TESIS DE LA UNIVERSIDAD DE ZARAGOZA
2021
51

Alba Legarda Lisarri

Disentangling Eocene/Oligocene ocean changes in the NW Atlantic using planktic foraminifera, stable isotopes and other proxies

Departamento
Ciencias de la Tierra

Director/es
Arenillas Sierra, Ignacio
Coxall, Helen Katherine

ISSN 2254-7606

Prensas de la Universidad
Universidad Zaragoza

ISSN 2254-7606

Universidad Zaragoza
1542

Tesis Doctoral

DISENTANGLING EOCENE/OLIGOCENE OCEAN CHANGES IN THE NW ATLANTIC USING PLANKTIC FORAMINIFERA, STABLE ISOTOPES AND OTHER PROXIES

Autor

Alba Legarda Lisarri

Director/es

Arenillas Sierra, Ignacio
Coxall, Helen Katherine

UNIVERSIDAD DE ZARAGOZA

Ciencias de la Tierra

2019

Universidad Zaragoza
1542

Stockholm University

PhD Thesis

Disentangling Eocene/Oligocene ocean changes in the NW Atlantic using planktic foraminifera, stable isotopes and other proxies

Alba Legarda Lisarri

Zaragoza, 2019

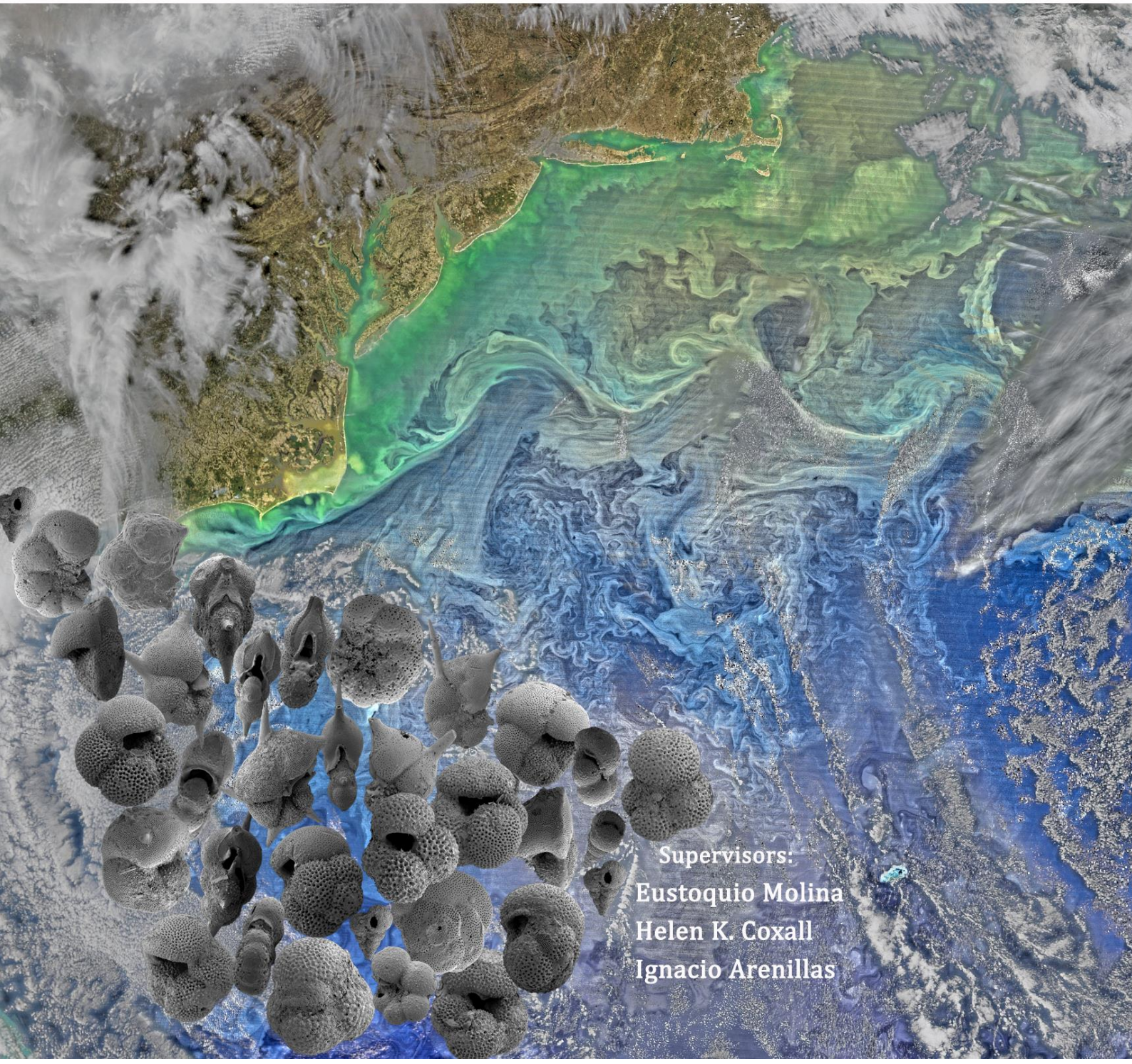

Disentangling Eocene/Oligocene ocean changes in the NW Atlantic using planktic foraminifera, stable isotopes and other proxies

Alba Legarda Lisarri

Cover: Site 612 planktic foraminifera overlying “The Turbulent North Atlantic” Image collected on March 9, 2016 by the Visible Infrared Imaging Radiometer Suite on NASA-NOAA's Suomi NPP satellite. It shows the relatively laminar flow of the Gulf Stream (left) opposed to the more turbulent western North Atlantic Ocean (right). The turbulence — visible due to the high content of pigmented phytoplankton — extends across the entire North American Basin from Anegada to Bermuda to Cape Cod. Courtesy of *NASA/Ocean Biology Processing Group, NASA Goddard Space Flight Center.*

A mi familia,

A quienes han estado a mi lado durante todo este tiempo,

A quienes han partido para siempre.

”Izarren hautsa egun batean
bilakatu zen bizigai,
hauts hartatikan ustekabean
noizpait ginaden gu ernai.

Eta horrela bizitzen gera
sortuz ta sortuz gure aukera
atsedenik hartu gabe:
lana eginaz goaz aurrera
kate horretan denok batera
gogorki loturik gaude.”

Xabier Lete, “Izarren hautsa” (1976)
(Stardust)

Table of contents

Abstract

The Eocene-Oligocene climate transition (EOT) was associated with pronounced global cooling and changes in ocean circulation that culminated in the onset of Antarctic glaciation ~34 Ma ago. A growing body of sedimentologic, geochemical and micropaleontologic evidence recognizes consistent changes in the Northern Hemisphere that imply an important role for North Atlantic Ocean circulation during the EOT. This PhD thesis contributes new insights about the oceanographic and climatic events occurred between 36 and 33 Ma based on micropaleontological assemblage analysis (planktic foraminifera, benthic foraminifera and calcareous nannofossils) and stable isotope data ($\delta^{18}O$ and $\delta^{13}C$) on exceptionally well preserved (glassy) foraminifera from DSDP Site 612 on the western North Atlantic margin. This midlatitude site (paleolatitude 41°18'N, 48°54'W) is located on the New Jersey Continental Slope (palaeodepth ~1000 m). In the present, as well as likely during EOT time, it sits at the confluence of today's north flowing Gulf Stream and south flowing Labrador surface currents. Today Site 612 seafloor is bathed by North Atlantic Deep Water. Isotopic and biostratigraphic data indicate that the first phase of the EOT (EOT-1 and the Eocene/Oligocene boundary, EOB) is captured in Site 612 sediments but the rest, i.e. the Oi-1 Antarctic glaciation event, is truncated by a hiatus, with only a sliver of early Oligocene strata surviving.

According to recognized micropaleontological assemblages and oxygen and carbon stable isotope measurements on benthic and planktic foraminifera, significant changes in surface and deep-water conditions have been identified in the 2.87 Myrs of the late Eocene and early Oligocene. This period can be divided into four paleoenvironmental phases, which can reflect the changes in nutrient supply and vertical mixing occurred during the 2.5 Myrs prior to the EOB in the North Atlantic. These changes are consistent with shifting influence of surface currents linked here to strengthening of northern-sourced deep water production, from 36 Ma. The

results of this PhD thesis are important for piecing together the global events associated with the rapid expansion of the cryosphere in the early Oligocene.

Resumen

El tránsito Eoceno-Oligoceno (*EOT* en siglas inglesas) estuvo asociado a un enfriamiento pronunciado del océano y a cambios en la circulación oceánica que culminó con la formación inicial del casquete polar de la Antártida hace ~34 Ma. Un conjunto creciente de evidencias sedimentológicas, geoquímicas y micropaleontológicas en el Hemisferio Norte sugieren que la circulación oceánica del Atlántico Norte jugó un importante rol en los cambios climáticos ocurridos durante el EOT. Esta Tesis Doctoral contribuye con una revisión de los eventos oceanográficos y climáticos ocurridos entre hace 36 y 33 Ma basada en el análisis de las asociaciones micropaleontológicas (foraminíferos planctónicos, foraminíferos bentónicos y nanofósiles calcáreos) y de los isótopos estables ($\delta^{18}O$ y $\delta^{13}C$) obtenidos de las conchas excepcionalmente bien preservadas de foraminíferos provenientes del margen Oeste del Atlántico Norte (DSDP Site 612). Este sondeo es de latitud media (paleolatitud 41°18'N, 48°54'W) y está situado en el talud continental de New Jersey (paleoprofundidad ~1000 m). En la actualidad, probablemente como en el EOT, se halla en la confluencia de la Corriente del Golfo, que fluye hacia el norte, y la Corriente del Labrador, que fluye hacia el sur, mientras que el fondo oceánico es bañado por el Agua Profunda del Atlántico Norte (*NADW* en siglas inglesas). Los datos isotópicos y bioestratigráficos indican que la primera fase del EOT (EOT-1 y el límite Eoceno/Oligoceno, o EOB en siglas inglesas) está registrada en los sedimentos del Sondeo 612. Sin embargo, el evento de glaciación Antártica Oi-1 está truncado por un hiato, sobre el cual se conserva únicamente una fina capa del Oligoceno.

El estudio cuantitativo de las asociaciones micropaleontológicas y las mediciones isotópicas de oxígeno y carbono en conchas de foraminíferos planctónicos y bentónicos han permitido identificar cambios significativos en las condiciones de las aguas superficiales y profundas del Atlántico Norte durante los 2.87 Ma estudiados del Eoceno tardío y Oligoceno temprano. Este periodo puede dividirse en cuatro fases paleoambientales, las cuales pueden reflejar los cambios en el aporte de nutrientes y mezcla vertical acontecidos durante los 2.5 Ma anteriores al EOB en

el Atlántico Norte. Estos cambios son consistentes con la intensificación de las aguas profundas provenientes del norte que venía ocurriendo desde hace 36 Ma y que provocó alteraciones en las corrientes superficiales. Los resultados de esta Tesis Doctoral son importantes para entender los eventos globales asociados con la rápida expansión de la criosfera en el Oligoceno temprano.

1. Introduction

The Eocene-Oligocene climate transition (EOT) is associated with pronounced ocean and atmospheric cooling, changes in ocean circulation and biotic turnover that culminated in the onset of glaciation on Antarctica ~34 Ma (Coxall & Wilson, 2011; Kennett, 1977; Lear et al., 2008; Zanazzi et al., 2007). Much of the focus has been on southern high latitude ocean changes associated with Southern Ocean gateway reconfigurations and the local oceanic and climatic impacts of the emplacement of a continental-scale Antarctic ice sheet (Bohaty et al., 2012; Goldner et al., 2014; Kennett et al., 1974; Kennett, 1977; Murphy & Kennett, 1986; Nong et al., 2000; Scher & Martin, 2006; Toggweiler & Bjornsson, 2000). However, there is increasing evidence that there was a critical change in North Atlantic Ocean circulation closely associated with or prior to the onset of Antarctic glaciation, possibly signaling the start of a stronger Atlantic Meridional Overturning Circulation (AMOC), the large scale system of surface and deep currents responsible for northward heat transport in the current oceanic setting (Coxall et al., 2018; Davies et al., 2001; Ferreira et al., 2018; Miller & Tucholke, 1983; Via & Thomas, 2006). To test this idea, detailed reconstructions of the state and evolution of ocean structure and temperature in the North Atlantic are essential. This will help improve understanding of climate forcing mechanisms during the EOT, especially in relation to global oceanic heat transport, biota and biogeochemical cycling during the early stages of Antarctic glaciation. Past studies have extensively looked at processes at the seafloor and/or uppermost layer of the water column (Coxall et al., 2018; Katz et al., 2008; Pagani et al., 2011). To have a better understanding of the water column structure and therefore, dynamics, it would be ideal to, simultaneously, analyze and compare tracers of different depths of the water column in regions most sensitive to circulation changes.

A variety of previous micropaleontological and geochemical studies have documented oceanic and biotic changes in the Southern Hemisphere, tropical Oceans and shallow shelf regions of the western North Atlantic (e.g. Bohaty et al., 2012; Diester-Haass & Zahn, 2001; Dunkley Jones et al.,

2008; Egan et al., 2013; Erhardt et al., 2013; Moore et al., 2014; Persico & Villa, 2004; Schumacher & Lazarus, 2004; Wade et al., 2012; Wade & Pearson, 2008). In the Southern Ocean these have been associated with the strengthening of circumpolar circulation, intensification of wind driven upwelling and nutrient supply to polar and subpolar waters (Diester-Haass & Zahn, 2001; Egan et al., 2013; Persico & Villa, 2004). In the tropics, some Atlantic settings suggest increased production (Diester-Haass & Zachos, 2003). Equatorial Pacific records consistently suggest decreased production associated with Oi-1 and the E/O boundary (EOB; Moore et al., 2014; Schumacher & Lazarus, 2004), however, a variety of proxies document a peak in export productivity in the eastern equatorial Pacific coincident with a peak in the Southern Ocean before the EOT onset close to the precursor glaciation EOT-1 (Egan et al., 2013; Erhardt et al., 2013). The importance of primary production relies on its potential role for increasing the biologic pump and drawing down CO_2 (Martin, 1990; Sarnthein et al., 1988; Volk & Hoffert, 1985).

The EOT is associated with major changes in surface and deep ocean circulation including regions of deep-water formation. A variety of evidence argues for intensification of Southern Ocean Deep water formation around the EOT. In parallel there is evidence for cessation of North Pacific deep water production sometime in the late Eocene and start up or intensification of deep water production in the North Atlantic (Cramer et al., 2009; Ferreira et al., 2018; McKinley et al., 2019; Scher & Martin, 2008; Thomas et al., 2014; Via & Thomas, 2006), which is a prediction of ocean circulation theory and modeling that finds a competition between NA and North Pacific sinking due to interbasinal, salt budgets and advection (Hutchinson et al., 2019). The precise order of these changes and the implications of each for driving ocean climate feedbacks remains uncertain.

A recent study found evidence that the intensification of North Atlantic deep water production predated the glaciation of Antarctic by approximately 1 million years (Coxall et al., 2018). Various proxies show that the first pulse of proto- North Atlantic Deep water, which it is here referred to as Northern Component Water (NCW), began at ~35.5 Ma and was fingerprinted with a low $\delta^{13}C$ signature that could be traced downstream, including at Site DSDP Site 612. Site, 612, therefore,

appears to be sensitively positioned to monitor the arrival of NCW on the Deep Western Boundary Current (Coxall et al., 2018). Strengthening of the deep limb of the AMOC should be associated with changes in the surface ocean on the New Jersey Margin, including potential changes in sea surface temperature and other changes in ocean structure linked to corresponding changes in the surface branch of the strengthening AMOC.

This doctoral thesis explores this hypothesis further by investigating the planktic foraminiferal assemblages and multi-species stable isotopes across EOT at Site 612 (from the mid Priabonian to the early Rupelian), together with other micropaleontological groups, in order to reconstruct the water column structure, surface and deep ocean response and the local marine ecosystem in general on the western North Atlantic Margin. Initial treatments of the calcareous nannofossils, siliceous microfossils, benthic and planktic foraminifera from this Site (Abbott, 1987; Bukry, 1987; Miller & Hart, 1987; Miller & Katz, 1987; Palmer, 1987) imply highly productive waters at Site 612 during Eocene and Oligocene but detail is missing for the EOT, and specially EOB (33.7 Ma, according to Cande & Kent, 1995; 33.9 Ma according to Gradstein et al., 2012). These results fill this gap and contribute new insights into the ocean environment on the western NA margin during the EOT. The multiproxy approach gives insight into stratification/mixing and paleotemperatures, all built on existing frameworks for interpretation of paleoecologies (Aze et al., 2011; Corliss, 1985; Villa et al., 2008). Specifically, this doctoral thesis presents the first continuous ~ 2 million year stable isotope geochemical record of the entire water column in NA mid latitudes and compare complementary information from phyto- and zooplankton (planktic foraminifera and calcareous nannofossils), and the dependents at the seafloor, benthic foraminifera.

This thesis is written as a monograph but the work include several papers and manuscripts. It began In Zaragoza University under supervision of Eustoquio Molina and Ignacio Arenillas with training in taxonomy and biostratigraphy. It continued with a collaborative project with Jorijntje Henderiks, Helen Coxall, Manuela Bordiga and Nicoletta Mancin, with training in Uppsala University under supervision of Jorijntje Henderiks focused in sample preparation and multiproxy data integration.

Finally, at Stockholm University under supervision of Helen Coxall, training and experience was acquired in order to learn about and apply $\delta^{18}O$ and $\delta^{13}C$ proxies for reconstructing Eocene-Oligocene palaecology and ocean-climate interactions. As a result, papers Bordiga et al. (2015b), Coxall et al. (2018), Legarda-Lisarri et al. (2014) and an unpublished manuscript were produced. This research used samples and data provided by the IODP. Benthic foraminiferal counts were performed by Nicoletta Mancin and Calcareous nannofossil counts by Manuela Bordiga, who also helped drawing the main initial interpretations on these groups, together with Jorijntje Henderiks and Helen Coxall. Nika Nordanstorm, student doing her bachelor thesis under Helen Coxall and my supervision, prepared, studied and carried benthic foraminiferal isotopical analysis in some additional samples.

2. Objectives

The central hypothesis to be tested is that the strengthening of the deep limb of the Atlantic Meridional Overturning Circulation (AMOC) should be associated with disturbances in the surface ocean on the New Jersey Margin, including potential changes in sea surface temperature and ocean structure linked to corresponding alterations in the surface branch of the strengthening AMOC.

The overarching goal of this PhD thesis is to investigate whether there was a critical change in North Atlantic circulation, implying the initiation of a stronger AMOC on the western margin associated with the onset of Antarctic glaciation. Detailed paleoceanographic reconstructions of the state and evolution of ocean structure and temperature in the North Atlantic were carried out in order to improve understanding of climate mechanisms that forced the change from a greenhouse (Eocene) to icehouse climate (Oligocene) in the EOT, especially in relation to global oceanic heat transport, biota and biogeochemical cycles during the early stages of Antarctic glaciation.

This PhD thesis has the following specific aims:

1) To analyse planktic foraminiferal assemblages and multi-species stable isotopes ($\delta^{18}O$ and $\delta^{13}C$) across the EOT at Site 612, together with benthic foraminiferal and calcareous nannofossil assemblages, in order to perform paleoenvironmental interpretations and reconstruct the water column structure and local marine ecosystem on the western North Atlantic Margin.

2) To appraise the stratification/mixing and palaeotemperatures on the western NA margin during the EOT.

3) To explore whether the strengthening of the deep limb of the AMOC is associated with changes in the surface ocean on the New Jersey Margin, such as sea surface temperature.

2. Objetives

4) To assess the erosional history of the New Jersey Margin and wider North Atlantic by examining Site 612 unconformities associated with depositional hiatuses, and re-evaluate their significance in relation to the new proxy data suite.

5) To develop an improved chronologic framework and build an age model.

6) To closely analyse the planktic foraminifera and produce a revised taxonomic assessment for Site 612.

7) To investigate the source of a ^{13}C-depleted carbon signature (low $\delta^{13}C$) in foraminifera during the early Oligocene (Rupelian) and assess the regional or global significance.

8) To investigate whether the decrease in $\delta^{13}C$ that occurred ~36 Ma ago (mid Priabonian) originated from a northern sourced deep water imprinted with 'old carbon' as previously proposed, or whether more local mechanisms related to export production and oxygen conditions might explain the $\delta^{13}C$ patterns.

3. Materials and methods

3.1. DSDP Site 612: Oceanic and geological setting

DSDP Leg 95 Site 612 (38°49.21'N and 72°46.43'W, Atlantic Ocean; Figure 1) was drilled in 1983 at bathyal water depth (1404 m) in the middle part of the New Jersey lower continental slope, at the Baltimore Canyon (Poag et al., 1987) (paleolatitude 41°18'N, 48°54'W according to Pagani et al., 2011; paleodepth ~1000 m according to Miller & Katz, 1987). This site contains a 6m long sequence of marine sediments through the late Eocene to early Oligocene. The E/O itself is known to be punctuated with at least one hiatus (Poag et al., 1987). Therefore, while there are gaps there are also important continuous windows into late Eocene and earliest Oligocene. The sediments comprise hemipelagic clays rich in calcareous and siliceous microfossils. Significantly, diverse planktic and benthic foraminifera occur that demonstrate test calcite preservation of an extremely high quality (glassy).

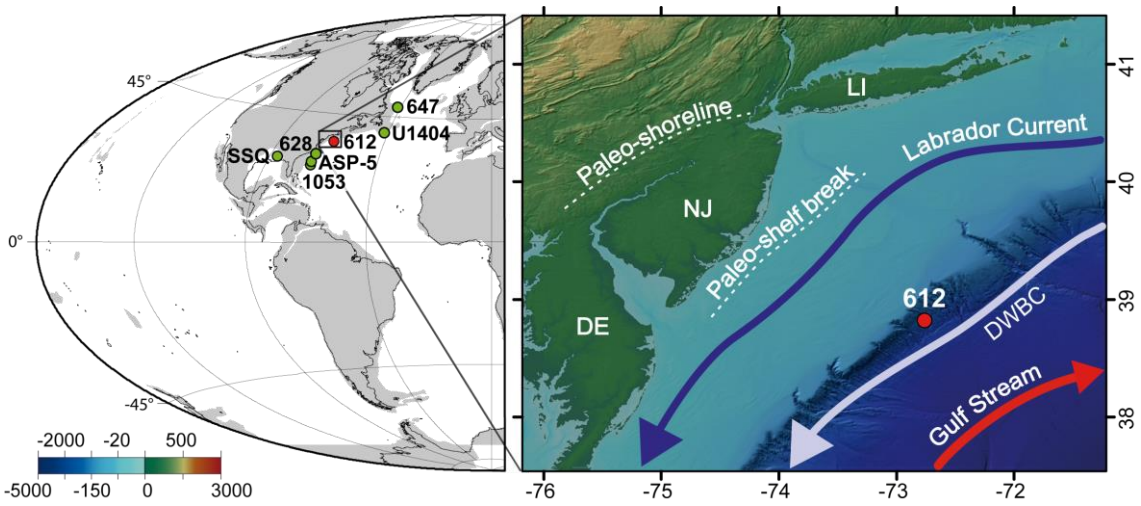

Figure 1. Modern and paleogeographic location of Sites investigated in this study; DSDP Sites 612 (red dot) and 647, ODP Sites 1053 and 628, IODP Site U1404, core ASP-5 and onshore-section SSQ (green dots) at 33.9 Ma (Ocean Drilling Stratigraphic Network, www.odsn.de). Zoomed view shows modern oceanic setting around New Jersey (National Geophysical Data Center, https://maps.ngdc.noaa.gov/), with generalized late middle Eocene paleo-shoreline and -shelf break (Poag & Low, 1987). The Labrador and Gulf Stream arrows represent cold (blue) and warm (red) surface currents respectively. Deep Western Boundary Current (DWBC) is the main southward conduit of Modern NADW (grey). (DE: Delaware, NJ: New Jersey, LI: Long Island). Color scale for bathymetry.

Stable oxygen and carbon isotopes ($\delta^{18}O$ and $\delta^{13}C$)(Miller et al., 1991; Pusz et al., 2009) and microfossils occurring across the EOB (Abbott, 1987; Bukry, 1987; Miller & Hart, 1987; Miller & Katz, 1987; Palmer, 1987) have been already investigated at a low resolution. This study has a 6-20 times greater resolution (See Appendix IV, Tables l and m).

The recent suggestion by Coxall et al. (2018) that major changes in deep water circulation occurred at this site (inferred from ^{13}C depleted benthic foraminiferal $\delta^{13}C$) requires a new examination of the entire water column to investigate whether the low $\delta^{13}C$ signature indeed originated from a northern sourced deep water imprinted with 'old carbon' as proposed, or whether more local mechanisms related to export production and oxygen conditions might explain the $\delta^{13}C$ patterns.

3.1.1. Modern oceanographic setting

Modern surface oceanographic conditions at Site 612 are governed by two major current systems: the equatorward flowing Labrador Current (LC) that hugs the shelf and the poleward flowing Gulf Stream (GS), in the form of eddies that advect warm salty water towards the slope (Townsend et al., 2006). The great (150 to 200 km today) width of the broad continental shelf plays an important role in controlling these conditions, allowing the existence of the two differentiated water masses. At their confluence, which is not fixed, cold and relatively fresh LC waters (Labrador Slope Water; LSW) and warm GS waters interact to induce abrupt changes in temperature (Figure 2a; 25°C - 15°C annual temperature range) and other properties (Townsend et al., 2006). Overall primary production is high and is dominated by a clear seasonal signal, with peak production occurring during the spring bloom when shelf-slope frontal interactions promote nutrient fluxes, and combined to estuarine-like physical processes, nutrients became available in the surface (Falkowski et al., 1980). The depth of the thermocline in summer (June)

is ~50 m with a SST of 25°C, and in winter (December) at ~150 m with an SST of 15°C (WOA (World Ocean Atlas) annual average 1955-2012; Locarnini et al., 2013) (Fig.2 b, c).

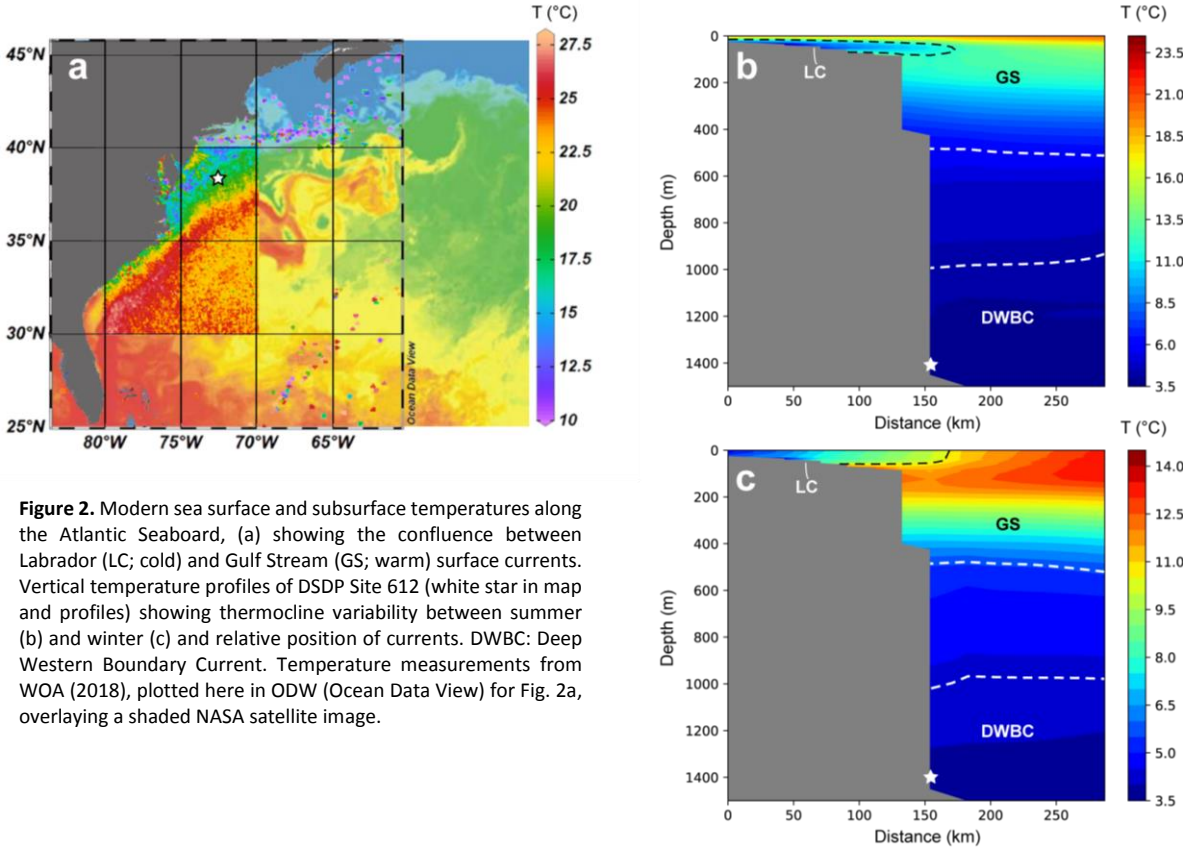

Figure 2. Modern sea surface and subsurface temperatures along the Atlantic Seaboard, (a) showing the confluence between Labrador (LC; cold) and Gulf Stream (GS; warm) surface currents. Vertical temperature profiles of DSDP Site 612 (white star in map and profiles) showing thermocline variability between summer (b) and winter (c) and relative position of currents. DWBC: Deep Western Boundary Current. Temperature measurements from WOA (2018), plotted here in ODW (Ocean Data View) for Fig. 2a, overlaying a shaded NASA satellite image.

At the seafloor Site 612 is influenced by the Deep Western Boundary Current (DWBC), the thermohaline-driven deep water contour current that flows south along the western Atlantic margin constrained by geostrophic flow and the shape of the ocean basin at depths of approximately 1,000-4,500 m (Fine & Molinari, 1988; Richardson et al., 1981; Schmitz & McCartney, 1993). Today the DWBC is an important part of the AMOC and responsible for transporting the cold, high-salinity northern sourced deep water known as North Atlantic Deep Water (NADW), which is formed periodically by sinking of chilled salty surface waters in the Nordic and Labrador Seas (Ferreira et al., 2018; Fine & Molinari, 1988; McCartney & Talley, 1982). Changes in AMOC strength are considered to be an important driver of abrupt climate change in the glacial past and the future, (Broeker, 1991; Coxall et al., 2018; Delworth et al.,

2008; Ferreira et al., 2018; Rahmstorf, 2006) but its origin and subsequent early Cenozoic history is a subject of current debate (Ferreira et al., 2018).

3.1.2. Paleoceanography

Certainly, the paleoceanography of the EOT contrasts to that in the present, although there are multiple similarities too. This passive US middle Atlantic margin has been the subject of various studies directed at unravelling sea-level history and the response of sedimentation to sea-level changes during the Cretaceous to Recent (Miller et al., 2014). In terms of paleoceanography, one of the key features that was different in Eocene-Oligocene time and influenced the study site is the location of the paleo-shoreline and paleo-shelf break, which is reconstructed to have been 100 km landward compared to present (Poag & Low, 1985). This resulted in a sediment-starved shelf and slope with low siliciclastic and high pelagic carbonate inputs associated with early and middle Eocene warm climates (maximum Cenozoic sea level), and increased siliciclastic sedimentation at the expense of carbonate deposition during the middle Eocene and earliest Oligocene, as cooling events and falling sea level took over (Miller et al., 2006; Miller et al., 2014; Mountain et al., 1998; Pekar et al., 2001). Backstripping approaches to reconstructing sea level on this margin imply glacioeustatic lowering of ~55 m associated with the initiation of Antarctic glaciation (Oi-1 $\delta^{18}O$ event) (Pekar et al., 2001). On the other hand, a similar feature to the current circulation is the presence of the geostrophic Gulf Stream surface current, which has likely existed since the Early Cretaceous when the Atlantic basin became wide enough for northern gyre circulation (Tucholke & Mountain, 1986).

A long standing challenge to reconstructing early Eocene-Oligocene Atlantic circulation is the lack of continuous sedimentary records through this interval as a consequence of widespread unconformities, especially in the northeastern Atlantic, that have been associated with invigoration of abyssal circulation at this time (Boyle et al., 2017; Miller & Tucholke, 1983; Miller

et al., 2014; Tucholke & Mountain, 1986). Whether this is linked to NCW startup (Borrelli et al., 2014; Davies et al., 2001; Hohbein et al., 2012; Huber & Sloan, 2001; Via & Thomas, 2006) is still uncertain, since an alternate view proposes that not until the late Miocene were significant amounts of northern sourced deep water produced (Wright & Miller, 1996). Therefore, the potential role of northern sourced deep-water production as a climatic force during the EOT is still under debate. That aside, increasing evidence points to the late Eocene as being a critical phase in the evolution of the AMOC that may have had a role in priming the Earth for Antarctic glaciation (Abelson & Erez, 2017; Coxall et al., 2018; Elsworth et al., 2017; Hutchinson et al., 2018a).

3.1.3. Samples and sample preparation

Fifty-four 10 cc core samples, consisting mainly of clayey siliceous foraminiferal nannofossil ooze (Poag et al., 1987), were prepared for a variety of paleoceanographic analyses (Appendix IV, Table IV.l). Samples were collected from between 135.37 and 141.46 meters below seafloor (mbsf) at 6 cm intervals in the Oligocene and 10-20 cm in the Eocene, except around the expected EOB, where the sampling was every 3 cm (See Appendix IV, Table IV.m) to accurately quantify the biostratigraphic changes and, ultimately the extinction level of the genus *Hantkenina*, which denotes the E/O boundary in open marine settings. The biostratigraphic age-depth model, updated here using new biostratigraphic constraints (Section 4.2.), indicates that the newly sampled and studied interval spans ~ 2 million years, ranging from 34.96 to 32.95 Ma (Cande & Kent, 1995; CK95). Constraints from this new sample suite are examined together with the longer-term middle Eocene sedimentary and foraminiferal stable isotope data sets from Site 612 of Miller et al. (1991), Pusz et al. (2009) and Coxall et al. (2018). Sand-fraction samples for sediment fraction abundance (weight %) and foraminiferal analyses were prepared by first drying the bulk sediment samples in an oven at 40°C, then recording the total dry weight before

soaking in deionized water and eventually wet-sieving over a 38 µm mesh. For calcareous nannofossil analysis, slides were prepared with the drop technique (Bordiga et al., 2015a). Siliceous microfossil counts were made on the same slides. They were examined with a transmitted light microscope under polarized light (LM) at 1000X magnification. Sand fraction samples (foraminifera and radiolarian fractions) were examined using a binocular light microscope. A camera set up was used to image foraminifera at some intervals. See Appendix V for additional information on sample preparation.

3.2. Scanning Electron Microscope (SEM) analysis

SEM imaging was carried out to document biostratigraphically useful taxa and investigate foraminiferal preservation, supplemented at some intervals with light microscope imaging. Specimens were mounted on a 20 mm SEM stub and gold-coated with a Leica ion beam coater to maximize the backscattering of secondary electrons for optimal topographic imaging. Imaging was conducted under high vacuum using a Carl Zeiss MERLIN™ field emission SEM at Universidad de Zaragoza.

3.3. Oxygen and Carbon stable isotopes

Planktic and benthic foraminiferal tests were screened for preservation quality and those deemed well preserved, i.e. having no significant overgrowth or infilling of diagenetic calcite, and smooth translucent looking test surfaces, were picked for analysis. Samples from 141.46 to 135.37 mbsf were studied to obtain monospecific/monogeneric $\delta^{18}O$ and $\delta^{13}C$ records that sample physical and chemical conditions in the water column. As inferred from this and previous isotopic paleoecology studies (Pearson et al., 2006; Pearson et al., 2001), *Pseudohastigerina micra* and *P. naguewichiensis* were chosen to monitor the uppermost surface mixed layer,

Turborotalia ampliapertura and *T. increbescens* slightly deeper mixed layer conditions, and *Catapsydrax dissimilis* and *C. unicavus* thermocline to subthermocline conditions. The benthic species *Cibicidoides* spp. and *Hanzawaia ammophila* provide a bottom water signal (Katz et al., 2003). The choice of species was controlled by the availability of sufficient specimens throughout the section. In the case of planktic foraminifera, given the uneven availability of some species, specimens corresponding to two species -same genera- with the same isotopic signature were selected (Arthur et al., 1989; Boersma et al., 1987; van Eijden & Ganssen, 1995; Moore et al., 2014; Pearson & Wade, 2009; Pearson et al., 2001; Poore & Matthews, 1984; Sexton et al., 2006; Spezzaferri & Pearson, 2009; Wade et al., 2007; Wade & Pearson, 2008). The minimum required $CaCO_3$ mass for analysis at Stockholm University Geological Sciences Isotope Lab (SIL) was 10 µg. The number of analyzed planktic specimens required to achieve this ranged from 6-14 and depended on size fraction (>250 µm; except *Pseudohastigerina*, picked 53-79 specimens from >106 µm fraction). For benthic, 2-5 specimens were picked from >250 µm fraction, and where no *Cibicidoides* was present, *Hanzawaia ammophila* was picked.

$\delta^{18}O$ and $\delta^{13}C$ were measured on a ThermoFinnigan MAT 252 IRMS coupled with a Finnigan Gasbench II device at the Stockholm University SIL lab. Carbonate samples were reacted in 100 % ortophosphoric acid at 90°C for 15 min and the resultant CO_2 was analyzed. Results are reported in per mil (‰) deviations relative to Vienna Pee Dee belemnite standard (VPDB). Standard external analytical precision is better than 0.07‰ for $\delta^{13}C$ and 0.15‰ for $\delta^{18}O$, based on replicate analysis of in-house standards (Carm-1 and $CaCO_3$ Merck) calibrated to international standards (NBS19, IAEA-CO-1 and IAEA-CO-8).

The measured $\delta^{18}O$ and $\delta^{13}C$ values of *Hanzawaia ammophila* values were adjusted to equivalent *Cibicidoides* spp. values using adjustment factors determined by Katz et al. (2003) with the following equations:

$$\delta^{18}O_{Cibicidoides} = (\delta^{18}O_{Hanzawaiia} - 0.16)/0.62 \quad (1)$$

$$\delta^{13}C_{Cibicidoides} = \delta^{13}C_{Hanzawaiia} + 0.08 \quad (2)$$

This facilitates comparison with previous late Eocene/ early Oligocene *Cibicidoides* spp. records from this and other sites (Miller et al., 1991; Pusz et al., 2009).

3.3.1. $\delta^{18}O$ Paleotemperature estimates

The oxygen stable isotope ratio ($\delta^{18}O$) of biogenic calcite has long been used as a paleothermometer, due to the temperature dependency of $^{18}O/^{16}O$ fractionation during calcite formation, and the shells of foraminifera are the most widely used fossil archive for reconstructing temperature on geological time scales (Emiliani, 1954; Urey, 1947). In practice there are many factors that complicate this application, including the need to know the value of local sea water $\delta^{18}O$ at the time the foraminifera was calcifying and local seawater salinity, both of which vary significantly on Cenozoic time scales as a consequence of changes in global ice volume and hydrological cycling, and locally in the ocean due to latitude and evaporation/precipitation patterns (Cramer et al., 2011; Pearson, 2012; Rohling & Cooke, 1999; Tindall et al., 2010). During late Eocene time, before significant ^{16}O had been locked into the Antarctic ice sheet, $\delta^{18}O$ of seawater related to terrestrial ice storage should be simpler to constrain. Therefore, assuming only minor local-salinity-related fluctuations at Site 612, ocean temperatures on the Eastern seaboard were reconstructed using planktic and benthic foraminiferal $\delta^{18}O$. For this, the following $\delta^{18}O$ temperature equations were used. For planktic foraminifera, Kim & O'Neil (1997), calibrated using synthetic calcite in the laboratory over a temperature range of 10-40°C, and for benthic foraminifera Lynch-Stieglitz et al. (1999) as arranged by Cramer et al. (2011), empirically tested using *Cibicidoides* and *Planulina:*

$$T\,(^{\circ}C) = 16.1 - 4.76\left[\delta^{18}O_{CC(bf)} - 0.27 - (\delta^{18}O_{SW} - LC)\right], \quad (3)$$

where 0.27 is the SMOW to VDBP conversion factor and LC stands for latitude correction. The equation of Kim & O'Neil (1997) was chosen over the classically used Erez & Luz, (1983) that significantly overestimates temperatures by about 2°C (Mulitza et al., 2003), and has a more suitable temperature range. Lynch-Stieglitz et al. (1999) was chosen because it is the best-constrained field calibration, as it is based on a large data set. EOT sea-water $\delta^{18}O_{(sw)}$ (VSMOW) value is the greatest unknown in this method. Therefore, I experimented with multiple surface and deep $\delta^{18}O_{sw}$ values (Table 1) to build an envelope of realistic temperatures, after converting them to ‰ VPDB (Pearson, 2012) and applied the latitudinal conversion to SST values (Zachos et al., 1994), as expressed in the following equation:

$$y = 0.576 + 0.041x - 0.0017x^2 + 1.35 * 10^{-5}x^3 , \quad (4)$$

where *y* represents $\delta^{18}O_{sw}$ and *x* is absolute latitude in the range of 0 ° to 70 °.

Table 1. The range of estimated $\delta^{18}O_{sw}$ (VSMOW) (‰) values relevant to EOT time applied to build the paleotemperature envelopes.

Estimated $\delta^{18}O_{sw}$ (VSMOW) (‰)	Reference	Comments
-1.00	Shackleton & Kennett (1975)	Ice-free world global ocean (also used for ice-free conditions in Zachos et al., 1994)
-0.80 -0.40	Zachos et al. (1994)	Late Eocene (mean ocean water) Early Oligocene (mean o.w.)
-0.43 -0.37	Tindall et al. (2010)	Modelled for Eocene (surface/bottom of mixed layer-50m-)
-0.30	Roberts et al. (2009)	Modelled for Paleogene surface waters
-0.28 -0.53	Huber et al. (2003)	Modelled for Paleogene surface waters (upper limit/Lower limit)
-0.89	Cramer et al. (2011)	Assuming minimal ice; 1/3 isostatic subsidence
0.33	Katz et al. (2008)	Calculated for SSQ (Gulf of Mexico; 50m paleodepth) after Mg/Ca data

3.4. Quantitative microfossil assemblage analysis and sediment fractions weigh %

Quantitative assemblage analysis was performed for three microfossil groups to explore phyto- and zooplankton assemblage composition, water column and seafloor conditions, and export production. Species range data generated during this was used to provide additional

biostratigraphic constraints were applicable (see Section 4.2.). Weight percentages (wt%, contributions of the various grain size classes) were also quantified, as a physical proxy for current speed and/or erosion potential on the western Atlantic margin during the EOT (Kleiven et al., 2011; McCave et al., 2017; Thornalley et al., 2013). The theory behind this is that selective erosion of finer components (winnowing) can result in concentration of coarser grains by producing intermittent erosion horizons marked by a coarse silt–sand lag (McCave et al., 2017; McLaren & Bowles, 1985). To obtain the wt %, the residue with particle diameter greater than 38 μm (ø >38 μm) was wet sieved into three sub-fractions that were subsequently dry weighed: sortable silt (SS; 38> ø <63 μm), fine sand (63> ø <106 μm) and coarse sand (ø >106 μm) - the latter two compose the coarse fraction (CF). Fine fraction (FF; ø <38 μm) weight was obtained after subtracting the residue from the initial weight.

For planktic foraminifera abundance surveys, counts are based on at least 300 specimens, identified and classified to species or genus level (see Appendix II). For benthic foraminifera, a minimum of 200 specimens (limited by availability) were counted. Foraminiferal taxonomies followed are Pearson et al. (2006) and Wade et al. (2018) for planktic foraminifera and a variety of works for the benthic foraminifera (Hayward et al., 2012; Kaminski & Gradstein, 2005; Kaminski & Ortiz, 2014; Loeblich & Tappan, 1988; Van Morkhoven et al., 1986; Ortiz & Kaminski, 2012; Ortiz & Thomas, 2006; Tjalsma & Lohmann, 1983). For siliceous plankton, at least 300 specimens were counted and classified into two basic classes: diatoms and other siliceous plankton, which was mostly radiolaria. Both relative (%) and absolute abundances (number of specimens per gram of dry bulk; N g^{-1}) are reported to observe the influence of dilution and sedimentation rate, and the real fluctuations in abundance of single species or group of taxa. Glauconite content, which is common at several horizons, was visually estimated (%) while performing the foraminiferal counts. This provides a course proxy for sea-level lowering and/or decreased carbonate production evidenced by increased sand input (Diester-Haass et al., 2002). Diversity was assessed for each micropaleontological group using the Fisher's alpha parametric

index of diversity, which assumes that the abundance of species follows the log series distribution (Fisher et al., 1943).

A new treatment of the biostratigraphy was carried out using planktic microfossil groups that builds on previous studies (Miller et al., 1991; Poag et al., 1987) and the latest higher resolution sampling. The biozonation scheme follows Agnini et al. (2014) for calcareous nannofossil, Wade et al. (2012) for planktic foraminifera and Kamikuri et al. (2012) for radiolaria. The age-depth model was improved upon from the Leg 95 initial reports version by the inclusion of new biostratigraphic data produced here. Sample ages are calculated using linear interpolation between biostratigraphic datums, calibrated to the timescales of both CK95 (Cande & Kent, 1995) and GPTS 2012 (Gradstein et al., 2012) (Appendix IV, tables a and b). All the sample ages in this manuscript are plotted respective to CK95, to facilitate simple comparison to existing studies.

3.5. Microfossil eco-groups and Eocene-Oligocene evolutionary histories

Eocene-Oligocene planktic microfossil assemblages can provide insights into upper ocean conditions including primary production and stratification (Diester-Haass & Zahn, 2001; Dunkley Jones et al., 2008). Benthic foraminifera provide further perspectives on productivity in relation to organic matter export from the upper ocean to the seafloor, as well as insights into water depth, deep water oxygenation and current activity (Fraile et al., 2008; Mackensen et al., 1995; Ortiz & Kaminski, 2012; Thomas & Gooday, 1996).

From a broad evolutionary perspective, planktic foraminifera underwent an enhanced turnover at the EOT, especially of surface dwellers (Pearson et al., 2008; Wade & Pearson, 2008). Calcareous nannoplankton also underwent significant restructuring during the EOT, marked by a rapid diversity decline, from a maximum during the warm Eocene to a minimum in the early

Oligocene, accompanied with near-terminal extinction of four taxa (Bown et al., 2004). Benthic foraminifera experienced a significant evolutionary turnover (Thomas, 1990), marked by a diversity decrease, at the expenses of cylindrical taxa decline (Hayward et al., 2012; Thomas, 2007) and increase in eutrophic opportunistic species after the EOT (Thomas & Gooday, 1996).

For benthic foraminifera, understanding the paleoenvironmental tolerances of Eocene and Oligocene foraminiferal species is inferred from knowledge of modern communities, contemporary environmental and lithological settings and stable isotope signatures (Table 2; Corliss, 1985; Sen Gupta & Machain-Castillo, 1993; Jorissen et al., 2007; Van Morkhoven et al., 1986). Regarding the relationship between benthic foraminiferal assemblages and deep water conditions, infaunal forms are more tolerant to low-oxygen conditions and/or high organic matter fluxes (Bernhard, 1986; Kaiho & Hasegawa, 1994), while epifaunal taxa become generally less abundant under those conditions. In this aspect, proxies like the Epifaunal/Infaunal ratio (E/I; *Epifaunal taxa (%)/ Total assemblage (%)*), can show major changes in the ecological factors controlling benthic foraminiferal assemblages. Comparative environment and assemblage based interpretations can also be used to infer planktic ecologies but planktic stable isotope depth profiling has also become especially helpful (Birch et al., 2012; Pearson et al., 2006; Pearson et al., 1997; Sexton et al., 2006; Spezzaferri, 1994, 1995, 2002; Wade et al., 2007, 2018). This doctoral thesis follows the isotope based classification of Aze et al (2011) which divides EOT planktic foraminifera into various ecological groups (‘eco-groups’) according to water column habitat: mixed layer, thermocline and sub-thermocline dwellers (Table 3). An additional surface opportunistic eco-group has been considered that includes occasionally abundant microperforate taxa, such as tenuitellids and chiloguembelinids, not treated by Aze et al. (2011), based on paleoecology interpretations of Pearson et al. (2006), Pearson et al. (1997), Pearson & Wade (2009), Poore & Matthews (1984), Smart & Thomas (2006) and Wade et al. (2018).

In the case of coccolithophores, their geographical distribution and abundance are controlled by the availability of light, temperature, nutrient availability and salinity (e.g. Winter et al., 1994). In the fossil record, the ecological preferences of calcareous nannoplankton are still controversial and unresolved. Nevertheless, some paleo-environmental/climatic preferences have been proposed (see Table 3 in Villa et al., 2008 for a comprehensive summary of paleoecological interpretations for the main nannofossil taxa occurring across the EOT).

Although the main focus and detail in this study concerns planktic and benthic foraminifera and calcareous nannofossils, components of the siliceous plankton as diatoms and radiolaria are relevant to understand the Eocene/Oligocene climatic transition, a time of enhanced siliceous ooze accumulation including a threshold increase in diatom abundance (Falkowski et al., 2004). Oceanic diatoms are an important group of protistan phytoplankton usually dominant in upwelling regions and high latitudes that thrive under high nutrient conditions. They account for ca. 45% of net primary productivity and play a major role in the biogeochemical cycling of nutrients such as silica (Benoiston et al., 2017). During the EOT they underwent a significant turnover, a major diversity increase (Baldauf, 1992; Suto, 2006) that has been attributed to increased Si availability in the ocean surface (Falkowski et al., 2004).

The other important siliceous group are radiolaria. Modern radiolarians are a zooplankton group that prefer regions seaward of the continental slope, where upwelling makes food available and they bloom seasonally in response to changes in food, silica content, currents and water masses (Armstrong & Brasier, 2005). Similar to planktic foraminifera, they commonly have photosymbionts. This group is useful for biostratigraphy and as a paleoceanographic indicator. In fact, they record a dramatic turnover during the EOB, marked by the extinction of several taxa and expansion of cool-water taxa (Funakawa et al., 2006; Moore et al., 2015). This has been linked to changes in seasonal upwelling in the tropics and an overall increase in nutrient supply to the photic zone, providing sufficient nutrients to support a diatom flora (Moore et al., 2015):

Table 2. Benthic foraminiferal species paleoecologic affinities and taxonomic list used for this study. *1 sensu Miller & Katz, (1987). References: 1) Corliss (1985); 2) Corliss & Chen, (1988); 3) De & Gupta, (2010); 4) de Mello e Sousa et al. (2006); 5) Den Dulk et al. (2000); 6) de Stigter et al. (1998); 7) Fontanier et al. (2002); 8) Fontanier et al. (2005); 9) Hayward et al. (2012); 10) Jorissen et al. (1995); 11) Jorissen et al. (2007); 12) Kaminski & Gradstein, (2005); 13) Mackensen et al. (1995); 14) Mojtahid et al. (2010); 15) Phipps et al. (2012); 16) Rathmann & Kuhnert, (2008); 17) Schmiedl et al. (2000); 18) Sen Gupta & Machain-Castillo, (1993); 19) Schönfeld, (2002); 20) Sun et al. (2006); 21) Van Morkhoven et al. (1986); 22) Gooday, (1988); 23) Ortiz & Kaminski, (2012); 24) Thomas, (2007).

BENTHIC TAXA	WATER DEPTH (m)								LIFE MODE		FOOD SUPPLY	OXYGEN CONTENT	SUBSTRATE	OTHER REMARKS	ECOLOGICAL REMARKS				REF.
	CONTINENTAL SHELF			CONTINENTAL SLOPE			ABYSSAL	ABYS. PLAIN							Epifaunal Phyto–detritus taxa	Infaunal			
	NERITIC			BATHYAL			ABYSSAL									Flattened-biserial	Conical	Elongated group	
	0-50	50-100	100-200	200-600	600-1000	1000-2000	2000-4000	>4000	Infaunal	Epifaunal									
Alabamina cf. *A. dissonata* *1				x	x	x				x	seasonally high		muddy to sandy	Morphologically and ecologically similar to the extant Alabaminella *weddellensis*. The Eocene forms with a developed keel usually occur at abyssal depths.	x				3, 20, 21
Anomalinoides alazanensis				x	x					x	low								1, 2, 21
Bolivina-Brizalina spp.				Not indicative					deep		high sustained	low	muddy	Typical of sapropelitic layers and an important foraminiferal component of the OMZ		x			1, 2, 5, 10, 11, 17, 18
Bulimina alazanensis				x	x				x		high sustained	low	muddy				x		18, 21
Bulimina mexicana				x	x				deep		high sustained	low	muddy to sandy	Typical of coastal upwelling and high productivity areas			x		1, 2, 8, 10, 11, 18, 21
Bulimina tuxpamensis				x	x	x	x		deep		high sustained	low	muddy				x		1, 2, 10, 11, 21
Cibicidoides hadjibulakensis				x	x	x				x	low (pulsed)	high		Morphologically closed to *C. eoceanus;* less tolerant to low oxygen conditions					1, 2, 4, 11, 21
Cibicidoides mundulus						x	x			x	low (pulsed)	high							1, 2,10, 21
Chrysalogonium spp.					x	x	x		x		high	low	muddy to sandy					x	1, 2, 5, 9, 13, 23
Epistominella exigua					x	x	x			x	seasonally high				x				20
Eponides abatissae						x	x	x		x				Ecologically similar to *Cibicidoides havanensis*					1, 2, 4, 21
Glandulonodosaria spp.									x		high		muddy to sandy					x	23
Globocassidulina subglobosa					x	x	x		facultative	x	low (pulsed)	high	sandy and elevated	Mainly cold bottom-water with strong and persistent near-bottom currents					
Gyroidinoides girardanus				x	x				shallow		low								1, 2, 11, 21
Hanzawaia ammophila			x	x						x	low			Locally abundant at abyssal depth					1, 2, 11, 21
H. grimsdalei						x	x	x		x				Max. abundance 2000-4000m water-depth					1, 2, 21
H. mexicana					x	x				x				Can tolerate carbonate depleted waters					1, 2, 21
Lenticulina spp.					x	x				x	low								1, 2, 5, 9, 21
Melonis affinis						x	x		shallow		high	intermediate							1, 2, 6, 7, 14, 15
Mucronina spp.			x	x	x	x			x		high	low	muddy to sandy						1, 2, 5, 9, 13, 18
Neugeborina longiscata					x	x	x		x		high	low	muddy to sandy					x	1, 2, 5, 9, 13, 18
Oridorsalis umbonatus						x	x	x	shallow	x(2)	low (pulsed)			Cold deep waters, can tolerate hypoxic bottom water					1-3, 11, 13, 16, 19, 21
Orthomorphina cf. *jedlitschkai*						x	x		x		high	low	muddy to sandy					x	1, 2, 5, 9, 13, 18, 23
Osangularia cf. *O. plummerae*						x	x	x		x	seasonally high			Morphologically similar to the modern *Nuttallides umbonifera*. Opportunistic (24).					3, 20, 21
Planulina (Cibicidoides) renzi				x	x	x				x (raised epibenthic)	low (pulsed)	high	elevate	Morphologically closed to *C. wuellerstorfi*; high-energy environments with bottom current					1-3, 11, 13, 19, 21
Pleurostomella spp.						x	x		x		high	low	muddy to sandy					x	1, 2, 5, 9, 13, 18, 23
Pullenia bulloides					x	x	x		x		intermediate	low	muddy						1-4, 6, 10, 14, 15, 21
Siphonodosaria spp.						x	x		x		high		muddy to sandy					x	1, 2, 5, 9, 13, 18, 23
Strictocostella spp.						x	x		x		high		muddy to sandy					x	1, 2, 5, 9, 13, 18, 23
Textularia spp.	x	x	x	x					x				sandy						12
Trifarina spp.					x	x			x		high		coarse-grained	*T. angulosa* occurs on the shelf			x		3, 14, 15, 21
Uvigerina galloway-mexicana			x	x	x	x			x		high		muddy				x		1, 2, 18, 21
Uvigerina rippensis					x	x			x		high	low	muddy	Morphologically similar to the modern *U. peregrina*; it can tolerate low oxygen conditions with refractory organic matter			x		1-4, 6, 10, 11, 14, 15, 21
Vulvulina spinosa				x	x				x				sandy						12

Table 3. Planktic foraminiferal species paleoecologic affinities and taxonomic list used for this study. References: (1) Wade et al. (2007); (2) Pearson et al. (1997); (3) Spezzaferri et al. (2002); (4) Sexton et al. (2006); (5) Pearson et al. (2006); (6) Spezzaferri, (1995); (7) Spezzaferri, (1994); (8) Wade et al. (2018). ML stands for mixed layer; T for thermocline; ST for sub-thermocline, according to Aze et al. (2011). S=Surface; D=deep; H=high; L=low; TR=more tropically restricted. Notes: Notes: 1* deep zone; 2* shelf environment; 3* common in upwelling regions; 4* cold water; 5* only pre-adult; 6* shallow habitat for pre-adult forms, deepening in the adult stage; 7* microperforated; 8*common; 9* absent from deep-sea oligotrophic settings and cold water preferred; 10* predicted from *T. munda* and *T. angustiumbilicata* stable isotope paleobiology; 11* alternatively, vital effect; 12* tychopelagic.

PLANKTIC TAXA	Water column habitat				Geographic distribution			High productivity affinity	Other remarks	Eco-groups
	Surface (S)		Thermocline (D)	Subthermocline (D)	High latitudes (H)	Cosmopolitan, no diagnostic	Low & Mid latitudes (L)			
	Mixed layer	Shallow subsurface								
Turborotalia cocoaensis	(4)	(5)					(5)		TR (5)	ML
Turborotalia cunialensis							(5)		TR (5)	ML
Turborotalia cerroazulensis		(5)				(5)				ML
Turborotalia increbescens	(5)					(5)				ML
Turborotalia ampliapertura	(3,5)					(5)				ML
Hantkenina alabamensis	(5)						(5)			ML
Hantkenina compressa	(5)						(5)			ML
Hantkenina nanggulanensis	(5)*1						(5)			ML
Hantkenina primitiva	(5)						(5)		(5)*2	ML
Cribrohantkenina inflata	(5)						(5)			ML
Pseudohastigerina micra	(5)						(5)			ML
P. naguewichiensis	(5)						(5)			ML
Catapsydrax unicavus			(8)	(2,4,5,8)	(7)	(5)				ST
Catapsydrax dissimilis				(2,5,8)	(7)	(5)		(6)*3		ST
Subbotina angiporoides			(4)(5)		(5)	(5)			(8*4)	T
Subbotina linaperta			(4)(5)			(5)				T
Subbotina eocaena			(1)	(3,5)			(5)			T
Subbotina corpulenta				(5)			(5)			T
Subbotina gortanii				(5)			(5)			T
Subbotina hagni							(5)			T
Subbotina yeguaensis					(5)					T
Subbotina projecta			(8)				(5)			T
Dentoglobigerina galavisi			(3)(4)	(5,8)			(5)			T
Dentoglobigerina tripartita				(5)			(5)			T
D. pseudovenezuelana			(8)							T
D. venezuelana		(8)*5	(3)	(8)		(6)	(8)		(8)*6	T
Globoturborotalita ouachitaensis	(4,5)						(5)			ML
Chiloguembelina cubensis	(5)		(1)			(5)			(5)*7	ML
Streptochilus martini						(5)			(5)*7	ML
Chiloguembelina ototara	(5)					(5)			(5)*7	ML
Paragloborotalia nana				(4,5)			(5)			T
Globigerina officinalis	(3,5)	(3,5)					(5)			ML
Ciperoella anguliofficinalis	(5)	(2)					(5,6)			ML
Globoturborotalita martini	(5)						(5,6)			ML
Globorotaloides eovariabilis				(8)	(5)*8	(5)		(8)		ST
Globorotaloides quadrocameratus				(8)	(5)*8	(5)		(8)		ST
Paragloborotalia griffinoides				(5)				(5)	(5)*9	T
Turborotalita praequinqueloba							(5)			Others
Tenuitella gemma	(8)*10	(8)*10				(5)		(8)	(5)*7	ML
Tenuitella praegemma				(5)	(5)			(8)	(5)*7*11	ML
Tenuitella patefacta						(5)		(8)	(5)*7	ML
Acarinina collactea						(5)				ML
Dipsidripella danvillensis				(8)*12		(5)			(5)*7	ST

During the Eocene stratified ocean scenario, radiolaria Si source was the aphotic zone (Moore et al., 2015; Olivarez Lyle & Lyle, 2006). At the EOB, diatoms may have started to win the competition for dissolved silica over radiolaria in the photic zone, as diatoms are a very efficient Si cycling group (Harper & Knoll, 1975; Lazarus et al., 2009).

3.6. Factor Analysis

Using Statistica 6.0 © software, a Q mode Factor Analysis (FA) on the log-transformed relative abundances of each of the three microfossil groups was performed. This powerful data reduction and structure detection method allowed us to (1) identify inter-taxa abundance relationships within and between samples that permit them to be arranged into statistically coherent groups (factors) and (2) observe which taxa dominate in each Factor (F). See Appendix III for details on statistical approach. To extrapolate the environmental and oceanographic significance of the main factors, previously published assignments to paleoecological eco-groups were taken into account (see 'Microfossil eco-groups' section above and Tables 2 and 3), together with the new oxygen and carbon isotope analyses presented below.

4. Results

4.1. Microfossil preservation

SEM imaging (Plate 1) revealed high quality preservation of test calcite (glassy) as indicated by smooth surface and preservation of ultrastructures, including pores (2c), keel architecture (5d), pustules and aperture features (5e) with minimal/no secondary recrystallization. This is the case for most samples, although some samples show mild surface etching implying some weak dissolution in some specimens (2c). This confirms initial light microscope observations and verifies the reliability of isotopic analysis performed on Site 612 EOT foraminiferal material to capture near original ocean chemistry and environmental conditions (Sexton et al., 2006).

4.2. Biostratigraphy and age model

Age modelling was based on biostratigraphic data (Table 4). An important horizon for EOT stratigraphy is the extinction of *Hantkenina* spp., which is used to denote the E/O boundary worldwide (Premoli Silva & Jenkins, 1993). As shown previously (Coxall et al., 2018), all five hantkeninid morphospecies (*H. primitiva*, *H. compressa*, *H. alabamensis*, *H. nanggulanensis*, and *Cribrohantkenina inflata*) disappear abruptly at Site 612 in sample 16X-CC, 10-12 cm (136.025 mbsf). This occurs simultaneously with the dwarfing (i.e. sudden reduction in size) of *Pseudohastigerina* (observed qualitatively as a shift in size fraction from > 106 µm to 63-106 µm) (Table S3 in Coxall et al., 2018) (Table 4, Fig. 3) and the extinction of the *Turborotalia cerroazulensis* group. The age model used here is very similar to that used by Coxall et al. (2018), but differs through small revisions in the depths of the highest occurrence of *Discoaster*

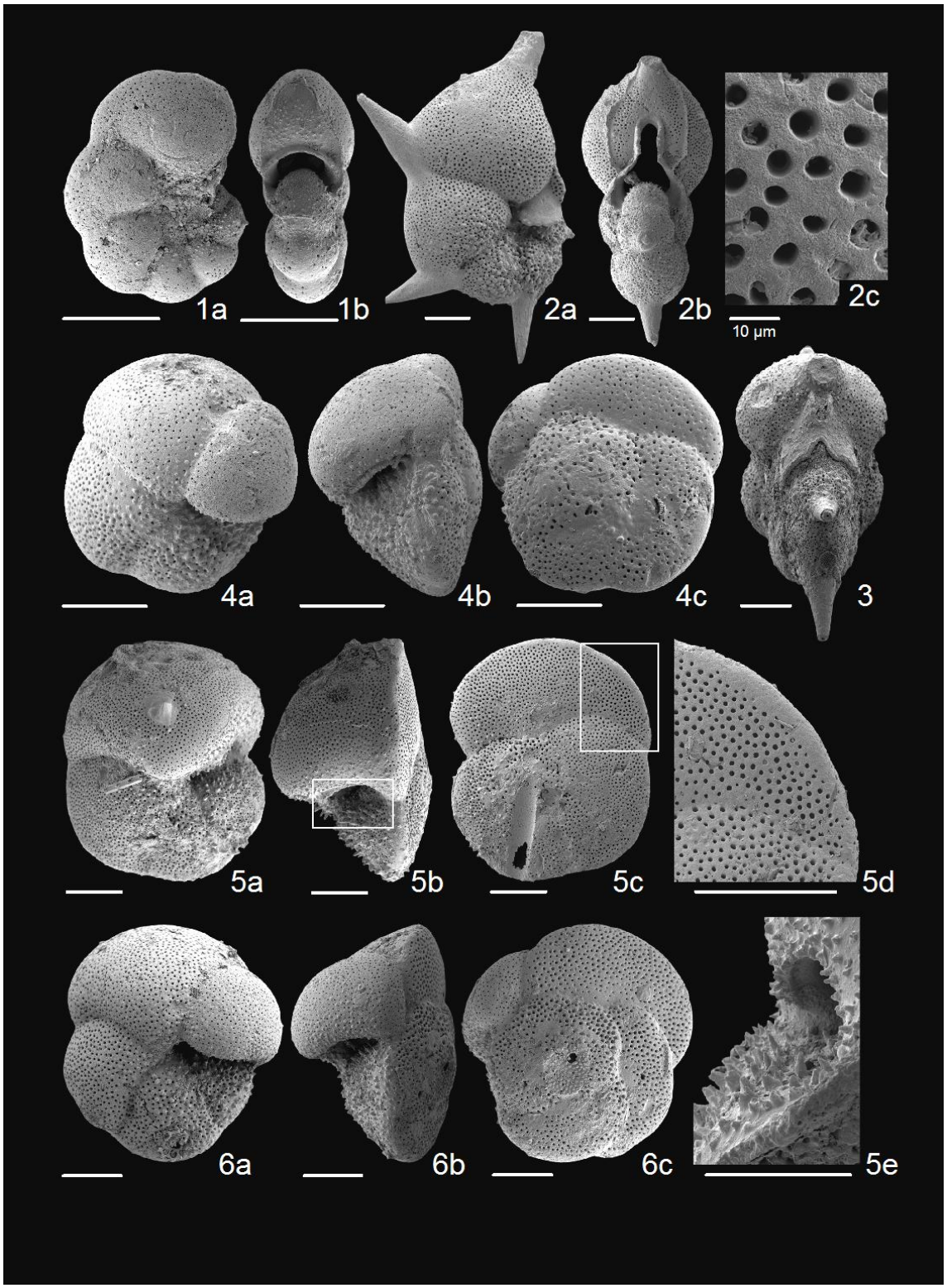

Plate 1. SEM micrographs of biostratigraphically useful planktic foraminiferal species from DSDP Site 612, Zone E15/16. Scale bars indicate 100 µm. **1a-b** *Pseudohastigerina micra* (Cole, 1927). Umbilical and edge views (same specimen). Sample 612-17X-2, 47-49 cm. **2a-c** *Hantkenina alabamensis* (Cushman, 1925). Umbilical and edge views and wall close-up. **2a**, sample 612-16X-CC, 10-12 cm. **2b-c**, sample 612-17X-1, 0-2 cm. **3** *Cribrohantkenina inflata* (Howe, 1928). Umbilical and edge views. Sample 612-17X-1, 39-41 cm. **4a-c** *Turborotalia cerroazulensis* (Cole, 1928). Umbilical, edge and spiral views (same specimen). Sample 612-16X-CC, 10-12 cm. **5a-e** *Turborotalia cunialensis* (Toumarkine and Bolli, 1970). Umbilical, edge and spiral views and close-ups showing the keel and the umbilical aperture with spines (a-d same specimen). Sample 612-17X-1, 20-22 cm. **6a-c** *Turborotalia cocoaensis* (Cushman, 1928). Umbilical, edge and spiral views (same specimen). Sample 612-17X-1, 59-61 cm.

saipanensis and *D. barbadiensis* and the use of a 'Maximum age envelope' for the early Oligocene based on the presence of *P. micra* in the uppermost Oligocene sample (must be older than the calibrated extinction of *P. micra* at 32.0 Ma; Berggren et al., 1995). In the studied interval the following biozones were recognized: planktic foraminifera E15/E16 (Berggren & Pearson, 2005), calcareous nannofossil CNE19/CNE20 O1 (Agnini et al., 2014) and radiolarian RP19 and RP20 (Kamikuri & Wade, 2012) were recognized. Ages reported in the text are based on the chronology of CK95 (while the tables also include ages in GPTS 2012; Gradstein et al., 2012). Core recovery is 100% or more in the sampled cores (Cores 612-16X and 612-17X). The age model reveals moderately high oceanic sedimentation rates of 20.5-53.75 m/my during the late Eocene interval studied. Close to the E/O boundary two closely spaced hiatuses are recognized, one at 136.375 mbsf and second at 136.025 mbsf (Table 4, Fig. 3). The first lasts

Table 4. Microfossil datum table used for age modelling of the Eocene-Oligocene section of Site 612 revised here after Bordiga et al. (2017) and Coxall et al. (2018). Note that recent biostratigraphic observations (refs, 1-3) provide important new constraints on the position of the E/O boundary compared to Poag et al. (1987). Detailed bioevents of planktic foraminifera (*), calcareous nannofossils (x) and radiolaria (+), and interpreted hiatuses with depth and age. Datums in bold were used as age-depth tie points for the age-model. Midpoint depth corresponds to the depth between the sample of the last occurrence (of the species) and the consecutive sample in which the species was absent. T = Top. B = Base. H= *Hantkenina*. D= *Discoaster*. G= *Globigerinatheka*. Tu= *Turborotalia*. Th=*Thyrsocyrtis*. I= *Isthmolithus*. 1, This study; 2, Coxall et al. (2018); 3, Bordiga et al. (2017); 4, Miller et al. (1991); 5, Poag et al. (1987); 6, Miller & Hart, (1987).

Type	Datum / Event		Used in this study		Shipboard Scientific Party[5]	Age (Ma)		Reference
			Interval (core-section, cm)	Midpoint depth (mbsf)	Average depth (mbsf)	CK95	GTS12	
T	***P. micra***	*	> 16X-6, 127-129	135.47	-	32	32.1	1
T	***Hantkenina* spp.**	*	16X-CC, 10-12	136.03		33.7	33.89	2
Size reduction	*Pseudohastigerina* dwarfing	*	16X-CC, 10-12	136.03	142.42			2
T	***Tu. cerroazulensis* group**	*	16X-CC, 10-12	136.03		33.8	34.03	2
T	***D. saipanensis***	x	17X-1, 20-22	136.38	136.4	34.2	34.44	3
T	*D. barbadiensis*	x	17X-1, 20-22	136.38	136.4	34.38	34.77	3
T	***Th. bromia***	+	18X-3, 110-113	148.3	148.3	35.09	35.44	4
T	***G. semiinvoluta***	*	19X-4, 50-51	160	160	35.3	35.66	4
T	***Th. rhizodon***	+	19X-CC	163.5	163.5	35.43	35.79	4
T	***Th. triacantha***	+	21X-1, 119-112	174.75	174.75	35.99	36.34	4
Bc	*I. recurvus*	x	21X-5, 111	181.3	181.37	36.73	36.84	5
	Hiatus 3 (H3)			136.03	-	33.86-33.67		1
	Hiatus 2 (H2)			136.38	136.4	34.87-34.15		4, 6
	Hiatus 1 (H1)			181.3	181.37	36.73-36.3		4, 6

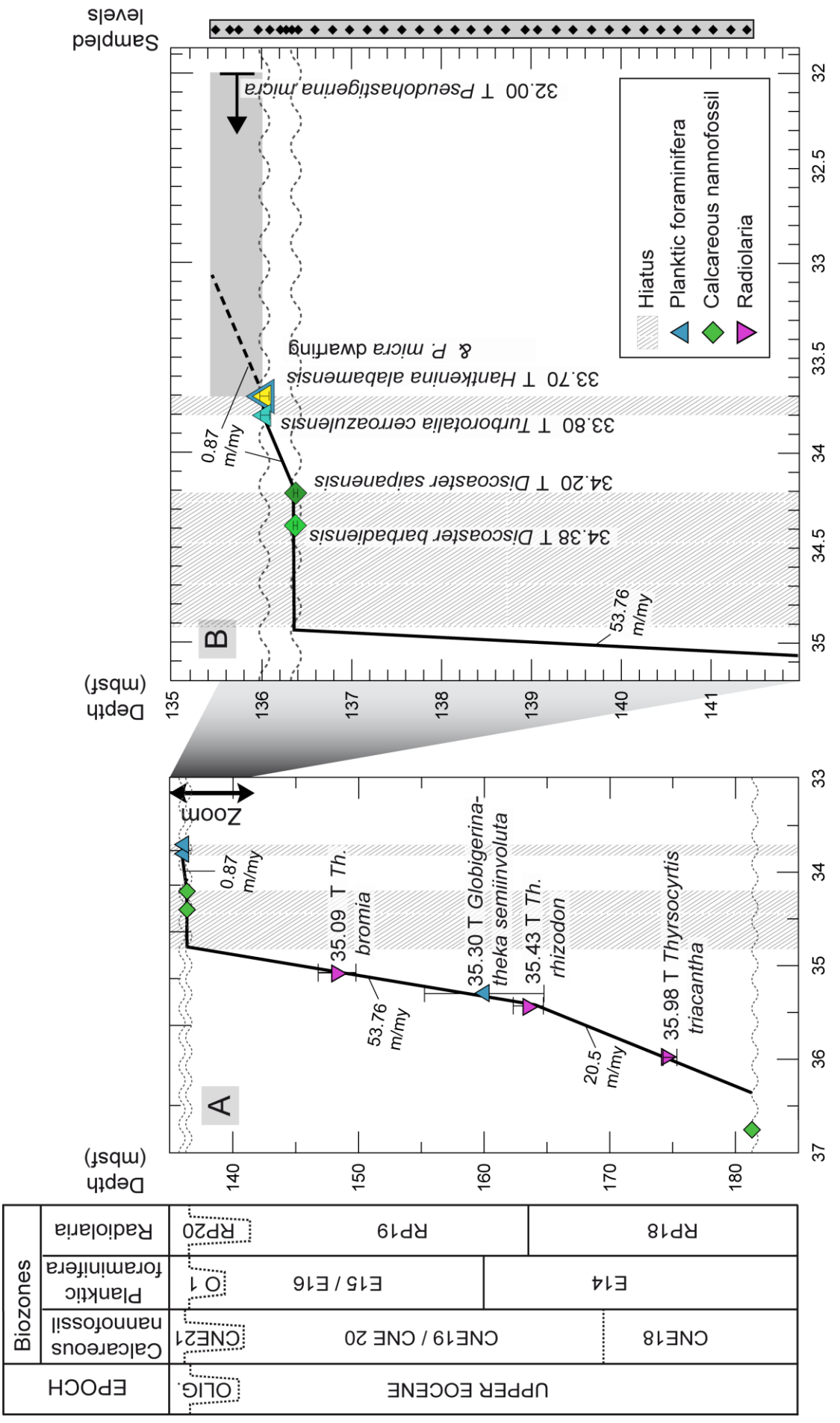

Figure 3. DSDP Site 612 age-depth plot (solid line) and associated sedimentation rates (m/my), based on biostratigraphic datums (see Table 4, ages plotted in Cande & Kent, (1995), improved after Bordiga et al. (2017); Coxall et al. (2018); Miller & Hart, (1987); Miller & Katz, (1987). n = 35 samples. Expanded (A) and magnified (B). "Zoom" arrow identifies the interval magnified in (b) in which the new multiproxy study was performed. Wavy lines indicate unconformities and associated hiatuses (intervals dashed with diagonal lines). Biozonations with calcareous nannofossils (Agnini et al., 2014), planktic foraminifera (Berggren & Pearson, 2005) and radiolaria (Kamikuri & Wade, 2012). Core recovery = 100%. Gray rectangle shows the potential area of T *Pseudohastigerina micra*.

~0.72 Myrs. The duration of the second is uncertain due to the lack of biostratigraphic constraints in the early Oligocene. A short interval (0.35 m) of condensed (estimated sedimentation rate of 0.875 m/my) but apparently coherent sediments containing *Hantkenina, T. cerroazulensis* and 'large' (i.e. > 106 µm) *P. micra* exists between the hiatuses. This observation is the reason to identify two rather than one hiatuses, as described previously (Miller & Hart, 1987). A deeper hiatus has been recognized previously at 181.3 mbsf (Miller et al., 1991; Miller & Hart, 1987). This appears to truncate the *I. recurvus* calcareous nannofossil datum, which is thus, not used as a constraint in the lower portion of the age model (Fig. 3). Because of the large differences in sedimentation rate in the lower compared to upper part of the section, the various proxy data sets here reported were first plotted in the depth domain, with an analysis in the age domain later when synthesizing the records.

4.3. Benthic and planktic foraminiferal oxygen and carbon stable isotopes from DSDP Site 612

New foraminiferal stable-isotope measurements (118) provide three monogeneric planktic records (six species) and one benthic record (combination of *Cibicidoides* spp. and *Hanzawaia ammophila*). The data are here presented with previously published data from Site 612 (Coxall et al., 2018), including previously published late Eocene benthic data that provide important broader context to the paleoceanographic evolution (35.0-36.3 Ma; Miller et al., 1991; Pusz et al., 2009), (Figure 4.; Appendix IV. Tables l and m). Due to higher sedimentation rates below 145 mbsf (53.76 m/my compared with 0.87 m/my calculated here, Fig. 3) the graph axis is broken at 141 mbsf and switches to a different scale.

Stable isotope series show clear taxon-specific separation throughout the studied interval. For the benthic isotopic record, a combination of 2 different species was used, reflecting the availability of the different taxa at Site 612, i.e. common *H. ammophila* compared to less common *Cibicidoides* spp. After experimentation we found that *H. ammophila* $\delta^{18}O$ and $\delta^{13}C$ compared well to raw *Cibicidoides* spp values,

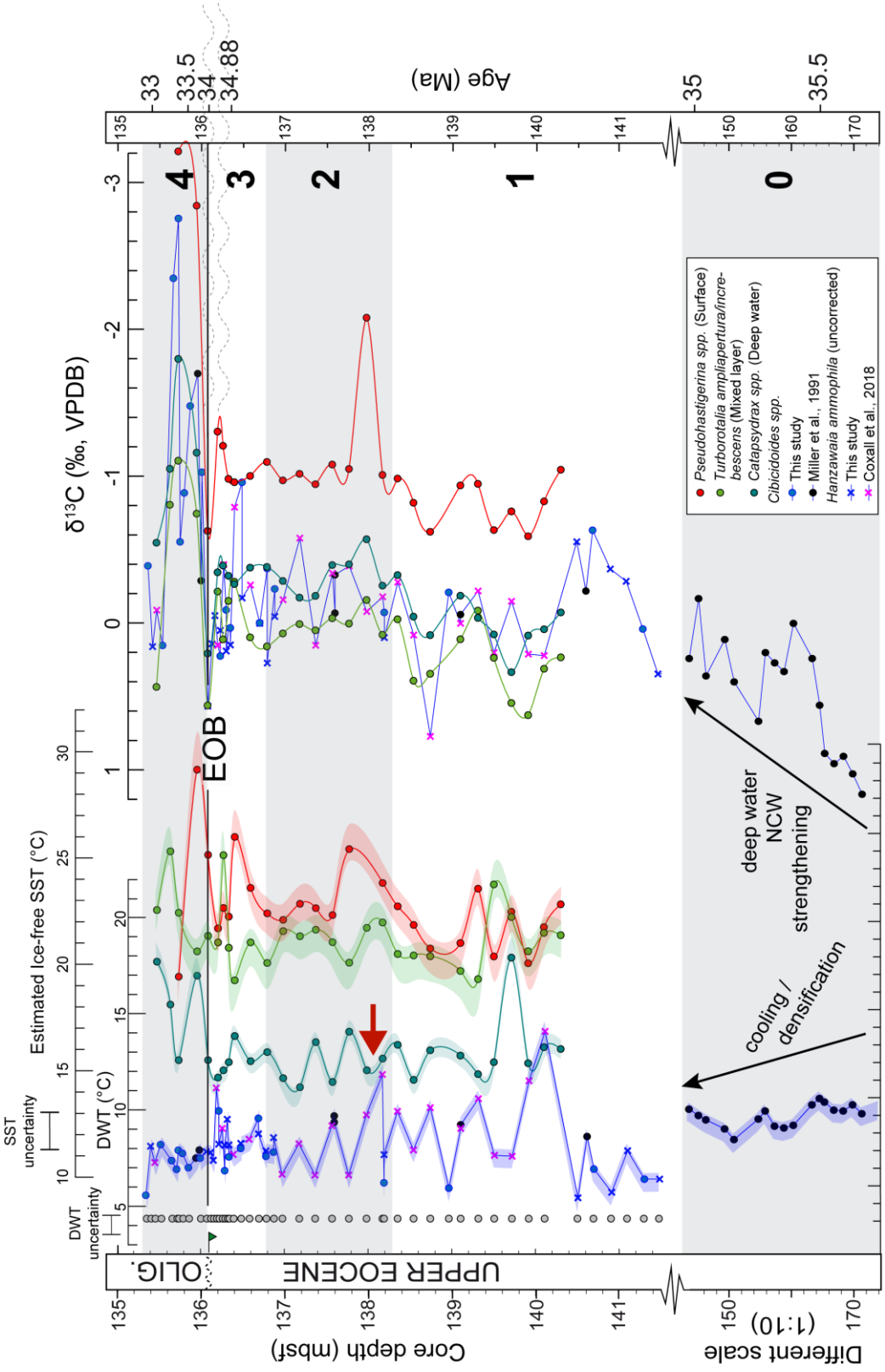

Figure 4. Stable isotope (δ18O and δ13C) records of surface, mixed layer, thermocline and benthic foraminifera through the EOT of Site 612 and estimated paleotemperatures. EOB=Eocene/Oligocene Boundary, as identified by the extinction of Hantkenina spp. and synchronous dwarfing of Pseudohastigerina micra at 136.05 mbsf, as determined in this study. Estimated ice-free sea-surface (SST) and deep water paleotemperatures (DWT) using the equations of Kim and O'Neil. (1997) and Lynch-Stieglitz et al. (1999) respectively, envelopes calculated after multiple δ18OSW values (Table 1). Note that Oligocene paleotemperatures were estimated with an ice-free δ18OSW. Bold numbers in the right side indicate the identified oceanographic phases. Red arrow indicates the timing of the low-nutrient NCW (Northern Component Water) pulse peak (Coxall et al., 2018). Cibicidoides spp. data from: (1) this study; (2) Coxall et al. (2018); (3) Miller et al. (1991) and Pusz et al. (2009). Age (Ma) according to CK95 timescale. Note that the age axis is not to scale but shows relative age tie points based on biostratigraphic datum events. Grey diamonds in the left represent sampled levels.

including previous data (Miller et al., 1991; Pusz et al., 2009). Therefore we do not apply the habitat adjustment factor suggested by (Katz et al., 2003).

Benthic $\delta^{18}O$ record shows a long-term trend to increasing values up-section and with significant changes in amplitude variability along the way (Fig. 3). The data run in different labs (Miller et al., 1991; Pusz et al., 2009) compared to Coxall et al. (2018) and this study are coherent, including exact reproduction of 0.66 ‰ value at 136.01 and 135.96 mbsf between this and Miller et al. (1991) data sets, and very similar values at 137.6 and 137.57 mbsf (0.26; 0.3‰) and 139.1 mbsf (0.29; 0.33‰) between Coxall et al. (2018) and Miller et al. (1991) data sets. This gives confidence that the data sets can be integrated and interpreted together. At the base of the studied interval (ca. 150-170 mbsf) values range between 0 to 0.5 ‰ and are relatively stable. From ~141.5 mbsf (i.e. from where the present sampling begins) to ca. 140.5 mbsf values are higher 0.5-1.0 ‰ and much more variable, with amplitude changes on the order of 0.75-1.0 ‰. This high $\delta^{18}O$ variability continues to ~136.8 mbsf but with on average lower values of 0-0.5 ‰, with an apparent more extreme excursion (described by only 2 data points) to a minimum of -1.5 ‰ at ~142 mbsf. Values return to a more stable pattern above 136.8 mbsf with lower amplitude variability. A second late Eocene negative $\delta^{18}O$ excursion on the order of 1 ‰ and decreasing to -0.45 ‰, occurs at ca. 136.3 mbsf.

Across the EOB there is minimal benthic $\delta^{18}O$ change, although values are slightly higher above the EOB by ~0.6 ‰. For both $\delta^{18}O$ and $\delta^{13}C$, and planktics as well as benthics, the systematic variability is probably a result of changes on orbital cycles, which is mostly under sampled in the study. The higher resolution sampling close to the EOT better captures some of the cyclic change, yet at the same time supports the idea that the final phase of the late Eocene and the earliest Oligocene was isotopically more stable, especially with respect to benthic foraminifera.

Planktic data exhibit separations between taxa and the benthic record involving a trend of increasing foraminiferal $\delta^{18}O$ and decreasing $\delta^{13}C$ with increasing inferred paleodepth habitat

(Figure 4). For $\delta^{18}O$, the shallow mixed layer dweller *Pseudohastigerina* shows the isotopically lowest values (an average of -2.18 ‰), followed by the deeper mixed layer dweller *T. ampliapertura/increbescens* (-1.85 ‰), sub-thermocline dweller *Catapsydrax* (-0.56 ‰) and benthic *Cibicidoides* spp. (0.3 ‰) showing higher values. For $\delta^{13}C$, *T. ampliapertura/increbescens* displays the highest values (0.02 ‰), *Catapsydrax* shows lower values (-0.32 ‰) and benthic *Cibicidoides* spp. (0.08 ‰) lies in between those records. *Pseudohastigerina* is significantly offset from the rest of the records exhibiting the lowest $\delta^{13}C$ values (-1.14 ‰). The interspecies offsets remain fairly consistent through the studied section, apart from during negative $\delta^{18}O$ excursions when there tends to be some convergence of planktic and benthic values.

In terms of the down core planktic variability, Late Eocene *Catapsydrax* $\delta^{18}O$ typically ranges between -0.2 to -0.8 ‰ and is generally negatively offset from the benthic $\delta^{18}O$ by ca 0.5-1 ‰. The exception is at the base of the *Catapsydrax record* (138.17-140.30 mbsf) and 136.2 mbsf, where *Catapsydrax* $\delta^{18}O$ is higher than, or similar to the benthic values. A late Eocene minimum of ca. -1.6 ‰ occurs at 139.71 mbsf. Following the EOB (136.4 mbsf) *Catapsydrax* $\delta^{18}O$ is lower, with three of the 4 samples registering values between -1.0 to -2.0 ‰ (standard deviation increases from 0.1 down core to 0.75). *Turborotalia ampliapertura/increbescens* and *Pseudohastigerina* records generally co-vary up-core and show a systematic excursion to lower values in the early Oligocene. Prior to and after the EOB the curves show high variability, with negative peaks detectable in both taxa (1.5 and 0.9 ‰ decrease at 136.3 and 136.4 mbsf respectively) following the *Catapsydrax* records and showing excursions to lower $\delta^{18}O$, although with phase differences between taxa. *Pseudohastigerina* abundance was too low to generate analyses in the youngest early Oligocene samples.

Planktic $\delta^{13}C$ also shows rhythmic variability and several excursions similar to $\delta^{18}O$ but with some differences. A strong negative excursion is seen in benthic and all planktic species $\delta^{13}C$ in the early Oligocene, with values decreasing by as much as 2.5 ‰ (benthics) and 1.2 ‰ in

Pseudohastigerina (minima of -2.8 and -3.2 ‰ respectively) before returning to pre-EOB values by 135.54 mbsf.

4.3.1. Paleotemperature estimates

Foraminiferal $\delta^{18}O$ paleotemperature estimates, calculated assuming negligible salinity and ice-volume fluctuations (Table 1, Figure 5; Appendix IV. Table b), show late Eocene (35-34 Ma) averages of 22.6°C for the upper mixed layer (*Pseudohastigerina*), 21°C for the lower mixed layer (*T. ampliapertura and T. increbescens)*, 12.9°C for sub-thermocline waters (*Catapsydrax*) and 9.4°C for bottom waters (benthics) (Figure 4). From 36-33 Ma, bottom waters show cooling from a maximum of 11°C to 5-7°C in the basal Oligocene at ~33 Ma, comprising an estimated net EOT

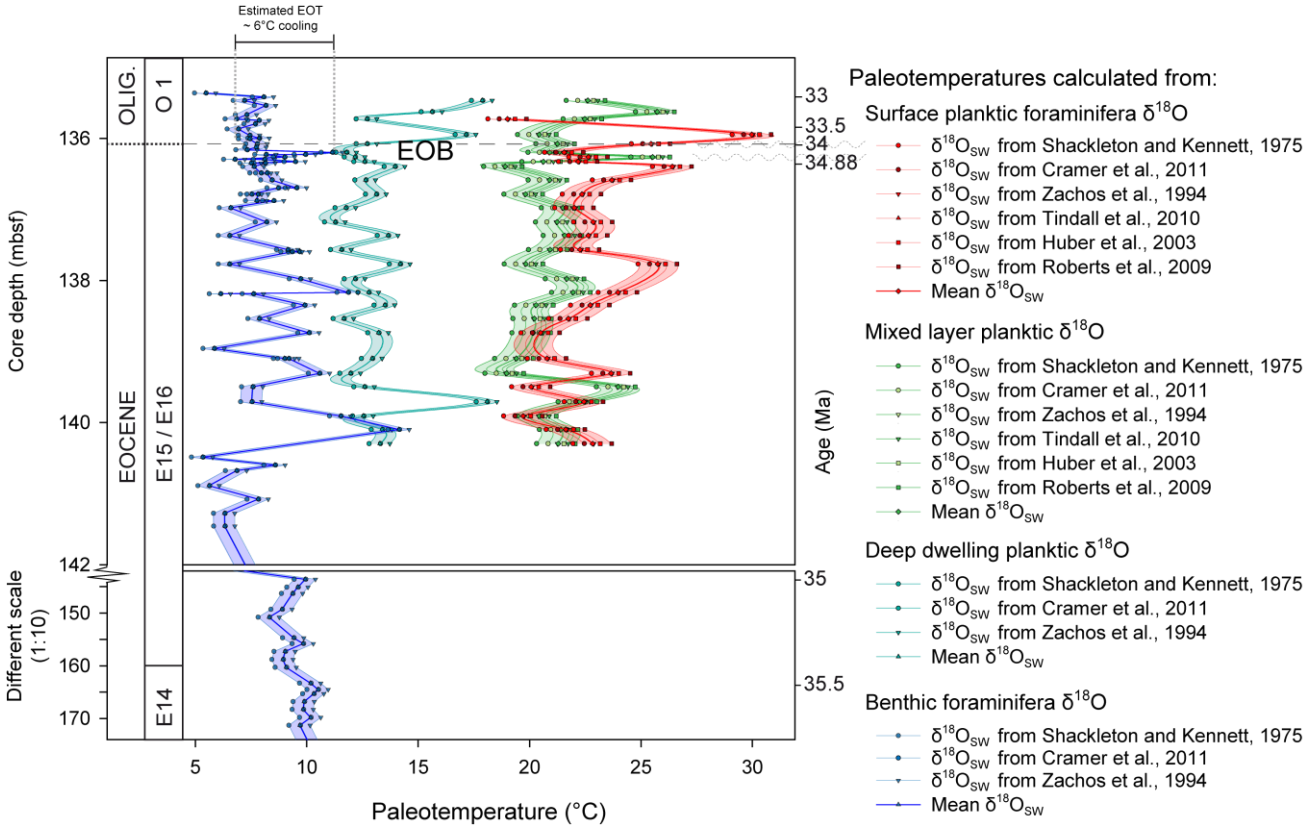

Figure 4. Site 612 $\delta^{18}O$ paleotemperatures and uncertainty envelopes for surface (*Pseudohastigerina* spp.), mixed layer (*Turborotalia ampliapertura/increbescens*), subthermocline (*Catapsydrax* spp.) and bottom waters (*Hanzawaia ammophila* and *Cibicidoides* spp. compilation) calculated using multiple $\delta^{18}O_{sw}$ values (Table 1). Lines represent calculated paleotemperatures with different $\delta^{18}O_{sw}$ values, thick lines represent mean paleotemperatures and shaded areas, the envelope of potential paleotemperatures. In the benthic record and across the EOT, the shift between vertical dashed lines represents the estimated ~6°C cooling. Interval from 174 to 142 mbsf plotted in a different scale (1:10) to show the general trend of previous paleotemperatures, creating an artificial space between the two series. Epoch and planktic foraminifera biozones stated in the left, age tie points in the right, and gray dashed line marking the EOB. Age (Ma) according to CK95 timescale. Note that the age axis is not to scale but shows relative age tie points based on biostratigraphic datum events.

benthic cooling of maximum 6°C on the New Jersey margin (see annotation on Figure 5). The high $\delta^{18}O$ variability between 136.8 to 141.5 mbsf implies equally high bottom water temperature variability with a cooling to a minimum of 4°C at 140.3 mbsf, warming to a maximum of 17°C at ~140.1 mbsf.

The late Eocene planktic $\delta^{18}O$ temperatures imply warm stratified upper ocean conditions with probable cyclic variability on the order of 3-5°C, that is largely isolated and varying independently from the seafloor. If the early Oligocene $\delta^{18}O$ increase seen in all planktic species around 135.5-136 mbsf, is related to increased temperature, then this would equate to as much as 6°C warming (maximum 29°C) of the mixed layer in the basal Oligocene. Both mixed layer and SST show a maximum during or after the EOB.

4.4. Microfossil assemblages, eco-groups and factor analysis

Site 612 raw microfossil counts (Appendix IV. Tables d1, e1, f1 and g) were transformed into relative abundances (number of specimens per gram of dry bulk, N g-1). Abundance patterns for selected species are shown in Figure 6; for planktic foraminifera, species showing high scores in factor analysis were selected (Table 5) and for benthic foraminifera and calcareous nannofossils, the most significant species in terms of abundance or paleoecological affinities. Late Eocene microfossil assemblages and categorized eco-groups display both long-term and transient changes across the investigated interval (Figure 7).

4.4.1. Benthic foraminiferal assemblages

Starting with benthic foraminifera, over 100 species were recognized throughout the entire record (Figure 6; census in Appendix IV, table e1). The assemblages can be described as moderately diverse (Fisher's α varies from 6 to 18, Figure 7) with relatively high absolute

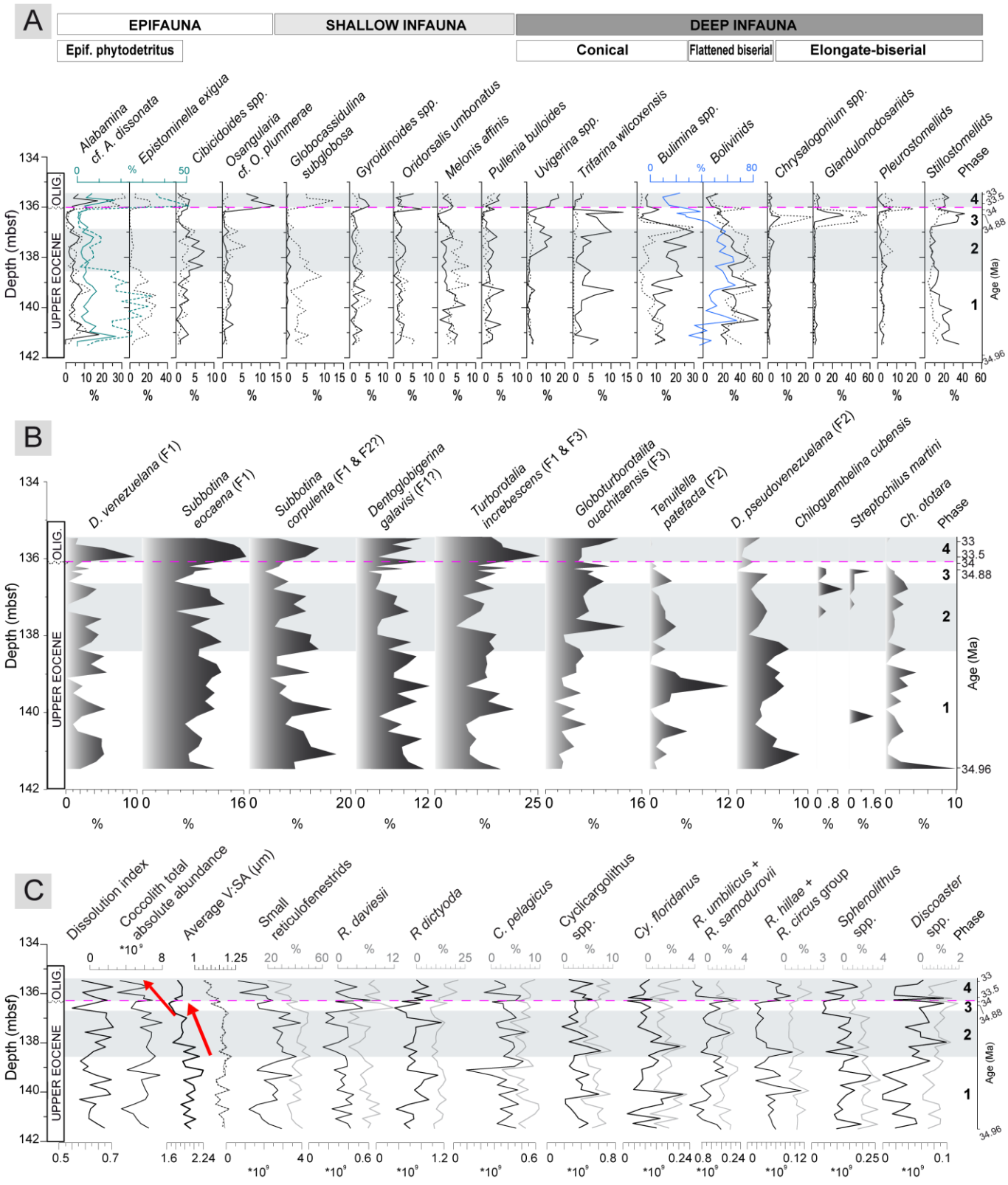

Figure 5. Relative abundances of selected species of (a) benthic foraminifera (%), (b) planktic foraminifera (%) and (c) calcareous nannofossil (Ng^{-1}) plotted against depth (mbsf). Bold numbers in the right indicate the oceanographic phase. Pink dashed line corresponds to EOB. (a) In-box, species ecological preferences designations. Solid lines correspond to abundances in the >106 µm fraction and dashed lines to those in >63-106 µm. In dark green, epifaunal taxa Σ; in dark blue, deep infaunal conical and flattened biserial Σ (high food supply). (b) In brackets, the Factor they score in. (c) large Reticulofenestra are presented by bold lines, alkenone-producer taxa by solid lines and placolith-bearing taxa by dashed lines. Bars are out of scale for (a) and (b). Age tie points provided in the right with age (Ma) according to CK95 timescale. Note that the age axis is not to scale but shows relative age tie points based on biostratigraphic datum events.

Table 5. Factor analysis of each micropaleontological group showing selected Factors, corresponding highest scoring species and associated paleoecological meaning. Expl. Var. = explained variance; Ecol. meaning= species ecological affinity; F1=Factor 1; BF= Benthic foraminifera; PF= Planktic foraminifera; CN= Calcareous nannofossils.

BF	$F1_{BF}$		$F2_{BF}$		$F3_{BF}$			Tot.
Expl.Var.	46%		17%		13%			75%
Scoring species	*Brizalina tectiformis*	*Bulimina alazanensis*	*Strictocostella* spp.	*Glandulo-nodosariidae*	*Uvigerina galloway*	*Osangularia cf. plummerae*	*Siphonodosaria* spp.	
Score	2.88	2.00	2.73	1.65	1.81	1.73	1.68	
Ecol. meaning	Need high sustained O.M.		Elongate group (elongated deep infaunal taxa)		Mostly Oligotrophic & linked to seasonal food pulses			

PF	$F1_{PF}$			$F2_{PF}$		$F3_{PF}$		Tot.
Expl.Var.	38%			22%		15%		75%
Scoring species	*Dentoglobigerina venezuelana*	*Subbotina corpulenta*	*Subbotina eocaena*	*Tenuitella patefacta*	*Dentoglobigerina pseudovenezuelana*	*Globoturborotalita ouachitaensis*	*Turborotalia increbescens*	
Score	1.79	1.16	1.14	1.86	1.32	2.00	1.38	
Ecol. meaning	Open ocean thermocline			Surface -opportunistic	Open ocean thermocline (?)	Open ocean Mixed Layer		

CN	$F1_{CN}$		$F2_{CN}$		$F3_{CN}$		Tot.
Expl.Var.	33%		28%		23%		84%
Scoring species	*Reticulofenestra dictyoda*	*Sphenolithus tribulosus*	*Reticulofenestra scrippsae*	*Dictyococcites daviesii*	*Pontosphaera* spp.	*Clausicoccus subdistichus*	
Score	1.97	1.61	1.78	1.75	1.60	1.42	
Ecol. meaning	?		*R. daviesii*: cosmopolitan		*Pontosphaera* spp. related to warm water conditions		

abundances in both >106 µm and 63-106 µm fractions (80-2274 N g^{-1} and 135-3048 N g^{-1} respectively). In this doctoral thesis, the down core changes in terms of the three a priori determined benthic eco-groups are described. Deep-infaunal morphogroups (*sensu* Corliss & Chen, 1988) constitute most of the assemblage (~75%); flattened-biserial taxa show highest abundance (*Brizalina*, *Bolivina* and *Bolivinoides*), followed by conical (*Bulimina*, *Uvigerina* and *Trifarina*) and elongate cylindrical genera (*Siphonodosaria*, *Strictocostella*, and *Orthomorphina*), the latter belonging to the Elongate Group (*sensu* Ortiz & Kaminski, 2012) (Figure 6, Table 2). Other significant components of the benthic assemblage are the epifaunal phytodetritus species (*Alabamina cf. A. dissonata* and *Epistominella exigua*; Gooday et al., 1992 (mostly in the smaller fraction)) and the shallow-infaunal taxa (*Gyroidinoides girardanus*, *Melonis affinis*, *Pullenia bulloides* and *Oridorsalis umbonatus*) (Figure 6, Table 2).

Using apriori morphological and eco-groupings (Table 2), distinct phases and horizons were

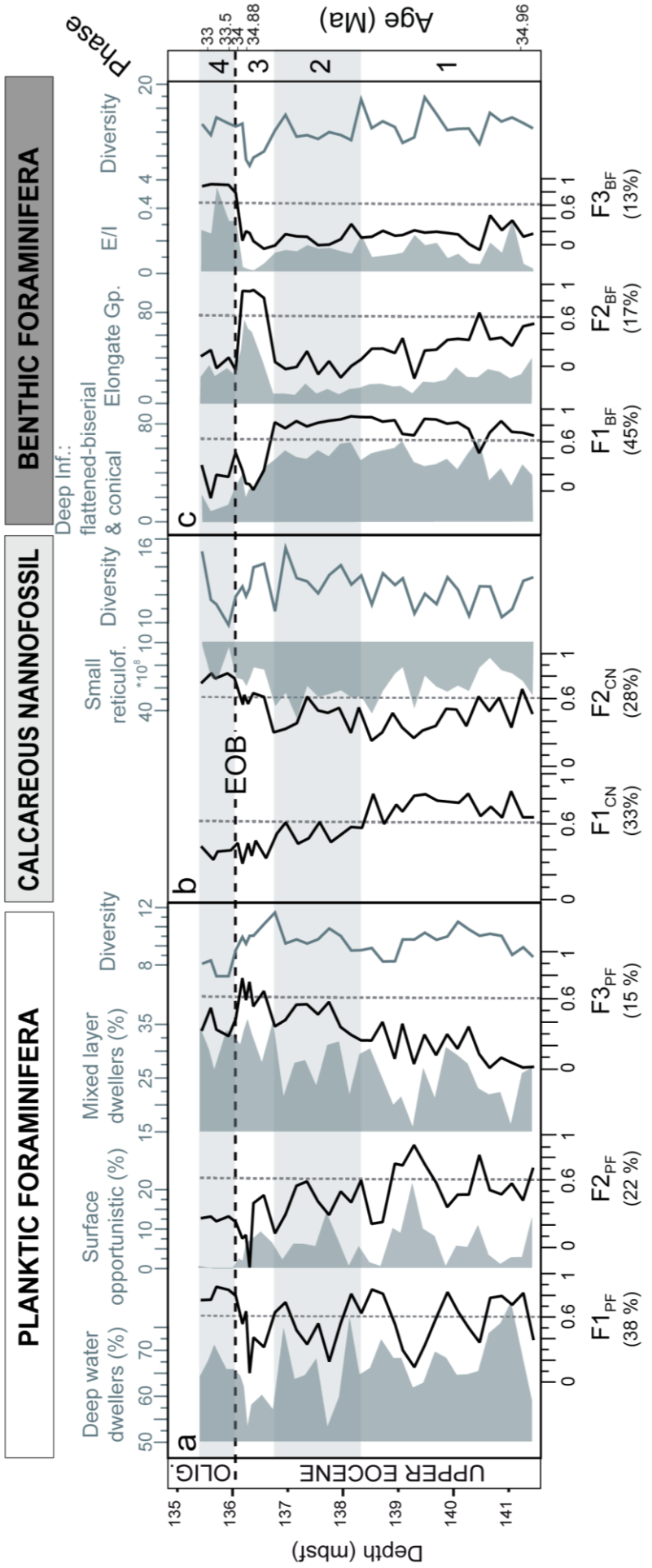

Figure 7. Diversity, ecology and statistically determined assemblage factors for the three microfossil groups through the EOT of Site 612. In each case (planktic foraminifera, calcareous nannofossils and benthic foraminifera), black lines represent the main factors, thin dashed line, diversity (Fisher's α) and grey area curves show eco-groups. Small Reticulofenestra axis is reversed to emphasize negative correlation with F2CN. Numbered intervals 1-4 to the right represent phases of biologic and oceanographic change identified in this study. See main text for definitions of the microfossil eco-groups. Age tie points provided in the right with age (Ma) according to CK95 timescale. Note that the age axis is not to scale but shows relative age tie points based on biostratigraphic datum events.

recognized as defined by dominant groups and shifts in dominance: at 138.35, 136.8 and 136.08 mbsf (Figure 7). At the base of the record (141.46-138.35 mbsf) flattened biserial taxa, part of the 'deep infaunal' group, slightly dominate (33%) (Figure 6). Towards the middle of the record (138.35-136.8 mbsf) flattened biserial taxa show a decrease, paired with a simultaneous increase of conical taxa (Figure 6). In the interval prior to the EOB (136.8-136.2 mbsf), deep infaunal taxa reach maximum abundance (95%), driven by the peak (73%) in the elongate-cylindrical taxa (Elongate Gp.), also signaled by the minimum in E/I ratio (~0%) (Figure 7). The youngest shift occurs at 136.08 mbsf and corresponds to the EOB, where a profound change is registered by all three benthic eco groups during the early basal Oligocene (136.08-135.47 mbsf): deep infaunal taxa - including Elongate Gp. -, show a rapid abundance decrease (Figure 6), concordant with a positive shift and maximum in epifaunal taxa (E/I ratio) (Figure 7), particularly epifaunal phytodetritus species (43% in the small fraction) (Figure 6). Absolute abundance of benthic foraminifera increases first at 138.35 mbsf (from an average of ~400 to 930 N g^{-1}) and has a second major increase at 136.8, reaching its maximum value later at 136.4 mbsf (930 N g^{-1}). After that it has a sharp decrease to reach the minimum value of 80 N g^{-1} just above the EOB (135.95 mbsf).

Q-mode Factor Analysis (FA) performed on benthic foraminiferal assemblages identified three main factors ($F1_{BF}$, $F2_{BF}$ and $F3_{BF}$), which explain 75% of the total variance after a maximized variance (VARIMAX) rotation (Klovan & Miesch, 1975) (45%, 17% and 13%, respectively)(Figure 7, Table 5 and Appendix IV. Table j) and similarly identify the three horizons of change (138.35, 136.8 and 136.08 mbsf). The highest scoring species in each factor define and allow us to interpret the ecological meaning of each factor, which is further explained in the discussion section.

4.4.2. Planktic foraminiferal assemblages

In total, 43 species were recorded (stratigraphic distribution of entire assemblage in Figure 8; selected species in Figure 6; full census in Appendix IV Table d), composing a moderately diverse assemblage (Fisher's α from 5 to 11, Figure 7). Tropical taxa (mixed layer and low/mid latitude species (Table 3) that go extinct in the EOB) are present prior to the EOB, and show a moderately high abundance within the total sediment content (135 to 2034 N g^{-1} in the >106 μm fraction). Thermocline dwellers (with an average relative abundance of 37.5%) constitute the largest proportion of the assemblage, followed by subthermocline dwellers (28.5%) and mixed layer dwellers (28%). The most common species are *T. increbescens* (12% average relative abundance of total assemblage), *S. eocaena* (10%), *S. corpulenta* (9%) and *D. galavisi* (7%) (Figure 7). As in many sites, *Hantkenina* spp. and *Cribrohantkenina inflata* are rare, however, all five late Eocene hantkeninid species are recorded and found to go extinct simultaneously recording the E/O boundary.

At the base of the record (141.46-136.8 mbsf), deep dwellers (belonging to the genera *Subbotina*, *Dentoglobigerina*, *Paragloborotalia* and *Catapsydrax*, and including thermocline and subthermocline habitats) dominate (~68%), showing a marked decrease prior to the EOB (57% at 136.8 mbsf) and a rapid subsequent recovery after the boundary (66% at 136.08 mbsf) (Figure 7). Mixed layer dwellers display gradual increasing abundance, from an average of 25% at the base (141.46-136.8 mbsf) to 33% prior to the EOB (136.8 to 136.2 mbsf). Surface opportunistic taxa (*Chiloguembelina* and *Tenuitella*), another significant component of the assemblage (5.5%), show high variability, peaking in the intervals where deep dwellers decrease, these two groups having a moderately good correlation (r=-0.5; all reported correlations are statistically significant; p-value < 0.003). Diversity fluctuates through the record, showing a peak prior to the EOB and a rapid negative shift after (136.08-135.47 mbsf), in an interval coinciding with the abundance peak of the most common species (Figures 6 and 7). Absolute planktic foraminiferal

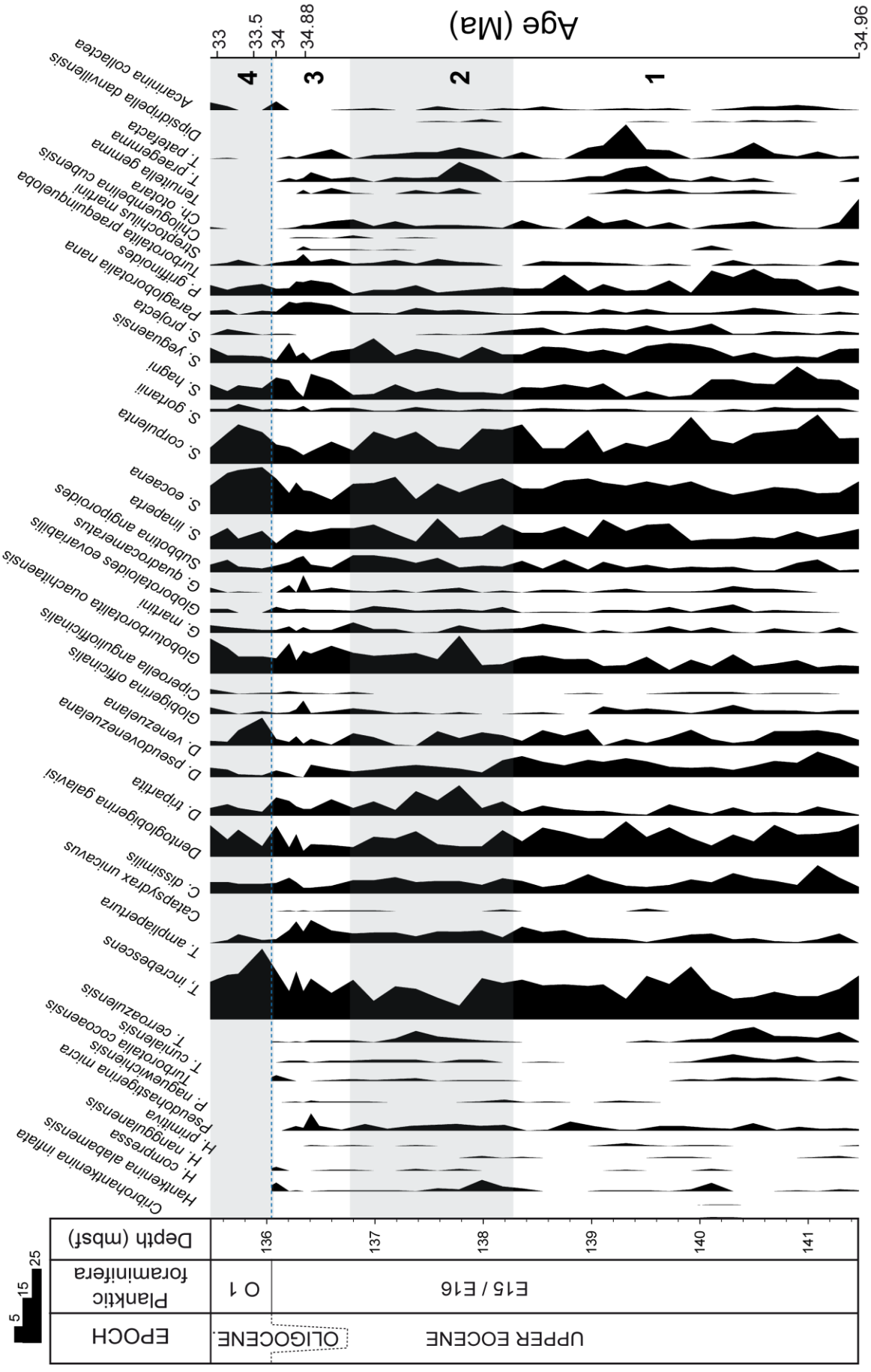

Figure 8. Site 612 stratigraphic distribution of planktic foraminifera. EOB depicted by a dashed blue line: observe the absence of the taxa in the left on top of the line, showing the extinction of taxa with tropical affinities. Reference for abundance scale, top left. Numbered intervals 1-4 to the right represent phases of biologic and oceanographic change identified in this study. Age tie points provided in the right with age (Ma) according to CK95 timescale. Note that the age axis is not to scale but shows relative age tie points based on biostratigraphic datum events.

abundance has a good visual anti-correlation with benthic $\delta^{18}O$ and is highest during three intervals (137.57 to 137.18 mbsf; 136.59 to 136.4 mbsf; and 136.265 to 136.2 mbsf). The two uppermost intervals are punctuated by two hiatuses.

Factor Analysis of the planktic foraminiferal assemblage data identified three main factors ($F1_{PF}$, $F2_{PF}$ and $F3_{PF}$), which explain 75% of the total variance after Varimax rotation (38%, 22% and 15%, respectively) (Figure 7, Table 5 and Appendix IV. Table j). These broadly correspond with the Deep water, Surface opportunistic and Mixed layer groups respectively (according to Aze et al., 2011) in terms of variability.

4.4.3. Calcareous nannofossil assemblages

A total of 80 morphospecies were recognized through the sequence, contributing to high assemblage diversity (Fisher's α from 9.8 to 15.4; Figures 6 and 7; census in Appendix IV. Table f) with high nannofossil abundance ($8*10^9$ to $3*10^9$ N g^{-1}; average $5.8*10^9$ N g^{-1}) against the background hemipelagic clay fraction (Fig. 6). Nannofossils are extremely well preserved with the exception of one sample just above the EOB (135.73 mbsf), where nannofossils are highly dissolved (planktic foraminifera show some dissolution evidence in the following sample, 135.63mbsf). This level is also characterized by high abundance of amorphous glassy fragments that are not obviously attributable to diatoms/siliceous plankton or mikrotektites, they are structureless. Prior to the EOB, absolute nannofossil abundance slightly decreases, probably due to the decrease of the most abundant taxa, the bloom associated small *Reticulofenestra* spp. (< 3 μm) (40% of total assemblage), which could be related either to reduced surface productivity or increased dissolution, affecting small coccoliths preferentially. Only in correspondence with the high dissolution interval diversity decreases significantly. The most abundant species, small *Reticulofenestra* spp. (shown in Fig. 6), dominates the assemblages together with *Reticulofenestra dictyoda* (12%). Small *Reticulofenestra* spp. is an r-selected blooming placolith (Young, 1994) that responds to nutrient enrichment with significant population growth (Hulbert

& Corwin, 1969). It is a high productivity and/or upwelling (Okada & Wells, 1997) and fertile water indicator (Bolton et al., 2010; Flores et al., 1995; Flores et al., 2000; Wells & Okada, 1996). The abundance of small *Reticulofenestra* spp. increases from 140.8 mbsf reaching over ~40% and becoming more stable in the central part (138.35 to 136.8 mbsf), then declines to ~20% prior to EOB and into the basal Oligocene. The abundance of large *Reticulofenestra dictyoda* anti-correlates with small *Reticulofenestra* spp. (r=-0.7). Similarly, V:SA (cell volume to surface area) curves for these taxa record shifts at similar cored depths as to small *Reticulofenestra* spp. and *Reticulofenestra dictyoda*: 1) large reticulofenestrids average V:SA drops from ~138.35 mbsf to prior to EOB; where 2) placolith-bearing taxa average V:SA decreases till the top of the record corresponding to the decrease of small *Reticulofenestra*. The first event is not recorded by the placolith-bearing taxa V:SA curve because the high abundance of small *Reticulofenestra* spp. compensates the loss of large ones (Fig. 6). (See Appendix V for details on the entire assemblage).

Factor Analysis was performed on the nannofossil assemblages, excluding the most dominant taxon, *Reticulofenestra spp.*, in order to extract information from the rest of the assemblage and use this taxon as an independent proxy. Two main factors were extracted ($F1_{CN}$ and $F2_{CN}$), which explained 61% of the total variance after Varimax rotation (33% and 27%, respectively) (Fig. 6, Table 5).

4.5. Siliceous microfossils and other sedimentary components

Siliceous microfossils, as seen as remains in smear-slide view (see materials and methods section) represent a relatively constant contribution to the sediments throughout the section until 136.8 mbsf, where there is a sharp temporary increase by ca. 40%, both in diatom and other siliceous plankton records curves (Figure 9; census in Appendix IV. Table g). This corresponds to the phase 3 increase in benthic foraminifera. Major variation in weight

percentage of particle-size fractions (wt%) occurs at 138.35 mbsf, where fine fraction (%FF) shows a decrease (from an average of 82 to 78 wt %) that is, in turn, mirrored by a gradual increase of %SS (~8 to 12 wt %) and coarse sand fraction (~6 to 10 wt %) (Figure 9). Prior to the EOB, at 136.8 mbsf, %FF decreases and reaches minimum values (70 wt %) before recovering, whereas the rest of the fractions increase. After the EOB, particle-size fractions show a highly fluctuating pattern. Glauconite is absent from the base to 138.35 mbsf, showing an increase to became a common content of the sediment at 136.08, prior to EOB, where it becomes frequent till the top.

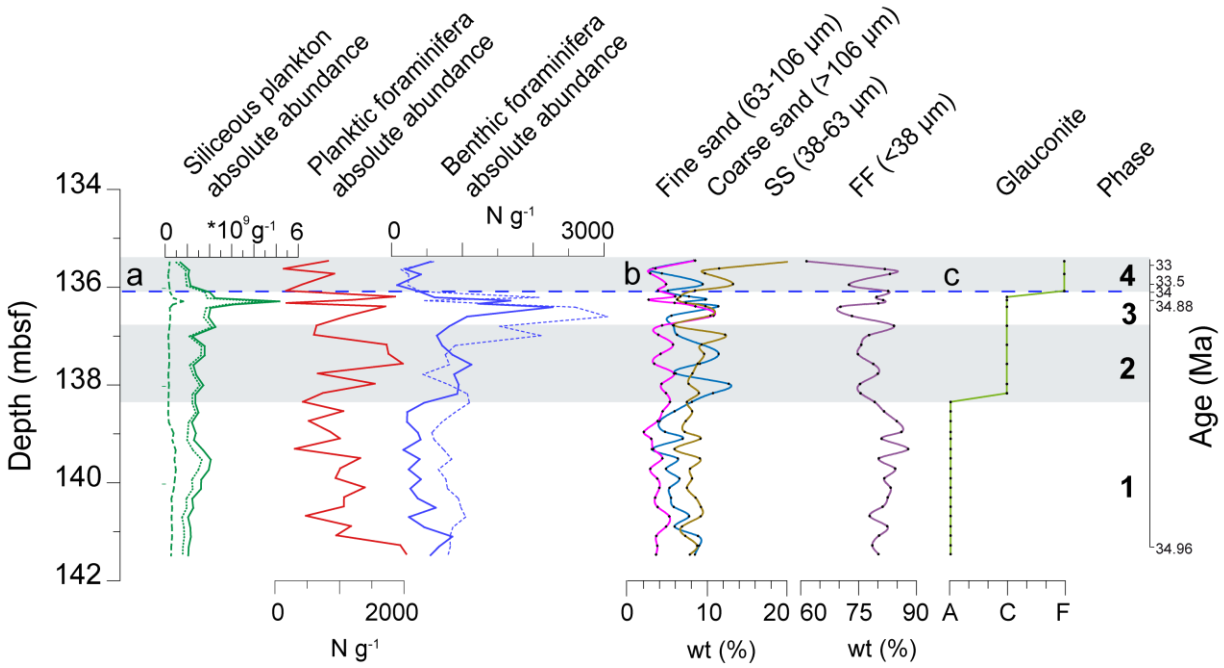

Figure 6. Other sedimentological proxies at Site 612: (a) Absolute abundances of siliceous plankton (N g^{-1}) (diatoms, green dotted line; other siliceous plankton, green dashed line; and total siliceous plankton, green bold line), planktic foraminifera (red) and benthic foraminifera (>106 µm fraction, blue bold line; >63-106 µm fraction, blue dashed line), (b) weight percentage of sediment fractions and (c) glauconite visual estimation (A=absent; C= common; F= frequent) plotted against depth (mbsf). Bold numbers in the right indicate the oceanographic phase. Blue dashed horizontal line corresponds to EOB. FF stands for fine fraction (<38µm) and SS for sortable silt (38-63 µm). Age tie points provided in the right with age (Ma) according to CK95 timescale. Note that the age axis is not to scale but shows relative age tie points based on biostratigraphic datum events.

5. Discussion

5.1. Age model and timing of western North Atlantic hiatuses

The refined biostratigraphy studies (published in Coxall et al. (2018) and updated here) allowed a different interpretation of the position of the E/O compared to the age model of Poag et al. (1987). Elsewhere the *Turborotalia cerroazulensis* group extinction (comprising *T. cerroazulensis*, *T. cocoaensis* and *T. cunialensis*) has been shown to predate the hantkeninid extinction by ~65 kyrs (Berggren, 2005; Pearson et al., 2008). That the *Hantkenina* and *Turborotalia* events coincide at Site 612 implies there is a hiatus between 33.8 and 33.7 Ma (Fig. 3), or that the extremely slow sedimentation at this level is unable to resolve these events in the sample/depth domain. On the basis of the nannofossil content, CNE20 and CNE21 biozones (Agnini et al., 2014) were recently identified by Bordiga et al. (2017), characterized by the Top of *Discoaster saipanensis/Discoaster barbadiensis* at 136.33 mbsf. The abundance of these two taxa is very sporadic and rare along the studied sequence, which creates uncertainties in the identification of the top. The close spacing (136.08-136.33 mbsf; 0.57 Myrs; CK95) between the planktic foraminiferal bioevents defining the EOB and T *D. saipanensis/D. barbadiensis* may be caused by the presence of another hiatus, as previously suggested by the Shipboard Party at the same level (Poag et al., 1987), rather than a drastic change in the sedimentation rate.

Although these uncertainties exist in the age control, and other constraints, including magnetostratigraphic data, are missing, the age model presented here sheds new light on the EOT interval at Site 612 by; (1) highlighting the complexity and incompleteness of the boundary at this location, (2) revealing a condensed interval with different sedimentation rates punctuated by two hiatuses close to the EOB and (3) identifying an intact but condensed sedimentary interval between the extinctions of *D. saipanensis* and *Hantkenina* spp. From the age model, three sedimentary regimes or intervals, punctuated and separated by two hiatuses,

are interpreted: interval (1) (34.96-34.87 Ma) with a sedimentation rate of 53.76 m/my and interval (2) (34.15-33.86 Ma) and (3) (33.67-33.06 Ma) with a sed. rate 0.87 m/my. The hiatuses have an approximate duration of 0.72 Myrs (34.87-34.15) and 0.19 Myrs (33.86-33.67) (Table 6).

Table 6. Sedimentary intervals and hiatuses depth, age and duration. *= Data from Miller et al. (1991) and Miller & Hart, (1987); new interpretation in this study.

Sedimentation interval/Event	Depth/depth range (mbsf)	Age range (Ma)(CK95)	Sedimentation rate/ hiatus duration	Source
Interval 3	136.03-135.37	33.67-32.94	0.87 m/my	This study
Hiatus 3 (H3)	136.03	33.86-33.67	0.19 Myrs	This study
Interval 2	136.38-136.03	34.15-33.86	0.87 m/my	This study
Hiatus 2 (H2)	136.38	34.87-34.15	0.72 Myrs	*
Interval 1	181.3-136.38	36.3-34.87	53.76 m/my	This study
Hiatus 1 (H1)	181.3	36.73-36.3	0.43 Myrs	*

5.2. Shifting ocean-climate regimes during the EOT in the New Jersey margin

By assessing the foraminiferal isotopic data and assemblage data of the three microfossil groups in the depth domain, three distinct phases can be identified, separated by horizons of change at 138.35 (34.9 Ma), 136.8 (34.89 Ma) and 136.08 mbsf (34.87 Ma) (Figure 7). The intervals in between horizons were interpreted as different paleoceanographic phases: P1 (base to 138.35 mbsf), P2 (138.35 to 136.8 mbsf), P3 (136.8 to 136.08 mbsf) and P4 (136.08 mbsf to top). The diagnostic features are summarized in Table 7, compiled in Figure 10 and discussed in section 5.2.2.5.

5.2.1. Isotopic perspectives on thermal and nutrient stratification on the New Jersey margin

The isotopic separations between taxa provide isotopic depth orderings that are consistent with previous paleoecological interpretations (Aze et al., 2011; Pearson et al., 2006), the various species generally displaying a trend of increasing foraminiferal $\delta^{18}O$ and decreasing $\delta^{13}C$ with (inferred) depth (Figure 4). The isotopic depth orderings corresponds to decreasing temperature

(e.g. Fairbanks et al., 1982) regarding $\delta^{18}O$ and surface-removal of ^{12}C by biological production compared to increasing remineralization of $^{12}CO_2$ in subsurface waters regarding $\delta^{13}C$ (e.g. Kroopnick, 1985), although there are important caveats to the $\delta^{13}C$ interpretations (see below). *Pseudohastigerina* and *Turborotalia* inhabited shallower and deeper mixed layer niches as suggested by isotopically low $\delta^{18}O$ and high *Turborotalia* $\delta^{13}C$ values. *Pseudohastigerina* $\delta^{13}C$ is also consistent with previous work (Pearson et al., 2001), showing consistently low values that oppose the $\delta^{18}O$ depth-ranking model. This likely corresponds to a metabolic fractionation process that preferentially affects small test individuals (Birch et al., 2013). In contrast, higher $\delta^{18}O$ and lower $\delta^{13}C$ values in *Catapsydrax* support a sub-thermocline habitat influenced by a water mass that has thermal properties similar to the bottom water, i.e. benthic record.

The multispecies $\delta^{18}O$ pattern implies thermal stratification of the water column over the New Jersey Slope in the late Eocene. The $\delta^{18}O$ values (*T. ampliapertura* $\delta^{18}O$ -1.79 ‰, 33.86-35 Ma) are closely comparable to species-equivalent data sets from the western North Atlantic Eocene for the same interval, including Site 647 to the north (Southern Labrador Sea; *T. ampliapertura* $\delta^{18}O$ -1.84 ‰) and St. Stephens Quarry (SSQ; *T. ampliapertura* $\delta^{18}O$ -1.68 ‰) (Fig.1), both of which contain similarly well-preserved 'glassy' foraminifera (Coxall et al., 2018; Wade et al., 2012). They also fall close to sparse late Eocene Site 612 surface $\delta^{18}O$ measured previously (0.75; Zachos et al., 1994). Benthic $\delta^{18}O$ isotopic values (~0.51‰, 32.95-35 Ma) are lower than the long-term benthic stack (~1.6 ‰; Zachos et al., 2001) and previous studies at Site 612 (1.01 ‰; Zachos et al., 1994) for pre-EOB, while on the same range as ASP-5 (0.45‰, 600 m paleodepth; Katz et al., 2011), slightly higher than the shallower SSQ (-0.17‰, 50-100 m, Katz et al., 2008) and slightly lower than the deeper site ODP 1053 (0.72‰, 1600m, Cramer et al., 2009), for the same interval.

Concerning the $\delta^{18}O$ gradient between benthic (~0.3‰) and deep dwelling planktic foraminifera (~-0.56‰), this is approximately ~1-0.5‰ (<2 °C) and highly variable in much of the section due

to the high variability in the benthic $\delta^{18}O$, but stabilizes in the uppermost Eocene (34.89 Ma; ~138 mbsf; red arrow in Fig.4). From where it increases somewhat to 1.4‰ (~6 ΔT°C). This probably reflects arrival of a cooler more saline northern-sourced deep water, while the isotopic composition of planktic foraminiferal remains nearly unchanged. This densification event might be coincident with that described in Coxall et al. (2018) starting at ~34.6 Ma, as the major $\delta^{18}O$ gradient between deep planktic and benthic - starting at 138 mbsf- coincides with the low nutrient $\delta^{13}C$ peak. Further south on the Gulf coast, a similar late Eocene reorganization of ocean structure was inferred from fossil mollusk shell $\delta^{18}O$, involving greater cooling of the thermocline and deep waters compared to surface waters (Kobashi et al., 2004). The negative $\delta^{18}O$ fluctuations in the early Oligocene of Site 612 imply either transient warmings or transient changes in surface ocean salinity and thus seawater $\delta^{18}O$.

$\delta^{13}C$ values provide further insights into water column structure. Regarding benthic $\delta^{13}C$, in the base of the record they are similar to other mid Atlantic sites (~0.7 ‰), but diverge towards more negative $\delta^{13}C$ values (~-0.5 ‰) thereafter, as seen throughout the Atlantic in EOT benthic isotope compilations (Coxall et al., 2018). At around 141 mbsf and then again at ~138 mbsf benthic $\delta^{13}C$ reach minima that are also evident in the planktic records (Figure 4). Overall the benthic stable isotope records imply increasing influence of bottom water with a low $\delta^{13}C$ signature indicative of high nutrient content, while the $\delta^{18}O$ records imply a general positive trend, indicating a cooling.

Vertical planktic-benthic $\delta^{13}C$ offsets can be used as a tool to speculate about water mass nutrients, stratification and primary productivity. Taking *T. increbescens/ampliapertura* as the surface ocean indicator (lower mixed layer), overall $\delta^{13}C$ surface-to-deep offsets at Site 612 profiles are small relative to today. The *T. increbescens/ampliapertura* surface $\delta^{13}C$ is lower compared to equivalent species records from the tropical Indian Ocean (0.75-1.0‰) in *T. ampliapertura* from Tanzania (Pearson et al., 2001, 2008), but similar to Sites 647 and U1411

(compared to 0-0.5 ‰) over the same interval (Coxall et al., 2018). Strikingly ^{13}C negative values were observed in all the Site 612 planktic taxa at the early Oligocene. Interestingly this negative ^{13}C excursion is not a unique observation: is the first time it has been observed and reported in the NA margin, although it has been detected in the nearby site SSQ (Wade pers. comm.) and Malaysia (Cotton et al., 2014). Modern $\delta^{13}C$ gradients in the western North Atlantic at the same latitude are approximately 1‰ (Sites 29 and 30 in Kroopnick, 1980), while the Eocene/Oligocene profiles show offsets of 0.1 – 0.5 ‰. Specifically, $\delta^{13}C$ values between deep mixed layer (~0 ‰) and deep dwellers (~-0.35 ‰) show an average offset of 0.35 ‰, while that between deep dwellers (~-0.35 ‰) and benthic (~-0.1 ‰) show an average offset of 0.2 ‰.

The scenario of low $\delta^{13}C$ Site 612 benthic foraminifera is consistent with the presence of subsurface waters with relatively low $\delta^{13}C$ below the mixed layer, as seen in other North Atlantic sites and potentially linked to a pulse of low DIC (dissolved inorganic carbon) $\delta^{13}C$ northern sourced deep water initiating in the uppermost Eocene (Coxall et al., 2018). There are various possible explanations for the low surface $\delta^{13}C$ and thus the low overall surface to seafloor $\delta^{13}C$ gradient. One option is that the site was influenced by upwelling during EOT time, bringing ^{12}C and nutrients up to the mixed layer, thus depressing mixed layer planktic shell $\delta^{13}C$ and the vertical $\delta^{13}C$ gradient. This would lead to enhanced primary productivity, and abundant opportunistic surface dwellers, such as *Pseudohastigerina*. High abundance of small taxa such as *Tenuitella*, inferred to be indicative of high food availability, is consistent with this idea. That the upper mixed-layer tracer *Pseudohastigerina* has a strong biological fractionation effect (and, therefore, more negative values than the other planktic taxa) makes it harder to test this scenario in surface waters. Water column DIC patterns and resulting foraminiferal calcite $\delta^{13}C$ under modern upwelling conditions, however, do not appear to work like this. Nutrients upwell from beneath the mixed layer but phytoplankton quickly respond, photosynthesis acting to strip out ^{12}C from surface water DIC as primary production accelerates, leaving resident planktic foraminiferal shells with high $\delta^{13}C$ signatures (Grant & Dickens., 2002). Moreover, if modern and

EOT $\delta^{13}C$ profiles are compared, it can be noted that all the species have more negative (~1 ‰) average values than those in the modern profile (Kroopnick, 1980, 1985), i.e. both planktic and benthic foraminiferal species (Fig. 4).

Surface $\delta^{13}C$ composition of dissolved inorganic carbon (DIC) in the modern surface ocean reflects a combination of external inputs, air-sea gas exchange, chemical and biological fractionations and ocean circulation and is typically between 0.5 and 2.5 ‰ (Gruber et al., 1999; Tagliabue & Bopp, 2008). While this average could be higher or lower in the past depending on prevailing global organic carbon storage budgets or rate of ocean ventilation (Zachos et al., 2001), other mid to late Eocene DIC $\delta^{13}C$ inferred from non-symbiotic mixed layer planktic foraminifera largely fall within this modern range (Tanzania, ~0.5-1.5‰; Adriatic Sea, 0.75 ‰; eastern North Atlantic) (Bornemann et al., 2016; Pearson et al., 2001). The relatively low mixed layer planktic $\delta^{13}C$ noted in the late Eocene of Site 612 surface (~0.0-0.5‰), also found at more northerly sites on the western Atlantic margin (Coxall et al., 2018) and the Gulf Coast (Pearson et al., 2001), are thus anomalous. Such low mixed layer values could reflect unknown vital effects in *T. ampliapertura* and *T. increbescens* in these regions, but it seems unlikely because the same species were analyzed in Tanzania and elsewhere. Instead, it could reflect additions of terrestrial sourced DIC with low ^{13}C content to the offshore environment.

Low early Oligocene $\delta^{13}C$ Site 612 mixed layer values are comparable to the anomalously low (0.5-0‰) surface ocean DIC $\delta^{13}C$ measured or reconstructed in several modern shelf seas in tropical or temperature regions, including the Gulf of Thailand and Anderman Sea (Tagliabue & Bopp, 2008). These regions and their characteristic surface ocean $\delta^{13}C$ signatures, which are of interest for their role as CO_2 and/or nutrient sources or sinks, are coastally-sourced, and result from export of terrestrial carbon from large rivers, tropical mangroves or temperate salt marshes, including modern salt marshes to the south of Site 612, offshore Georgia (Cai et al., 2003; Miyajima et al., 2009; Tagliabue & Bopp, 2008). These mangrove and marsh cases are of

special interest because of the 'high quality' of organic carbon they contain, which, being younger than river-sourced carbon is more readily available for bacterial decomposition and CO_2 release (Cai et al., 2003). Importantly, significant quantities of marsh derived DIC (2 Million tons of carbon yr^{-1}) has shown to be exported across the Georgia shelf to the open Atlantic, implying this mechanism is significant for global ocean carbon cycling (Cai et al., 2003). This could have occurred on a greater scale during the late Eocene, when high sea level (at least 50 m > modern) (Kominz & Pekar, 2001; Pekar et al., 2000, 2001) created large shelf seas. Sea-margins experienced a sea level fall and record a pulse of ^{12}C enriched carbon, potentially a feedback from exhumed neritic/blue carbon. Moreover, paleobotanical records recorded in marine sediments reveal expansive fringing swamp lands (Kotthoff et al., 2014), that could have been an important contributor of low $\delta^{13}C$ DIC to coastal waters and offshore slope environments, including Site 612.

5.2.1.1. Temperature increase in NW Atlantic upper water column

Paleotemperature envelopes for surface, mixed layer, thermocline and deep waters were created with a range of realistic paleotemperature estimates obtained after applying different $\delta^{18}O_{sw}$ (VSMOW) values (Figure 5, Table 1). The estimated temperatures using globally homogeneous $\delta^{18}O_{sw}$ values based on estimates of ice volume change (Cramer et al., 2011; Shackleton & Kennett, 1975; Zachos et al., 1994) and applying an offset reflecting the modern variability of $\delta^{18}O_{sw}$ with latitude (Zachos et al., 1994), are lower than those obtained using lat/long specific $\delta^{18}O_{sw}$ values derived from isotope-enabled GCMs (General Circulation Models) (Huber et al., 2003; Roberts et al., 2009; Tindall et al., 2010). When using $\delta^{18}O_{sw}$ calculated at a nearby site (SSQ) determined by paired Mg/Ca and $\delta^{18}O$ paleothermometry for a 50 m paleodepth (Katz et al., 2008), SST values increase on the order of 3.2°C regarding the average.

The averaged $\delta^{18}O_{sw}$ value used for estimating SSTs (-0.35 ‰ VSMOW) falls well within the range of GCM derived values (Huber et al., 2003; Roberts et al., 2009; Tindall et al., 2010), consistent with other SST estimates from the late Eocene western North Atlantic. Temperature fluctuation is mirrored at Site U1411, a NA site in the same latitude, with an average of 26.5°(C) (TEX_{86}; Liu et al., 2018). In a more southerly site (28°N) a value of ~27°(C) was reported ($U^{K'}_{37}$; Site 628; Liu et al., 2009). The calculated late Eocene SSTs at 41°N of 19-28°C, based on *Pseudohastigerina*, are within the range of Tex 86 estimates (27-28°C, likely summer maxima) for the same site by Pagani et al. (2011), within range of $\delta^{18}O$ summer estimates (22-28°C) from fossil mollusk shells from Alabama (Kobashi et al., 2004) and also Tex86 and *T. ampliapertura* Mg/Ca SST estimates (27-33°C) from the SSQ (Late Eocene, ~31°N, Wade et al., 2012). The latter SST were higher most probably due to the shallow nature of the site and the more restricted conditions inside the gulf compared to those in the open ocean.

Long term trends of Site 612 appear to be more significant when compared to previously published records, as in the latest compilation of EOT benthic isotopic records (Coxall et al., 2018; initial Site 612 benthic isotopic record included) and specially when compared to ODP 647, located ~8° north to this site and also under the influence of the DWBC. The authors reconstructed 3 oceanic regimes and demonstrated the start-up of the Northern Component Water (NCW) in two broad steps reflecting the progressive densification of subpolar waters, as they recorded a novel difference in water mass characteristics, which has been interpreted as the initiation of Northern Component Water (NCW). The isotopic signature of NCW initiation is characterized by a trend to lower $\delta^{13}C$ and higher $\delta^{18}O$ values in the high latitude NA sites, and $\delta^{13}C$ negative signal is propagated from north to south, as the sign of a first NCW export. Both densification steps, that are the starting event of Regime 2 and 3 respectively, are detectable in this site after the new data reported here.

5. Discussion

At Site 612, there is a clear $\delta^{13}C_{Cib}$ excursion to lower values coupled to a $\delta^{18}O_{Cib}$ positive excursion spanning Phase 0 and 1, that is probably the first densification step to Regime 2, as seen in Site 647 (Coxall et al., 2018). The $\delta^{18}O$ offset and same range $\delta^{13}C$ values between benthic and planktic values during Phase 2, could be indicating the second densification step towards Regime 3. The similar $\delta^{13}C$ values between deep and mixed layer planktic and the offset with benthic values during Phase 3 agree with Regime 3 in Coxall et al. (2018). The limited age model doesn't allow us to properly asses the timing of this events in the site.

According to different climate models, during the late Eocene deep water formation occurs in the Pacific while the North Atlantic is strongly stratified and poorly ventilated (Baatsen et al., 2018; Hutchinson et al., 2018b). This is in agreement with the initial isotopic values at Phase 0.

Another oceanic characteristic inferred from the data is an SST increase during the EOB that could be linked to the oceanic changes triggered by the NCW initiation.

Paleotemperature estimates after surface planktic foraminiferal $\delta^{18}O$ increase throughout the record, and show higher values at the top. This observation evidences that mixed layer waters became warmer, especially during and after the EOB. Simultaneously, paleotemperature estimates after thermocline dwellers and benthic foraminiferal diverge, showing a general cooling throughout the record and an increase after the EOB in the case of thermocline dwellers.

To account for the SST increase, two alternative mechanistic explanations can be considered: (1) the initiation of deep water formation in the North Atlantic (NCW) implies that the thermohaline circulation is pulled downwards in polar latitudes – at formation site – triggering a more energetic surface circulation and, therefore, pushing the near-to tropical warm waters to higher latitudes, i.e. Gulf Stream to Site 612. (2) The alternative explanation involves a poleward shift in westerly winds causing the northward migration of the front between the warm and salty North Atlantic Subtropical Gyre and the cold and fresh Polar Gyre. These gyres are separated by

the westerly wind energy maximum, so a shift in westerly winds would change the gyre position, ultimately leading to the same effect: bringing warmer waters northwards.

The first mechanism seems to be more plausible, i.e. the pull originated by the initiation of the NCW formation due to densification (salinification increase). In fact, this mechanism has been previously suggested by several authors (Borrelli et al., 2014; Coxall et al., 2018; Via & Thomas, 2006). Moreover, according to Wade & Kroon, (2002) high-amplitude variability of SST (>4 °C) or $\delta^{18}O$ (>1‰) during the late Eocene at the nearby Site 1052 may occur due to latitudinal displacement of the Gulf Stream front, a mechanism suggested after Paleogene seismic stratigraphy studies (Pinet et al., 1981). This variability is mirrored by Site 612 mixed-layer planktic foraminifera that reveal prominent and rapid $\delta^{18}O$ oscillations (Figures 4 and 10). This is particularly evident at 138 mbsf, where $\delta^{18}O$ values shift from -1.5‰ to 0.0‰. Remarkably, another study north to this site (Site U1404; 40°N) shows no evidence of surface cooling in the North Atlantic directly coinciding with the EOT, interpreted as a northwards expansion of warm subtropical gyre waters (Liu et al., 2018). The isotopic shifts agree well with predicted $\delta^{18}O$ variations in the climatic model of Huber et al. (2003). Furthermore, it has been shown that cooling events increase the velocity of the Gulf Current from Miocene to present (Kaneps, 1979).

The alternative hypothesis seems unlikely because global cooling shift westerlies equatorward as observed during the LGM (Durand et al., 2018), an analogous scenario, and not poleward, as it would be needed for the explained scenario.

5.2.2. Plankton and benthos community responses and evolving North Atlantic circulation

Micropaleontological proxies use existing understanding of the paleoecology of different taxa to make inferences about paleonvironmental changes. Planktic and benthic foraminifera have been widely studied in this respect, both in terms of modern biology and as far as possible, the

Table 7. Upsection observation and interpretation summary (read following the direction of the arrow, from bottom to top). Numbers in the left (0-4) indicate oceanographic phases - as identified in Figures 4 and 7, and summarized in Fig. 10 - and ranges beneath correspond to depths. > = higher, relative to the average; < = lower, relative to the average. r = Pearson correlation coefficient between the bracketed variables (corresponding p-value <0.003); $F1_{BF}$= Benthic foraminifera Factor 1, identified by factor analysis ($F1_{PF}$=Planktic foraminifera F1; $F1_{CN}$=Calcareous Nannofossil F1); ML= mixed layer; DW= deep water; SO= surface opportunistic; BW= bottom water; V:SA= volume Vs surface area ratio; Δ=gradient; SS=Sortable Silt (38-63µm); FF=fine fraction (<38 µm); O.M.=Organic matter; P.P.=Primary productivity; OC=Organic carbon.

PHASE Depth (mbsf)	OBSERVATIONS						Strongest signals that lead to →	INTERPRETATION
	Benthic foraminifera	**Planktic foraminifera**	**Nannoplancton (Phyto)**	**$\delta^{18}O$**	**$\delta^{13}C$**	**Others**		
4 **136.08-135.47**	> Epif. phytodetritus ↳ Opportunistic Oligotrophic > $F3_{BF}$ (r=0.77) < Elongate gp.	> Deep water dwellers > $F1_{PF}$ (r=0.65) < Diversity	>*R. daviesii* : Cosmopolitan >> $F2_{CN}$ >Discoaster (warm/oligotrophic) · Variable Small *Reticulofenestra* spp. <Placolith-bearing taxa V:SA	· (-) peak in all planktic species (~1-2‰) · $\delta^{18}O_{cib}$ stable	· (-) peak in all species (~2‰)	· Hiatus 3 · Relatively low sed. Rate >SS variable FF >> Glauconite · Low biosilica	· Ecological turnover (BF): Elongate gp. replaced by opportunistic (Epif. Phytodetritus) · $\delta^{13}C$ (-) peak (all species) → · $\delta^{18}O$ (-) peak (Planktic sp.) → >> Glauconite →	· Elongate gp. specific food source (phyoplanton/procaryote) directly impacted by cooling/climate transition a) Methane hydrate release? b) Input of continental sourced O.M.? SST rise? · Sedimented after lowered sea level
3 **136.8-136.08**	> Elongate gp. > $F2_{BF}$ (r=0.85) · MAX total abundance < Diversity < Agglutinated	Mixed layer dwellers peak > $F3_{PF}$ (r=0.58) > Total abundance	< Small *Reticulofenestra* spp. > $F2_{CN}$ (r=-0.7) > *R. daviesii* ↳ · Cosmopolitan taxa with ecological plasticity · Decreasing diversity · Placolith-bearing taxa V:SA drop	· $\delta^{18}O_{cib}$ (-) highly variable: pre-EOB shift (~1‰) · $\delta^{18}O_{ML}$ (-) excursion (~1‰)	· Pre-EOB $\delta^{13}C_{cib}$ (+) shift to near-initial values (~1‰; pre-NCW)	· Biosilica (MAX) · Hiatus 2 · Relatively low sed. rate << FF (-) peak (MIN) (variable) >>106 µm Ø grain size fraction >SS (MAX)	· Winnowing (<<FF (MIN)) >Elongate Gp: feed on refractory C? < Agglutinated benthic → · Biosilica (MAX) → · $\delta^{13}C_{cib}$ (+) shift in the top → · $\delta^{18}O_{cib}$ (-) shift: low salinity/warm waters?	· Enhanced circulation (>BW current velocity); Refractory C input by lateral advection→ <export P.P. > Ventilation DSi Input after erosion of seafloor/margins enhances Bsi productivity · NCW with younger ^{13}C-rich $\delta^{13}C$ (End of (-)ve sourced NCW) a) Local continental input? b) Related to turbidites?
2 **138.35-136.8**	> Conical ↳ Eutrophic (r=0.6) (Vs Conical+Fl. Biserial) > $F1_{BF}$ >Total abundance	· No clear dominance · ML: plateau · DW & SO: shifting > Total abundance	>> Small *Reticulofenestra* spp ↳ · Eutrophic / warm · Large Reticulofenestra V:SA drop	> $\Delta\delta^{18}O_{Cat-Cib}$	· $\delta^{13}C_{cib}$ (-) trend continues (from P1), stable MAX values	· Relatively high sed. rate >SS; >>106 µm grain size fraction < FF · Low biosilica	>>S. Reticulofenestra spp. → > $\Delta\delta^{18}O_{Cat-Cib}$: < BW T(°C) · Pref. pres. 106µm = Winnowing · SS Vs δ18Ocat (r=0.57) > Deep Infaunal (flattened-biserial & conical) related to →	· Enhanced productivity · Enhanced bottom current velocity and density when > SS% and > $\delta^{18}O$. Winnowing evidence. > O.M. flux to sea floor (> export production)
1 **141.46-138.35**	> Flattened biserial ↳ Eutrophic (r=0.6) (Vs Conical+Fl. Biserial) > $F1_{BF}$	> Deep water dwellers (vs $F1_{PF}$) (r=0.65) · Ocassional SO peaks (vs $F2_{PF}$) (r=0.61) $F1_{PF}$ $F2_{PF}$ peak alternance	>Small *Reticulofenestra* spp ↳ · Eutrophic / warm > $F1_{CN}$	· $\delta^{18}O_{cib}$ (+) trend continues (from P0) · $\Delta\delta^{18}O_{Cat-Cib} \approx 0$	· $\delta^{13}C_{cib}$ (-) trend continues (from P0)	· Relatively high sed. rate > FF · Low biosilica	· Continuation of trend to (+) $\delta^{18}O_{cib}$ & (-) $\delta^{13}C_{cib}$ → · Relative high sed. rate & >FF→ > Deep Infaunal (flattened-biserial & conical) related to →	· Further local BW cooling & export of Arctic-imprinted, nutrient-rich NCW · Relat. lower DW velocity conditions > O.M. flux to sea floor (> export production)
0 **181.38-141.46**	< abundance of *Bolivina* sp. (%) ↳ · Related to > O.M. input	(No data)		· Trend to enriched (+) $\delta^{18}O_{cib}$ values	· Trend to depleted (-) $\delta^{13}C_{cib}$ values	· Hiatus 1 in the base	· Trend to (+) $\delta^{18}O_{cib}$ → · Trend to (-) $\delta^{13}C_{cib}$ → · < abundance of *Bolivina* spp.	· Local BW cooling, NCW export · Export of Arctic-imprinted, nutrient-rich NCW · Sustained low OC in deep waters

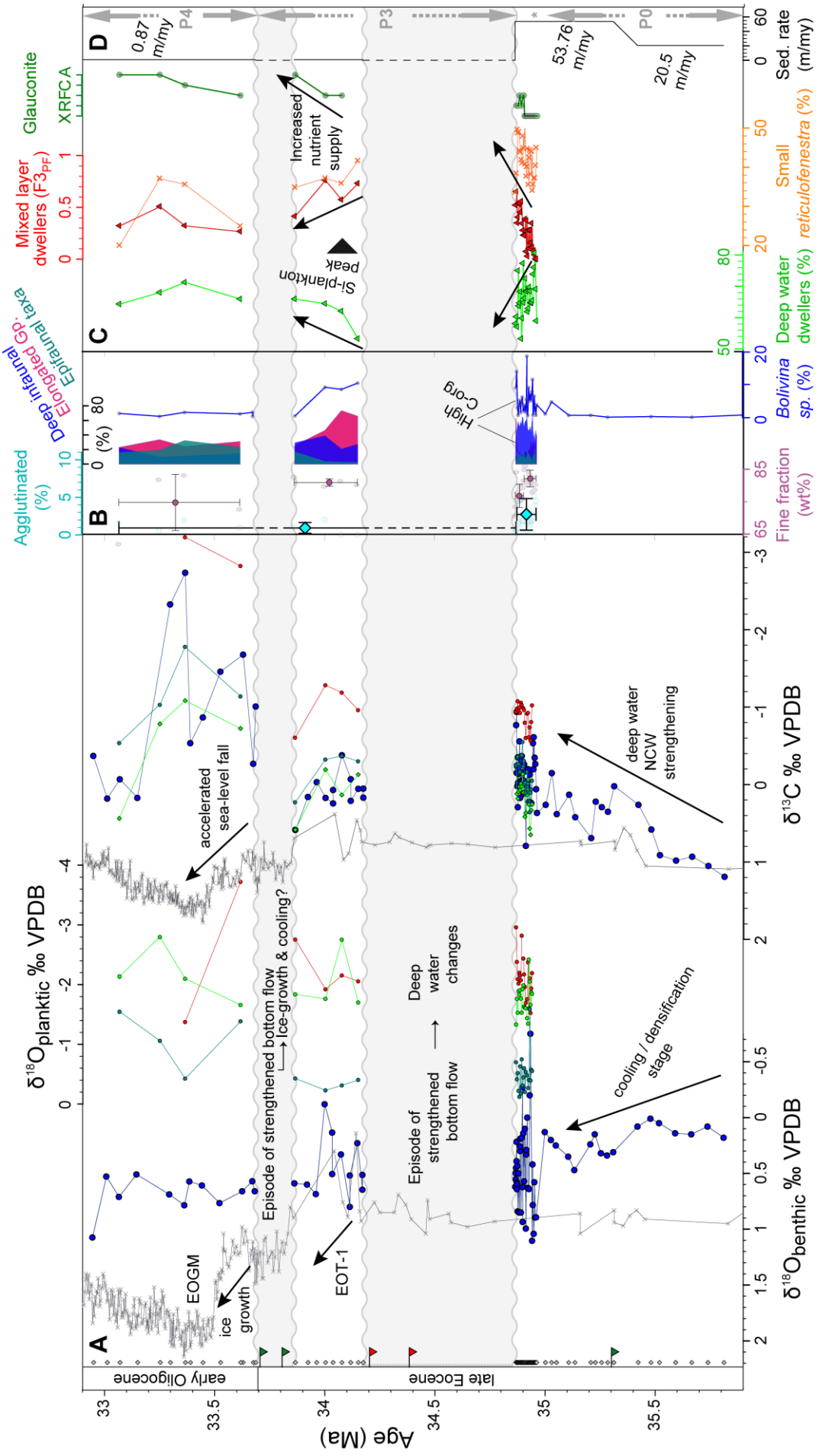

Figure 10. Compilation of a suite of the strongest surface and deep ocean records through the late Eocene to early Oligocene of Site 612, plotted against age (Ma) according to CK95 timescale. Note the hiatuses, represented as gray intervals bounded by light wavy lines. A) Stable isotope (δ18O and δ13C) records of planktic foraminifera (dots) from thermocline (cyan), mixed layer (green) and surface (red); and benthic foraminifera (blue dots) from Site 612, compared to Site 1218 benthic records (grey crosses) (Coxall et al., 2005). B) Deep water conditions expressed by fine particle size-fraction (weight percentages; wt%) and benthic assemblage selected (Agglutinated, deep infaunal flattened-biserial and conical, Elongated Gp., Epifaunal taxa, Bolivina sp.) abundance records. Depicting means and standard deviation of a-priori recognized zones to aid visual representation and trends. C) Surface water conditions expressed by deep (%) and mixed layer (Factor 3) planktic foraminiferal dwellers, small Reticulofenestra calcareous nannofossil (%), siliceous plankton and glauconite abundance records (X= absent; R= rare; F= few; C= common; A= abundant). D) Sedimentation rate, indicating the variable sedimentation rate (m/my). Grey diamonds in the left represent sampled levels. Inverse green triangles indicate LO of planktic foraminifera (1) Hantkenina spp. and synchronous dwarfing of Pseudohastigerina micra; (2) Turborotalia cerroazulensis group. Inverse red triangles indicate Top of calcareous nannofossils (3) Discoaster saipanensis and (4) D. barbadiensis. Gray numbers on the right side indicate the identified oceanographic phases (P0 to P4; P1-2 marked with *).

paleoecology. The geographic and vertical distribution of modern planktic foraminifera is known to be controlled by physiological requirements, feeding preferences, sea surface temperature, salinity, water depth, water column stratification and food supply (Schiebel & Hemleben, 2017). The distribution of deep water (bathyal types) benthic foraminifera of the type found at Site 612, is strongly controlled by food supply, as well as bottom water chemistry, including oxygen and carbonate content (Corliss, 1985; Sen Gupta & Machain-Castillo, 1993; Jorissen et al., 2007; Van Morkhoven et al., 1986).

5.2.2.1. Benthic foraminiferal assemblages

Benthic foraminifera (BF) Factor 1 ($F1_{BF}$) explains 45% of the total variance, and in consequence, characterizes the ecological parameter that is most important for explaining benthic assemblages in the records. $F1_{BF}$ curve shows a significant (loading >0.6) high stable pattern (141.46 to 136.8 mbsf) until immediately before the EOB, when it decreases at 136.8 mbsf, remains depressed until 135.47 mbsf, then temporarily increases around the E/O before decreasing again (Fig. 7, Table 5; Appendix IV. Table j). This factor is defined by *Brizalina tectiformis*, *Bulimina alazanensis*, *Siphonodosaria* spp. and *Bolivina* spp. in order of importance (Fig. 7, Table 5), deep-infaunal taxa that require high sustained organic matter (Corliss, 1985; Van Morkhoven et al., 1986; Table S2a). The pattern is paralleled by the apriori eco-grouping with a significant correlation (r=0.77), deep-infaunal conical and flattened biserial taxa dominates the assemblage up to 136.8 mbsf then rapidly decline. Its record mirrors $F1_{BF}$ with a significant correlation (r=0.77) (Fig. 7), reassuring the Factor Analysis. This suggests that $F1_{BF}$ represents the quantity of organic matter (OM) reaching the seafloor.

The benthic Factor 2 loadings ($F2_{BF}$) curve (exp. var. 17%; Fig. 7; Appendix IV. Table j) shows an almost inverse pattern to $F1_{BF}$, increasing dramatically at 136.8 mbsf up to the E/O. This factor is largely characterized by the deep infaunal taxa *Strictocostella* spp., Glandulonodosariids,

Bolivinoides crenulatus, *Brizalina carinata* and *Siphonodosaria* spp. (Table 5). These taxa are inferred to be tolerant of hypoxic conditions within the substratum (Sen Gupta & Machain-Castillo, 1993; Jorissen et al., 2007; Levin, 2003; Table 2) but can also proliferate in response to high fluxes of refractory organic matter reaching the seafloor, including when laterally advected offshore by turbidity currents. In this latter situation bacterial recycling of the refractory carbon under anaerobic conditions within the sediment makes the organic matter available to benthic foraminifera (Fontanier et al., 2005; Jorissen et al., 2007; Murray, 2006). Thus, it is reasonable to suppose that $F2_{BF}$ relates to the degree of oxygenation at the seafloor or, alternatively, the quality (labile or refractory) of organic matter. In the same stratigraphic interval, both Fisher's α diversity and richness index record an abrupt drop (Fig. 7), indicating increasingly stressful conditions at the seafloor (Gooday et al., 2000; Levin, 2003). The low oxygen hypothesis, however, is here discarded since there is a lack of other sedimentological evidence indicative of poor oxygenation, such as dark coloured and/or laminated sediments. The alternative explanation would lead us to assume that the controlling factor forcing the assemblage change is food quality, involving a shift from labile to refractory organic matter.

Compared to records from elsewhere and the chronology produced here, this interval corresponds to the Antarctic cooling event EOT-1 (see Coxall & Wilson, 2011), involving the first of two stepped increases in benthic $\delta^{18}O$ and $\delta^{13}C$, as well as evidence for a major increase in NCW export, as implied from benthic $\delta^{18}O$ from the Southern Labrador Sea (Coxall et al., 2018). The stable isotope records, when plotted in the age domain (Figure 10) are broadly consistent with this, although the isotopic changes are rather noisy. The species that characterize $F2_{BF}$, (*Strictocostella* spp., Glandulonodosariids and *Siphonodosaria* spp.) are elongate cylindrical taxa with complex apertural structures that belong to the 'Elongate Group', which has high correlation (r=0.86) with $F2_{BF}$. In fact, the Elongate group shows a peak in this interval at Site 612 (34.87 – 33.86 Ma) (70 % relative abundance), which is also seen in other high latitude sites at this time in the North Atlantic (76 % at Site 647, mid C13r, ~34.2-34 Ma; Ortiz & Kaminski, 2012),

40 % in a compilation of several sites (Sites 548, 608, 980, 982, and 1055; ca. 34.2-33.8 Ma; Hayward et al., 2010) and the Southern Ocean (34.8-33.8 Ma) (70 % at 689 and 690; Thomas, 1990, 2007; Thomas et al., 2000). Elongate group's complex apertural structures have also been linked to specialization to a specific food-source, most probably detrital phytoplankton or bottom-dwelling microbes (Hayward et al., 2007; Thomas, 2007). Its peak occurrence in the late Eocene North Atlantic has also been linked to vigorous bottom water ocean circulation (Ortiz & Kaminski, 2012), $F2_{BF}$ suggesting that the switch in food supply to more refractory organic matter was associated with stronger bottom water flow or turbidity currents. A simultaneous, sharp depletion of agglutinated benthic foraminiferal taxa (Appendix IV, Table i), also identified at Site 647 immediately before EOT-1 (34-34.2 Ma) in the Southern Labrador Sea (Kaminski & Ortiz, 2014), supports this hypothesis. The loss of agglutinated (Fig. 10) and subsequent increase in calcareous species was similarly interpreted as indicating stronger bottom currents and improved ventilation, to which calcareous benthic species are better suited.

Both the benthic assemblage changes and the two hiatuses (in the record at 136.375 and 136.025 mbsf) during the $F2_{BF}$ peak interval, are probably linked to increased deep water flow at the seafloor, modifying food availability and at times creating erosive or non-depositional surfaces respectively. The hiatuses recognized here, are in agreement with an erosional unconformity in the entire continental slope and rise (marked by Horizon A^U /seismic reflector recorded at Site 612 and elsewhere (Mountain & Tucholke, 1985; Tucholke & Mountain, 1979; Tucholke & McCoy, 1986; Tucholke & Mountain, 1986) and other erosive features in the North Atlantic (Berton & Vesely, 2018; Boyle et al., 2017). Moreover, on the New Jersey margin these hiatuses have been linked to sequence boundaries associated with a 50-60 m sea level fall (Miller et al., 2005a; Pekar et al., 2001) close to the C13r/C13n boundary, associated with the rapid continental scale glaciation on Antarctica. The unusually wide and shallow sloping shelves of the New Jersey (Miller et al., 2014) margins mean that this region would be especially sensitive to this sea level fall, rapidly shrinking the shelf seas and, thus potentially, the sediment and nutrient

fluxes from the hinterland. This process has been well studied on the New Jersey margin (e.g. Browning et al., 2008; Miller et al., 2014; S. Pekar & Miller, 1996). The late Eocene has been defined as a time of relatively high sea level, carbonate production but generally sediment starvation on the shelf, diagnostic glauconite sands during associated with High Systems Tracts (HSTs). After the early Oligocene sea level fall sedimentation rates were even slower, likely because carbonate production ceased on the shelf. Increasing inputs of quartz sand occur, together with extensive reworking of older glauconite (Browning et al., 2008). The sea level change to impact interactions of shelf-waters and oceanic water masses over Site 612 is also expected.

Factor 3 explains a smaller fraction of the assemblage diversity (exp. var. 13%; (Fig. 7, Table 5) this element of the assemblage is relatively stable up to the EOB (136.08 mbsf) after which there is a dramatic increase. The species describing this factor are *Uvigerina galloway*, *Osangularia* cf. *O. plummerae, Siphonodosaria* spp. and *Alabamina cf. A. dissonata* (Table 5), indicative of high seasonal food supply to seafloor (Table 2; Jorissen et al., 2007; Sun et al., 2006). Therefore, $F3_{BF}$ can be considered as high seasonal organic flux. $F3_{BF}$ shows high correlation with the epifaunal: infaunal ratio (E/I ratio) (r=0.75) and epifaunal phytodetritus taxa (r=0.63 and r=0.436 from 63-106 and >106 µm respectively), taxa that mimic $F3_{BF}$ curve (database in appendix IV, Table i). Epifaunal phytodetritus taxa, such as recent and fossil *Epistominella exigua* or *Alabaminella weddellensis* (morphologically similar to the Site 612 *Alabamina* cf. *A. dissonata*, characteristic of $F3_{BF}$) (Table 2), are associated with opportunistical blooming in response to the spring phytoplankton bloom and resulting phytodetritus dump to the seafloor (Thomas et al., 1995). These taxa show a temporarily decline during phase 3 before the E/O but peak during the early Oligocene at Site 612 (33.67 Ma) in both sediment fractions (Figure 6). Linking this to the sharp decrease of the Elongate Gp. According to these data from the early Oligocene, it is possible to postulate that conditions changed again in the late Oligocene, and the Elongate group was out-competed by small opportunistic, seasonal phytodetritus-feeding-species after the EOB. This

scenario is consistent with observations from the Southern Ocean and Indian Ocean at this time (Gooday, 2003; Nomura, 1995; Thomas et al., 2000; Thomas & Gooday, 1996) that suggest a switch to a seasonally fluctuating food supply, especially at high latitudes, during the transition.

5.2.2.2. Planktic foraminiferal assemblages

Planktic foraminifera (PF) Factor 1 ($F1_{PF}$) displays a fluctuating pattern that shows intermittent significant values (loading >0.6) during the first half of the record until a major disruption (141.46-136.8 mbsf), and it becomes significant again after EOB (136.08 mbsf; (Fig. 7). It is characterized by *Dentoglobigerina venezuelana*, *Subbotina corpulenta* and *S. eocaena*, subthermocline dweller taxa (Table 5) and shows high correlation with deep dwellers (r=0.65) and surface opportunistic (r=-0.83) eco-groups, suggesting that $F1_{PF}$ dominantly reflects deeper, i.e. thermocline dwelling taxa abundance. Moreover, the subthermocline dweller *Catapsydrax* has a moderately high score in this factor (Table 5), giving confirmation on the interpretation. Food is the predominant factor affecting planktic foraminiferal distribution under favorable temperatures (Ortiz et al., 1995), therefore, the parameter driving $F1_{PF}$ is probably either (1) the depth of the thermocline, as its variability has the ability to expand/contract niches (mixed layer/thermocline/subthermocline) and enhance/diminish primary productivity; (2) the temperature variability of surface waters or (3) an intertwining of both mechanisms. $F1_{PF}$ shows variability but no net change over the studied interval. $F2_{PF}$ (22%) drops through the record (141.46-138.35 mbsf; Fig. 7). It is characterized by *Tenuitella patefacta*, an opportunistic species related also to high productivity conditions, and by *D. pseudovenezuelana*, thermocline dweller (Tables 2 and 5). High correlation with surface opportunistic eco-group (r=0.61) indicates that $F2_{PF}$ is related either to some kind of variability in surface conditions, likely related to surface production. That the $F2_{PF}$ loadings are lowest in the early Oligocene suggests a shift in surface regime following the E/O. $F3_{PF}$ (15%) shows a steady increasing trend until it reaches significant values (loading >0.6), showing a peak up to EOB (138.35-136.08 mbsf) before decreasing

somewhat. It is characterized by *Globoturborotalita ouachitaensis* and *Turborotalia increbescens*, mixed layer species (Table 5), and correlates with the mixed layer dwellers eco-group (r= 0.58) (Fig. 7). The shift in assemblage structure towards more abundant mixed layer dwellers (MLD) prior to 136.8 mbsf, i.e. before the pre-EOB interval (136.8-136.08 mbsf), could have been caused by variability of the thermocline depth, or reflect changes in the surface water mass influencing Site 612. A stronger deep water formation in the northern North Atlantic can be suggested as a result of a stronger Gulf Stream and possibly a great influence of warm eddies peeling off the warm current and close to the New Jersey margin (see section 5.2.2.1.).

5.2.2.2.1. Thermocline effect on the zooplankton

Changes in the position of the thermocline are fundamental in maintaining marine plankton communities (Leckie & Olson, 2003). Specifically, planktic foraminiferal distribution is mainly determined by food availability under favorable temperatures (Ortiz et al., 1995) that, in turn, is limited by primary productivity and nutrient availability, factors controlled by the position of the thermocline and nutricline (Mutti & Hallock, 2003). The shift in assemblage structure from deep dweller dominance to an increase in mixed layer dwellers abundance (Fig. 7), could have been caused by variability of the thermocline depth as it follows; (1) when the thermocline is shoaled the underlying nutricline permits nutrient supply making them available for primary producers (by upwelling or mixing) and sustains abundant MLD and DD populations (Mutti & Hallock, 2003), whereas (2) in a deepened thermocline scenario (and therefore, nutricline), high nutrient waters are isolated from the surface, making this nutrients unavailable for primary producers. Therefore, primary productivity decreases and becomes a limited trophic resource, resulting in preferential grazing by mixed layer dwellers versus deep dweller populations, since food decreases as depth increases, making DD populations relatively less abundant in comparison to MLD ones (Leckie, 1989; Spezzaferri et al., 2002). In the Global Stratotype Section and Point (GSSP) for the Eocene-Oligocene boundary at Massignano, the same effect - as in the case of

shallowed thermocline- has been observed: higher abundance of DD increases over MLD at late Eocene (Spezzaferri et al., 2002). They attribute the turnover to a shallowing of the thermocline coeval to a contraction of the mixed and surface layers, linked to the enhanced cooling. Similarly, this observation and interpretation has been made for a number of Sites at the EOB (Keller, 1983). An alternative explanation, however, can be related to the effect that elevated temperature has in nutrient availability, and its consequences in primary productivity and sustaining zooplankton populations. According to isotopic data, a temperature increase over a range of ~2-5°C can be inferred in the entire water column at Site 612 prior to EOB, being higher in surface waters (~8°C). High temperatures inhibit the availability of nutrients in the mixed layer, suppressing nutrient supply by enhanced stratification (Roemmich & McGowan, 1995), therefore primary productivity becomes a limited trophic resource, favoring the increase of MLD population, and resulting in the same scenario as that in the initial explanation. This would make P3 an interval of deeper thermocline, therefore more ML dwellers. Alternatively, if the enhanced seasonality enhances atmospheric dynamics (i.e. storms), in a scenario of deeper mixing, primary production would increase, and the ML dwellers could increase rapidly, outnumbering the deep dwellers. However, calcareous nannofossil data does not completely support this interpretation, showing a decrease of bloom-related taxa (small *Reticulofenestra*) during Phase 3 to the top of the record.

5.2.2.3. Calcareous nannofossil assemblages

The contribution of calcareous nannofossil (CN) $F1_{CN}$ gradually decreases from ~138.2 mbsf and towards the Oligocene. It is characterized by *Sphenolithus tribulosus* and *R. dictyoda* (Figure 7, Table 5), whose paleoecological preferences have not yet been clearly defined. Nevertheless, the genus *Sphenolithus* has been linked with high-productivity intervals across the EOT (Bordiga et al., 2015b; Dunkley Jones et al., 2008) and in the early Oligocene (Wade & Pälike, 2004). Although the loading species do not show any particular size distribution along the first factor,

$F1_{CN}$ displays high correlation with large reticulofenestrids V:SA (r=-0.58). Moreover, a correlation of 0.59 with $F2_{PF}$ and with all the planktic $\delta^{13}C$ records (surface, r=0.44; mixed layer, r=0.55; thermocline, r=0.59) could be indicative of a link between $F1_{CN}$ and the amount of organic matter produced by the phytoplankton. More challenging is to link $F1_{CN}$, i.e. the average size of large *Reticulofenestra*, to a defined environmental parameter. The unusually low surface and deep (benthic) $\delta^{13}C$ (see above) prevent the traditional approaches of identifying high primary production by high surface $\delta^{13}C$ or strong planktic to benthic $\delta^{13}C$ gradients. Moreover, no pCO_2 alkenone-derived data are available across the EOB at high northerly latitudes to verify if the large reticulofenestrids have been affected by lower pCO_2 conditions, as previously documented by Bordiga et al. (2015b), Henderiks & Pagani (2008) and Pagani et al. (2011). $F2_{CN}$ shows a slowly decreasing pattern at the base of the record (141.46-138.35 mbsf), until it exhibits a rapid increase followed by a posterior decrease (138.35-136.8 mbsf), displaying a recovery in the upper part of the record (136.8 mbsf-top) and reaching significant values after the EOB during a maximum peak (136.08 mbsf-top). It is characterized by *Reticulofenestra scrippsae* and *Reticulofenestra daviesii*, respectively described as taxa with undefined ecological affinity and a cosmopolitan one with a significant ecological plasticity (Bordiga et al., 2017). $F2_{CN}$ has high negative correlation with small *Reticulofenestra* (r=-0.7), considered an external paleoproductivity proxy – it was not included into the factor analysis due to its high abundance (see Appendix III). Moreover, $F2_{CN}$ negatively correlates with $F1_{BF}$ (r=-0.69) – i.e. the quantity of OM – and positively with $F2_{BF}$ (r=0.56) – i.e. the seasonality of OM fluxes. Thus, it is reasonable to presume that $F2_{CN}$ represents the primary productivity/nutrient supply, which was high (low values of $F2_{CN}$) throughout the sequence, and decreased towards the top, as shown in $F1_{BF}$ curves (Figure 7). The absence of holococcoliths, which have found to be indicative of oligotrophic conditions (e.g. Cros et al., 2000; Winter et al., 1994), provides additional support for a highly productivity regime at Site 612 throughout the studied interval.

5.2.2.4. *Other components of the sediment*

Variability in particle-size fractions, siliceous microfossil abundance and glauconite abundance show parallels with changes found in some the isotope and calcareous microfossil proxies. Coarse sand wt% correlates with planktic foraminiferal abundance (r=0.53) (Figure 9), implying they constitute a major component of this fraction, as well as $CaCO_3$. Weigh percentage of SS is anticorrelated to $\delta^{18}O$ (Vs $\delta^{18}O_{Catapsydrax}$ (sub-thermocline), r=-0.57; Vs $\delta^{18}O_{Cibicidoides}$ (benthic, good visual correlation)), suggesting density-driven %SS deposition. On the other hand, correlation between %SS and $F3_{BF}$ (r=0.55) and the parameter associated with it, i.e. epifaunal phytodetritus taxa (r=0.42), could be indicative of lower availability of organic matter when selective erosion of finer components (winnowing) occurs (Tesi et al., 2016). A minimum in sediment fine fraction is coeval with Elongate benthic group peak, supporting the idea of current winnowing removing fine particles, as this group is linked to enhanced current strength associated with stronger deep water circulation in the NA (Ortiz & Kaminski, 2012).

Biosilica, including diatoms, radiolaria and silicoflagelates, is abundant in the late Eocene of Site 612 with typically temperate, not tropical affinities (Bukry, 1987; Palmer, 1987). This is interpreted to reflect bathyal depths and high biological productivity along the New Jersey slope (Palmer, 1987). Moreover, it has been suggested that upwelling fronts may have been more prominent along the fore-shelf edge off New Jersey during the high sea-level stands of late Eocene compared today (Poag, 1987). The new records capture this pattern but also show a further peak in siliceous fossils involving an increase of 40% (136.8-136.08 mbsf), both in diatom and other siliceous plankton records curves (Figures 9 and 10), immediately preceding the E/O. This points to high availability of Si that could be originated either by enhanced deep water circulation, which strengthened at this time (Coxall et al., 2018) weathering seafloor basalt (Frings et al., 2016) and bringing dissolved Si to the Site by advection, or associated changes in surface currents interacting close to the shelf-break due to strengthening of the Gulf Stream and

potentially the opposing Labrador Current. The glauconite counts show a sustained increase after 33.61 Ma (136.08 to 135.47) supporting previous findings of increased concentrations of reworked glauconite associated with lowered sea level of the early Oligocene (Browning et al., 2008), both on the shelf and offshore at Site 612. However, the new data pinpoint this, and reveal how this immediately follows the Si peak. The increased glauconite at Site 612 depths may be the result of increased gravity flow mechanisms dispersing shelf sediments to the continental slope, as the hinterland moved progressively seaward (Diester-Haass et al., 2002; Poag, 1987).

5.2.2.5. Identification of shifting ocean-climate regimes at Site 612: Phases 0-4

To summarize the first stage of interpretations, after analyzing the various proxies at Site 612 (foraminiferal C and O isotopes, microfossil assemblages and other components of the sediment), a series of proxy and environmental regime shifts that occur at similar depths in the section among the various proxies have been recognized, allowing to define 5 successive environmental phases or episodes. The phases are largely defined based on all the proxies. However, benthic foraminiferal assemblages seem to be the proxy that shows highest sensitivity to variability, making possible the recognition of all the phases within its record. Other proxies (i.e. $\delta^{13}C$ and biosilica) do not record such a clear signal throughout the entire record, but they exhibit strikingly distinctive shifts during some of the phases that are essential for the interpretation. The depths of the regime shifts and respective phases are as follows; Phase 0 (below the base of the new sampling) 181.38 – 141.46 mbsf; Phase 1, 141.46 – 138.35 mbsf; Phase 2, 138.35 – 136.8 mbsf; Phase 3, 136.8 – 136.08 mbsf and Phase 4, above 136.08 mbsf. These are identified in Figs. 4 and 7, summarized and compiled in Table 7 and Figure 10 and described fully below and in relation to the previous perspectives on the evolution of

paleoproductivity on the western Atlantic margin and wider Atlantic Ocean circulation during the late Eocene by Coxall et al. (2018).

5.2.2.5.1. Phase 0 (P0): 181.38 – 141.46 mbsf (36.3-34.96 Ma)

Is characterized by a $\delta^{18}O_{Cib}$ trend to enriched values (0.5‰) and a $\delta^{13}C_{Cib}$ trend to depleted values (1.4‰), most likely indicating a local bottom water cooling or/and an inflow of older water masses. Interpretations can only be based on the isotopic data by previous authors (Miller et al., 1991; Pusz et al., 2009) due to the limitation/lack of microfossil assemblage data. However, the record of *Bolivina* -deep infaunal taxa associated to high availability of organic C- as reported by Miller and Katz, (1987) shows a period of sustained low organic C content in deep waters (Fig.10).

5.2.2.5.2. Phase 1 (P1): 141.46 – 138.35 mbsf (34.96-34.9 Ma)

Characterized by (1) high abundance and stability of deep planktic dwellers ($F1_{PF}$; representing ~60% of the assemblage) and occasional abundance of surface opportunistic species, probably indicative of intermittent upwelling and enhanced productivity conditions; (2) increasing nannoplankton most abundant species ($F2_{CN}$; small *Reticulofenestra*, a species linked to blooms; ~40%); and (3) high abundance of deep benthic infaunal taxa that need high sustained organic matter fluxes ($F1_{BF}$). Therefore, primary productivity remained constantly high during this phase, supporting organic matter fluxes to the seafloor, also supported by an increase in *Bolivina* record (Figure 10). (4) All species $\delta^{18}O$ point towards an stratified water column, being thermocline and benthic values within the same range; (5) benthic $\delta^{18}O$ shows a shifting record with a general trend towards enriched values – continuation of P0 -, which can be interpreted as local bottom water cooling; (6) $\delta^{13}C$ shows a negative trend - continuation from P0- possibly indicating an

inflow of older water masses and (7) high FF wt % and sedimentation rate are linked to relatively low deep water velocity conditions (Fig. 10, Table 7).

5.2.2.5.3. Phase 2 (P2): 138.35 – 136.8 mbsf (34.9-34.87 Ma)

Characterized by (1) long term stability of planktic mixed layer dwellers ($F3_{PF}$) abundance and high variability of surface opportunistic ($F2_{PF}$) and deep water dwellers ($F1_{PF}$) – being the later the most abundant group of the assemblage, as in P1 –; (2) low variability and high abundance of small *Reticulofenestra* (50%), species related to eutrophic and warm conditions, supporting that P2 is an enhanced productivity interval; (3) high abundance of deep benthic infaunal taxa that need high sustained organic matter fluxes ($F1_{BF}$); (4) more positive $\delta^{18}O_{Cib}$ values and an increased gradient between this and thermocline *Catapsydrax* $\delta^{18}O$ record reflects the long-term bottom water cooling and salinification, while the isotopic composition of planktic foraminiferal $\delta^{18}O$ remains nearly unchanged; (5) $\delta^{13}C$ negative trend continues from the previous intervals, reaching more stable and maximum values, probably signature of a densification event coincident with that described in Coxall et al. (2018) starting at ~34.6 Ma, as the major $\delta^{18}O$ gradient coincides with the low nutrient $\delta^{13}C$ peak; (6) relatively high sedimentation rate, low preservation of fine fraction wt% and preferential preservation of higher fractions (SS and 106 µm) point towards winnowing, probably due to enhanced ventilation and bottom current velocity (Fig. 10, Table 7).

5.2.2.5.4. Phase 3 (P3): 136.8 – 136.08 mbsf (34.87-33.86 Ma)

Characterized by (1) high abundance of benthic foraminiferal elongate group -linked to more vigorous (than in P2) ocean ventilation - that correlates with $F2_{BF}$, probably indicative of laterally advected high nutrient fluxes of refractory organic matter, as in an scenario of low export

productivity; (2) and low BF diversity, as in an scenario of stressing conditions at the seafloor; (3) agglutinated taxa near to 0 values, as reported for other high latitude NA sites under strong deep current flow (Fig.10); (4) planktic foraminiferal mixed layer dwellers ($F3_{PF}$) peak, as in an scenario of deep thermocline; (5) regarding calcareous nannofossils, decreasing small *Reticulofenestra* spp. ($F2_{CN}$) related to high productivity conditions, increasing *R. daviesii* (cosmopolitan) and drop of placolith-bearing taxa V:SA point towards an ecological turnover in calcareous nannofossil assemblage (Figure 6); (6) highly variable $\delta^{18}O_{Cib}$; (9) $\delta^{18}O_{ML}$ negative excursion (~1‰), probably indicating a warm pulse of mixed layer waters; (8) pre-EOB $\delta^{13}C_{Cib}$ positive shift to near-initial values (~1‰; to pre-NCW pulse values), probably indicating the end of a negative sourced NCW and a NCW with younger ^{13}C-rich $\delta^{13}C$; (9) maximum biosilica peak, probably indicating input of Si-rich water-after erosion of seafloor and/or margins- that enhanced biosilica productivity. (10) The above considerations match with the existence of a hiatus, relatively low sedimentation rate, minimum FF wt% peak, maximum 106 µm Ø particle size fraction- probably responsible of the benthic maximum and relatively high planktic total abundance - and are in agreement with an erosional unconformity found in North Atlantic Sites indicating enhanced bottom current ventilation (Fig. 10, Table 7).

5.2.2.5.5. Phase 4 (P4): 136.08-135.47 (33.86-32.94 Ma)

Characterized by (1) low diversity index showed in planktic microfossil assemblages; (2) ecological turnover showed by the benthic foraminiferal assemblage, as the Elongate Gp. was replaced by the opportunistic Epifaunal Phytodetritus group, probably because the specific food source for Elongate Gp. (phytoplankton or prokaryotes) was directly impacted by the cooling; (3) planktic foraminiferal deep water dwellers ($F1_{PF}$) abundance recovered to values more similar to P1 and P2; (4) calcareous nannofossil *R. daviesii* cosmopolitan species increased, as well as $F2_{CN}$ and *Discoaster* (related to warm and/or oligotrophic conditions); (5) while small

Reticulofenestra spp. showed high variability and placolith-bearing taxa V:SA decreased (Figure 6). (6) The second hiatus in the record is present in this Phase (Table 6), that together with relatively low sedimentation rate, (7) high SS and variable FF wt% (Fig. 9) point towards relatively high ventilated bottom waters, but not as strong velocities as in P3, decreasing the erosive action. (8) Therefore, it most likely affected the biosilica decrease to average abundance values. (9) High glauconite content could be related to sedimentation after lowered sea level, evidencing a previous eustatic fall (Fig. 10). (10) While $\delta^{18}O_{Cib}$ remains stable and relatively positive, planktic $\delta^{18}O$ shows no evidence of surface cooling during the EOT, with a negative peak in all planktic species (~1-2‰). (11) This is coupled with a negative $\delta^{13}C$ shift (~2‰) in all species, probably linked to input of continental sourced O.M. or a methane hydrate release due to slope instability triggered by the already mentioned eustatic fall (Fig. 10, Table 7).

5.2.2.6. Ecological turnover across EOT affected by oceanographic regimes

Phase 3 is the interval of major ecological turnover within the studied record. Interestingly, benthic foraminiferal assemblage data suggest a major change in Site 612 was the modality of food supply to the seafloor, which became more seasonal and pulsed during P4. This favored the development of opportunistic phytodetritus species (i.e. *Alabamina* cf. *dissonata*, *Osangularia* cf. *dissonata* and *O. umbonatus*, scoring Factor 3, see multivariate analysis, Table 5, Fig. 7) that out-competed the deep-infaunal taxa that need high sustained nutrient fluxes (i.e. decrease of Ext. Gp.; increase of I/E index). During the same interval, planktic foraminiferal thermocline dwellers abundance decreases while ML dwellers abundance increases, probably caused by the stratification of water and deepening of thermocline, isolating nutrient rich deep waters from the mixed layer and suppressing primary productivity (extended discussion below). In fact, small *Reticulofenestra* abundance, a species related to blooms, decreases during P3. Increased (but intermittent) abundance of *Discoaster* spp. and *Dictyococcites daviesii* during P3

and P4 (Fig. 6) probably indicates enhanced but intermittent or seasonal upwelling due to the intensification of deep water circulation, supported by the peak of biosilica during P3, attributable to remineralization of Si recycled from ventilated seafloor sediments/rocks. In the same interval, the shift from high small *Reticulofenestra* abundance to Si-bearing microfossils very near to the EOB (~136.3 mbsf, Fig. 10) could indicate a shift in the type of productivity from calcareous to siliceous organisms, caused by an alteration in Si fluxes (also proposed for other sites according to Diester-Haass & Zahn, 1996, 2001 and Ehrmann & Mackensen, 1992). Continental shelves are massive biogenic silica (BSi) pools due to proximity to continental nutrients and higher preservation efficiencies (DeMaster, 2002). Remobilization of continental shelf sediments after sea level lowstands has been proposed as one of the major Si input to ocean during LGM (Frings et al., 2016). Sea-level lowering after Antarctica ice-sheet formation could have followed the same mechanism, enhancing regional Si input from newly exposed land surfaces of continental shelf. According to Frings et al. (2016), changes in associated dissolved silica (DSi) flux during LGM related to continental shelf BSi deposit remobilization account for 20 %. At Site 612 BSi increased 40%, therefore, another Si source might have played an important role; dissolved Si can also be supplied from weathering of seafloor basalt (Frings et al., 2016). This is a plausible scenario of greater input of Si by the DBWC enhanced ventilation. This is in agreement with Berggren and Hollister (1974) proposal, who suggested that increased early to middle Eocene deposition of biosiliceous sediments in the North Atlantic correlates with the first formation, sinking, and upwelling of cold, deep waters in the northern North Atlantic.

5.2.3. Continent-ocean interactions and shelf carbon release at the opening of the Cenozoic Ice house

A key finding of this study is the negative $\delta^{13}C$ excursion (~2 ‰ in all the species) recorded by all foraminiferal species during P4 lasting ca. 0.53 Myrs (33.68-33.15) (Figure 10). This coincides

with a negative $\delta^{18}O$ excursion, equivalent to ~8°C SST increase, from surface to thermocline depths (Figure 10). This is the first time this has been described in this setting, probably due to lower sampling of previous studies and the condensed nature of the Site 612 section. The source of the negative $\delta^{13}C$ excursion is unclear. One option is locally sourced input of isotopically depleted marsh/mangrove ("blue carbon") $\delta^{13}C$ associated with the rapid global sea-level fall of ~55 m (Miller et al., 2005a; Pekar et al., 2001) and subsequent exhumation of terrigenous sediments. An equivalent excursion in bulk carbonates (also ~2 ‰) from a shallow water section in Malaysia, was interpreted as indicating the formation of an exposure horizon due to sea-level fall (Cotton et al., 2014). It is possible that this was happening on a large scale around continental margins. Since this Indian Ocean site is coeval to Site 612, this excursion could be explained alternatively by a rapid release of methane hydrates from the seafloor, due to slope instability triggered by the already mentioned eustatic fall, as it has already been suggested by other studies (Armstrong McKay et al., 2016; Berger, 2007). It seems plausible that during the precursor cooling (Coxall et al., 2005) methane was sequestered in clathrates (Berger, 2007), and the sea-level fall destabilized hydrates on the margin, suddenly releasing the carbon to the atmosphere. In this way, the negative $\delta^{13}C$ signature of methane seepage was instantly propagated from deep to surface waters, and after warming the atmosphere due to its greenhouse effect, registered in shallow water $\delta^{18}O$ and propagated to deep waters. This is supported by the existence of two Atlantic-wide unconformities (Berton & Vesely, 2018; Boyle et al., 2017; Mountain & Tucholke, 1985; Tucholke & Mountain, 1979; 1986; Tucholke & McCoy, 1986) associated with hiatuses in Site 612 - beneath or in the same level as the $\delta^{13}C$ peak-, probably related to sea-level changes and/or enhanced deep ventilation. Weathering feedbacks in the early Oligocene associated with Antarctic glaciation are of considerable interest and while continental margins have been suggested as a source of high $\delta^{13}C$ associated with the exposure and erosion of neritic limestone that could help explain the positive $\delta^{13}C$ excursion associated with the EOT (Armstrong McKay et al., 2016; Merico et al., 2008), it is possible that exposure of

organic carbon on some shelves could be at least a transient source that ameliorated the effects of the EOGM. The Eastern Seaboard Shelf for example was not a carbonate platform but a siliciclastic shelf, of considerably large extent at that, although with low accumulation rates, and erosion of this material by sea level fall could have been significant. Moreover, exhumation of large carbon stocks in massive-scale coastal swamps and marshes, as reconstructed from pollen (Kotthoff et al., 2014) could be globally important.

6. Conclusions

1. DSDP Site 612, positioned in the western North Atlantic margin (New Jersey), has a key location to analyze the vertical structure of the ocean in North Hemisphere mid-latitudes during the Eocene-Oligocene transition (EOT). The micropaleontological and isotopical records ($\delta^{13}C$ and $\delta^{18}O$ stable isotopes measured in foraminifera shells) suggest a thermally stratified water column over 1000 m in the late Eocene.

2. Despite not being an objective of this PhD thesis, this work includes a revision of Site 612 EOT planktic foraminifera, and has been compared with Fuente Caldera section (Granada, Spain) in the western Tethys. In total 43 planktic foraminifera have been recognized, comprising 18 genera. For paleoenvironmental interpretations, these species were paleoecologicaly characterized applying a factor analysis to Site 612 and Fuente Caldera planktic foraminifera assemblages, and reviewing previous paleoecologic and isotopic studies, aiming to arrange the species into eco-groups.

3. A detailed study of the planktic foraminifera biostratigraphy provides constrains to build a new age model for the studied series in Site 612, which spans between 34.96 and 33.06 Ma (~ 2 Myrs). The EOB was positioned in Site 612 according to the last occurrence of *Hantkenina* spp. The age model indicates a very low sedimentation rate and the continuity of the record in the major part of the upper Priabonian (upper Eocene) and the presence of two hiatuses (H2 and H3) across the EOB. The hiatus likely recorded episodes of intense erosion caused by intensified deep water currents interacting with the North American continental margin.

4. Hiatus H2 spans between 34.87 and 34.15 Ma (0.72 Myrs) of upper Priabonian. The interval between the last occurrences of calcareous nannofossil *D. saipanensis* and *Hantkenina* spp. is very condensed, suggesting a third hiatus (H3). Hiatus H3, identified

in this study for the first time, affects the EOB and lower Rupelian (lower Oligocene), between 33.86 and 33.67 Ma (0.19 Myrs), is truncated by the stratigraphic ranges of the *Hantkenina* species, preceded by further changes in benthic foraminiferal assemblages and signaled by a negative excursion in benthic foraminiferal $\delta^{13}C$, indicative of further bottom current strengthening.

5. The age model enables the division of the studied series in 3 time intervals with different sedimentary regimes separated by H2 and H3 hiatus: (1) interval between 34.96-34.87 Ma, with a sedimentation rate of 53.76 m/my, (2) interval between 34.15 and 33.86 Ma, with a sedimentation rate of 0.87 m/my and (3) interval between 33.67 and 33.06 Ma, with a sedimentation rate 0.87 m/my.

6. Several studies suggest that the first pulse of proto- North Atlantic Deep Water (NADW) or Northern Component Water (NCW) started at the EOT, but is not yet clear why and when. New micropaleontological and foraminiferal stable isotope data in Site 612 support recent studies suggesting intensification in deep water flow in the western North Atlantic starting from 2 Myrs before Antarctic glaciation and continuing to the EOB. At the seabed, benthic foraminifera $\delta^{13}C$ and $\delta^{18}O$ indicate densification of this water, which supports the salinity increase in the North Atlantic as a result of the Arctic closure suggested by Coxall et al. (2018) and Hutchinson et al. (2019). Across the EOT, benthic foraminifera $\delta^{18}O$ increased by 1‰, which could be interpreted either as a net cooling of maximum 6°C, a salinity increase, or a combination of the two.

7. Other sedimentary proxies support the interpretation of intensified water ventilation: During this period, taxa related to increased deep water ventilation dominates benthic foraminifera assemblage; two hiatuses punctuate the record, likely recording episodes of intense erosion caused by the intensified ventilation; a minimum in the fine fraction weight % associated with winnowing coincides with the interval of increased ventilation;

as well as a peak in biosilica, that points to high availability of Si that could be originated by enhanced deep water circulation.

8. Benthic foraminiferal assemblages varies from a dominance period of taxa that need high sustained organic matter fluxes (Phases 1 and 2; 34.96-34.87 Ma), followed by a dominance period of taxa related to increased deep water ventilation (Phase 3, 34.87-33.86 Ma) and, after the EOB and during the earliest Oligocene (Phase 4; 33.86-32.94 Ma), a takeover of taxa that bloom opportunistically when a spring plankton bloom results in seasonal deposition of phytodetritus on the seafloor.

9. In this record, there is no sea surface temperature (SST; estimated from planktic $\delta^{18}O$ data) cooling evidence during the EOT, as it would be expected from the long-term benthic stack (Zachos et al., 2001). There is rather a warming of 6°C in the basal Oligocene - also observed in a more Easterly location (Site U1404). This suggests strong asymmetric surface temperature response during EOT, indicative of transient thermal decoupling of North Atlantic from Southern Ocean. Another possibility is the northwards migration of the inter tropical convergence zone (ITCZ) as it has previously been proposed.

10. Large negative excursions in surface and thermocline planktic foraminiferal $\delta^{18}O$ and $\delta^{13}C$ (-1.2 and -1.5 ‰ over ~0.5 Myrs) during the lowermost Oligocene documented here for the first time, are attributed to increased cross-shelf transport of shelf water to the continental slope due to reorganization of surface currents and seaward advance of the shelf-break after sea level fall, possibly with increased inputs of exhumed terrestrial "blue carbon" and warm or fresh neritic waters.

11. The importance of exhumed neritic C in continental margins during the EOT and its role in the associated C cycle perturbation and global cooling is not yet clear, and needs further investigation.

12. Planktic foraminifera assemblage was dominated by deep dwellers but an abundance increase of mixed layer dwellers was identified (from 34.9 and predominantly from 34.87 to 32.94 Ma). This abundance increase might be related to variability of thermocline depth but the link to the climate turnover needs to be investigated.

13. Identical results in the Site 612 inter-lab comparison (Pusz et al., 2009; Miller et al., 1991) and coherent when compared to other synchronous western NA sites (647, SSQ, ASP-5 and ODP 1053) showed that 'glassy' foraminiferal tests from Site 612 are good past tracers.

Conclusiones

1. El DSDP Site 612 situado en el margen occidental del Atlántico Norte (Nueva Jersey) es un punto clave para analizar la estructura vertical del océano en latitudes medias del Hemisferio Norte durante el tránsito Eoceno-Oligoceno (EOT). El registro micropaleontológico e isotópico (relaciones isotópicas $\delta^{13}C$ y $\delta^{18}O$ medidas sobre conchas de foraminíferos) sugiere en este lugar una columna de agua bien estratificada térmicamente sobre 1000 m de profundidad durante el Eoceno tardío.

2. Aunque no fue un objetivo de esta Tesis Doctoral, se ha realizado una revisión de la taxonomía de foraminíferos planctónicos del EOT en el Site 612, comparándola con la de la sección de Fuente Caldera (Granada) del Tetis occidental. En total se han reconocido 43 especies de foraminíferos planctónicos pertenecientes a 18 géneros. Para las interpretaciones paleoambientales, se caracterizaron paleoecológicamente estas especies aplicando un análisis factorial a las asociaciones de foraminíferos planctónicos de Site 612 y de Fuente Caldera, y revisando estudios paleoecológicos e isotópicos previos, con el objetivo de agrupar las especies en ecogrupos.

3. Un detallado estudio bioestratigráfico de foraminíferos planctónicos ha proporcionado nuevos límites para construir el modelo de edad para la serie estudiada en el Site 612, que abarca entre 34.96 y 33.06 Ma (~ 2 Myrs). El EOB ha sido situado en Site 612 con el último registro de *Hantkenina* spp. El modelo de edad indica una tasa de sedimentación muy baja, la continuidad del registro en la mayor parte del Priaboniense superior (Eoceno superior) y la presencia de dos hiatos (H2 y H3) entorno al límite Eoceno/Oligoceno (EOB). Estos hiatos parecen estar ocasionados por importantes cambios en la circulación oceánica, principalmente por episodios de intensa erosión

provocados por la intensificación de corrientes profundas en el margen continental de Norte América.

4. El hiato H2 abarca entre 34.87 y 34.15 Ma (0.72 Myrs de duración) del Priaboniense superior. El intervalo entre los últimos registros del nanofósil calcáreo *Discoaster saipanensis* y *Hantkenina* spp. está muy condensado, lo que sugiere un tercer hiato (H3). El hiato H3, que es identificado en este estudio por vez primera, afecta al EOB y al Rupeliense inferior (Oligoceno inferior), entre 33.86 y 33.67 Ma (0.19 Myrs de duración). Está marcado por el truncamiento aparente de los rangos estratigráficos de las especies de *Hantkenina*, una excursión negativa del $\delta^{13}C$ en foraminíferos bentónicos y precedido por cambios bruscos en las asociaciones de foraminíferos bentónicos, indicativos del fortalecimiento de la corriente del fondo.

5. El modelo de edad permite dividir la serie estudiada en tres intervalos de tiempo con diferentes regímenes sedimentarios y separados por los hiatos H2 y H3: (1) intervalo entre 34.96 y 34.87 Ma, con una tasa de sedimentación de 53.76 m/my, (2) intervalo entre 34.15 y 33.86 Ma, con una tasa de sedimentación de 0.87 m/my, y (3) intervalo entre 33.67 y 33.06 Ma, con una tasa de sedimentación de 0.87 m/my.

6. Diferentes estudios sugieren que el primer pulso de la proto-corriente de Agua Profunda del Atlántico Norte (NADW en siglas inglesas) comenzó en el EOT, pero aún no está claro cuándo y por qué causa. Los nuevos indicadores micropaleontológicos e isotópicos en Site 612 corroboran estudios recientes que sugieren la intensificación del flujo de aguas profundas en el Atlántico Norte occidental comenzando 2 millones de años antes de la glaciación antártica y continuando hasta el EOB. En el fondo marino, los isotopos estables de $\delta^{13}C$ y $\delta^{18}O$ medidos en foraminíferos bentónicos indican la densificación de estas aguas, lo cual confirma el incremento en salinidad en el Atlántico Norte como resultado del cierre del Ártico, sugerido por Coxall et al. (2018) y Hutchinson et al.

(2019). En el EOT, el $\delta^{18}O$ medido en foraminíferos bentónicos incremento por un 1‰, siendo posible interpretarlo como un enfriamiento neto máximo de 6°C, un incremento de la salinidad o la combinación de ambos.

7. Durante este periodo, otros indicadores sedimentarios respaldan la intensificación de la ventilación en aguas profundas interpretada: La asociación de foraminíferos bentónicos es dominada por taxones relacionados con mayor ventilación de aguas profundas; dos hiatos interrumpen el registro, probablemente indicando episodios de intensa erosión; un mínimo en el porcentaje en peso de la fracción fina asociado con selección por corrientes (*winnowing*) coincide con el intervalo de mayor ventilación; y un brusco incremento de la biosílice sugiere una alta disponibilidad de Si debido a una circulación de aguas profundas intensificada.

8. Las asociaciones de foraminíferos bentónicos varían desde un predominio de taxones que necesitan flujos de materia orgánica altos y sostenidos (*Phase* 1 y 2; 34.96 - 34.87 Ma), seguidos de un predominio de taxones relacionado con una mayor ventilación de aguas profundas (*Phase* 3; 34.87 - 33.86 Ma) y, tras el EOB y durante el Oligoceno más temprano (*Phase* 4; 33.86 - 32.94 Ma), una proliferación de taxones oportunistas debido a floraciones primaverales de plancton que provocan el depósito estacional de fitodetritos en el fondo marino.

9. En Site 612 no hay evidencia de enfriamiento en la temperatura de las aguas superficiales (SST) durante el EOT como pudiera sugerir la compilación global de $\delta^{18}O$ de foraminiferos bentonicos (Zachos et al., 2001). Por el contrario, se puede interpretar un calentamiento de 6°C en el Oligoceno más temprano, lo que también fue identificado previamente en un sondeo más oriental en el Atlántico Norte (Site U1404). Estos datos sugieren una respuesta asimétrica de la temperatura de las aguas superficiales entre el Atlántico Norte y el Océano Antártico durante el EOT, indicativo de un desacoplamiento

térmico transitorio entre ambos hemisferios. Otra alternativa es la migración hacia el norte de la Zona de Convergencia Intertropical (ITCZ en siglas inglesas) como se había propuesto previamente.

10. En Site 612 han sido identificadas por primera vez dos importantes excursiones negativas del $\delta^{13}C$ y $\delta^{18}O$ en foraminíferos planctónicos habitantes de aguas superficiales y de la termoclina en el Oligoceno más inferior. Esas excursiones isotópicas han sido atribuidas al transporte de aguas de plataforma al talud continental provocado por una reorganización de las corrientes superficiales y el avance hacia el mar de la ruptura de plataforma tras una caída del nivel del mar. Esto provocó posiblemente mayores entradas de carbono azul (^{12}C) proveniente de aguas continentales y de aguas neríticas cálidas o de menor salinidad.

11. Son necesarias investigaciones más detalladas respecto a la importancia del C nerítico exhumado en márgenes continentales durante el EOT, y su rol en la perturbación del ciclo del carbono y en el enfriamiento global asociados.

12. La asociación de foraminiferos planctónicos esta dominada por los habitantes de aguas profundas, pero se observa un aumento en abundancia de los habitantes de la capa de mezcla desde hace 34.9 Ma y, sobre todo, desde 34.87 a 32.94 Ma. Este cambio pudo ser causado por la variabilidad de la profundidad de la termoclina, pero su relacion con el cambio climático debe ser investigada.

13. Los resultados isotópicos obtenidos son idénticos al compararlos con los de otros laboratorios para el mismo sondeo (Pusz et al., 2009; Miller et al., 1991) y son coherentes al compararlos con otros sondeos sincrónicos del Atlántico Norte occidental (Site 647, SSQ, ASP-5 y ODP 1053), por lo que las conchas de foraminíferos con apariencia vítrea del Site 612 son excelentes archivos del pasado.

Acknowledgements

This thesis is a contribution to the projects CGL2011-23077, CGL2014-58794 and CGL2015-64422-P (MINECO/FEDER-UE) and Aragonian DGA group E05. I also thank the Spanish Economy and Competitiveness Ministry for the BES-2012-058945 grant. I would like to acknowledge the use of the *Servicio General de Apoyo a la Investigacion-SAI, Universidad de Zaragoza*, the Stockholm University Stable Isotope Lab (SIL) and Uppsala University micropaleontology lab. This research used samples and data provided by the IODP. Benthic foraminiferal counts were performed by Nicoletta Mancin and Calcareous nannofossil counts by Manuela Bordiga, who also helped drawing the main initial interpretations on these groups, together with Jorijntje Henderiks and Helen Coxall.

I extend my gratitude to Heike Siegmund for her assistance with handling the isotopic samples, Nicolàs Campione for assistance with *R*, David Hutchinson for his help in *Python* and oceanography questions, Natalia Barrientos for her comments to help improve the initial manuscript, Jenny Sjöström for the every day support and to the external reviewer Agatha deBoer for taking time to read and validate this document.

I dedicate this thesis to Eustoquio Molina, who sadly passed away a year ago (30 September 2018). He introduced me to Planktic foraminifera during the master thesis, and was one of this thesis supervisors until he passed away. He had a unique way for understanding planktic foraminiferal taxonomy given by his vast experience, which will certainly be missed by the community. However, his work will still be kept alive; recently species that were very important for him (*Globigerinella molinae* (Popescu and Brotea, 1989) and *Globigerinella navazuelensis* (Molina, 1979)) were endorsed and updated in the Atlas of Oligocene planktic foraminifera (Wade et al., 2018).

Also, this thesis could have not been the same without the initial guidance of Jorijntje Henderiks and the great supervision of Helen Coxall and Ignacio Arenillas.

Special mention to all the people that encouraged me on the way to completing this thesis. Thank you, Eskerrik asko, Gracias, Tack: you know who you are!

References

Abbott, W. H. (1987). Diatom occurrences, Deep Sea Drilling Project sites 612 and 613. *Initial Reports of the Deep Sea Drilling Project*, *95*, 417.

Abelson, M., & Erez, J. (2017). The onset of mondern-like Atlantic Meridional overturning circulation at the Eocene-Oligocene transition: Evidence, causes and possible implications for global cooling. *Geochemistry, Geophysics, Geosystems*, *18*, 2177–2199. https://doi.org/10.1002/2017GC006826.

Agnini, C., Fornaciari, E., Raffi, I., Catanzariti, R., Pälike, H., Backman, J., & Rio, D. (2014). Biozonation and biochronology of Paleogene calcareous nannofossils from low and middle latitudes. *Newsletters on Stratigraphy*, *47*(2), 131–181. https://doi.org/10.1127/0078-0421/2014/0042

Armstrong, H., & Brasier, M. D. (2005). *Microfossils* (2nd ed.). Cornwall: Blackwell Publishing Ltd.

Armstrong McKay, D. I., Tyrrell, T., & Wilson, P. A. (2016). Global carbon cycle perturbation across the Eocene-Oligocene climate transition. *Paleoceanography*, *31*(2), 311–329. https://doi.org/10.1002/2015PA002818

Arthur, M. A., Dean, W. E., Zachos, J. C., Kaminski, M., Hagerty Reig, S., & Elmstrom, K. (1989). Geochemical Expression of Early Diagenesis in Middle Eocene-Lower Oligocene Pelagic Sediments in the Southern Labrador Sea, Site 647, ODP Leg 105. In *Proceedings of the Ocean Drilling Program, 105 Scientific Results*. Ocean Drilling Program. https://doi.org/10.2973/odp.proc.sr.105.157.1989

Aze, T., Ezard, T. H. G., Purvis, A., Coxall, H. K., Stewart, D. R. M., Wade, B. S., & Pearson, P. N. (2011). A phylogeny of Cenozoic macroperforate planktonic foraminifera from fossil data. *Biological Reviews*, *86*(4), 900–927. https://doi.org/10.1111/j.1469-185X.2011.00178.x

Baatsen, M., von der Heydt, A. S., Huber, M., Kliphuis, M. A., Bijl, P. K., Sluijs, A., & Dijkstra, H. A. (2018). Equilibrium state and sensitivity of the simulated middle-to-late Eocene climate. *Climate of the Past Discussions*, (April), 1–49. https://doi.org/10.5194/cp-2018-43

Baldauf, J. G. (1992). MIDDLE EOCENE THROUGH EARLY MIOCENE DIATOM FLORAL TURNOVER. In Donald R Prothero & W. A. Berggren (Eds.), *Eocene-Oligocene Climatic and Biotic Evolution* (pp. 310–326). Princeton University Press. Retrieved from http://www.jstor.org/stable/j.ctt7zvp65.19

Benoiston, A. S., Ibarbalz, F. M., Bittner, L., Guidi, L., Jahn, O., Dutkiewicz, S., & Bowler, C. (2017). The evolution of diatoms and their biogeochemical functions. *Philosophical Transactions of the Royal Society B: Biological Sciences*, *372*(1728). https://doi.org/10.1098/rstb.2016.0397

Berger, W. H. (2007). Cenozoic cooling, Antarctic nutrient pump, and the evolution of whales. *Deep-Sea Research Part II: Topical Studies in Oceanography*, *54*(21–22), 2399–2421. https://doi.org/10.1016/j.dsr2.2007.07.024

Berggren, W. A. (2005). A revised Tropical To Subtropical Paleogene Planktonic Foraminiferal Zonation. *The Journal of Foraminiferal Research*, *35*(4), 279–298. https://doi.org/10.2113/35.4.279

Berggren, W. A., Kent, D. V., Aubry, M. P., & Hardenbol, J. (1995). *Geochronology, time scales and global stratigraphic correlation; unified temporal framework for an historical geology*. *Geochronology, Time Scales and Global Stratigraphic Correlation*.

BERGGREN, W. A., & HOLLISTER, C. D. (1974). PALEOGEOGRAPHY, PALEOBIOGEOGRAPHY AND THE HISTORY OF CIRCULATION IN THE ATLANTIC OCEAN. In *Studies in Paleo-Oceanography* (pp. 126–186). Special Publications of SEPM. https://doi.org/10.2110/pec.74.20.0126

Bernhard, J. M. (1986). Foraminiferal biotopes in Explorers Cove, McMurdo Sound, Antarctica. *The Journal of Foraminiferal Research*, *16*(4), 207–215. https://doi.org/10.2113/gsjfr.17.4.286

Berton, F., & Vesely, F. F. (2018). Origin of buried, bottom current-related comet marks and associated submarine bedforms from a Paleogene continental margin, southeastern Brazil. *Marine Geology*, *395*(January), 347–362. https://doi.org/10.1016/j.margeo.2017.11.015

Birch, H., Coxall, H. K., Pearson, P. N., Kroon, D., & O'Regan, M. (2013). Planktonic foraminifera stable isotopes and water column structure: Disentangling ecological signals. *Marine Micropaleontology*, *101*, 127–145. https://doi.org/10.1016/j.marmicro.2013.02.002

Birch, H. S., Coxall, H. K., & Pearson, P. N. (2012). Evolutionary ecology of Early Paleocene planktonic foraminifera: size, depth habitat and symbiosis. *Paleobiology*, *38*(03), 374–390. https://doi.org/10.1666/11027.1

Boersma, A., Silva, I. P., & Shackleton, N. J. (1987). Atlantic Eocene planktonic foraminiferal paleohydrographic indicators and stable isotope paleoceanography. *Paleoceanography*, *2*(3), 287–331. https://doi.org/10.1029/PA002i003p00287

Bohaty, S. M., Zachos, J. C., & Delaney, M. L. (2012). Foraminiferal Mg/Ca evidence for Southern Ocean cooling across the Eocene-Oligocene transition. *Earth and Planetary Science Letters*, *317–318*, 251–261. https://doi.org/10.1016/j.epsl.2011.11.037

Bolton, C. T., Gibbs, S. J., & Wilson, P. A. (2010). Evolution of nutricline dynamics in the equatorial Pacific during the late Pliocene. *Paleoceanography*, *25*(1), 1–13. https://doi.org/10.1029/2009PA001821

Bordiga, M., Bartol, M., & Henderiks, J. (2015a). Absolute nannofossil abundance estimates: Quantifying the pros and cons of different techniques. *Revue de Micropaleontologie*, *58*(3), 155–165. https://doi.org/10.1016/j.revmic.2015.05.002

Bordiga, M., Henderiks, J., Tori, F., Monechi, S., Fenero, R., Legarda-Lisarri, A., & Thomas, E. (2015b). Microfossil evidence for trophic changes during the Eocene-Oligocene transition in the South Atlantic (ODP Site 1263, Walvis Ridge). *Climate of the Past*, *11*(9), 1249–1270. https://doi.org/10.5194/cp-11-1249-2015

Bordiga, M., Sulas, C., & Henderiks, J. (2017). Reticulofenestra daviesii: Biostratigraphy and paleogeographic distribution across the Eocene–Oligocene boundary. *Geobios*, *50*(5–6), 349–358. https://doi.org/10.1016/j.geobios.2017.07.002

Bornemann, A., D'haenens, S., Norris, R. D., & Speijer, R. P. (2016). The demise of the early Eocene greenhouse – Decoupled deep and surface water cooling in the eastern North Atlantic. *Global and Planetary Change*, *145*, 130–140. https://doi.org/10.1016/j.gloplacha.2016.08.010

Borrelli, C., Cramer, B. S., & Katz, M. E. (2014). Bipolar Atlantic deepwater circulation in the

middle-late Eocene: Effects of Southern Ocean gateway openings. *Paleoceanography*, *29*(4), 308–327. https://doi.org/10.1002/2012PA002444

Bown, P. R., Lees, J. A., & Young, J. R. (2004). Calcareous nannoplankton evolution and diversity through time. In H. R. Thierstein & J. R. Young (Eds.), *Coccolithophores* (pp. 481–508). Berlin, Heidelberg: Springer Berlin Heidelberg. https://doi.org/10.1007/978-3-662-06278-4_18

Boyle, P. R., Romans, B. W., Tucholke, B. E., Norris, R. D., Swift, S. A., & Sexton, P. F. (2017). Cenozoic North Atlantic deep circulation history recorded in contourite drifts, offshore Newfoundland, Canada. *Marine Geology*, *385*, 185–203. https://doi.org/10.1016/j.margeo.2016.12.014

Broeker, W. (1991). The Great Ocean Conveyor. *Oceanography*, *4*(2), 79–89. https://doi.org/10.5670/oceanog.1991.07

Browning, J. V., Miller, K. G., Sugarman, P. J., Kominz, M. A., Mclaughlin, P. P., Kulpecz, A. A., & Feigenson, M. D. (2008). 100 Myr record of sequences, sedimentary facies and sea level change from Ocean Drilling Program onshore coreholes, US Mid-Atlantic coastal plain. *Basin Research*. https://doi.org/10.1111/j.1365-2117.2008.00360.x

Bukry, D. (1987). Eocene Siliceous and Calcareous Phytoplankton, Deep Sea Drilling Project Leg 95. In *Initial Reports of the Deep Sea Drilling Project, 95*. U.S. Government Printing Office. https://doi.org/10.2973/dsdp.proc.95.112.1987

Cai, W. J., Wang, Z. A., & Wang, Y. (2003). The role of marsh-dominated heterotrophic continental margins in transport of CO2 between the atmosphere, the land-sea interface and the ocean. *Geophysical Research Letters*, *30*(16), 1–4. https://doi.org/10.1029/2003GL017633

Cande, S. C., & Kent, D. V. (1995). Revised calibration of the geomagnetic polatiry timescale for the Late Cretaceous and Cenozoic. *Journal of Geophysical Research*, *100*(B4), 6093–6095.

Cattell, R. B. (1966). The Scree Test For The Number Of Factors. *Multivariate Behavioral Research*. https://doi.org/10.1207/s15327906mbr0102_10

Corliss, B. H. (1985). Microhabitats of benthic foraminifera within deep-sea sediments. *Nature*, *314*(6010), 435–438. https://doi.org/10.1038/314435a0

Corliss, B. H., & Chen, C. (1988). Morphotype patterns of Norwegian Sea deep-sea benthic foraminifera and ecological implications. *Geology*, *16*(8), 716. https://doi.org/10.1130/0091-7613(1988)016<0716:MPONSD>2.3.CO;2

Cotton, L. J., Pearson, P. N., & Renema, W. (2014). Stable isotope stratigraphy and larger benthic foraminiferal extinctions in the Melinau Limestone, Sarawak. *Journal of Asian Earth Sciences*, *79*(PA), 65–71. https://doi.org/10.1016/j.jseaes.2013.09.025

Coxall, H.K., Huck, C. E., Huber, M., Lear, C. H., Legarda-Lisarri, A., O'Regan, M., et al. (2018). Export of nutrient rich Northern Component Water preceded early Oligocene Antarctic glaciation. *Nature Geoscience*, *11*(3). https://doi.org/10.1038/s41561-018-0069-9

Coxall, Helen K., & Wilson, P. A. (2011). Early Oligocene glaciation and productivity in the eastern equatorial Pacific: Insights into global carbon cycling. *Paleoceanography*, *26*(2), 1–18. https://doi.org/10.1029/2010PA002021

Coxall, Helen K., Wilson, P. A., Palike, H., Lear, C. H., & Backman, J. (2005). Rapid stepwise onset of Antarctic glaciation and deeper calcite compensation in the Pacific Ocean. *Nature*, 53–57.

Coxall, Helen K., Huck, C. E., Huber, M., Lear, C. H., Legarda-Lisarri, A., O'Regan, M., et al. (2018). Export of nutrient rich Northern Component Water preceded early Oligocene Antarctic glaciation. *Nature Geoscience*, *11*(3), 190–196. https://doi.org/10.1038/s41561-018-0069-9

Cramer, B. S., Toggweiler, J. R., Wright, J. D., Katz, M. E., & Miller, K. G. (2009). Ocean overturning since the late cretaceous: Inferences from a new benthic foraminiferal isotope compilation. *Paleoceanography*, *24*(4), 1–14. https://doi.org/10.1029/2008PA001683

Cramer, B. S., Miller, K. G., Barrett, P. J., & Wright, J. D. (2011). Late Cretaceous-Neogene trends in deep ocean temperature and continental ice volume: Reconciling records of benthic foraminiferal geochemistry (δ18O and Mg/Ca) with sea level history. *Journal of Geophysical Research: Oceans*, *116*(12), 1–23. https://doi.org/10.1029/2011JC007255

Cros, L., Kleijne, A., Zeltner, A., Billard, C., & Young, J. R. (2000). New examples of holococcolith–heterococcolith combination coccospheres and their implications for coccolithophorid biology. *Marine Micropaleontology*, *39*(1–4), 1–34. https://doi.org/10.1016/S0377-8398(00)00010-4

Davies, R., Cartwright, J. A., Pike, J., & Line, C. (2001). Early Oligocene initiation of North Atlantic Deep Water formation. *Nature*, *410*(6831), 917–920. https://doi.org/10.1038/35073551

De, S., & Gupta, A. K. (2010). Deep-sea faunal provinces and their inferred environments in the Indian Ocean based on distribution of Recent benthic foraminifera. *Palaeogeography, Palaeoclimatology, Palaeoecology*. https://doi.org/10.1016/j.palaeo.2010.03.012

Delworth, T. L., Clark, P. U., Holland, M., Johns, W. E., Kuhlbrodt, T., Lynch-Stieglitz, J., et al. (2008). The Potential for Abrupt Change in the Atlantic Meridional Overturning Circulation. *Abrupt Climate Change*, 258–359. Retrieved from http://citeseerx.ist.psu.edu/viewdoc/download?doi=10.1.1.184.709&rep=rep1&type=pdf%5Cnhttp://downloads.climatescience.gov/sap/sap3-4/sap3-4-final-report-ch4.pdf

DeMaster, D. J. (2002). The accumulation and cycling of biogenic silica in the Southern Ocean: revisiting the marine silica budget. *Deep Sea Research Part II: Topical Studies in Oceanography*, *49*(16), 3155–3167. https://doi.org/10.1016/S0967-0645(02)00076-0

Diester-Haass, L., & Zachos, J. (2003). The Eocene-Oligocene transition in the Equatorial Atlantic (ODP Site 925); paleoproductivity increase and positive d13C excursion. In D.R. Prothero, L. C. Ivany, & E. A. Nesbitt (Eds.), *From greenhouse to icehouse; the marine Eocene-Oligocene transition*. New York, NY, United States (USA): Columbia University Press.

Diester-Haass, L., & Zahn, R. (1996). Eocene-Oligocene transition in the Southern Ocean: History of water mass curculation and biological productivity. *Geology*, *24*(2), 163–166. https://doi.org/10.1130/0091-7613(1996)024<0163:EOTITS>2.3.CO

Diester-Haass, L., & Zahn, R. (2001). Paleoproductivity increase at the Eocene - Oligocene climatic transition: ODP/DSDP sites 763 and 592. *Palaeogeography, Palaeoclimatology, Palaeoecology*, *172*(1–2), 153–170. https://doi.org/10.1016/S0031-0182(01)00280-2

Diester-Haass, L., Meyers, P. A., & Vidal, L. (2002). The late Miocene onset of high productivity in the Benguela Current upwelling system as part of a global pattern. *Marine Geology*,

180(1–4), 87–103. https://doi.org/10.1016/S0025-3227(01)00207-9

Den Dulk, M., Reichart, G. J., Van Heyst, S., Zachariasse, W. J., & Van Der Zwaan, G. J. (2000). Benthic foraminifera as proxies of organic matter flux and bottom water oxygenation? A case history from the northern Arabian Sea. *Palaeogeography, Palaeoclimatology, Palaeoecology*. https://doi.org/10.1016/S0031-0182(00)00074-2

Dunkley Jones, T., Bown, P. R., Pearson, P. N., Wade, B. S., Coxall, H. K., & Lear, C. H. (2008). Major shifts in calcareous phytoplankton assemblages through the Eocene-Oligocene transition of Tanzania and their implications for low-latitude primary production. *Paleoceanography*, *23*(4). https://doi.org/10.1029/2008PA001640

Durand, A., Chase, Z., Noble, T. L., Bostock, H., Jaccard, S. L., Townsend, A. T., et al. (2018). Reduced oxygenation at intermediate depths of the southwest Pacific during the last glacial maximum. *Earth and Planetary Science Letters*, *491*, 48–57. https://doi.org/10.1016/j.epsl.2018.03.036

Egan, K. E., Rickaby, R. E. M., Hendry, K. R., & Halliday, A. N. (2013). Opening the gateways for diatoms primes Earth for Antarctic glaciation. *Earth and Planetary Science Letters*, *375*, 34–43. https://doi.org/10.1016/j.epsl.2013.04.030

Ehrmann, W. U., & Mackensen, A. (1992). Sedimentological evidence for the formation of an East Antarctic ice sheet in Eocene/Oligocene time. *Palaeogeography, Palaeoclimatology, Palaeoecology*. https://doi.org/10.1016/0031-0182(92)90185-8

van Eijden, A. J. M., & Ganssen, G. M. (1995). An Oligocene multi-species foraminiferal oxygen and carbon isotope record from ODP Hole 758A (Indian Ocean): paleoceanographic and paleo-ecologic implications. *Marine Micropaleontology*, *25*(1), 47–65. https://doi.org/10.1016/0377-8398(94)00028-L

Elsworth, G., Galbraith, E., Halverson, G., & Yang, S. (2017). Enhanced weathering and CO 2 drawdown caused by latest Eocene strengthening of the Atlantic meridional overturning circulation. *Nature Geoscience*, *10*(3), 213–216. https://doi.org/10.1038/ngeo2888

Emiliani, C. (1954). Temperatures of pacific bottom waters and polar superficial waters during the tertiary. *Science*, *119*(3103), 853–855. https://doi.org/10.1126/science.119.3103.853

Erez, J., & Luz, B. (1983). Experimental paleotemperature equation for planktonic foraminifera. *Geochimica et Cosmochimica Acta*, *47*(6), 1025–1031. https://doi.org/10.1016/0016-7037(83)90232-6

Erhardt, A. M., Pälike, H., & Paytan, A. (2013). High-resolution record of export production in the eastern equatorial Pacific across the Eocene-Oligocene transition and relationships to global climatic records. *Paleoceanography*, *28*(1), 130–142. https://doi.org/10.1029/2012PA002347

Esparza-Alvarez, M. A., Herguera, J. C., & Lange, C. (2007). Last century patterns of sea surface temperatures and diatom (> 38 µm) variability in the Southern California current. *Marine Micropaleontology*, *64*(1–2), 18–35. https://doi.org/10.1016/j.marmicro.2007.01.001

Fairbanks, R. G., Sverdlove, M., Free, R., Wiebe, P. H., & Bé, A. W. H. (1982). Vertical distribution and isotopic fractionation of living planktonic foraminifera from the Panama Basin. *Nature*, *298*(5877), 841–844. https://doi.org/10.1038/298841a0

Falkowski, P., Hopkins, T. S., & Walsh, J. J. (1980). An analysis of factors affecting oxygen

depletion in the New York Bight. *J. Mar. Res.*, *38*, 479–506. Retrieved from papers2://publication/uuid/DC9D30BE-52D4-4240-AA9C-B0AA73ECD66B

Falkowski, P. G., Knoll, A. H., Quigg, A., Raven, J. A., Schofield, O., & Taylor, F. J. R. (2004). The evolution of modern eukaryotic phytoplankton. *Science*, *305*(July), 354–360. Retrieved from http://science.sciencemag.org/

Ferreira, D., Cessi, P., Coxall, H. K., De Boer, A., Dijkstra, H. A., Drijfhout, S. S., et al. (2018). Atlantic-Pacific Asymmetry in Deep Water Formation. *Annu. Rev. Earth Planet. Sci*, *46*, 327–52. https://doi.org/10.1146/annurev-earth-082517

Fine, R. A., & Molinari, R. L. (1988). A continuous deep western boundary current between Abaco (26.5°N) and Barbados (13°N). *Deep Sea Research Part A, Oceanographic Research Papers*, *35*(9), 1441–1450. https://doi.org/10.1016/0198-0149(88)90096-9

Fisher, R. A., Corbet, A. S., & Williams, C. B. (1943). The Relation Between the Number of Species and the Number of Individuals in a Random Sample of an Animal Population. *The Journal of Animal Ecology*, *12*(1), 42–58. https://doi.org/10.2307/1411

Flores, J.-A., Sierro, F. J., & Raffi, I. (1995). Evolution of the Calcareous Nannofossil Assemblage as a Response to the Paleoceanographic Changes in the Eastern Equatorial Pacific Ocean from 4 to 2 Ma (Leg 138, Sites 849 and 852). *Proceedings of the Ocean Drilling Program, 138 Scientific Results*, *138*, 163–176. https://doi.org/10.2973/odp.proc.sr.138.109.1995

Flores, J. A., Bárcena, M. A., & Sierro, F. J. (2000). Ocean-surface and wind dynamics in the Atlantic Ocean off Northwest Africa during the last 140 000 years. *Palaeogeography, Palaeoclimatology, Palaeoecology*, *161*(3–4), 459–478. https://doi.org/10.1016/S0031-0182(00)00099-7

Fontanier, C., Jorissen, F. J., Licari, L., Alexandre, A., Anschutz, P., & Carbonel, P. (2002). Live benthic foraminiferal faunas from the Bay of Biscay: Faunal density, composition, and microhabitats. *Deep-Sea Research Part I: Oceanographic Research Papers*, *49*(4), 751–785. https://doi.org/10.1016/S0967-0637(01)00078-4

Fontanier, C., Jorissen, F. J., Chaillou, G., Anschutz, P., Grémare, A., & Griveaud, C. (2005). Live foraminiferal faunas from a 2800 m deep lower canyon station from the Bay of Biscay: Faunal response to focusing of refractory organic matter. *Deep Sea Research Part I: Oceanographic Research Papers*, *52*(7), 1189–1227. https://doi.org/10.1016/J.DSR.2005.01.006

Fraile, I., Schulz, M., Mulitza, S., & Kucera, M. (2008). Predicting the global distribution of planktonic foraminifera using a\rdynamic ecosystem model. *Biogeosciences*, *5*, 891–911.

Frings, P. J., Clymans, W., Fontorbe, G., De La Rocha, C. L., & Conley, D. J. (2016). The continental Si cycle and its impact on the ocean Si isotope budget. *Chemical Geology*, *425*, 12–36. https://doi.org/10.1016/j.chemgeo.2016.01.020

Funakawa, S., Nishi, H., Moore, T. C., & Nigrini, C. A. (2006). Radiolarian faunal turnover and paleoceanographic change around Eocene/Oligocene boundary in the central equatorial Pacific, ODP Leg 199, Holes 1218A, 1219A, and 1220A. *Palaeogeography, Palaeoclimatology, Palaeoecology*. https://doi.org/10.1016/j.palaeo.2005.07.014

Goldner, A., Herold, N., & Huber, M. (2014). Antarctic glaciation caused ocean circulation changes at the Eocene-Oligocene transition. *Nature*, *511*(7511), 574–577. https://doi.org/10.1038/nature13597

Gooday, A. J. (1988). A response by benthic Foraminifera to the deposition of phytodetritus in the deep sea. *Nature*, *332*, 70. Retrieved from http://dx.doi.org/10.1038/332070a0

Gooday, A. J. (2003). Benthic foraminifera (protista) as tools in deep-water palaeoceanography: Environmental influences on faunal characteristics. *Advances in Marine Biology*, *46*, 1–90. https://doi.org/10.1016/S0065-2881(03)46002-1

Gooday, A. J., Levin, L. A., Linke, P., & Heeger, T. (1992). The Role Of Benthic Foraminifera in Deep-Sea Food Webs and Carbon Cycling. *Deep-Sea Food Chains and the Global Carbon Cycle*. Dordrecht: Springer Netherlands. https://doi.org/10.1007/978-94-011-2452-2_5

Gooday, A. J., Bernhard, J. M., Levin, L. A., & Suhr, S. B. (2000). Foraminifera in the Arabian Sea oxygen minimum zone and other oxygen-de " cient settings : taxonomic composition , diversity , and relation to metazoan faunas. *Deep-Sea Research Part II: Topical Studies in Oceanography*, *47*(Deep-Sea Research II), 25–54. https://doi.org/10.1016/S0967-0645(99)00099-5

Gradstein, F. M., Ogg, J. G., Schmitz, M. D., & Ogg, G. M. (2012). *The Geologic Time Scale 2012*. Elsevier.

Grant, K. M., & Dickens, G. R. (2002). Coupled productivity and carbon isotope records in the southwest Pacific Ocean during the late Miocene-early Pliocene biogenic bloom. *Palaeogeography, Palaeoclimatology, Palaeoecology*, *187*(1–2), 61–82. https://doi.org/10.1016/S0031-0182(02)00508-4

Gruber, N., Keeling, C. D., Bacastow, R. B., Guenther, P. R., Lueker, T. J., Wahlen, M., et al. (1999). Spatiotemporal patterns of carbon-13 in the global surface oceans and the oceanic Suess effect. *Global Biogeochemical Cycles*, *13*(2), 307–335. https://doi.org/10.1029/1999GB900019

Sen Gupta, B. K., & Machain-Castillo, M. L. (1993). Benthic foraminifera in oxygen-poor habitats. *Marine Micropaleontology*, *20*(3–4), 183–201. https://doi.org/10.1016/0377-8398(93)90032-S

Hair, J. F., Anderson, R. E., Tatham, R. L., & Black, W. C. (1998). Multivariate Data Analysis. *International Journal of Pharmaceutics*. https://doi.org/10.1016/j.ijpharm.2011.02.019

Harper, H. E., & Knoll, A. H. (1975). Silica, diatoms, and Cenozoic radiolarian evolution. *Geology*. https://doi.org/10.1130/0091-7613(1975)3<175:SDACRE>2.0.CO;2

Hayward, Bruce W., Kawagata, S., Grenfell, H. R., Sabaa, A. T., & O'Neill, T. (2007). Last global extinction in the deep sea during the mid-Pleistocene climate transition. *Paleoceanography*, *22*(3). https://doi.org/10.1029/2007PA001424

Hayward, Bruce W., Johnson, K., Sabaa, A. T., Kawagata, S., & Thomas, E. (2010). Cenozoic record of elongate, cylindrical, deep-sea benthic foraminifera in the North Atlantic and equatorial Pacific Oceans. *Marine Micropaleontology*, *74*(3–4), 75–95. https://doi.org/10.1016/j.marmicro.2010.01.001

Hayward, Bruce William, Kawagata, S., & Sabaa, A. (2012). *The Last Global Extinction (Mid-Pleistocene) of Deep-sea Benthic Foraminifera (Chrysalogoniidae, Ellipsoidinidae, Glandulonodosariidae, Plectofrondiculariidae, Pleurostomellidae, Stilostomellidae): Their Late Cretaceous-Cenozoic History and Taxonomy* (Vol. 43). Cushman Foundation for Foraminiferal Research, Spec. Pub.

Henderiks, J., & Pagani, M. (2008). Coccolithophore cell size and the Paleogene decline in atmospheric CO2. *Earth and Planetary Science Letters*, *269*(3–4), 575–583. https://doi.org/10.1016/j.epsl.2008.03.016

Hohbein, M. W., Sexton, P. F., & Cartwright, J. A. (2012). Onset of North Atlantic deep water production coincident with inception of the Cenozoic global cooling trend. *Geology*, *40*(3), 255–258. https://doi.org/10.1130/G32461.1

Huber, M., & Sloan, L. C. (2001). Heat transport, deep waters, and thermal gradients: Coupled simulation of an Eocene greenhouse climate. *Geophysical Research Letters*, *28*(18), 3481–3484. https://doi.org/10.1029/2001GL012943

Huber, M., Sloan, L. C., & Shellito, C. (2003). Early Paleogene oceans and climate: A fully coupled modeling approach using the NCAR CCSM. *Special Paper 369: Causes and Consequences of Globally Warm Climates in the Early Paleogene*, 25–47. https://doi.org/10.1130/0-8137-2369-8.25

Hulbert, E. M., & Corwin, N. (1969). Influence of the Amazon River outflow on the ecology of the western tropical Atlantic III -The plankton flora between the Amazon River and the Windward Islands. *Journal of Marine Research*, *27*, 55–72.

Hutchinson, D. K., de Boer, A. M., Coxall, H. K., Caballero, R., Nilsson, J., & Baatsen, M. (2018a). Climate sensitivity and meridional overturning circulation in the late Eocene using GFDL CM2.1. *Climate of the Past Discussions*, (2016), 1–46. https://doi.org/10.5194/cp-2017-161

Hutchinson, D. K., Coxall, H. K., O'Regan, M., Nilsson, J., Caballero, R., & de Boer, A. M. (2019). Arctic closure as a trigger for Atlantic overturning at the Eocene-Oligocene Transition. *Nature Communications*, *10*(1), 3797. https://doi.org/10.1038/s41467-019-11828-z

Jorissen, F. J., de Stigter, H. C., & Widmark, J. G. V. (1995). A conceptual model explaining benthic foraminiferal microhabitats. *Marine Micropaleontology*. https://doi.org/10.1016/0377-8398(95)00047-X

Jorissen, F. J., Fontanier, C., & Thomas, E. (2007). Chapter Seven Paleoceanographical Proxies Based on Deep-Sea Benthic Foraminiferal Assemblage Characteristics. *Developments in Marine Geology*, *1*(07), 263–325. https://doi.org/10.1016/S1572-5480(07)01012-3

Kaiho, K., & Hasegawa, T. (1994). End-Cenomanian benthic foraminiferal extinctions and oceanic dysoxic events in the northwestern Pacific Ocean. *Palaeogeography, Palaeoclimatology, Palaeoecology*. https://doi.org/10.1016/0031-0182(94)90346-8

Kaiser, H. F. (1960). The Application of Electronic Computers to Factor Analysis. *Educational and Psychological Measurement*. https://doi.org/10.1177/001316446002000116

Kamikuri, S.-I., Moore, T. C., Ogane, K., Suzuki, N., Pälike, H., & Nishi, H. (2012). Early Eocene to early Miocene radiolarian biostratigraphy for the low-latitude Pacific Ocean. *Stratigraphy*, *9*(1), 77–108. Retrieved from http://www.scopus.com/inward/record.url?eid=2-s2.0-84867635016&partnerID=40&md5=5f8a68aff13429779e5770d028864df2

Kamikuri, S. ichi, & Wade, B. S. (2012). Radiolarian magnetobiochronology and faunal turnover across the middle/late Eocene boundary at Ocean Drilling Program Site 1052 in the western North Atlantic Ocean. *Marine Micropaleontology*, *88–89*(May 2012), 41–53. https://doi.org/10.1016/j.marmicro.2012.03.001

Kaminski, M.A., & Gradstein, F. M. (2005). *Atlas of Paleogene cosmopolitan deep-water*

agglutinated foraminifera. Krakow: Grzybowski Foundation.

Kaminski, M.A., & Ortiz, S. (2014). The Eocene-Oligocene turnover of deep-water agglutinated Foraminifera at ODP Site 647, southern Labrador Sea (North Atlantic). *Advances in Agglutinated Foraminiferal Research; the Ninth International Workshop on Agglutinated Foraminifera (IWAF-9)*, *60*(1), 53.

Kaneps, A. G. (1979). Gulf Stream: Velocity Fluctuations During the Late Cenozoic. *Science*, *204*(4390), 297–302. Retrieved from http://science.sciencemag.org/content/204/4390/297

Katz, M. E., Katz, D. R., Wright, J. D., Miller, K. G., Pak, D. K., Shackleton, N. J., & Thomas, E. (2003). Early Cenozoic benthic foraminiferal isotopes: Species reliability and interspecies correction factors. *Paleoceanography*, *18*(2), 1–12. https://doi.org/10.1029/2002PA000798

Katz, M. E., Miller, K. G., Wright, J. D., Wade, B. S., Browning, J. V., Cramer, B. S., & Rosenthal, Y. (2008). Stepwise transition from the Eocene greenhouse to the Oligocene icehouse. *Nature Geoscience*, *1*(5), 329–334. https://doi.org/10.1038/ngeo179

Katz, M. E., Cramer, B. S., Toggweiler, J. R., Esmay, G., Liu, C., Miller, K. G., et al. (2011). Impact of Antarctic circumpolar current development on Late Paleogene ocean ctructure. *Science*, *332*(6033), 1076–1079. https://doi.org/10.1126/science.1202122

Keller, G. (1983). Paleoclimatic analyses of Middle Eocene through Oligocene planktic foraminiferal faunas. *Palaeogeography, Palaeoclimatology, Palaeoecology*, *43*, 73–94.

Kennett, J. P., Houtz, R. E., Andrews, P. B., Edwards, A. R., Gostin, V. A., Hajos, M., et al. (1974). Development of the Circum-Antarctic Current. *Science*, *186*(4159), 144–147. https://doi.org/10.1126/science.186.4159.144

Kennett, James P. (1977). Cenozoic evolution of Antarctic glaciation, the circum-Antarctic Ocean, and their impact on global paleogeography. *J. Geophys. Res.*, *82*(27). Retrieved from http://dx.doi.org/10.1029/JC082i027p03843

Kim, S.-T., & O'Neil, J. (1997). Equilibrium and nonequilibrium oxygen isotope effects in synthetic carbonates. *Geochimica et Cosmochimica Acta*, *61*(16), 3461–3475.

Kleiven, H. K. F., Hall, I. R., McCave, I. N., Knorr, G., & Jansen, E. (2011). Coupled deep-water flow and climate variability in the middle pleistocene North Atlantic. *Geology*, *39*(4), 343–346. https://doi.org/10.1130/G31651.1

Klovan, J., & Miesch, A. (1975). Extended CABFAC and QMODEL computer programs for Q-mode factor analysis of compositional data. *Computers & Geosciences*, *1*(3), 111.

Klovan, J. E., & Imbrie, J. (1971). An algorithm and Fortran-iv program for large-scale Q-mode factor analysis and calculation of factor scores. *Journal of the International Association for Mathematical Geology*. https://doi.org/10.1007/BF02047433

Klovan, J. E., & Miesch, A. T. (1976). Extended cabfac and Qmodel computer programs for Q-mode factor analysis of compositional data. *Computers and Geosciences*. https://doi.org/10.1016/0098-3004(76)90004-2

Kobashi, T., Grossman, E. L., Dockery, D. T., & Ivany, L. C. (2004). Water mass stability reconstructions from greenhouse (Eocene) to icehouse (Oligocene) for the northern Gulf

Coast continental shelf (USA). *Paleoceanography*, *19*(1), n/a-n/a. https://doi.org/10.1029/2003PA000934

Kominz, M. A., & Pekar, S. F. (2001). Oligocene eustasy from two-dimensional sequence stratigraphic backstripping. *Bulletin of the Geological Society of America*, *113*(3), 291–304. https://doi.org/10.1130/0016-7606(2001)113<0291:OEFTDS>2.0.CO;2

Kotthoff, U., Greenwood, D. R., McCarthy, F. M. G., Müller-Navarra, K., Prader, S., & Hesselbo, S. P. (2014). Late Eocene to middle Miocene (33 to 13 million years ago) vegetation and climate development on the North American Atlantic Coastal Plain (IODP Expedition 313, Site M0027). *Climate of the Past*, *10*(4), 1523–1539. https://doi.org/10.5194/cp-10-1523-2014

Kroopnick, P. M. (1980). The distribution of 13C in the Atlantic Ocean. *Earth and Planetary Science Letters*, *49*, 469–484.

Kroopnick, P. M. (1985). The distribution of 13C of ΣCO2 in the world oceans. *Deep Sea Research Part A, Oceanographic Research Papers*, *32*(1), 57–84. https://doi.org/10.1016/0198-0149(85)90017-2

Lazarus, D. B., Kotrc, B., Wulf, G., & Schmidt, D. N. (2009). Radiolarians decreased silicification as an evolutionary response to reduced Cenozoic ocean silica availability. *Proceedings of the National Academy of Sciences*. https://doi.org/10.1073/pnas.0812979106

Lear, C. H., Bailey, T. R., Pearson, P. N., Coxall, H. K., & Rosenthal, Y. (2008). Cooling and ice growth across the Eocene-Oligocene transition. *Geology*, *36*(3), 251–254. https://doi.org/10.1130/G24584A.1

Leckie, R. MARK, & Olson, H. C. (2003). Foraminifera As Proxies for Sea-Level Change on Siliciclastic Margins. *Micropaleontologic Proxies for Sea-Level Change and Stratigraphic Discontinuities*, (75), 5–19. https://doi.org/10.2110/pec.03.75.0005

Leckie, R M. (1989). A Paleoceanographic Model for the Early Evolutionary History of Planktonic-Foraminifera. *Palaeogeography Palaeoclimatology Palaeoecology*, *73*(1–2), 107–138.

Legarda-Lisarri, A. (2016). *Variabilidad de la comunidad de foraminíferos planctónicos a traves del límite Eoceno-Oligoceno en el corte de Fuente Caldera, Cordilleras Béticas, España*. Universidad del Mar.

Legarda-Lisarri, A., Molina, E., Arenillas, I., & Esparza-Alvarez, M. A. (2014). Cambios paleoambientales basados en foraminíferos planctónicos del Tetis durante el tránsito Eoceno-Oligoceno. In G. Arreguín-Rodríguez, J. Colmenar, E. Díaz-Berenguer, J. Galán, A. Legarda-Lisarri, J. Parrilla-Bel, et al. (Eds.), *NEW INSIGHTS ON ANCIENT LIFE* (pp. 156–159).

Levin, L. A. (2003). Oxygen Minimum Zone Benthos: Adaptation and Community Response To Hypoxia, *41*, 1–45.

Liu, Z., Pagani, M., Zinniker, D., DeConto, R., Huber, M., Brinkhuis, H., et al. (2009). Global cooling during the eocene-oligocene climate transition. *Science*, *323*(5918), 1187–1190. https://doi.org/10.1126/science.1166368

Liu, Z., He, Y., Jiang, Y., Wang, H., Liu, W., Bohaty, S. M., & Wilson, P. A. (2018). Transient temperature asymmetry between hemispheres in the Palaeogene Atlantic Ocean. *Nature Geoscience*, 1. https://doi.org/10.1038/s41561-018-0182-9

Locarnini, R. A., Mishonov, A. V., Antonov, J. I., Boyer, T. P., Garcia, H. E., Baranova, O. K., et al. (2013). *World Ocean Atlas 2013. Vol. 1: Temperature. S. Levitus, Ed.; A. Mishonov, Technical Ed.; NOAA Atlas NESDIS*. https://doi.org/10.1182/blood-2011-06-357442

Loeblich, A. R., & Tappan, H. (1988). *Foraminiferal Genera and Their Classification*. https://doi.org/10.1007/978-1-4899-5760-3

Lynch-Stieglitz, J., Curry, W. B., & Slowey, N. (1999). A geostrophic transport estimate for the Florida Current from the oxygen isotope composition of benthic foraminifera. *Paleoceanography*, *14*(3), 360–373. https://doi.org/10.1029/1999PA900001

Mackensen, A., Schmiedl, G., Harloff, J., & Giese, M. (1995). Deep-Sea Foraminifera in the South Atlantic Ocean: Ecology and Assemblage Generation. *Micropaleontology*, *41*(4), 342. https://doi.org/10.2307/1485808

Martin, J. H. (1990). Glacial-interglacial CO2 change: The Iron Hypothesis. *Paleoceanography*, *5*(1), 1–13. https://doi.org/10.1029/PA005i001p00001

McCartney, M. S., & Talley, L. D. (1982). The Subpolar Mode Water of the North Atlantic Ocean. *Journal of Physical Oceanography*, *12*, 1169–1188. Retrieved from papers://f554698c-bc30-43aa-8c0c-c8de8adb48e4/Paper/p1321

McCave, I. N., Thornalley, D. J. R., & Hall, I. R. (2017). Relation of sortable silt grain-size to deep-sea current speeds: Calibration of the 'Mud Current Meter.' *Deep-Sea Research Part I: Oceanographic Research Papers*, *127*(May), 1–12. https://doi.org/10.1016/j.dsr.2017.07.003

McKinley, C. C., Thomas, D. J., LeVay, L. J., & Rolewicz, Z. (2019). Nd isotopic structure of the Pacific Ocean 40–10 Ma, and evidence for the reorganization of deep North Pacific Ocean circulation between 36 and 25 Ma. *Earth and Planetary Science Letters*, *521*, 139–149. https://doi.org/10.1016/j.epsl.2019.06.009

McLaren, P., & Bowles, D. (1985). The Effects of Sediment Transport on Grain-Size Distributions. *SEPM Journal of Sedimentary Research*, *Vol. 55*(January 1985). https://doi.org/10.1306/212F86FC-2B24-11D7-8648000102C1865D

de Mello e Sousa, S. H., Passos, R. F., Fukumoto, M., da Silveira, I. C. A., Figueira, R. C. L., Koutsoukos, E. A. M., et al. (2006). Mid-lower bathyal benthic foraminifera of the Campos Basin, Southeastern Brazilian margin: Biotopes and controlling ecological factors. *Marine Micropaleontology*. https://doi.org/10.1016/j.marmicro.2006.05.003

Merico, A., Tyrrell, T., & Wilson, P. A. (2008). Eocene/Oligocene ocean de-acidification linked to Antarctic glaciation by sea-level fall. *Nature*, *452*(7190), 979–982. https://doi.org/10.1038/nature06853

Miller, K. G., Wright, J. D., Katz, M. E., & Wade, B. S. (2006). The Eocene-Oligocene Climate Transition: Antarctic Ice Takes Over. *American Geophysical Union, Fall Meeting 2006, Abstract Id. PP23E-06*. Retrieved from http://adsabs.harvard.edu/abs/2006agufmpp23e..06m

Miller, K.G., & Hart, M. B. (1987). Cenozoic Planktonic Foraminifers and Hiatuses on the New Jersey Slope and Rise: Deep Sea Drilling Project Leg 95, Northwest Atlantic. In *Initial Reports of the Deep Sea Drilling Project, 95*. U.S. Government Printing Office. https://doi.org/10.2973/dsdp.proc.95.106.1987

Miller, K.G., & Tucholke, B. E. (1983). Development of Cenozoic abyssal circulation south of the Greenland-Scotland Ridge. In *New Methods and Concepts* (pp. 549–589). https://doi.org/10.1007/978-1-4613-3485-9_27

Miller, K.G., Berggren, W. A., Jijun Zhang, & Palmer-Julson, A. A. (1991). Biostratigraphy and isotope stratigraphy of Upper Eocene microtektites at Site 612: how many impacts? *Palaios*, *6*(1), 17–38. https://doi.org/10.2307/3514951

Miller, K G, & Katz, M. E. (1987). Eocene Benthic Foraminiferal Biofacies of the New Jersey Transect. *Initial Reports of the Deep Sea Drilling Project*, *95*, 267–298.

Miller, Kenneth G, Kominz, M. A., Browning, J. V, Wright, J. D., Mountain, G. S., Katz, M. E., et al. (2005). The phanerozoic record of global sea-level change. *Science*, *310*(5752), 1293–1298. https://doi.org/10.1126/science.1116412

Miller, Kenneth G, Browning, J. V, Mountain, G. S., Sheridan, R. E., Peter, J., Glenn, S., et al. (2014). Chapter 3 History of continental shelf and slope sedimentation on the US middle Atlantic margin Chapter 3 History of continental shelf and slope sedimentation on the US middle Atlantic margin. https://doi.org/10.1144/M41.3

Mix, A. C., Morey, A. E., Pisias, N. G., & Hostetler, S. W. (1999). Foraminiferal faunal estimates of paleotemperature: Circumventing the no-analog problem yields cool ice age tropics. *Paleoceanography*. https://doi.org/10.1029/1999PA900012

Miyajima, T., Tsuboi, Y., Tanaka, Y., & Koike, I. (2009). Export of inorganic carbon from two Southeast Asian mangrove forests to adjacent estuaries as estimated by the stable isotope composition of dissolved inorganic carbon G01024. *Journal of Geophysical Research: Biogeosciences*, *114*(1), 1–12. https://doi.org/10.1029/2008JG000861

Mojtahid, M., Griveaud, C., Fontanier, C., Anschutz, P., & Jorissen, F. J. (2010). Les foraminifères benthiques vivants le long d'un transect bathymétrique (140-4800m) dans le Golfe de Gascogne (Atlantique NE). *Revue de Micropaleontologie*, *53*(3), 139–162. https://doi.org/10.1016/j.revmic.2010.01.002

Molina, E., Gonzalvo, C., & Keller, G. (1993). The Eocene-Oligocene planktic foraminiferal transition: Extinctions, impacts and hiatuses. *Geological Magazine*, *130*(4), 483–499. https://doi.org/10.1017/S0016756800020550

Moore, J. C., Wade, B. S., Westerhold, T., Erhardt, A. M., Coxall, H. K., Baldauf, J., & Wagner, M. (2014). Equatorial Pacific productivity changes near the Eocene-Oligocene boundary. *Paleoceanography*, *29*(9), 825–844. https://doi.org/10.1002/2014PA002656

Moore, T. C., Kamikuri, S. ichi, Erhardt, A. M., Baldauf, J., Coxall, H. K., & Westerhold, T. (2015). Radiolarian stratigraphy near the Eocene-Oligocene boundary. *Marine Micropaleontology*, *116*(February), 50–62. https://doi.org/10.1016/j.marmicro.2015.02.002

Van Morkhoven, F. P. C. ., Berggren, W. A., Edwards, A. S., & Oertli, H. . (1986). Cenozoic Cosmopolitan Deep-Water Benthic Foraminifera. *Bulletin Des Centres de Recherches Exploration-Production Elf-Aquitaine Mem 11*, 1–431.

Mountain, G. S., & Tucholke, B. E. (1985). Mesozoic and Cenozoic Geology of the U.S. Atlantic Continental Slope and Rise. In C. W. Poag (Ed.), *Geologic evolution of the United States Atlantic Margin* (p. 382). Van Nostrand Reinhold. Retrieved from http://oceanrep.geomar.de/33361/

Mountain, G. S., Kominz, M., Christie-Blick, N., Katz, M. E., Browning, J. V., Miller, K. G., et al. (1998). Cenozoic global sea level, sequences, and the New Jersey Transect: Results From coastal plain and continental slope drilling. *Reviews of Geophysics*, *36*(4), 569–601. https://doi.org/10.1029/98rg01624

Mulitza, S., Boltovskoy, D., Donner, B., Meggers, H., Paul, A., & Wefer, G. (2003). Temperature: δ18O relationships of planktonic foraminifera collected from surface waters. *Palaeogeography, Palaeoclimatology, Palaeoecology*, *202*(1–2), 143–152. https://doi.org/10.1016/S0031-0182(03)00633-3

Murphy, M. G., & Kennett, J. P. (1986). Development of Latitudinal Thermal Gradients during the Oligocene: Oxygen-Isotope Evidence from the Southwest Pacific. In J.P. Kennett & C. C. von der Borch (Eds.), *Initial Reports of the Deep Sea Drilling Project, 90* (pp. 1347–1460). Washington DC. https://doi.org/10.2973/dsdp.proc.90.140.1986

Murray, J. W. (2006). *Ecology and applications of benthic foraminifera*. Cambridge University Press. Retrieved from https://eprints.soton.ac.uk/42204/

Mutti, M., & Hallock, P. (2003). Carbonate systems along nutrient and temperature gradients: Some sedimentological and geochemical constraints. *International Journal of Earth Sciences*, *92*(4), 465–475. https://doi.org/10.1007/s00531-003-0350-y

Nomura, R. (1995). Paleogene to Neogene Deep-Sea Paleoceanography in the Eastern Indian Ocean: Benthic Foraminifera from ODP Sites 747, 757 and 758. *Micropaleontology*, *41*(3), 251. https://doi.org/10.2307/1485862

Nong, G. T., Najjar, R. G., Seidov, D., & Peterson, W. H. (2000). Simulation of ocean temperature change due to the opening of Drake Passage. *Geophysical Research Letters*. https://doi.org/10.1029/1999GL011072

Okada, H., & Wells, P. (1997). Late Quaternary nannofossil indicators of climate change in two deep-sea cores associated with the Leeuwin Current off Western Australia. *Palaeogeography, Palaeoclimatology, Palaeoecology*, *131*(3–4), 413–432. https://doi.org/10.1016/S0031-0182(97)00014-X

Olivarez Lyle, A., & Lyle, M. W. (2006). Missing organic carbon in Eocene marine sediments: Is metabolism the biological feedback that maintains end-member climates? *Paleoceanography*. https://doi.org/10.1029/2005PA001230

Ortiz, J. D., Mix, A. C., & Collier, R. W. (1995). Environmental control of living symbiotic and asymbiotic foraminifera of the California Current. *Paleoceanography*, *10*(6), 987–1009. https://doi.org/10.1029/95PA02088

Ortiz, S., & Kaminski, M. A. (2012). Record of Deep-Sea, Benthic Elongate-Cylindrical Foraminifera Across the Eocene-Oligocene Transition in the North Atlantic Ocean (ODP Hole 647A). *The Journal of Foraminiferal Research*, *42*(4), 345–368. https://doi.org/10.2113/gsjfr.42.4.345

Ortiz, S., & Thomas, E. (2006). Lower-middle Eocene benthic foraminifera from the Fortuna Section (Betic Cordillera, southeastern Spain). *Micropaleontology*, *52*(2), 97–150. https://doi.org/10.2113/gsmicropal.52.2.97

Pagani, M., Huber, M., Liu, Z., Bohaty, S. M., Henderiks, J., Sijp, W., et al. (2011). The role of carbon dioxide during the onset of antarctic glaciation. *Science*, *334*(6060), 1261–1264. https://doi.org/10.1126/science.1203909

Palmer, A. A. (1987). Cenozoic Radiolarians from Deep Sea Drilling Project Sites 612 and 613 (Leg 95, New Jersey Transect) and Atlantic Slope Project Site ASP 15. In *Initial Reports of the Deep Sea Drilling Project, 95*. U.S. Government Printing Office. https://doi.org/10.2973/dsdp.proc.95.110.1987

Pearson, P., Olsson, R. K., Huber, B. T., Hemleben, C., & Berggren, W. A. (Eds.). (2006). Atlas of Eocene Planktonic Foraminifera. *Cushman Foundation Special Publication*, *41*, 513.

Pearson, P. N., & Wade, B. S. (2009). Taxonomy and Stable Isotope Paleoecology of Well-Preserved Planktonic Foraminifera From the Uppermost Oligocene of Trinidad. *The Journal of Foraminiferal Research*, *39*(3), 191–217. https://doi.org/10.2113/gsjfr.39.3.191

Pearson, P. N., Shackleton, N. J., & Hall, M. A. (1997). Stable isotopic evidence for the sympatric divergence of Globigerinoides trilobus and Orbulina universa (planktonic foraminifera). *Journal of the Geological Society*, *154*(2), 295–302. https://doi.org/10.1144/gsjgs.154.2.0295

Pearson, P N, Ditchfield, P. W., Singano, J., Harcourt-brown, K. G., Nicholas, C. J., Oissonns, R. K., et al. (2001). Warm tropical sea surface temperatures in the Late Cretaceous ands Eocene epochs. *Nature*, *413*, 481–487.

Pearson, Paul N., McMillan, I. K., Wade, B. S., Jones, T. D., Coxall, H. K., Bown, P. R., & Lear, C. H. (2008). Extinction and environmental change across the Eocene-Oligocene boundary in Tanzania. *Geology*, *36*(2), 179–182. https://doi.org/10.1130/G24308A.1

Pearson, Paul N. (2012). Oxygen Isotopes in Foraminifera : Overview and Historical Review. *The Paleontological Society Papers*, *18*, 1–38. https://doi.org/10.1017/S1089332600002539

Pekar, S., & Miller, K. G. (1996). New Jersey oligocene “Icehouse” sequences (ODP Leg 150X) correlated with global δ18O and Exxon eustatic records. *Geology*, *24*(6), 567–570. https://doi.org/10.1130/0091-7613(1996)024<0567:NJOISO>2.3.CO;2

Pekar, S. F., Miller, K. G., & Kominz, M. A. (2000). Reconstructing the stratal geometry of latest Eocene to Oligocene sequences in New Jersey: Resolving a patchwork distribution into a clear pattern of progradation. In *Sedimentary Geology* (Vol. 134, pp. 93–109). Elsevier. https://doi.org/10.1016/S0037-0738(00)00015-4

Pekar, S. F., Christie-Blick, N., Kominz, M. A., & Miller, K. G. (2001). Evaluating the stratigraphic response to eustasy from oligocene in New Jersey. *Geology*, *29*(1), 55–58. https://doi.org/10.1130/0091-7613(2001)?029<0055:ETSRTE>?2.0.CO

Persico, D., & Villa, G. (2004). Eocene-Oligocene calcareous nannofossils from Maud Rise and Kerguelen Plateau (Antarctica): Paleoecological and paleoceanographic implications. *Marine Micropaleontology*, *52*(1–4), 153–179. https://doi.org/10.1016/j.marmicro.2004.05.002

Phipps, M., Jorissen, F., Pusceddu, A., Bianchelli, S., & De Stigter, H. (2012). Live benthic foraminiferal faunas along a bathymetrical transect (282-4987 m) on the Portuguese margin (NE Atlantic). *The Journal of Foraminiferal Research*, *42*(1), 66–81. https://doi.org/10.2113/gsjfr.42.1.66

Pinet, P. R., & Popenoe, P. (1985). A scenario of Mesozoic-Cenozoic ocean circulation over the Blake Plateau and its environs. *Geological Society of America Bulletin*, *96*(5), 618–626. https://doi.org/10.1130/0016-7606(1985)96<618:ASOMOC>2.0.CO;2

Pinet, Paul R., Popenoe, P., & Nelligan, D. F. (1981). Gulf Stream: Reconstruction of Cenozoic flow patterns over the Blake Plateau. *Geology*, *9*(6), 266–270. https://doi.org/10.1130/0091-7613(1981)9<266:GSROCF>2.0.CO;2

Poag, C. W. (1987). The New Jersey Transect: Stratigraphic Framework and Depositional History of a Sediment-Rich Passive Margin. In *Initial Reports of the Deep Sea Drilling Project, 95*. U.S. Government Printing Office. https://doi.org/10.2973/dsdp.proc.95.132.1987

Poag, C. W., & Low, D. (1987). Unconformable Sequence Boundaries at Deep Sea Drilling Project Site 612, New Jersey Transect: Their Characteristics and Stratigraphic Significance. In *Initial Reports of the Deep Sea Drilling Project, 95*. U.S. Government Printing Office. https://doi.org/10.2973/dsdp.proc.95.117.1987

Poag, C. W., Watts, A. B., & Shipboard Scientific Party. (1987). *Initial reports of the Deep Sea Drilling Project covering Leg 95 of the cruises of the drilling vessel Glomar Challenger, St. John's, Newfoundland, to Ft. Lauderdale, Florida, August-September 1983*. (A. B. Watts, M. Cousin, D. Goldberg, M. B. Hart, K. G. Miller, G. S. Mountain, et al., Eds.). Ocean Drilling Program, College Station, TX, United States: Texas A & M University. https://doi.org/10.2973/dsdp.proc.95.1987

Poore, R. Z., & Matthews, R. K. (1984). Oxygen isotope ranking of late Eocene and Oligocene planktonic foraminifers: Implications for Oligocene sea-surface temperatures and global ice-volume. *Marine Micropaleontology*, *9*(2), 111–134. https://doi.org/10.1016/0377-8398(84)90007-0

Premoli Silva, I., & Jenkins, D. G. (1993). Decision on the Eocene-Oligocene boundary stratotype. *Episodes*, *16*(3), 379–382.

Pusz, A. E., Miller, K. G., Wright, J. D., Katz, M. E., Cramer, B. S., & Kent, D. V. (2009). Stable isotopic response to late Eocene extraterrestrial impacts. *Special Paper - Geological Society of America*, *452*, 83–95. https://doi.org/http://dx.doi.org/10.1130/2009.2452(06

Rahmstorf, S. (2006). Thermohaline Ocean Circulation. *Encyclopedia of Quaternary Sciences*, 1–10. https://doi.org/10.1016/B0-44-452747-8/00014-4

Rathmann, S., & Kuhnert, H. (2008). Carbonate ion effect on Mg/Ca, Sr/Ca and stable isotopes on the benthic foraminifera Oridorsalis umbonatus off Namibia. *Marine Micropaleontology*. https://doi.org/10.1016/j.marmicro.2007.08.001

Richardson, M. J., Wimbush, M., & Mayer, L. (1981). Exceptionally strong near-bottom flows on the continental rise of nova scotia. *Science*, *213*(4510), 887–8. https://doi.org/10.1126/science.213.4510.887

Roberts, C. D., LeGrande, A. N., & Tripati, A. K. (2009). Climate sensitivity to Arctic seaway restriction during the early Paleogene. *Earth and Planetary Science Letters*, *286*(3–4), 576–585. https://doi.org/10.1016/j.epsl.2009.07.026

Roemmich, D., & McGowan, J. (1995). Climatic Warming and the Decline of Zooplankton in the California Current. *Science*, *276*(5202), 1324–1326. Retrieved from http://www.jstor.org/stable/2885994

Rohling, E. J., & Cooke, S. (1999). Stable oxygen and carbon isotopes in foraminiferal Carbonate Shells. In B. K. Sen Gupta (Ed.), *Modern Foraminifera* (Vol. 239–258, p. 1998).

Sarnthein, M., Winn, K., Duplessy, J. -C, & Fontugne, M. R. (1988). Global variations of surface

ocean productivity in low and mid latitudes: Influence on CO2 reservoirs of the deep ocean and atmosphere during the last 21,000 years. *Paleoceanography*, *3*(3), 361–399. https://doi.org/10.1029/PA003i003p00361

Scher, H. D., & Martin, E. E. (2006). Timing and climatic consequences of the opening of drake passage. *Science*. https://doi.org/10.1126/science.1120044

Scher, H. D., & Martin, E. E. (2008). Oligocene deep water export from the North Atlantic and the development of the Antarctic Circumpolar Current examined with neodymium isotopes. *Paleoceanography*, *23*(1), 1–12. https://doi.org/10.1029/2006PA001400

Schiebel, R., & Hemleben, C. (2017). *Planktic foraminifers in the modern ocean*. *Planktic Foraminifers in the Modern Ocean*. Berlin, Heidelberg: Springer Berlin Heidelberg. https://doi.org/10.1007/978-3-662-50297-6

Schmiedl, G., De Bovée, F., Buscail, R., Charrière, B., Hemleben, C., Medernach, L., & Picon, P. (2000). Trophic control of benthic foraminiferal abundance and microhabitat in the bathyal Gulf of Lions, western Mediterranean Sea. In *Marine Micropaleontology*. https://doi.org/10.1016/S0377-8398(00)00038-4

Schmitz, W. J., & McCartney, M. S. (1993). On the North Atlantic Circulation. *Reviews of Geophysics*, *31*(1), 29–49. https://doi.org/10.1029/92RG02583

Schönfeld, J. (2002). A new benthic foraminiferal proxy for near-bottom current velocities in the Gulf of Cadiz, northeastern Atlantic Ocean. *Deep-Sea Research Part I: Oceanographic Research Papers*. https://doi.org/10.1016/S0967-0637(02)00088-2

Schumacher, S., & Lazarus, D. (2004). Regional differences in pelagic productivity in the late Eocene to early Oligocene - A comparison of southern high latitudes and lower latitudes. *Palaeogeography, Palaeoclimatology, Palaeoecology*, *214*(3), 243–263. https://doi.org/10.1029/2002PA000804

Sexton, P. F., Wilson, P. A., & Pearson, P. N. (2006). Palaeoecology of late middle Eocene planktic foraminifera and evolutionary implications. *Marine Micropaleontology*, *60*(1), 1–16. https://doi.org/10.1016/j.marmicro.2006.02.006

Shackleton, N. J., & Kennett, J. P. (1975). Paleotemperature history of the Cenozoic and the initiation of Antarctic glaciation; Oxygen and carbon isotope analyses in DSDP sites 277, 279 and 281. *Initial Reports of the Deep Sea Drilling Project*, *29*, 743–755. https://doi.org/10.2973/dsdp.proc.37.1977

Smart, C. W., & Thomas, E. (2006). The enigma of early Miocene biserial planktic foraminifer. *Geology*, *34*(12), 1041–1044. https://doi.org/10.1130/G23038A.1

Spezzaferri, S. (1994). Planktonic foraminiferal biostratigraphy and taxonomy of the Oligocene and lower Miocene in the oceanic record. An overview. *Palaeontographia Italica*, *81*, 1–187.

Spezzaferri, S. (1995). Planktonic foraminiferal paleoclimatic implications across the Oligocene-Miocene transition in the oceanic record (Atlantic, Indian and South Pacific). *Palaeogeography, Palaeoclimatology, Palaeoecology*, *114*(1), 43–74. https://doi.org/10.1016/0031-0182(95)00076-X

Spezzaferri, S., & Pearson, P. N. (2009). Distribution and ecology of Catapsydrax indianus, a new Planktonic foraminifer index species for the late Oligocene-early Miocene. *The Journal of*

Foraminiferal Research, *39*(2), 112–119. https://doi.org/10.2113/gsjfr.39.2.112

Spezzaferri, S., Basso, D., & Coccioni, R. (2002). Late Eocene Planktonic Foraminiferal Response To an Extraterrestrial Impact At Massignano Gssp (Northeastern Appennines, Italy). *The Journal of Foraminiferal Research*, *32*(2), 188–199. https://doi.org/10.2113/0320188

de Stigter, H. C., Jorissen, F. J., & van der Zwaan, G. J. (1998). Bathymetric distribution and microhabitat partitioning of live (Rose Bengal stained) benthic Foraminifera along a shelf to bathyal transect in the southern Adriatic Sea. *The Journal of Foraminiferal Research*, *28*(1), 40–65. Retrieved from https://pubs.geoscienceworld.org/cushmanfoundation/jfr/article-abstract/28/1/40/76756

Sun, X., Corliss, B. H., Brown, C. W., & Showers, W. J. (2006). The effect of primary productivity and seasonality on the distribution of deep-sea benthic foraminifera in the North Atlantic. *Deep Sea Research Part I: Oceanographic Research Papers*, *53*(1), 28–47. https://doi.org/10.1016/J.DSR.2005.07.003

Suto, I. (2006). The explosive diversification of the diatom genus Chaetoceros across the Eocene/Oligocene and Oligocene/Miocene boundaries in the Norwegian Sea. *Marine Micropaleontology*. https://doi.org/10.1016/j.marmicro.2005.11.004

Tagliabue, A., & Bopp, L. (2008). Towards understanding global variability in ocean carbon-13. *Global Biogeochemical Cycles*, *22*(1), 1–13. https://doi.org/10.1029/2007GB003037

Tesi, T., Semiletov, I., Dudarev, O., Andersson, A., & Gustafsson, Ö. (2016). Matrix association effects on hydrodynamic sorting and degradation of terrestrial organic matter during cross-shelf transport in the Laptev and East Siberian shelf seas. *Journal of Geophysical Research: Biogeosciences*, *121*(3), 731–752. https://doi.org/10.1002/2015JG003067

Thomas, D. J., Korty, R., Huber, M., Schubert, J. A., & Haines, B. (2014). Nd isotopic structure of the Pacific Ocean 70-30 Ma and numerical evidence for vigorous ocean circulation and ocean heat transport in a greenhouse world. *Paleoceanography*, *29*(5), 454–469. https://doi.org/10.1002/2013PA002535

Thomas, E. (1990). Late Cretaceous through Neogene deep-sea benthic foraminifers (Maud Rise, Weddell Sea, Antarctica). *Proceedings of the Ocean Drilling Program, Scientific Results*, 571–594. https://doi.org/10.2973/odp.proc.sr.113.123.1990

Thomas, E, Booth, L., Maslin, M., & Shackleton, N. J. (1995). Northeastern Atlantic benthic foraminifera and implications of productivity during the last 40,000 years. *Paleoceanography*, *10*(3), 545–562. https://doi.org/10.1029/94PA03056

Thomas, Ellen. (2007). Cenozoic mass extinctions in the deep sea: What perturbs the largest habitat on Earth? *Special Paper 424: Large Ecosystem Perturbations: Causes and Consequences*, 1–23. https://doi.org/10.1130/2007.2424(01)

Thomas, Ellen, & Gooday, A. J. (1996). Cenozoic deep-sea benthic foraminifers: Tracers for changes in oceanic productivity? *Geology*, *24*(4), 355–358. https://doi.org/10.1130/0091-7613(1996)024<0355:CDSBFT>2.3.CO;2

Thomas, Ellen, Zachos, J., & Bralower, T. J. (2000). Deep-sea environments on a warm earth: lastest Paleocene-early Eocene. In B. T. Huber, K. G. MacLeod, & S. L. Wing (Eds.), *Warm Climates in Earth History* (pp. 132–160). New York: Cambridge University Press.

Thornalley, D. J. R., Barker, S., Becker, J., Hall, I. R., & Knorr, G. (2013). Abrupt changes in deep Atlantic circulation during the transition to full glacial conditions. *Paleoceanography*, *28*(2), 253–262. https://doi.org/10.1002/palo.20025

Tindall, J., Flecker, R., Valdes, P., Schmidt, D. N., Markwick, P., & Harris, J. (2010). Modelling the oxygen isotope distribution of ancient seawater using a coupled ocean-atmosphere GCM: Implications for reconstructing early Eocene climate. *Earth and Planetary Science Letters*, *292*(3–4), 265–273. https://doi.org/10.1016/j.epsl.2009.12.049

Tjalsma, R. C., & Lohmann, G. P. (1983). Paleocene-Eocene bathyal and abyssal benthic foraminifera from the Atlantic Ocean. *Paleocene-Eocene Bathyal and Abyssal Benthic Foraminifera from the Atlantic Ocean*, 1–90.

Toggweiler, J. R., & Bjornsson, H. (2000). Drake Passage and paleoclimate. *Journal of Quaternary Science*, *15*(4), 319–328. https://doi.org/10.1002/1099-1417(200005)15:4<319::AID-JQS545>3.0.CO;2-C

Townsend, D. W., Thomas, A. C., Mayer, L. M., & Thomas, M. A. (2006). Oceanography of the northwest Atlantic continental shelf. In A. R. Robinson & K. H. Brink (Eds.), *The Sea: The Global Coastal Ocean: Interdisciplinary Regional Studies and Syntheses* (Vol. 14, pp. 119–168). Harvard University Press, Cambridge.

Tucholke, B E, & Mountain, G. S. (1979). Seismic stratigraphy, lithostratigraphy and paleosedimentation patterns in the North American Basin. *Deep Drilling Results in the Atlantic Ocean; Continental Margins and Paleoenvironment.*, *3*, 58–86. https://doi.org/-

Tucholke, Brian E, & McCoy, F. W. (1986). Paleogeographic and paleobathymetric evolution of the North Atlantic Ocean. In *The Geology of North America. The western North Atlantic region* (Vol. M, pp. 589–602).

Tucholke, Brian E, & Mountain, G. S. (1986). Tertiary paleoceanography of the western North Atlantic Ocean. In *The Geology of North America (Vol. M): The Western North Atlantic Region* (pp. 631–650).

Urey, H. (1947). The Thermodynumic Properties of Isotopic Substances. *Journal of the Chemical Society*, (0), 562–581.

Via, R. K., & Thomas, D. J. (2006). Evolution of Atlantic thermohaline circulation: Early Oligocene onset of deep-water production in the North Atlantic. *Geology*, *34*(6), 441–444. https://doi.org/10.1130/G22545.1

Villa, G., Fioroni, C., Pea, L., Bohaty, S., & Persico, D. (2008). Middle Eocene-late Oligocene climate variability: Calcareous nannofossil response at Kerguelen Plateau, Site 748. *Marine Micropaleontology*, *69*(2), 173–192. https://doi.org/10.1016/j.marmicro.2008.07.006

Volk, T., & Hoffert, M. I. (1985). Ocean Carbon Pumps: Analysis of Relative Strengths and Efficiencies in Ocean-Driven Atmospheric CO 2 Changes. In E. T. Sundquist & W. S. Broecker (Eds.), *The Carbon Cycle and Atmospheric CO2: Natural Variations Archean to Present, Volume 32* (pp. 99–110). American Geophysical Union (AGU). https://doi.org/10.1029/GM032p0099

Wade, B., Olsson, R. K., Pearson, P. N., Huber, B. T., & Berggren, W. A. (Eds.). (2018). *Atlas of Oligocene Planktonic Foraminifera*. *Cushman Foundation For Foraminiferal Research Special Publication* (Vol. 46). Washington D.C. Retrieved from http://www.ucl.ac.uk/earth-sciences/research/micropalaeontology/research/atlas

Wade, B.S., & Kroon, D. (2002). Middle Eocene regional climate instability: Evidence from the western North Atlantic. *Geology*, *30*(11), 1011–1014. https://doi.org/10.1130/0091-7613(2002)030<1011:MERCIE>2.0.CO;2

Wade, Bridget S., & Pälike, H. (2004). Oligocene climate dynamics. *Paleoceanography*, *19*(4), 1–16. https://doi.org/10.1029/2004PA001042

Wade, Bridget S., & Pearson, P. N. (2008). Planktonic foraminiferal turnover, diversity fluctuations and geochemical signals across the Eocene/Oligocene boundary in Tanzania. *Marine Micropaleontology*, *68*(3–4), 244–255. https://doi.org/10.1016/j.marmicro.2008.04.002

Wade, Bridget S., Berggren, W. A., & Olsson, R. K. (2007). The biostratigraphy and paleobiology of Oligocene planktonic foraminifera from the equatorial Pacific Ocean (ODP Site 1218). *Marine Micropaleontology*, *62*(3), 167–179. https://doi.org/10.1016/j.marmicro.2006.08.005

Wade, Bridget S., Houben, A. J. P., Quaijtaal, W., Schouten, S., Rosenthal, Y., Miller, K. G., et al. (2012). Multiproxy record of abrupt sea-surface cooling across the Eocene-Oligocene transition in the Gulf of Mexico. *Geology*, *40*(2), 159–162. https://doi.org/10.1130/G32577.1

Wells, P., & Okada, H. (1996). Holocene and Pleistocene glacial palaeoceanography off southeastern Australia, based on foraminifers and nannofossils in Vema cored hole V18–222. *Australian Journal of Earth Sciences*, *43*(5), 509–523. https://doi.org/10.1080/08120099608728273

Winter, Amos., Jordan, R. W., & Roth, P. H. (1994). Biogeography of coccolithophores in ocean waters. In A. Winter & W. G. Siesser (Eds.), *Coccolithophores* (pp. 161–177). Cambridge University Press. Retrieved from http://www.cambridge.org/us/academic/subjects/earth-and-environmental-science/palaeontology-and-life-history/coccolithophores?format=PB#YoaXKBtVlYMlQfRA.97

Wright, J. D., & Miller, K. G. (1996). Control of North Atlantic deep water circulation by the Greenland-Scotland Ridge. *Paleoceanography*, *11*(2), 157–170. https://doi.org/10.1029/95PA03696

Young, J. (1994). Function of coccoliths. (Amos. Winter & W. G. Siesser, Eds.), *Coccolithophores*. Cambridge University Press. Retrieved from http://www.cambridge.org/us/academic/subjects/earth-and-environmental-science/palaeontology-and-life-history/coccolithophores?format=PB#6VuM2UbiyyVOktXy.97

Zachos, J., Pagani, M., Sloan, L., Thomas, E., & Billups, K. (2001). Trends, rythms and aberrations in global climate 65 Ma to present. *Science*, *292*(5517), 686–693.

Zachos, J. C., Stott, D., & Lohmann, K. C. (1994). Evolution of early Cenozoic marine temperatures at Equator. *Paleoceanography*, *9*(2), 353–387. https://doi.org/10.1029/93PA03266

Zanazzi, A., Kohn, M. J., Macfadden, B. J., & Jr, D. O. T. (2007). Large temperature drop across the Eocene – Oligocene transition in central North America, *445*(February), 639–642. https://doi.org/10.1038/nature05551

ArcGIS REST Services Directory. National Geophysical Data Center; [accessed 2016 Jan 20]. http://gis.ngdc.noaa.gov/arcgis/services

Bolin Centre for Climate Research Database http://bolin.su.se/data/Coxall-2018

Ocean Drilling Stratigraphic Network, 2011. Plate Tectonic Reconstruction Service; [accessed 2016 Apr 15]. http://www.odsn.de/odsn/services/paleomap/paleomap.html

Appendix I. Figure and table captions

Figure captions

Plate captions

Table captions

Appendix II. Taxonomy

The biostratigraphy, taxonomy and phylogenetic systematics of Eocene and Oligocene planktic foraminifera are extensively treated in two Atlas (Pearson et al., 2006; Wade et al., 2018). This section presents a modern treatment of the Site 612 planktic foraminifera assemblages using these recent frameworks. The goal of this appendix is to illustrate the morphospecies concept used by the author of this thesis to identify planktic foraminifera at Site 612 and reconstruct the assemblage. Comments are included to document any special features particular to the taphonomic settings investigated here. The results and interpretations of this Thesis are dependent on a strong taxonomy, as the interpretation of biostratigraphy and paleoenvironmental affinities of each species requires accurate identification of specimens.

In this appendix 43 species found in Site 612 (NW Atlantic Ocean) and Fuente Caldera section (Tethys) are described and listed here according to the taxonomies of Pearson et al. (2006) and revised by Pearson and Wade (2015) and Wade et al. (2018):

ORDER FORAMINIFERIDA D'Orbigny, 1826

Family HANTKENINIDAE Cushman, 1927

Genus *Cribrohantkenina* Thalmann, 1942

Cribrohantkenina inflata (Howe, 1928)

Genus *Hantkenina* Cushman, 1924

Hantkenina alabamensis Cushman, 1924

Hantkenina compressa Parr, 1947

Hantkenina nanggulanensis Hartono, 1969

Hantkenina primitiva Cushman and Jarvis, 1929

Family GLOBANOMALINIDAE Loebich and Tappan, 1984

Genus *Pseudohastigerina* Banner and Blow, 1959

Pseudohastigerina micra (Cole, 1927)

Pseudohastigerina naguewichiensis (Myatliuk, 1950)

Genus *Turborotalia* Cushman and Bermúdez 1949

Turborotalia cerroazulensis (Cole, 1928)

Turborotalia cocoaensis (Cushman, 1928)

Turborotalia cunialensis (Toumarkine and Bolli, 1970)

Turborotalia increbescens (Bandy, 1949)

Turborotalia ampliapertura (Bolli, 1957)

SUPERFAMILY GLOBIGERINOIDEA Loebich and Tappan, 1984

Family GLOBIGERINIDAE Carpenter, Parker and Jones, 1862

Genus *Catapsydrax* Bolli, Loebich and Tappan, 1957

Catapsydrax dissimilis (Cushman and Bermúdez, 1937)

Catapsydrax unicavus Bolli, Loeblich, and Tappan, 1957

Genus *Dentoglobigerina* Blow, 1979

Dentoglobigerina galavisi (Bermúdez, 1961)

Dentoglobigerina pseudovenezuelana (Blow and Banner, 1962)

Dentoglobigerina tripartita (Koch, 1926)

Dentoglobigerina venezuelana (Hedberg, 1937)

Genus *Ciperoella* Olsson and Hemleben, 2018

Ciperoella (Globoturborotalita) anguliofficinalis (Blow, 1969)

Genus *Globigerina* d'Orbigny, 1826

Globigerina officinalis Subbotina, 1953

Genus *Globoturborotalita* Hofker, 1976

Globoturborotalita ouachitaensis (Howe and Wallace, 1932)

Globoturborotalita martini (Blow and Banner, 1962)

Genus *Globorotaloides* Bolli 1957

Globorotaloides eovariabilis Huber and Pearson, 2006

Globorotaloides quadrocameratus Olsson, Pearson, and Huber, 2006

Genus *Subbotina* Brotzen and Pozaryska, 1961

Subbotina angiporoides (Hornibrook, 1965)

Subbotina linaperta (Finlay, 1939)

Subbotina eocaena (Guembel, 1868)

Subbotina corpulenta (Subbotina, 1953)

Subbotina gortanii (Borsetti, 1959)

Subbotina hagni (Gohrbandt, 1967)

Subbotina yeguaensis (Weinzierl and Applin, 1929)

Subbotina projecta Olsson, Pearson, and Wade, 2018

Genus *Paragloborotalia* Cifelli, 1982

Paragloborotalia nana (Bolli, 1957)

Paragloborotalia griffinoides Olsson and Pearson, 2006

Genus *Turborotalita* Blow and Banner, 1962

Turborotalita praequinqueloba Olsson and Hemleben, 2006

SUPERFAMILY BOLIVINOIDEA Glaessner, 1937

Family BOLIVINIDAE Glaessner, 1937

Genus *Streptochilus* Brönnimann and Resig, 1971

Streptochilus martini (Pijpers, 1933)

SUPERFAMILY GUEMBELITRIOIDEA Montanaro Gallitelli, 1957

Family CHILOGUEMBELINIDAE Reiss, 1963

Genus *Chiloguembelina* Loebich and Tappan, 1956

Chiloguembelina cubensis (Palmer, 1934)

Chiloguembelina ototara (Finlay, 1940)

SUPERFAMILY GLOBIGERINITOIDEA Bermúdez, 1961

Family GLOBIGERINITIDAE Bermúdez, 1961

Genus *Tenuitella* Fleisher, 1974

Tenuitella gemma (Jenkins, 1965)

Tenuitella praegemma (Li, 1987)

Tenuitella patefacta Li, 1995

Genus *Dipsidripella* Brotea, 1995

Dipsidripella danvillensis (Howe and Wallace, 1932)

Family TRUNCOROTALOIDIDAE Loebich and Tappan, 1961

Genus *Acarinina* Subbotina, 1953

Acarinina collactea (Finlay, 1939)

II.a. Description of planktic foraminifera species

Site 612 planktic foraminifera show good preservation. In fact, almost all specimens are well preserved or nearly well preserved, from near to glassy to glassy preservation. On the other hand, preservation of Fuente Caldera planktic foraminifera is frosty, showing recrystallization probably to severe dissolution and infilling during diagenesis. Basic distinction characteristics are detailed in the following section, and some of them quoted directly or slightly modified from the formal description presented in Pearson et al. (2006), Pearson and Wade (2015) and Wade et al. (2018). These are shown in italics.

Family HANTKENINIDAE Cushman, 1927

The species found in Site 612 and Fuente Caldera, belonging to Genus *Cribrohantkenina* and *Hantkenina* have a smooth wall, normal perforate, probably non-spinose. *Wall of tubulospines is imperforate, smooth or with fine striations. Test morphology is planispiral, biumbilical; with 5-6 closely appressed chambers; primary aperture is a single narrow, symmetrical equatorial arch, bordered by an imperforate lip. Adult chambers extend into a well-developed tubulospine, projecting radially or at a low angle with respect to the chamber periphery in the direction of coiling. The five species are stratigraphically useful and universally recognized, and they go extinct at the Eocene/Oligocene boundary.*

Genus *Cribrohantkenina* Thalmann, 1942

***Cribrohantkenina inflata* (Howe, 1928)**

PLATE 1, FIGURES 1 a-d

DESCRIPTION and DISTINGUISHING FEATURES.— *Primary aperture is a low arch, sometimes bifurcate. At least one, usually multiple, areal apertures. Tubulospines are mostly short and thick, to conical. Very inflated chambers, final one usually broader than tall in edge view. Generally large size, containing some of the largest individuals among modern and fossil planktic foraminifera, reaching shell sizes bigger than 1 mm. Distinguished from other hantkeninids by the presence of one or more areal apertures in addition to the primary aperture in the final adult chamber(s).*

DISCUSSION.— Specimen 1 a-b is interpreted as *Cribrohantkenina* based on the presence of what appears to be a single supplementary areal aperture in the edge view beneath the broken base of final tubular spine. Specimen 1 c-d from Fuente Caldera looks markedly different because they suffered from severe dissolution and infilling.

Genus *Hantkenina* Cushman, 1924

***Hantkenina alabamensis* Cushman, 1924**

PLATE 1, FIGURES 2 a-c

DESCRIPTION and DISTINGUISHING FEATURES.— *Aperture is broad and open; tubulospines are variable in length; chambers moderately inflated, usually taller than broad in edge view. Distinguished from H. compressa by the greater lateral inflation of the final 1-2 chambers, the more compact and involute coiling and more forward leaning tubulospines. It differs from H. primitiva in the greater lateral chamber inflation and by having a full complement of tubulospines in the adult whorl, and from H. nanggulanensis in the smaller size and absence of extremely globular final chambers.*

***Hantkenina compressa* Parr, 1947**

PLATE 1, FIGURES 3 a, b

DESCRIPTION AND DISTINGUISHING FEATURES.— *Aperture is tall, slit and with an inverted 'Y' shape; tubulospines are long and thin; chambers laterally compressed. Distinguished from H. alabamensis in lacking the subtangential adult tubulospines and in having more laterally compressed chambers. As in H. alabamensis, the final 2-3 tubulospines of H. compressa are in contact with the posterior wall of the adjacent chambers, but this is not as pronounced as in the former.*

***Hantkenina nanggulanensis* Hartono, 1969**

PLATE 1, FIGURES 4 a, b

DESCRIPTION AND DISTINGUISHING FEATURES.— Aperture is broad and open; tubulospines are mostly short and thick; *final chamber usually broader than tall in edge view* and chambers are strongly inflated and very large for the genus, since this morphospecies is transitional between *H. alabamensis* and *C. inflata*.

***Hantkenina primitiva* Cushman and Jarvis, 1929**

PLATE 1, FIGURES 5 a-c

DESCRIPTION AND DISTINGUISHING FEATURES.— *Somewhat evolute; aperture is tall, slit and with an inverted 'Y' shape; tubulospines are long, absent on early chambers; chambers are compressed. Distinguished from H. compressa by the absence of tubulospines on early adult chambers and the generally smaller test size. Lacks the forward leaning arrangement of tubulospines and lateral chamber inflation characteristic of H. alabamensis.* An interesting observation in 5c is that fine striations are visible not only on the tubulospines but also on the chamber surfaces in diverging patterns around the apertural system, indicative of externally flowing cytoplasm.

Family GLOBANOMALINIDAE Loebich and Tappan, 1984

Genus *Pseudohastigerina* Banner and Blow, 1959

The genus is characterized by a planispirally coiled, smooth-walled, normal perforate test, with an equatorial aperture which may vary from asymmetrical to symmetrical in position. The primary aperture may be singular or bipartite, arched openings bordered by a thin lip.

***Pseudohastigerina micra* (Cole, 1927)**

PLATE 1, FIGURES 6 a, b

DESCRIPTION AND DISTINGUISHING FEATURES.— *This species is characterized by its small compressed test, tightly coiled, involute, which is nearly circular in outline, pinched periphery with a peripheral imperforate band, globular chambers; in spiral view 6-7 chambers in ultimate whorl increasing slowly in size, straight and slightly depressed sutures, and rounded periphery in edge view. Maximum diameter of holotype 0.17 mm. The umbilicus tends to be crowded with minute pustules, as it is shown in Tanzanian specimens. It is distinguished from P. naguewichiensis by a more rapid increase in size of chambers, more compressed periphery and generally more involute coiling. In the Eocene is distinguished by its larger size, but both species are small in the Oligocene. In fact, there is a distinct decrease in the size of Pseudohastigerina micra at the same level as the extinction of the Hantkeninidae (i.e., the Eocene/Oligocene boundary) (Wade & Pearson, 2008) which serves as an alternative means of correlating the Eocene/Oligocene boundary when hantkeninids are rare or absent (Wade et al., 2011).* Specimen 6a shows scar of contact dissolution.

***Pseudohastigerina naguewichiensis* (Myatliuk, 1950)**

PLATE 1, FIGURES 7 a, b

DESCRIPTION AND DISTINGUISHING FEATURES.— *Characterized by its small size, much compressed test, tightly coiled, involute, circular in umbilical view slightly lobulate; globular chambers which increase very slowly in size, in umbilical view 6-8 chambers in ultimate whorl; sutures slightly depressed, straight to slightly curved, umbilicus circular in shape, inner coil of chambers may be partly visible; primary aperture a moderately high arch bordered by a thickened prominent lip, peripheral margin perforate and the appearance of a coarsely perforate test in adult tests. Wall in adult stage becomes thickened (gametogenetic calcite?) and openings to pores are enlarged, giving appearance of a coarsely perforate wall. The thickening of the wall in the terminal adult stage may indicate a change in its habitat in the water column (See P. micra description for distinguishing features).* Like other *P. naguewichiensis* found in Tanzania and the U.S. Gulf states (See PLATE 14.3, Figures 3-10), Site 612 *P. naguewichiensis* have well developed pustules in the umbilicus and early chambers.

Genus *Turborotalia* Cushman and Bermúdez 1949

T. cerroazulensis group (*T. cerroazulensis*, *T. cocoaensis* and *T. cunialensis*): *Smooth, normal perforate wall with pustulose earlier chambers and pustules around umbilicus; smooth calcification over proloculus; tendency to defoliate* (See PLATE 2, FIGURE 6 b)*; questionable sparse spine holes.*

***Turborotalia cerroazulensis* (Cole, 1928)**

PLATE 2, FIGURES 1 a-c

DESCRIPTION AND DISTINGUISHING FEATURES.— *Moderate trochospiral test, rounded-conical shape with 4-5 chambers in the final whorl; chambers appressed and embracing, strongly radially compressed and increasing moderately in size; final chamber commonly dorso-ventrally flattened; in edge view, showing obtuse or right angle at periphery and arching over towards umbilicus; dorsal sutures curved, flat or slightly depressed; aperture a broad arch, sometimes slit-like and in other specimens almost circular, generally not extending towards the periphery; an imperforate or pustulose lip is sometimes visible; more commonly it is obscured by inward folding of the final chamber; umbilicus very narrow; ventral sutures slightly curved, depressed. Holotype length 0.35 mm, breadth 0.26 mm.*

DISCUSSION.— *Turborotalia cerroazulensis has an obtuse periphery in edge view and it is clearly distinct from cocoaensis, which has an acute periphery.* However, it is an ongoing discussion where to place the boundaries between T. cerroazulensis group morphospecies, since they could belong to a single evolving population.

***Turborotalia cocoaensis* (Cushman, 1928)**

PLATE 2, FIGURES 2 a-c

DESCRIPTION AND DISTINGUISHING FEATURES.— *Large, low to moderate trochospiral, compressed conical to slightly biconvex test with 4-5 chambers in the final whorl; some specimens show imperforate band around periphery, or weak raised keel, especially on earlier chambers; chambers appressed and embracing, semicircular in dorsal view and wedge-shaped in ventral view, increasing moderately in size; final chamber distinctly acute at periphery in edge view; dorsal sutures strongly curved, flat or raised, commonly with imperforate band; aperture a broad arch, sometimes almost circular, generally not extending towards the periphery; an imperforate or pustulose lip is usually visible; umbilicus very narrow; ventral sutures moderately curved, depressed. Strong tendency for sinistral coiling. Holotype length 0.48 mm, breadth 0.33 mm. This species is distinguished from T. cunialensis by having a less acute periphery and a relatively flat spiral side. (See T. cerroazulensis description for more distinguishing features).*

***Turborotalia cunialensis* (Toumarkine and Bolli, 1970)**

PLATE 2, FIGURES 3 a-e, 6 a-b

DESCRIPTION AND DISTINGUISHING FEATURES.— *Low trochospiral, dorsoventrally strongly compressed biconvex test with 4-5 chambers in the final whorl; most specimens show imperforate keel around periphery, which can be distinctly raised; chambers appressed and embracing, wedge-shaped in ventral aspect and increasing moderately in size; final chamber distinctly acute (<40°) at periphery in edge view; dorsal sutures strongly curved, flat or raised with imperforate band; aperture a broad arch, sometimes almost circular, in extraumbilical position; umbilicus very narrow; ventral sutures moderately curved, depressed. Strong tendency for sinistral coiling. Holotype length 0.45 mm. Turborotalia cunialensis is a relatively rare form, although transitional cunialensis-cocoaensis specimens are more common. (See T. cerroazulensis and T. cocoaensis descriptions for distinguishing features).*

DISCUSSION.—Specimen 3 a-e is a *cunialensis-cocoaensis* transition, but closer to *T. cunialensis*; it shows the imperforate keel, as specimens in Pl. 15.4, Fig. 17 in Pearson et al.

(2006). Due to well preservation is possible to see smooth normal perforate wall, unperforated peripheral band and pustules on the earlier chambers.

***Turborotalia increbescens* (Bandy, 1949)**

PLATE 2, FIGURES 4 a-c

DESCRIPTION AND DISTINGUISHING FEATURES.— *High porosity, weakly cancellate and coarsely pustulose, often smooth on final chamber; tendency to defoliate (e.g., Leckie and others, 1993). Moderate to high trochospiral test, compact and rounded with 3½-4 chambers in the final whorl; chambers appressed and embracing, radially compressed and increasing moderately in size; final chamber commonly radially flattened; in edge view, showing rounded periphery with final chamber arching towards umbilicus; dorsal sutures curved, depressed; aperture a very broad arch in an intra-extraumbilical position, often irregular and elongate; an imperforate or pustulose lip is usually visible; umbilicus usually narrow to moderately open; ventral sutures slightly curved, depressed; usually a strong tendency for sinistral coiling. Holotype length 0.51 mm, breadth 0.47 mm. Turborotalia increbescens is distinguished from T. cerroazulensis by its more compact morphology, rounder periphery and more globular test shape. It is distinguished from T. ampliapertura by its longer inner whorl, distinctly more extraumbilical position of the aperture and less globular chamber shape, which gives the test a more 'globorotaliid' appearance.*

***Turborotalia ampliapertura* (Bolli, 1957)**

PLATE 2, FIGURES 5 a-c

DESCRIPTION AND DISTINGUISHING FEATURES.— *Smooth, to weakly cancellate wall in final chambers, frequently densely pustulose in earlier chambers; tendency to defoliate. Moderately high trochospiral, compact globular test with 3-4 chambers in final whorl. chambers inflated, appressed and embracing, increasing moderately in size; outline lobulate or rounded in edge view; dorsal sutures slightly curved, depressed; aperture a high arch, approaching circular, in umbilical-extraumbilical position; umbilicus wide and deep; ventral sutures moderately curved, depressed. Holotype length 0.49 mm, width 0.29 mm. Turborotalia ampliapertura is distinguished from T. increbescens by the wider, more open umbilicus, more umbilically centered aperture and more globular chamber shape.* Specimen 5c shows normal perforate wall in last chamber.

Genus *Catapsydrax* Bolli, Loebich and Tappan, 1957

Coarsely cancellate wall, sacculifer- type or ruber/sacculifer-type, probably spinose in life, with tendency to develop a thick (gametogenic) crust in some species. Test is globular, lobulate or compact, with 3-4 chambers in the final whorl; chambers moderately inflated, appressed; primary aperture is umbilical and nearly always covered by bulla with one or more infralaminal apertures in the adult stage; apertures are bordered by a continuous, narrow lip that may be thickened by gametogenetic calcification.

Catapsydrax dissimilis **(Cushman and Bermúdez, 1937)**

PLATE 3, FIGURES 2 a-c

DESCRIPTION AND DISTINGUISHING FEATURES.— *Wall coarsely cancellate, sacculifer-type, probably spinose; in adult stage wall becomes thickened. Test is moderately large, compact, low-moderate trochospiral of 2½-3 whorls, involute, lobate with 4 chambers in the final whorl, enlarging slowly. Later chambers are inflated, subglobular but slightly appressed and embracing. The early ontogenetic whorl, comprising 4½-5 chambers, is flattened or raised slightly above the adult whorl as seen in spiral view. Sutures are straight and depressed on the umbilical side and moderately depressed and slightly curved on spiral side. The primary aperture is a low umbilical arch covered by a single slightly inflated or flattened bulla less coarsely cancellate than the rest of test, with 2 or more (up to 4) rimmed infralaminal openings. The maximum diameter of holotype is ~0.5 mm, thickness ~0.3 mm. Distinguished from C. unicavus by having 2-4 infralaminal openings around the bulla compared to 1. The chambers of the final whorl are also usually of more similar size in C. dissimilis compared to C. unicavus, giving C. dissimilis a more lobed peripheral outline.*

DISCUSSION.— In the imaged specimen is not possible to see two infralaminal openings, characteristic of this taxon. However, the rather thin flat nature of the piece of bulla remaining is rather smooth and flat and reminiscent comparing to the bulla seen in typical dissimilis.

Catapsydrax unicavus **Bolli, Loeblich, and Tappan, 1957**

PLATE 3, FIGURES 1 a-c

DESCRIPTION AND DISTINGUISHING FEATURES.— *Cancellate wall with sacculifer-type texture, generally with heavy gametogenetic calcification in adult specimens. Moderately low trochospiral test, compact to slightly lobulate consisting of about 2½-3 whorls. Chambers globular, embracing, increasing rapidly in size with a terminal bulla extending over the umbilicus. The bulla may be flattened or inflated, and has a continuous, thickened imperforate rim and a single infralaminal aperture in a posterior position. The early ontogenetic whorl, comprising ~5 chambers, is somewhat flattened and typically raised slightly above the adult whorl. The adult whorl has 3-4 globular chambers increasing rapidly in size. Sutures, straight on the umbilical side, slightly curved on the spiral side and moderately depressed. The primary aperture small, semi-circular low umbilical arch, visible only when the bulla is broken or missing. The edge profile is an ovoid revealing the embracing bulla. Holotype maximum diameter is 0.22 mm, thickness 0.17 mm. Distinguished from Catapsydrax dissimilis by having a relatively compact test and a single infralaminal aperture which is always at the posterior (umbilical) end of the bulla. The chambers of the final whorl also typically increase more gradually in size.*

DISCUSSION.— *Catapsydrax unicavus is the most common and long-ranging species in the genus, extending from the early Eocene to early Miocene.*

Genus *Dentoglobigerina* Blow, 1979

Cancellate wall, normal perforate, probably spinose or sparsely spinose in life, commonly pustulose in umbilical region. Test is trochospiral, globular, rounded to lobulate in outline, final chamber leaning towards the umbilicus with an ill-defined apertural face in most species; weakly to coarsely pustulose with a concentration of pustules commonly seen around the umbilicus. Primary aperture umbilical, narrow to wide, commonly hidden in umbilical view, often with pustulose apertural lip or an asymmetrical triangular tooth, but in some species no tooth occurs, a bulla may be present, and is more common in late Oligocene and early Miocene forms.

Dentoglobigerina galavisi **(Bermúdez, 1961)**

PLATE 3, FIGURES 3 a-d, 4 a-d

DESCRIPTION AND DISTINGUISHING FEATURES.— *Wall is cancellate, honeycomb, normal perforate, probably spinose in life. Test trochospiral, globular, oval to quadrate in equatorial outline, chambers globular; in spiral view 3½ ovoid chambers in ultimate whorl, increasing rapidly in size, sutures moderately depressed, straight to slightly curved; in umbilical view 3-3½ ovoid chambers increasing rapidly in size, sutures deeply incised, straight; umbilicus small, enclosed by surrounding chambers, aperture centered over the umbilicus, bordered by a thin irregular, triangular shaped lip that is centered below an ill-defined apertural face; in edge view chambers ovoid in shape, projecting over the umbilicus, ultimate chamber shows a distinct bending and flattening into the umbilicus forming an indistinct umbilical face (modified from Olsson and others, 2006). Maximum diameter of holotype 0.46 mm, thickness 0.40 mm. It is the root-stock of the evolutionary radiation of dentoglobigerinids. It is distinguished from most species of Subbotina by its more quadrate shape, more appressed and radially compressed chambers, and the tendency for the final chamber to bend over the umbilicus (features which it shares with most other Dentoglobigerina).*

DISCUSSION.—Imaged specimen shows normal perforated and pustulose wall with pustulose early chambers, four chambers.

Dentoglobigerina pseudovenezuelana **(Blow and Banner, 1962)**

No images available for these sites. See Plate 11.9, Figures 9-16 (Wade et al., 2018).

DESCRIPTION AND DISTINGUISHING FEATURES.— *Wall is cancellate, normal perforate, probably spinose in life, pustulose in umbilical region. Test is large, trochospiral, compact, globular, subcircular in outline, chambers ovoid; in spiral view 3½ ovoid chambers in ultimate whorl, increasing moderately in size, sutures moderately depressed, straight; in umbilical view 3-3½ ovoid chambers increasing moderately in size, sutures deeply depressed, straight, umbilicus moderate in size, aperture centered over the umbilicus, bordered by an irregular pustulose lip or tooth; in edge view chambers ovoid in shape, embracing, ultimate chamber extends over the umbilicus, oval to subcircular in outline (modified from Olsson and others, 2006). Maximum diameter of holotype 0.51 mm, thickness 0.34 mm. Dentoglobigerina pseudovenezuelana is distinguished from its ancestor D. galavisi by its more inflated chambers and in typically having 3½ rather than 3 chambers in the final whorl. Although it is called pseudovenezuelana, the resemblance is not especially close. Dentoglobigerina venezuelana tends to have a more spherical overall morphology, with large, appressed, pillow-like chambers, the last of which is very*

commonly reduced in size, and in generally lacking the very pustulose, ragged lip which is characteristic of pseudovenezuelana.

***Dentoglobigerina tripartita* (Koch, 1926)**

No images available for these sites. See Plate 11.15, Figures 1-16 (Wade et al., 2018).

DESCRIPTION AND DISTINGUISHING FEATURES.— *Wall is cancellate, probably spinose in life, pustulose, with concentrations of pustules on the umbilical shoulders. Test is large, robust, globular, sub-spherical, outline sub-circular; in spiral view 3 embracing, elliptical shaped chambers, arranged in a moderate trochospire, that rapidly increase in size in final whorl, ultimate chamber may be reduced in size; in edge view globular, sub-circular in outline; in umbilical view 3 embracing chambers in final whorl that rapidly increase in size, final chamber commonly reduced in size, somewhat reniform, umbilicus small, triangular, open, aperture umbilical bordered by an irregular triangular shaped tooth covered in small pustules. Maximum diameter of holotype 0.52 mm, minimum diameter 0.50 mm.*

***Dentoglobigerina venezuelana* (Hedberg, 1937)**

PLATE 3, FIGURES 5 a-c

DESCRIPTION AND DISTINGUISHING FEATURES.— *Cancellate wall, probably spinose in life, pustulose, sometimes with concentrations of pustules on the umbilical shoulders. Test is large to very large, robust, globular, spherical, outline circular; in spiral view 3½-4 embracing, reniform chambers that slowly increase in size in the final whorl, final chamber commonly reduced in size and flattened, sutures weakly depressed; in edge view globular, oval in outline; in umbilical view 3½-4 appressed and embracing chambers in final whorl that slowly increase in size, final chamber commonly reduced in size, partially closing the umbilicus, sutures depressed; umbilicus small, commonly triangular in shape, aperture umbilical, often concealed, may be bordered by an irregular triangular tooth or a lip with no tooth. Maximum diameter of holotype 0.52 mm, minimum diameter 0.50 mm. The taxonomic concept of D. venezuelana* (in Wade et al., 2018) *is quite broad, and includes specimens that may contain a lip or a tooth. The holotype of D. venezuelana is a large specimen, these large sized forms are quite rare in the Oligocene. See under D. pseudovenezuelana for criteria for separating that species.*

DISCUSSION.— According to Wade et al. (2018) *D. venezuelana* does not evolve till Oligocene: It has a very uncertain range in the Eocene and is a typical Oligocene species. However, we find a very typical form and is abundant both in Site 612 and in Fuente Caldera. It might be characteristic from the North Atlantic. B. Wade (pers. Comm.) confirms that this has been observed elsewhere which supports the identification.

Genus *Ciperoella* Olsson and Hemleben, 2018

***Ciperoella anguliofficinalis* (Blow, 1969)**

No images available for these sites. See Plate 7.1, Figures 1-18 (Wade et al., 2018).

DESCRIPTION AND DISTINGUISHING FEATURES.— *Wall is normal perforate, spinose, Neogloboquadrina-type wall texture. Pore concentrations range from around 25-60 pores/50 µm² test surface area and pore diameters from around 0.9-2.5 µm. Test is moderately low trochospiral, globular, lobulate in outline, chambers globular; in spiral view 5 slightly embracing chambers in final whorl, increasing moderately in size, sutures depressed, straight; in umbilical view 5 slightly embracing chambers, increasing moderately in size, sutures depressed, straight, umbilicus large, open, enclosed by surrounding chambers, aperture umbilical, a rounded arch, bordered by a thin rim; in edge view chambers globular, slightly embracing, initial whorl slightly elevated. Maximum diameter 0.21-0.30 mm, minimum diameter 0.18-0.21 mm, maximum width 0.17 mm*. *The species is distinguished by its small lobulate test, globular chambers, large umbilical aperture, and* Neogloboquadrina-*type wall texture. Its sutures may be incised.*

DISCUSSION.— Synonymy: In Atlas of Eocene Planktonic Foraminifera (Pearson et al., 2008) described under *Globoturborotalita* as *Globoturborotalita anguliofficinalis* (Blow).

Genus *Globigerina* d'Orbigny, 1826

***Globigerina officinalis* Subbotina, 1953**

PLATE 4, FIGURES 1 a-c

DESCRIPTION AND DISTINGUISHING FEATURES.— *Wall is perforate and spinose, bulloides-type wall structure. Pore concentrations average 77 pores/50 µm² test surface area and pore diameters average 0.84 µm. Test is moderately high trochospiral consisting of 3 whorls, lobulate in outline, chambers globular; in spiral view 4 globular, slightly embracing chambers in ultimate whorl, increasing rapidly in size, sutures moderately depressed, straight, the last 4 chambers make up about 3/5 of the test size; in umbilical view 4 globular, slightly embracing chambers, increasing rapidly in size, sutures moderately depressed, straight, umbilicus small, open, enclosed by surrounding chambers, aperture umbilical, a low to high arch bordered by an imperforate rim; in edge view chambers globular in shape, slightly embracing (Olsson and others, 2006). Maximum diameter of holotype 0.14- 0.20 mm, thickness 0.11 mm. The species is characterized by its globular, slightly embracing, chambers with a moderately high arched, umbilical aperture bordered by a thickened imperforate rim, and its bulloides-type wall texture (Olsson and others, 2006). It differs from compact species of Globoturborotalita and Subbotina due to the possession of the wall with discrete spine collars and lack of a cancellate wall.*

Genus *Globoturborotalita* Hofker, 1976

***Globoturborotalita ouachitaensis* (Howe and Wallace, 1932)**

PLATE 4, FIGURES 2 a-d

DESCRIPTION AND DISTINGUISHING FEATURES.— *Wall is cancellate, normal perforate, spinose, ruber/sacculifer-type wall structure, an average of 27 pores/50 µm² test surface area. Test is small, moderately low trochospiral consisting of 4 whorls. The profile is diamond-shape and lobulate, chambers globular; in spiral view 4 globular, slightly embracing chambers in ultimate whorl, increasing slowly in size, sutures depressed, straight; in umbilical view 4 globular,*

slightly embracing chambers, increasing slowly in size, sutures depressed, straight. The last chamber is smaller than the previous ones. The umbilicus is small but open, enclosed by surrounding chambers, aperture umbilical tending towards the peripheral margin, a low arch, bordered by a lip; in edge view chambers globular in shape, slightly embracing, initial spire of chambers slightly elevated. Holotype maximum diameter 0.19 mm. It can be distinguished from the other species of Globoturborotalita by its overall smaller size, the rather gradual rate of chamber size increase in the final whorl, the reduced size of the final chamber compared to the penultimate, and the low arched aperture tending to the peripheral margin. These features give a distinctive diamond-shape to the peripheral outline.

***Globoturborotalita martini* (Blow and Banner, 1962)**

PLATE 4, FIGURES 3 a-c

DESCRIPTION AND DISTINGUISHING FEATURES.— *Wall is normal perforate, cancellate, spinose, ruber/sacculifer-type wall texture, an average of around 20 pores/50 µm^2 test surface area. Test is small, moderately low trochospiral, consisting of 3 whorls, globular, lobulated in outline, chambers globular; in spiral view 4 globular, slightly embracing chambers in ultimate whorl, increasing rapidly in size, sutures depressed, straight; in umbilical view 4 globular, slightly embracing chambers, increasing rapidly in size, final chamber reduced in size extending over and partially covering the umbilicus, sutures depressed, straight, umbilicus small, partially covered by the ultimate chamber, aperture umbilical, a rounded arch, bordered by thickened rim; in edge view chambers globular in shape, slightly embracing. Holotype maximum diameter 0.22 mm. Distinguished from the other species belonging to Globoturborotalita by its small size, 4 globular slightly embracing chambers in the last whorl and by the reduced last chamber that extends over and partially covers the umbilicus.*

Genus *Globorotaloides* Bolli 1957

***Globorotaloides eovariabilis* Huber and Pearson, 2006**

PLATE 4, FIGURES 4 a-d

DESCRIPTION AND DISTINGUISHING FEATURES.— *Wall is normal perforate, coarsely cancellate, sacculifer-type wall texture, often with corroded interpore ridges resulting in a remnant wall texture consisting of distinct 'rosettes' around pores. Possibly spinose. Test outline is lobate, subcircular in axial view, axial periphery rounded to slightly compressed and pinched, biconvex, oval to egg-shaped in edge view; 3- 3½ whorls of slightly inflated chambers arranged in a flattened to slightly elevated trochospire; 14-15 chambers in adult tests, 4½-6½ in the final whorl increasing moderately in size; umbilicus shallow to moderately deep and narrow; umbilical sutures moderately depressed, curved, radial; spiral sutures initially indistinct, later weakly depressed, radial; aperture a low umbilical-extraumbilical arch extending one-third towards the peripheral margin, surrounded by a broad lip that extends into the umbilical area; tendency to develop an imperforate peripheral band in some Oligocene forms. Holotype maximum diameter 0.18 mm, breadth 0.10 mm. It differs from Globorotaloides quadrocameratus in having greater*

than 4 (typically 5 but up to 6½) final whorl chambers that are less inflated and increase more gradually in size.

Globorotaloides quadrocameratus **Olsson, Pearson, and Huber, 2006**

PLATE 4, FIGURES 5 a-d

DESCRIPTION AND DISTINGUISHING FEATURES.— *Wall is spinose (?). Normal perforate, coarsely cancellate, sacculifer-type, wall structure. Test very low trochospiral, 2-2½ whorls, lobate in outline, chambers globular; in spiral view 4 globular, slightly embracing chambers in the ultimate whorl, increasing rapidly in size, sutures moderately depressed, straight; in umbilical view 4 globular, slightly embracing chambers, increasing rapidly in size, ultimate chamber may be directed towards the umbilicus, sutures moderately depressed, straight, umbilicus small, aperture umbilical-extraumbilical a low opening bordered by narrow thickened lip; in edge view chambers globular in shape, slightly embracing. Maximum diameter of holotype 0.18 mm, breadth 0.10 mm. It is characterized by its small, distinctly lobulate test, 4 chambers in the ultimate whorl, the umbilically directed ultimate chamber and rapidly enlarging final whorl chambers. It differs from Paragloborotalia griffinoides by the smaller size, more coarsely cancellate test, more open coiling and flattened spiral side. It differs from Catapsydrax unicavus in the greater number of final whorl chambers and umbilical-extraumbilical position of the aperture and lack of a bulla.*

Genus *Subbotina* **Brotzen and Pozaryska, 1961**

Low trochospiral, tripartite test consisting of 10-12 chambers, with 3-4 rapidly inflating, globular chambers in the ultimate whorl. Aperture interiomarginal, umbilical to slightly extraumbilical in most species, commonly with a low arch. Apertural lip varies from narrow to fairly broad with a distinct apparatus extending over the umbilicus, may have a projecting umbilical tooth in some species. Umbilicus small and nearly closed by tight coiling. Wall cancellate and spinose; spines set at juncture of the cancellate ridges with or without spine collars. Cancellate texture varies from weak to very strong and from moderate to very coarse or distinctly honeycombed (modified from Olsson and others, 2006). Distinguished from Dentoglobigerina by its globular chambers, lobate outline and spinose wall texture. In spiral view, Subbotina *chambers always appear more rounded, whereas* Dentoglobigerina *chambers appear subrectangular. Distinguished from* Globoturborotalita *by its generally larger size, less compact test, and more globular chambers.*

Subbotina angiporoides **(Hornibrook, 1965)**

No images available for these sites. See Plate 10.1, Figures 1-8 (Wade et al., 2018).

DESCRIPTION AND DISTINGUISHING FEATURES.— *Spinose wall, normal perforate, moderately cancellate, often thickened by addition of gametogenetic calcite,* ruber/sacculifer-*type wall. Test small to moderate size, non-umbilicate, spherical, quadrilobate, axial periphery rounded; chambers inflated, increasing moderately in size, 11-13 coiled in 3 whorls, usually 4 chambers in the final whorl that are often elongated along the radial axis; final chamber usually strongly embracing, kummerform, and extended over the umbilical sutures; sutures weakly depressed, radial to slightly curved; aperture a low, indistinct, interiomarginal slit bordered by a*

thick lip that extends the full width of the chamber face, opening in and sometimes beyond the umbilical area. Holotype maximum diameter 0.45 mm. Distinguished by often having a kummerform final chamber that resembles a bulla and extends over the umbilicus, and a low slit-like aperture that is bordered by a thick lip and is centered over the antepenultimate chamber. In S. angiporoides *the penultimate and ultimate chambers are about the same size giving rise to a test that appears compact. Furthermore, the lip appears continuous from one adjacent chamber to the other. It differs from* Catapsydrax unicavus *by its more compact test, well-defined lip and no bulla.*

***Subbotina linaperta* (Finlay, 1939)**

PLATE 5, FIGURES 1 a-c

DESCRIPTION AND DISTINGUISHING FEATURES.— *Wall is coarsely and symmetrically cancellate, normal perforate, spinose, sacculifer-type wall texture. Test is low trochospiral, globular, rounded in outline, chambers globular; in spiral view 3-3⅓globular, embracing chambers in ultimate whorl, increasing rapidly in size, sutures slightly to moderately depressed, straight to slightly curved, ultimate chamber broader than high, presenting a flattened appearance; in umbilical view 3-3⅓ globular, embracing chambers, increasing rapidly in size, sutures moderately depressed, straight to slightly curved, umbilicus very small, enclosed by surrounding chambers, aperture umbilical to somewhat extraumbilical, bordered by a thin, even lip, ultimate chamber broader than high, presenting a flattened appearance; in edge view chambers globular in shape, embracing; aperture visible as a low arch, bordered by a thin, even lip, ultimate chamber broader than high, presenting a flattened appearance. Maximum diameter of neotype 0.38 mm, thickness 0.27 mm. Differs from Subbotina eocaena (Guembel) by the faster rate of chamber size increase, 3-3½ rather than 4 chambers in the final whorl, equatorial flattening of final whorl chambers, and shallower umbilicus.*

***Subbotina eocaena* (Guembel, 1868)**

PLATE 5, FIGURES 2 a-c

DESCRIPTION AND DISTINGUISHING FEATURES.— *Wall is cancellate, normal perforate, spinose,* ruber/sacculifer-*type wall texture. Test is low trochospiral, globular, oval in outline, chambers globular arranged in three whorls; in spiral view 3½-4 globular, embracing chambers in ultimate whorl, increasing moderately rapidly in size, sutures moderately depressed, straight to slightly curved; in umbilical view 3½-4 globular, embracing chambers, increasing moderately in size, sutures moderately depressed, straight, umbilicus small, enclosed by surrounding chambers, aperture umbilical to slightly extraumbilical, directed somewhat anteriorly over the umbilicus, bordered by a thin, irregular lip; in edge view chambers globular in shape, embracing, aperture visible as a circular arch, bordered by a thin, irregular lip. Maximum diameter of neotype 0.69 mm, maximum thickness 0.45 mm.* Subbotina eocaena *is typified by its low rate of chamber size increase, globular chambers, open umbilicus, with a low arched aperture bordered by a thin irregular lip. It is distinguished from* S. corpulenta *by its well-developed lip and large, globular final chamber.*

***Subbotina corpulenta* (Subbotina, 1953)**

PLATE 5, FIGURES 3 a-c

DESCRIPTION AND DISTINGUISHING FEATURES.— *Wall is cancellate, normal perforate, spinose. Test is moderately high trochospiral, lobulate in outline, chambers globular, arranged in three whorls; in spiral view 4-4½ globular chambers in ultimate whorl, increasing moderately in size, sutures moderately depressed, straight to slightly curved; in umbilical view 4-4½ globular chambers, increasing moderately in size, often with a reduced ultimate chamber cantilevered over the umbilicus, sometimes centered and resembling a bulla, sutures moderately depressed, straight to slightly curved, umbilicus moderate in size, enclosed by surrounding chambers and often partly to entirely covered by the ultimate chamber, aperture umbilical, deep, with or without a lip; in edge view test with a moderately elevated initial whorl, chambers globular in shape, aperture generally not visible. Maximum diameter of holotype 0.57 mm, thickness 0.38 mm. It is characterized by its generally large adult size, moderately elevated initial spire, lobulate test, globular chambers and the cantilevered ultimate chamber directed over the umbilicus. It is distinguished from* Subbotina eocaena *by its less developed lip and common bulla-like ultimate chamber. The frequency of a bulla-like chamber on* S. corpulenta *could lead to confusion with the genus Catapsydrax and* Su*bbotina gortanii. However,* S. corpulenta *is distinguished from* C. unicavus *by its more lobate periphery, less compact coiling and generally more incised sutures, and from* S. gortanii *by its lower trochospire and more lobate periphery.*

***Subbotina gortanii* (Borsetti, 1959)**

No images available for these sites. See Plate 10.4, Figures 1-16 (Wade et al., 2018).

DESCRIPTION AND DISTINGUISHING FEATURES.—*Wall is cancellate, normal perforate, spinose,* ruber/sacculifer-*type wall texture. Test is high trochospiral, globular in outline, chambers globular; in spiral view 4 globular, loosely embracing chambers arranged in 3 whorls, increasing moderately in size, sutures deeply depressed, straight; in umbilical view 4 globular, loosely embracing chambers, increasing moderately in size, sutures deeply depressed, straight, umbilicus large, enclosed by surrounding chambers, aperture umbilical, bordered by a thickened, narrow rim; in edge view chambers arranged in a high, loosely coiled spire. Maximum diameter of holotype 0.62 mm, thickness 0.54 mm. The species is characterized by its trochospiral loosely coiled test, globular chambers, and umbilical aperture. It is distinguished from other Oligocene subbotinids and from species of* Catapsydrax *by its very high trochospire. Specimens are commonly large in size and may have a large inflated bulla-like chamber and may possess a tooth.*

***Subbotina hagni* (Gohrbandt, 1967)**

No images available for these sites. See Plate 6.11, Figures 1-17 (Pearson et al., 2006).

DESCRIPTION AND DISTINGUISHING FEATURES.— *Wall is cancellate, normal perforate, spinose, ruber/sacculifer-type wall texture. Test is low trochospiral, quadrate in outline, chambers globular; in spiral view 4 globular, somewhat embracing chambers in ultimate whorl, increasing moderately in size, sutures moderately depressed, straight; in umbilical view 4-4½ globular, somewhat embracing chambers, increasing moderately in size, sutures moderately depressed, straight, umbilicus small, enclosed by surrounding chambers, aperture umbilical to*

extraumbilical, bordered by a thin, irregular lip; in edge view chambers globular in shape, embracing; aperture visible as a low arch, bordered by a thin, irregular lip. Maximum diameter of holotype 0.58 mm, thickness 0.34 mm. The species is characterized by its generally large adult size, quadrate test, and globular, embracing, chambers with a lowarched, umbilical-extraumbilical aperture bordered by a thin irregular lip.

DISCUSSION.— *Subbotina hagni* has been reclassified as *Parasubbotina hagni* after Wade et al. (2018). However, the specimens assigned to *S. hagni* in Wade and Pearson (2008) with a stratigraphic range that extended into lower Oligocene Zone O1 are now considered to be *S. corpulenta* (Pearson and Wade, 2015).

***Subbotina yeguaensis* (Weinzierl and Applin, 1929)**

PLATE 5, FIGURES 4 a-c

DESCRIPTION AND DISTINGUISHING FEATURES.— *Wall is normal perforate, symmetrically cancellate, sacculifer-type wall texture, spinose. Test is moderately elevated, trochospiral, globular, lobulate in outline, chambers globular; in spiral view 3⅓ globular, slightly embracing chambers in ultimate whorl, increasing moderately in size, ultimate chamber may be equal to or smaller in size than penultimate chamber, sutures moderately depressed, straight; in umbilical view 3⅓ globular, slightly embracing chambers, increasing moderately in size, sutures moderately depressed, straight, umbilicus small, enclosed by surrounding chambers, aperture umbilical, bordered by a somewhat broad lip that tapers both anteriorly and posteriorly, ultimate chamber may be equal to or smaller than the penultimate chamber; in edge view moderately elevated trochospire, chambers globular in shape, somewhat embracing, aperture visible as a low rounded opening, bordered by a somewhat broad lip. Maximum diameter of holotype 0.52 mm, thickness 0.40 mm. The species is characterized by its lobulate test and moderately elevated trochospire, and the somewhat broad apertural lip that tapers both anteriorly and posteriorly.*

***Subbotina projecta* Olsson, Pearson, and Wade, 2018**

PLATE 5, FIGURE 5 a

DESCRIPTION AND DISTINGUISHING FEATURES.— *Wall is cancellate, spinose* ruber*/* sacculifer-*type wall texture. Test is large, globular, 10 to 13 chambers arranged in three whorls, in a moderately high trochospiral, lobate, oval in outline, chambers spherical to subspherical; in spiral view 3½- 4 globular, embracing chambers in final whorl, increasing gradually in size, sutures straight or gently curved, moderately incised; in umbilical view 3½ globular chambers, increasing moderately rapidly in size, sutures depressed to incised, straight, umbilicus wide, square, deep, aperture umbilical, usually with teeth projecting into umbilicus from one or more chambers. Teeth vary from small and triangular to narrow elongate projections, often with a distinct rim or lip around the edges of the tooth that connect with the apertural lip; in edge view chambers globular in shape, embracing, teeth leaning into the umbilicus. Maximum diameter of holotype 0.50 mm. The equatorial outline is in general diamond-shaped with chambers arranged in a cross. Subbotina projecta is distinguished by its high trochospiral coiling, wide, deep, and generally square umbilicus and detailed morphology of the teeth, which, although highly variable, can be quite elongate and are generally rimmed by a thin lip of constant thickness. It is*

distinguished from S. yeguaensis *by its smaller size, more globular chambers, more incised umbilical sutures and by possessing true teeth rather than a broad, tapering lip.*

Genus *Paragloborotalia* Cifelli, 1982

***Paragloborotalia nana* (Bolli, 1957)**

PLATE 6, FIGURES 1 a-c

DESCRIPTION AND DISTINGUISHING FEATURES.— *Wall is normal perforate, coarsely cancellate, probably sparsely spinose in life, heavy gametogenetic calcification is often present. Test is small to medium in size; very low trochospiral, quadrate to slightly lobulate in equatorial outline, chambers spherical to subspherical, inflated, embracing; typically 4-4½, occasionally 5 chambers in ultimate whorl, increasing slowly in size; in spiral view chambers moderately inflated, spherical to subspherical, arranged in 2 whorls, sutures slightly depressed, radial; in umbilical view chambers moderately inflated, sutures slightly depressed, radial, forming a cross, umbilicus very narrow, moderately deep, sometimes closed off by surrounding chambers, ultimate chamber may be slightly reduced in size; aperture umbilical-extraumbilical, low arch, bordered by a narrow, often thickened, continuous lip; in edge view chambers globular, spiral side flat, periphery broadly rounded. Maximum diameter of holotype 0.319 mm; maximum thickness 0.217 mm.*

***Paragloborotalia griffinoides* Olsson and Pearson, 2006**

PLATE 6, FIGURES 2 a-c

DESCRIPTION AND DISTINGUISHING FEATURES.— *Wall is normal perforate, coarsely cancellate, sacculifer-type, spinose. Test is very low trochospiral, globular, subquadrate in outline; chambers globular, much inflated, embracing; in spiral view 4, occasionally 4½ globular, embracing chambers in ultimate whorl, increasing rapidly in size; sutures slightly depressed, straight; last 4 chambers make up about three-quarters of the test, ultimate chamber may be slightly reduced in size; in umbilical view 4, occasionally 4½ globular, embracing chambers, increasing rapidly in size, sutures slightly depressed, straight; umbilicus very small opening, sometimes closed off by surrounding chambers; aperture umbilical-extraumbilical, bordered by a narrow, often thickened, continuous, lip; ultimate chamber may be slightly reduced in size; in edge view chambers globular, periphery rounded, aperture a high arch extending midway onto the peripheral edge, bordered by a thickened lip. Maximum diameter of holotype 0.41 mm, minimum diameter 0.39 mm, and maximum width 0.29 mm. P. griffinoides is distinguished by its small, very low trochospiral, compact, subquadrate test, coarsely cancellate wall, and aperture with a thickened continuous lip.*

Genus *Turborotalita* Blow and Banner, 1962

Turborotalita praequinqueloba **Olsson and Hemleben, 2006**

PLATE 6, FIGURE 3 a

DESCRIPTION AND DISTINGUISHING FEATURES.— Wall is n*ormal perforate, spinose, may be covered by a crust in adult stage. Test is very low trochospiral, lobulate in outline, chambers globular; in spiral view 4-4½ globular, slightly embracing chambers in ultimate whorl, increasing moderately in size, ultimate chamber sometimes reduced in size, sutures moderately depressed, straight; in umbilical view 4-4½ globular, slightly embracing chambers, increasing moderately in size, ampullate ultimate chamber often reduced and directed towards and over the umbilicus, sutures moderately depressed, straight, umbilicus small and often covered by ultimate chamber, aperture umbilical, a wide arch bordered by an imperforate rim or narrow thickened lip; in edge view chambers globular in shape, slightly embracing. Maximum diameter of holotype: approximately 0.27 mm, thickness 0.13 mm.*

Genus *Streptochilus* Brönnimann and Resig, 1971

Streptochilus martini **(Pijpers, 1933)**

No images available for these sites. See Plate 19.1, Figures 1-17 (Wade et al., 2018).

DESCRIPTION AND DISTINGUISHING FEATURES.— *Wall is microperforate, although low latitude forms may have macroperforations, smooth to finely pustulose. Test elongate, somewhat compressed, sometimes slightly twisted, gradually to moderately tapering, peripheral margin subrounded; chambers biserial, increasing gradually in size, sutures flush to slightly depressed and oblique in first two to three pairs of chambers, later more strongly depressed and nearly horizontal; aperture a semicircular arch with a thin lip that projects on one side more than the other and an internal toothplate that connects foramina of successive chambers. Syntype length 0.25 mm, width 0.19 mm, thickness 0.11 mm. It is distinguished from C. ototara by the more compressed and tapering test, smoother test surface, and presence of a toothplate.*

Genus *Chiloguembelina* Loebich and Tappan, 1956

Chiloguembelina cubensis **(Palmer, 1934)**

PLATE 6, FIGURES 4 a-d

DESCRIPTION AND DISTINGUISHING FEATURES.— Wall is m*icroperforate, bilamellar, 4-5 µm thick, the inner layer is usually very thin (0.4-0.5 µm), the outer layer has a submicron-scale, granular to columnar texture, granule size is 0.2-0.4 µm, (*ototara*-type wall); surface texture finely pustulose on youngest chambers, later becoming faintly but distinctly costate in rows aligned with the long axis of the test; the wall is evenly perforated by pores that are usually about 0.7-0.8 µm in diameter, but can exceed 1 µm as a result of dissolution, pore channels are straight. Test is biserial, elongate, subtriangular in outline, moderately expanding, periphery rounded*

rather than compressed; chambers increase moderately in size, up to 16 chambers in adult specimens; sutures depressed, perpendicular to slightly oblique to the growth axis; aperture a low, moderately narrow to broad symmetrical arch centered or slightly off-center from the base of the final chamber, bordered on one side by a narrow collar that thickens away from its attachment point on the chamber face. Apical angle varies from 35-45°. Hypotypes length 0.12-0.25 mm. Distinguished from Chiloguembelina ototara *by the presence of fine, generally continuous costae that are aligned parallel to the elongate axis of the test.*

***Chiloguembelina ototara* (Finlay, 1940)**

PLATE 6, FIGURES 5 a-c

DESCRIPTION AND DISTINGUISHING FEATURES.— Wall is m*icroperforate, bilamellar, (oto*tara-*type wall); uniformly finely pustulose, lacking pore mounds or costae. Test is biserial, elongate, moderately to rapidly expanding, subtriangular in outline with an apical angle of 50-55°; periphery rounded rather than compressed; chambers increasing moderately to rapidly in size, usually 11-12, and sometimes up to 15 in adult specimens; sutures depressed, perpendicular to slightly oblique to growth axis; aperture a moderately narrow to broad symmetrical arch centered or slightly off-center of the base of the final chamber, extending half-way up the final chamber face, bordered on one side by a narrow lip that thickens away from its attachment point on the chamber face; some specimens with an irregularly shaped terminal chamber. Paratype length, 0.17 mm, width 0.10 mm, breadth 0.07 mm. Distinguished from* C. cubensis *by the absence of costae on the wall surface and the shorter, more strongly tapering test.*

Genus *Tenuitella* Fleisher, 1974

***Tenuitella gemma* (Jenkins, 1965)**

PLATE 7, FIGURES 1 a-c

DESCRIPTION AND DISTINGUISHING FEATURES.— *Wall is microperforate* glutinata-*type wall, surface smooth to finely pustulose, pustules irregularly scattered on both sides of test.* Test is *small, very low trochospiral, equatorial periphery lobate, circular to elliptical in outline, axial periphery rounded; chambers globular, slightly compressed, 4½-6 in the final whorl, 10-12 comprising adult tests, increasing slowly in size; sutures slightly recurved, depressed on spiral and umbilical sides; umbilicus narrow, deep, sometimes nearly closed; aperture a very low arch bordered by a narrow lip, intra- to extraumbilical in position, sometimes extending to periphery (‘*neoclemenciae*’ morphotype). Holotype 0.16 mm diameter. Distinguished from* T. praegemma *by its slightly more compressed test, less lobate equatorial periphery and nearly closed umbilicus and by the absence of ovoid or subcrescentic chambers and secondary apertures.*

***Tenuitella praegemma* (Li, 1987)**

PLATE 7, FIGURES 2 a-c

DESCRIPTION AND DISTINGUISHING FEATURES.— *Wall is microperforate, surface smooth to finely pustulose, pustules irregularly scattered on umbilical and spiral sides of test.*

Test is small, lobate, circular in equatorial outline, equatorial periphery rounded; chambers globular, coiled in a low trochospire, increasing gradually in size, 4-5 in the final whorl, subcrescentic on spiral side, final chamber may be narrow, asymmetrical and pendulous; sutures depressed, curved on the spiral side, radial on umbilical side; umbilicus narrow, deep; aperture a low extraumbilical-umbilical arch bordered by a narrow, equidimensional lip that may extend to the spiral side, and may be accompanied by a secondary aperture or apertural lip along the spiral suture. Holotype maximum diameter: 0.16 mm. Distinguished from other tenuitellids by having either a low, interiomarginal aperture that extends from near the umbilicus to the spiral side or by presence of a low, narrow extraumbilical aperture accompanied by a supplementary aperture (or apertural lip) on or near the peripheral margin of the spiral suture; it further differs from Tenuitella gemma by having a more lobate equatorial outline.

***Tenuitella patefacta* Li, 1995**

PLATE 7, FIGURES 3 a-c

DESCRIPTION AND DISTINGUISHING FEATURES.— *Wall is microperforate, surface smooth to finely pustulose, pustules irregularly scattered on umbilical and spiral sides of test. Test is small, lobate circular in equatorial outline, equatorial periphery rounded; chambers globular, coiled in a very low trochospire, increasing gradually in size, 5-6 in the final whorl, nearly symmetrical in edge view; sutures depressed, curved on the spiral side, radial on umbilical side; umbilicus small; aperture a low extraumbilical-umbilical arch bordered by a narrow, equidimensional lip. Holotype maximum diameter: 0.16 mm. Differs from T. gemma by having a more lobate equatorial outline and a more oval equatorial outline, a more open umbilicus and an aperture that extends closer to the peripheral margin; differs from T. praegemma by lacking secondary apertures or apertural lips and having globular rather than oval or subcrescentic chambers.*

Genus *Dipsidripella* Brotea, 1995

***Dipsidripella danvillensis* (Howe and Wallace, 1932)**

PLATE 7, FIGURES 4 a-c

DESCRIPTION AND DISTINGUISHING FEATURES.— *Wall is micro- to medioperforate, surface smooth to moderately pustulose, hispid to bluntly pustulose, pustules randomly scattered on umbilical and spiral sides of test, radially crystalline in section (*glutinata-*type,* danvillensis-*subtype). Test is small, moderately lobate, subquadrate to circular or elliptical in equatorial outline, axial periphery rounded; chambers globular or radially extended, coiled in a low trochospire, increasing moderately in size, 4-6 in the final whorl; sutures radial and depressed on umbilical and spiral sides; umbilicus narrow to broad and moderately deep; aperture an interiomarginal, umbilical-extraumbilical arch that is narrow and high or broad and low, may or may not be bordered by a narrow, equidimensional lip; a semicircular accessory aperture may occur on the spiral side at the intersection of the spiral and and/ or penultimate chamber sutures. Holotype maximum diameter 110 µm, breadth 70 µm.*

Genus *Acarinina* Subbotina, 1953

***Acarinina collactea* (Finlay, 1939)**

PLATE 7, FIGURES 5 a-c

DESCRIPTION AND DISTINGUISHING FEATURES.— *Wall is moderately to coarsely muricate, normal perforate, nonspinose. Chambers arranged in a low to moderate trochospiral, test is compact, typically 4½ -5 chambers in the final whorl, slowly increasing in size; peripheral outline weakly lobate; chambers on the umbilical side wedge-shaped or triangular with blunt and blocky muricae; sutures distinct, straight, radial and wide; umbilicus narrow, deep; umbilical-extraumbilical aperture; weakly convex to flat; on spiral side 10-12 sub-circular chambers in three whorls; sutures weakly incised, curved; rounded to subangular peripheral margin in edge view. Maximum diameter of holotype 0.18 mm, thickness 0.13 mm.* Acarinina collactea *is characterized by its compact test, subangular chambers that increase slowly in size, and wide, incised sutures.*

DISCUSSION.— Evidence given recently by Wade et al. (2018) stated that acarininid lineage continued through the Oligocene, contrary to what previously thought, that they went extinct prior to the Eocene/Oligocene boundary (Berggren and others, 2006). Remarkably, evidence found at Site 612 supports the new statement, showing that this species occurs in Oligocene sediments.

PLATES

Plate 1. Family HANTKENINIDAE Cushman, 1927 and Genus *Pseudohastigerina* Banner and Blow, 1959

SEM micrographs of high quality glassy preserved biostratigraphically useful planktic foraminifera species from DSDP Site 612 and Fuente Caldera (1 c-d), upper Eocene Zone E15/16. **1 a-d** *Cribrohantkenina inflata* (Howe, 1928). Umbilical and edge views (**1 a, b** same specimen; Sample 612-17X-1, 39-41 cm) and close-up of imperforate lip and additional areal aperture, surrounded by an imperforated thickened rim (**1 c, d**; Sample 110-120 FC, 115 cm). **2 a-c** *Hantkenina alabamensis* (Cushman, 1925). Umbilical and edge views and wall close-up. **2 a**, sample 612-16X-CC, 10-12 cm (136.08 mbsf). **2 b-c** (same specimen), sample 612-17X-1, 0-2 cm (136.2 mbsf). **3 a, b** *Hantkenina compressa* Parr, 1947. Umbilical and edge views. Sample 612-17X-1, 39-41 cm (136.59 mbsf). **4 a, b** *Hantkenina nanggulanensis* Hartono, 1969. Umbilical and edge views (same specimen). Sample 612-17X-2, 28-30 cm (137.98 mbsf). **5a-c** *Hantkenina primitiva* Cushman and Jarvis, 1929. Umbilical and edge views and wall close-up, showing fine striations in the chamber surfaces (same specimen). 612-16X-CC, 10-12 cm (136.08 mbsf). **6 a-b** *Pseudohastigerina micra* (Cole, 1927). Umbilical and edge views (same specimen). Sample 612-17X-2, 47-49 cm (138.17 mbsf). **7 a-b** *Pseudohastigerina naguewichiensis* (Myatliuk, 1950). Umbilical and edge views (same specimen). Sample 612-17X-2, 47-49 cm (138.17 mbsf). Scale bar: 100 µm.

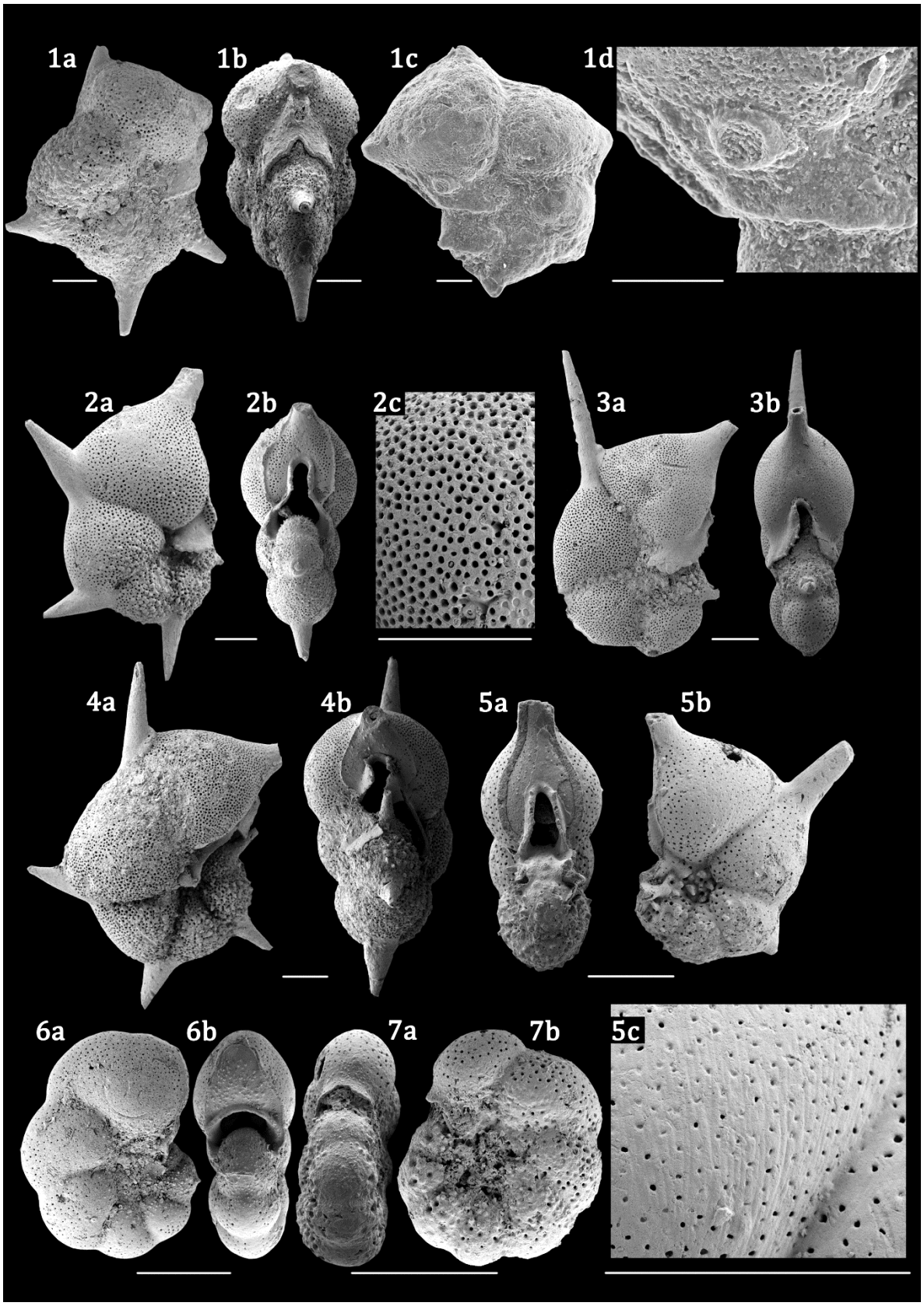

Plate 1. Family HANTKENINIDAE Cushman, 1927 and Genus *Pseudohastigerina* Banner and Blow, 1959

Plate 2. Genus *Turborotalia* Cushman and Bermúdez, 1949

SEM micrographs of high quality glassy preserved biostratigraphically useful planktic foraminifera species from DSDP Site 612, upper Eocene Zone E15/16 (**1-4, 6**) and lower Oligocene Zone O1 (**5**). **1 a-c** *Turborotalia cerroazulensis* (Cole, 1928). Umbilical, edge and spiral views (same specimen). Sample 612-16X-CC, 10-12 (136.08 mbsf). **4 a-c** *Turborotalia increbescens* (Bandy, 1949). Umbilical, edge and spiral views (same specimen). 612-17X-2, 47-49 cm (138.17 mbsf). **2 a-c** *Turborotalia cocoaensis* (Cushman, 1928). Umbilical, edge and spiral views (same specimen). Sample 612-17X-1, 59-61 cm (136.79 mbsf). **3 a-e** *Turborotalia cunialensis* (Toumarkine and Bolli, 1970). Umbilical, edge and spiral views and close-ups showing the keel and the umbilical aperture with spines (**a-d** same specimen). Sample 612-17X-1, 20-22 cm (136.4 mbsf). **5 a-c** *Turborotalia ampliapertura* (Bolli, 1957). Umbilical, edge and spiral views (same specimen). Sample 612-16X-7, 3-5 cm (135.73 mbsf). **6 a-b** *Turborotalia cunialensis* (Toumarkine and Bolli, 1970). Umbilical view and close-up showing *Turborotalia cerroazulensis* group characteristic defoliation (same specimen). Sample 612-17X-1, 0-2 cm, 136.2 mbsf. Scale bar: 100 µm.

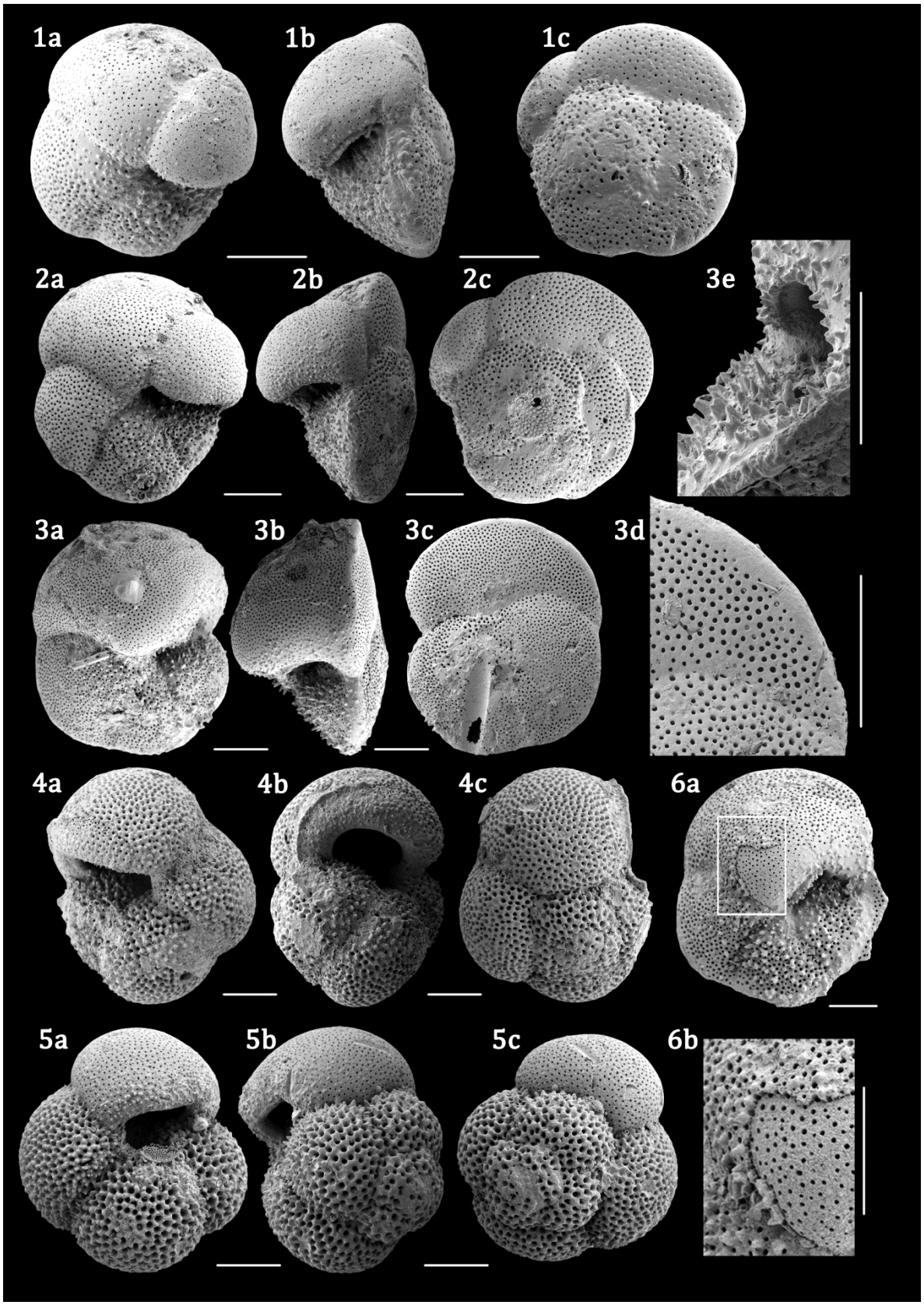

Plate 2. Genus *Turborotalia* Cushman and Bermúdez, 1949

Plate 3. Genus *Catapsydrax* Bolli, Loebich and Tappan, 1957 and Genus *Dentoglobigerina* Blow, 1979

SEM micrographs of high quality glassy preserved biostratigraphically useful planktic foraminifera species from DSDP Site 612, upper Eocene Zone E15/16. **1 a-c** *Catapsydrax unicavus* Bolli, Loeblich, and Tappan, 1957. Umbilical, edge and spiral views (same specimen). Sample 612-17X-1, 0-2 cm (136.2 mbsf). **2 a-c** *Catapsydrax dissimilis* (Cushman and Bermúdez, 1937). Umbilical, edge and spiral views (same specimen). Sample 612-17X-1, 0-2 cm (136.2 mbsf). **3, 4** *Dentoglobigerina galavisi* (Bermúdez, 1961). Umbilical, edge and spiral views and wall close-ups of three chambered (**3 a-d**, same specimen) and four chambered (**4 a-d**, same specimen) *D. galavisi*. Close-ups show the thin irregular, triangular-shaped lip (**3d**) and the normal perforated and pustulose wall (**4d**). Samples 612-17X-2, 47-49 cm (138.17 mbsf) and 612-17X-1, 0-2 cm (136.2 mbsf). **5 a-c** *Dentoglobigerina venezuelana* (Hedberg, 1937). Umbilical, edge and spiral views (same specimen). Sample 612-17X-1, 59-61 cm (136.79 mbsf). Scale bar: 100 µm.

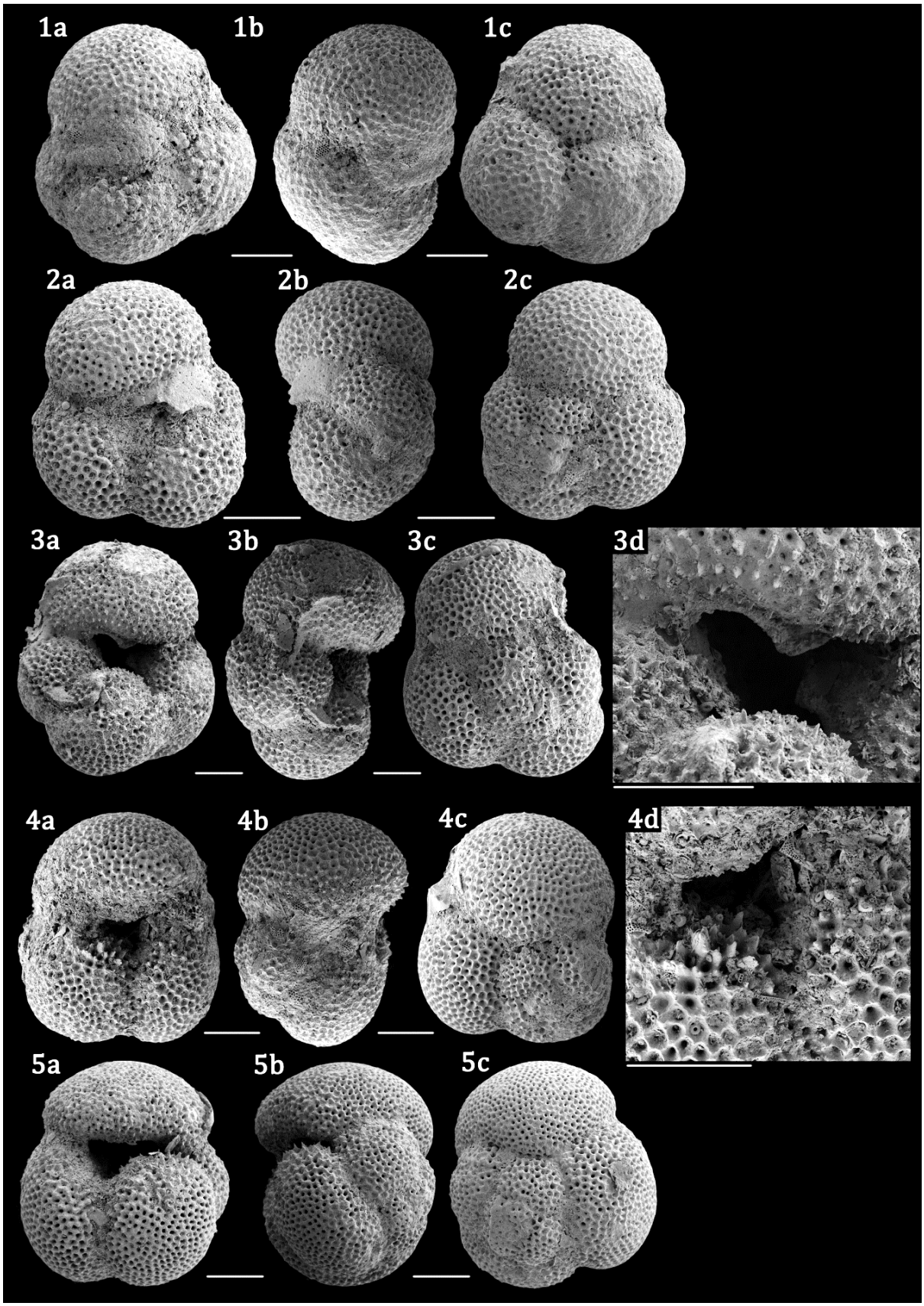

Plate 3. Genus *Catapsydrax* Bolli, Loebich and Tappan, 1957 and Genus *Dentoglobigerina* Blow, 1979

Plate 4. Genus *Globigerina* d'Orbigny, 1826, Genus *Globoturborotalita* Hofker, 1976 and Genus *Globorotaloides* Bolli 1957

SEM micrographs of high quality glassy preserved biostratigraphically useful planktic foraminifera species from DSDP Site 612, upper Eocene Zone E15/16, Sample 612-17X-1, 0-2 cm (136.2 mbsf). **1 a-c** *Globigerina officinalis* Subbotina, 1953. Umbilical, edge and spiral views (same specimen). **2 a-d** *Globoturborotalita ouachitaensis* (Howe and Wallace, 1932). Umbilical, edge and spiral views (**2 a-c** same specimen) and light microscope image showing umbilical view. **3 a-c** *Globoturborotalita martini* (Blow and Banner, 1962). Umbilical, edge and spiral views (same specimen). **4 a-d** *Globorotaloides eovariabilis* Huber and Pearson, 2006. Umbilical, edge and spiral views and close-up (same specimen). **5 a-d** *Globorotaloides quadrocameratus* Olsson, Pearson, and Huber, 2006. Umbilical, edge and spiral views and close-up (same specimen). **4 d** and **5 d** detailed views show *sacculifer*-type wall texture, with equally distributed pores and coarsely cancellate structure that is strongly symmetrically oriented (honeycomb structure). Scale bar: 100 μm.

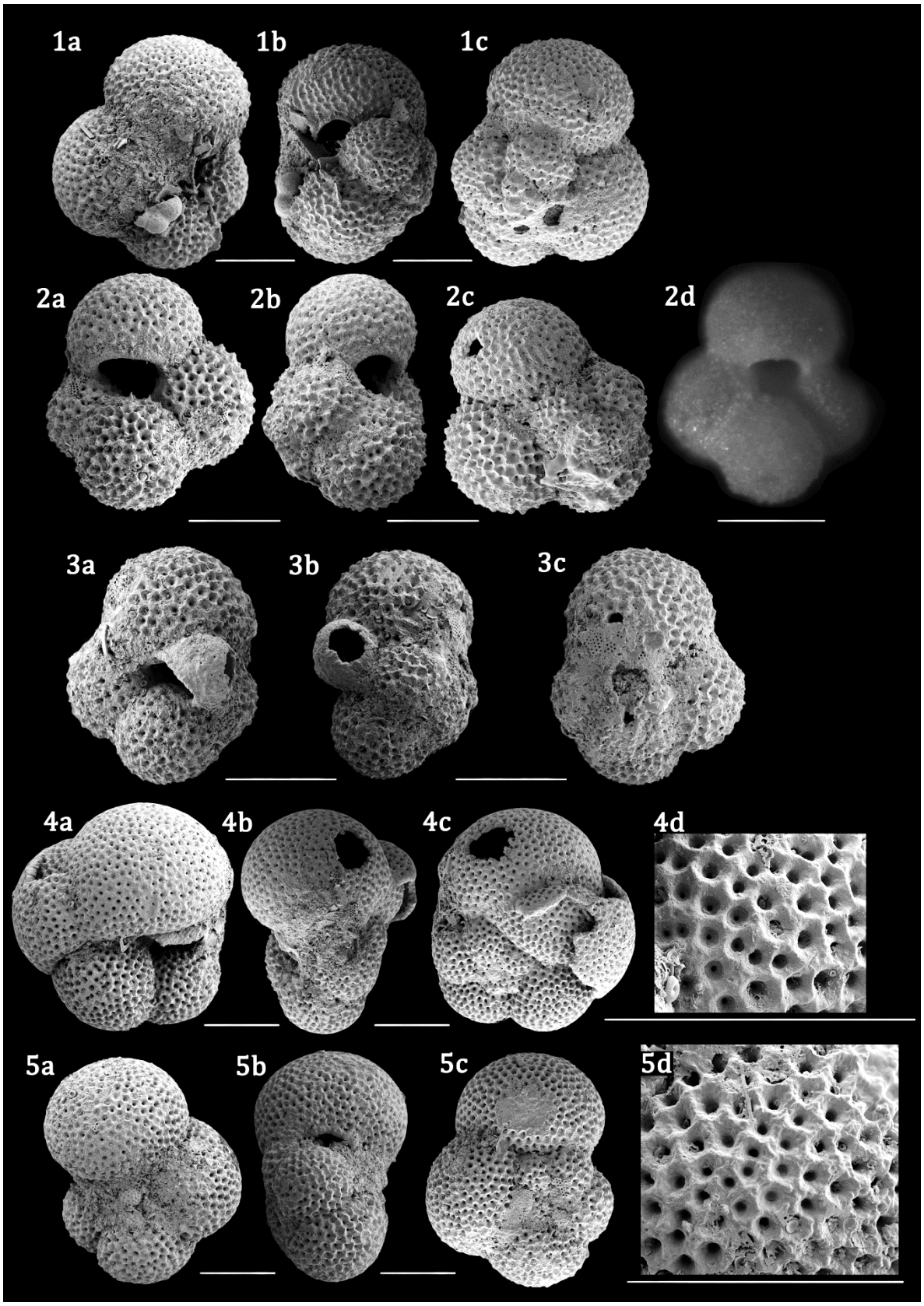

Plate 4. Genus *Globigerina* d'Orbigny, 1826, *Globoturborotalita* Hofker, 1976 and *Globorotaloides* Bolli 1957

Plate 5. Genus *Subbotina* Brotzen and Pozaryska, 1961

SEM micrographs of high quality glassy preserved biostratigraphically useful planktic foraminifera species from DSDP Site 612, upper Eocene Zone E15/16 (**1-5**) and lower Oligocene Zone O1 (**6**). **1 a-c** *Subbotina linaperta* (Finlay, 1939). Umbilical, edge and spiral views (same specimen). Sample 612-17X-1, 0-2 cm (136.2 mbsf). **2 a-c** *Subbotina eocaena* (Guembel, 1868). Umbilical, edge and spiral views (same specimen). Sample 612-17X-1, 0-2 cm (136.2 mbsf). **3 a-c** *Subbotina corpulenta* (Subbotina, 1953). Umbilical, edge and spiral views (same specimen). Sample 612-17X-1, 98-100 cm (137.18 mbsf). **4 a-c** *Subbotina yeguaensis* (Weinzierl and Applin, 1929). Umbilical, edge and spiral views (same specimen). Sample 612-17X-1, 0-2 cm (136.2 mbsf). **5 a** *Subbotina projecta* Olsson, Pearson, and Wade, 2018. Umbilical view. Sample 612-16X-6, 143-145 cm (135.63 mbsf). Scale bar: 100 µm.

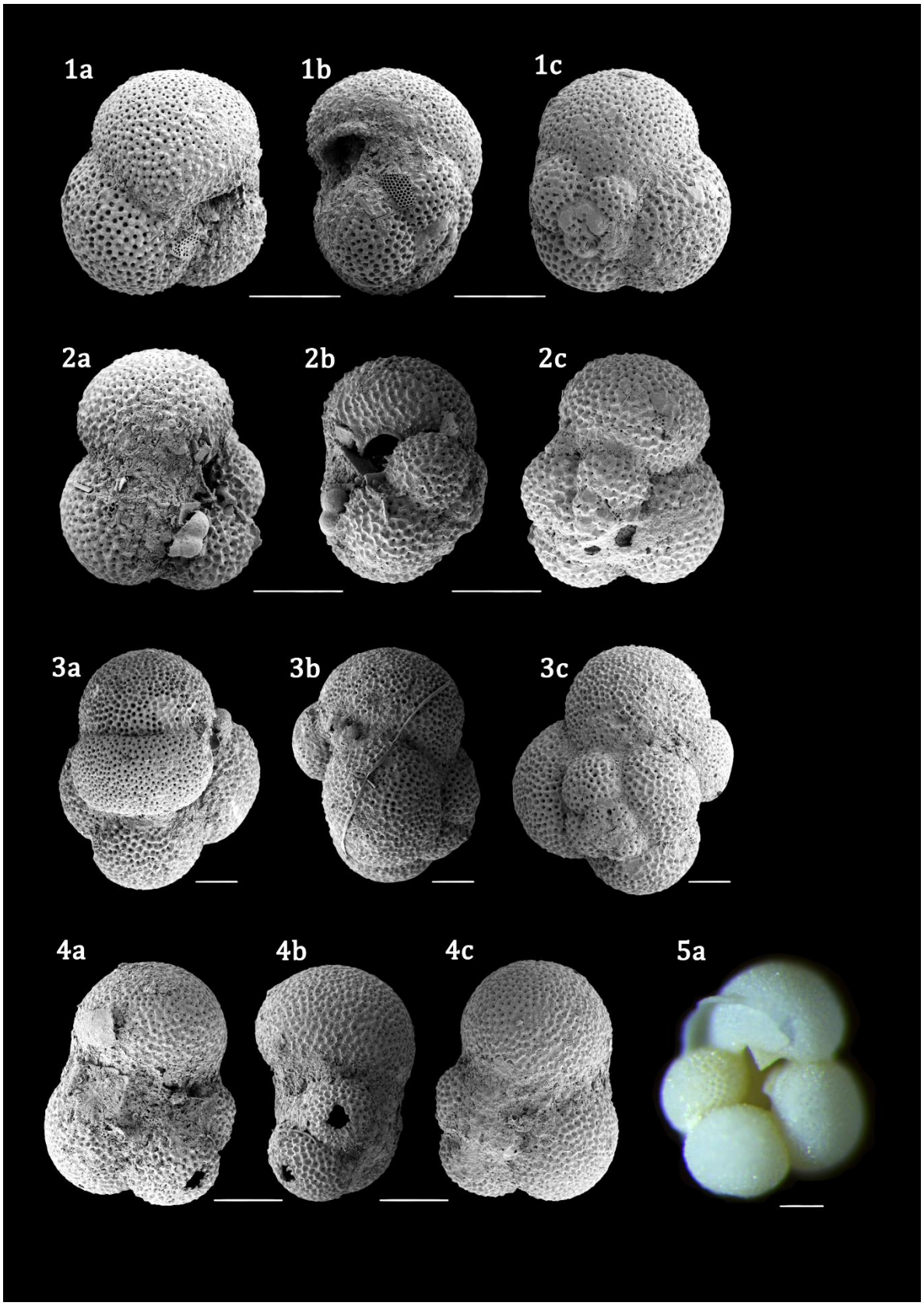

Plate 5. Genus *Subbotina* Brotzen and Pozaryska, 1961

Plate 6. Genus *Paragloborotalia* Cifelli, 1982, Genus *Turborotalita* Blow and Banner, 1962 and Genus *Chiloguembelina* Loebich and Tappan, 1956

SEM micrographs of high quality glassy preserved biostratigraphically useful planktic foraminifera species from DSDP Site 612, upper Eocene Zone E15/16. **1 a-c** *Paragloborotalia nana* (Bolli, 1957). Umbilical, edge and spiral views (same specimen). Sample 612-17X-3, 110-112 cm (140.3 mbsf). **2 a-c** *Paragloborotalia griffinoides* Olsson and Pearson, 2006. Umbilical, edge and spiral views (same specimen). Sample 612-17X-1, 0-2 cm (136.2 mbsf). **3 a** *Turborotalita praequinqueloba* Olsson and Hemleben, 2006. Umbilical view. Sample 612-17X-1, 0-2 cm (136.2 mbsf). **4 a-d** *Chiloguembelina cubensis* (Palmer, 1934). Specimen attached in the wall of a *Turborotalia* and close-ups show edge and umbilical views (same specimen). Sample 612-17X-1, 59-61 cm (136.79 mbsf). **5 a-c** *Chiloguembelina ototara* (Finlay, 1940). Umbilical and edge views. Sample 612-17X-3, 110-112 cm (140.3 mbsf). Scale bar: 100 µm.

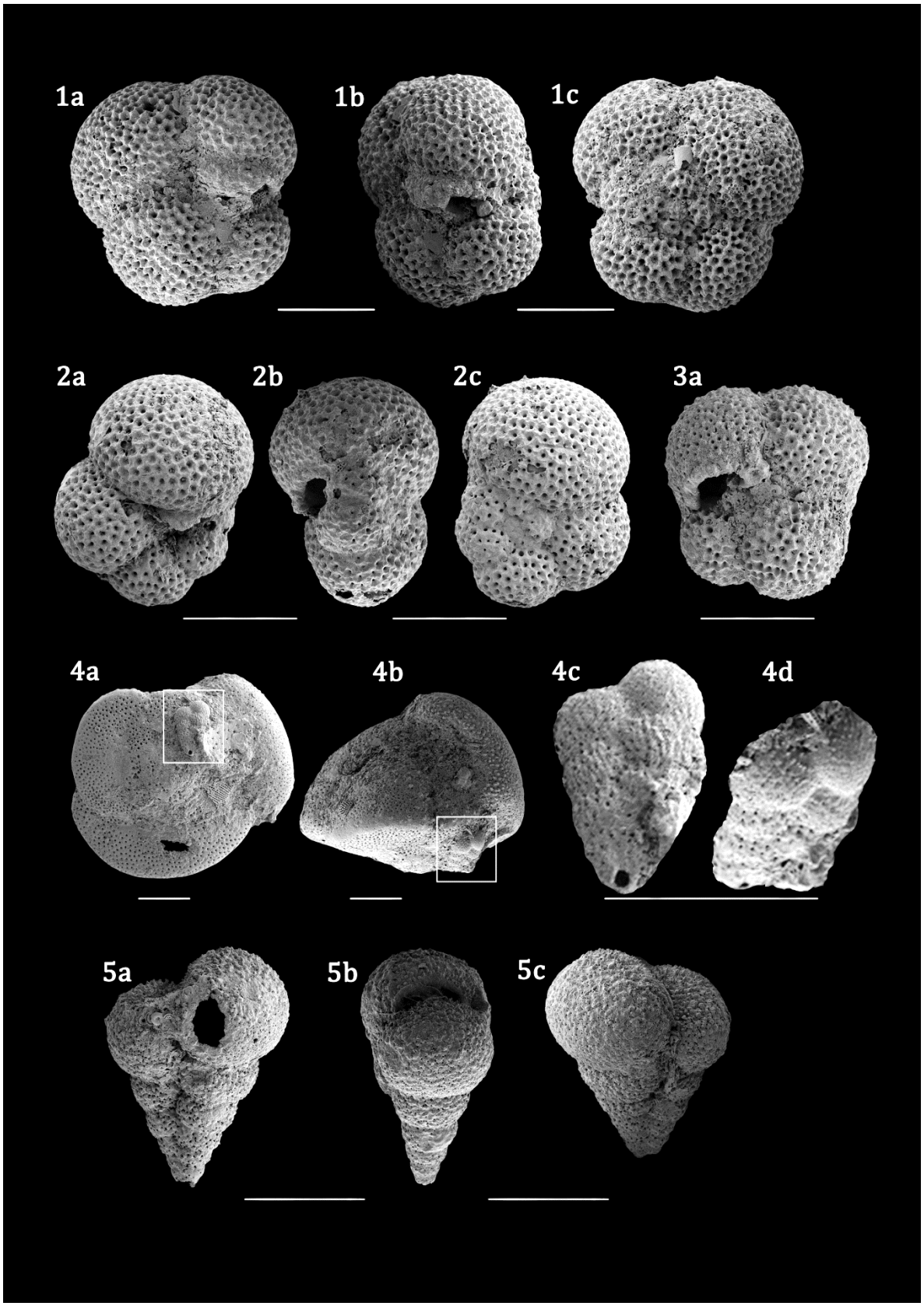

Plate 6. Genus *Paragloborotalia* Cifelli, 1982, *Turborotalita* Blow and Banner, 1962 and *Chiloguembelina* Loebich and Tappan, 1956

Plate 7. Family GLOBIGERINITIDAE Bermúdez, 1961 and Family TRUNCOROTALOIDIDAE Loebich and Tappan, 1961

SEM micrographs of high quality glassy preserved biostratigraphically useful planktic foraminifera species from DSDP Site 612, upper Eocene Zone E15/16 (**1-4, 5 b-c**) and lower Oligocene Zone O1 (**5a**). **1 a-c** *Tenuitella gemma* (Jenkins, 1965). Umbilical, edge and spiral views (same specimen). Sample 612-17X-1, 0-2 cm (136.2 mbsf). **2 a-c** *Tenuitella praegemma* (Li, 1987). Umbilical, edge and spiral views (same specimen). Sample 612-17X-1, 0-2 cm (136.2 mbsf). **3 a-c** *Tenuitella patefacta* Li, 1995. Umbilical, edge and spiral views (same specimen). Sample 612-17X-1, 59-61 cm (136.79 mbsf). **4 a** *Dipsidripella danvillensis* (Howe and Wallace, 1932). Umbilical view. Sample 612-17X-4, 76-78 cm (141.46 mbsf). **5 a-c** *Acarinina collactea* (Finlay, 1939). Umbilical and spiral views (**5 b, c** same specimen). Sample 612-16X-6,143-145 cm (135.63 mbsf) (**5a**) and 612-17X-2, 7-9 cm (137.77 mbsf) (**5 b-c**). Scale bar: 100 µm.

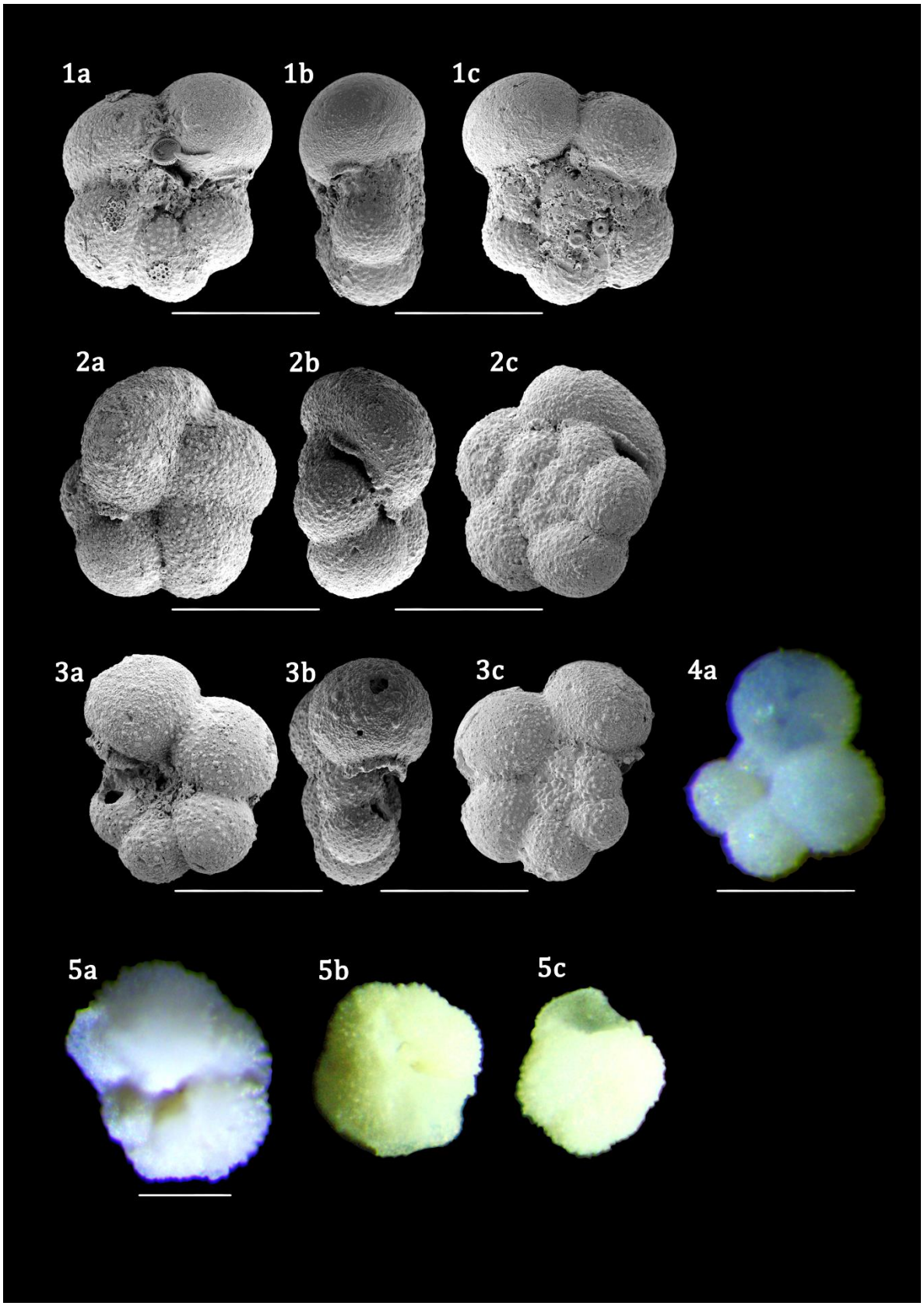

Plate 7. Family GLOBIGERINITIDAE Bermúdez, 1961 and TRUNCOROTALOIDIDAE Loebich and Tappan, 1961

Appendix III. Factor Analysis for paleoecological interpretations

Factor Analysis (FA) is an interdependence technique, and its main goals are (1) to reduce the number of variables and (2) to detect structure in the relationships between variables, that is to classify variables (Hair et al., 1998). The goal here is to find relationships between samples that allow us to arrange them into statistically coherent groups and detect the dominating taxa for each group. In this line, FA was applied as a data reduction and structure detection method of each taxa assemblage (Esparza-Alvarez et al., 2007). The data has to meet the following criteria: i) have a normal distribution, ii) heteroscedasticity and iii) linearity. For this purpose, a new database was built by removing the biostratigraphical markers, grouping some closely related species – at Genus level - with same paleoecological affinities and by taking in account only the major species or groups (a major species was defined as one composing >1% of the total population of the core). For calcareous nannofossil assemblage, small Reticulofenestra taxa were removed, because it would obscure the analysis due to its high abundance; instead, the rest of the assemblage was analyzed and compared it afterwards. Furthermore, to verify that the data fulfills the mentioned criteria, three data tests using R software on the new database with relative abundances were performed: i) Shapiro test to examine normality, ii) F-Test of variance for heteroscedasticity and iii) Harvey-Collier test for linearity. Due to the non-normal distribution observed (i.e. percentage of the species or group of planktic foraminifera (x) versus number of observations), a log-transformation of log (x + 1) was applied to the dataset to obtain a normal distribution. This transformation amplifies the importance of less abundant species, and compresses the dominance of few abundant species (Mix et al., 1999). Using Statistica 6.0. © Software, a Q mode FA of the log- transformed relative abundance of the fauna in each sample was performed for the three groups independently. FA calculation in Q mode is a correlation based on Euclidian distances between samples (variables), an expression of the degree of

vectors similitude between variables (Klovan & Imbrie, 1971; Klovan & Miesch, 1976). After Varimax rotation, two basis to retain the factors were used: 1) the Kaiser (1960) criterion that excludes all the factors with eigenvalues less than 1; and 2) the scree test (Cattell, 1966), a graphical method which selects the factors that explain more than 90% of the variability, which is usually found where the curve changes its slope.

In order to make paleoecological interpretations, Factor Analysis has been previously applied in Fuente Caldera (Legarda-Lisarri, 2016; Legarda-Lisarri et al., 2014), an analogous section in the Tethys ocean with an expanded upper Eocene-lower Oligocene record (Molina et al., 1993). The analysis shows similarities when compared to Site 612 (Table III.a; Figure III.a) but the lack of age control in Fuente Caldera prevented us to perform advanced correlations. However, the EOB position can still be located within the Fuente Caldera (FC) section, making possible to compare the changes in both sections. In FC, $F1_{PF}$ explained the major part of the variance (43%) and was characterized by deep water dwellers, $F2_{PF}$ (20%) by mixed layer dwellers, $F3_{PF}$ (12%) by surface dwellers and $F4_{PF}$ (5%) by mixed layer dwellers with tropical affinities; they either go extinct in

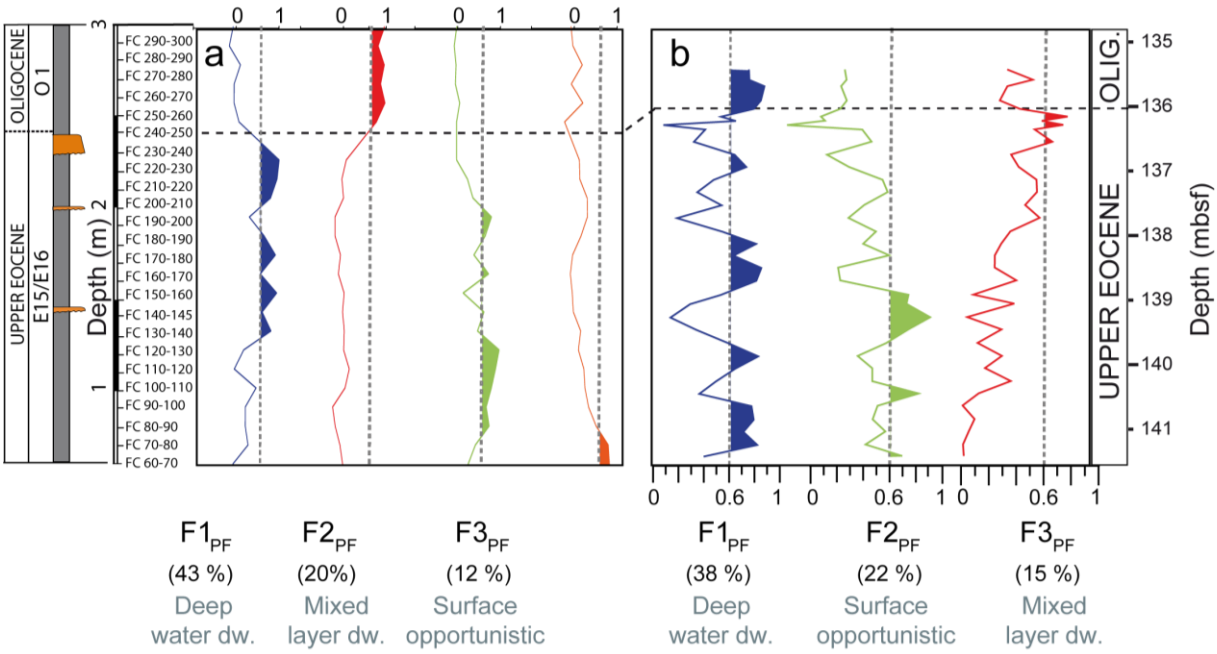

Figure III a. Table summarizing Factor analysis in Site 612 (upper part) and Fuente Caldera (lower part), showing selected Factors, corresponding highest scoring species and associated paleoecological meaning. Expl. Var. = explained variance; Ecol. meaning= species ecological affinity; F1=Factor 1; PF= Planktic foraminifera.

the EOB or suffer dwarfing effect. In Site 612 the extinct taxa were removed from the factor analysis so, if the remaining three factors ($F1_{PF}$ - $F3_{PF}$) are compared, the groups coincide, as well as the intervals in which they are significative.

In Fuente Caldera deep water dwellers dominate till EOB, while in Site 612 dominate till upper Eocene. Mixed layer dwellers show an abundance increase in both sites starting in the EOB and across the Oligocene. Surface opportunistic taxa show a shifting pattern across the record in both sites, with more significant (>0.6) values in the lower part of the record.

Table III a. Table summarizing Factor analysis in Site 612 (upper part) and Fuente Caldera (lower part), showing selected Factors, corresponding highest scoring species and associated paleoecological meaning. Expl. Var. = explained variance; Ecol. meaning= species ecological affinity; F1=Factor 1; PF= Planktic foraminifera.

	$F1_{PF}$			$F3_{PF}$		$F2_{PF}$		Tot.
Expl.Var.	38%			15%		22%		75%
Scoring sp.	*Dentoglobigerina venezuelana*	*Subbotina corpulenta*	*Subbotina eocaena*	*Globoturborotalita ouachitaensis*	*Turborotalia increbescens*	*Tenuitella patefacta*	*Dentoglobigerina pseudovenezuelana*	
Score	1.79	1.16	1.14	2	1.38	1.86	1.32	
	Dominate till upper Eocene			**> abundance: EOB and Oligocene**		**Shifting**		
Ecol. meaning	**Open ocean thermocline**			**Open ocean Mixed Layer**		**Surface-opportunistic**	**Open ocean thermocline (?)**	

FC PF	$F1_{PF}$			$F2_{PF}$				$F3_{PF}$	$F4_{PF}$			Tot.
Expl.Var.	43%			20%				12%	5%			79%
Scoring sp.	*Subbotina eocaena*	*Subbotina corpulenta*	*Catapsydrax dissimilis*	*Turborotalia increbescens*	*Globoturborotalita angulifficinalis*	*Tenuitellinata angustiumbilicata*	*Globigerina officinalis*	*Pseudohastigerina micra*	*Hantkenina alabamensis*	*Pseudohastigerina naguewichiensis*	*Cribrohantkenina lazzarii*	
Score	3	2.52	1.44	2.23	2.18	1.29	1.18	4.47	3.16	2.12	1.35	
	Dominate till upper EOB			**> abundance: EOB and Oligocene**				**Shifting**	> abundance: Base of the record			
Ecol. meaning	**Open ocean thermocline**			**Open ocean Mixed Layer**				**Surface**	Tropical, go extinct or dwarfing			

Appendix IV. Datasets

Table IV.a. Oxygen and Carbon stable isotopes

Table IV.b. Paleotemperatures

Table IV.c. Sediment fraction weigh

Table IV.d. Planktic foraminifera assemblage: Census, relative and absolute abundances

Table IV.e. Benthic foraminifera assemblage: Census, relative and absolute abundances

Table IV.f. Calcareous nannofossil assemblage: Census, relative and absolute abundances

Table IV.g. Siliceous plankton assemblage

Table IV.h. Planktic eco-groups

Table IV.i. Benthic eco-groups

Table IV.j. Factor analysis extended

Table IV.k. Initial observations of the sediment: Qualitative/semiquantitative data

Table IV.l. Examined Site 612 samples in this study

Table IV.m. Previously studied Site 612 samples

Table IV.n. Detailed biostratigraphy

Table IV a. Stable Oxygen and Carbon isotopes from foraminiferal shells. *The ages are shown on the paleomagnetic age framework of Cande and Kent (1995) (=CK95). Mbsf = meters below sea floor. Shaded, outlier. Cibs. adj. = contains *Hanzawaia ammophila* values adjusted to *Cibicidoides*, according to Katz *et al.* (2003). For the following tables in this Appendix, only depth is given; see this table for corresponding Sample ID and Age.

Sample ID	Depth (mbsf)	AGE (CK95)* (Ma)	AGE (GTS12) (Ma)	Species	$\delta^{18}O$ vs PDB unadj.	$\delta^{13}C$ vs PDB unadj.	Combined Cibs. adj. $\delta^{18}O$ ‰ VPDB	Combined Cibs. adj. $\delta^{13}C$ ‰ VPDB	Data source
612,16X-7, 3-5	135.73	33.36	33.54	*Pseudohastigerina micra & P. naguewichiensis*	-1.37	-3.22			This study
612,16X-7, 25-27	135.95	33.61	33.80	*Pseudohastigerina micra & P. naguewichiensis*	-3.72	-2.85			This study
612,16X-CC, 10-12	136.08	33.86	34.09	*Pseudohastigerina micra & P. naguewichiensis*	-2.76	-0.63			This study
612,17X-1, 0-2	136.20	34.00	34.24	*Pseudohastigerina micra & P. naguewichiensis*	-1.92	-1.31			This study
612,17X-1, 6.5-8.5	136.27	34.07	34.31	*Pseudohastigerina micra & P. naguewichiensis*	-2.15	-1.21			This study
612,17X-1, 13-15	136.33	34.15	34.39	*Pseudohastigerina micra & P. naguewichiensis*	-2.06	-0.99			This study
612,17X-1, 20-22	136.40	34.87	35.22	*Pseudohastigerina micra & P. naguewichiensis*	-2.96	-0.96			This study
612,17X-1, 39-41	136.59	34.87	35.23	*Pseudohastigerina micra & P. naguewichiensis*	-2.38	-1.01			This study
612,17X-1, 59-61	136.79	34.87	35.23	*Pseudohastigerina micra & P. naguewichiensis*	-2.09	-1.10			This study
612,17X-1, 78-80	136.98	34.88	35.23	*Pseudohastigerina micra & P. naguewichiensis*	-2.02	-0.98			This study
612,17X-1, 98-100	137.18	34.88	35.24	*Pseudohastigerina micra & P. naguewichiensis*	-2.20	-1.02			This study
612,17X-1, 117-119	137.37	34.88	35.24	*Pseudohastigerina micra & P. naguewichiensis*	-2.15	-0.95			This study
612,17X-1, 137-139	137.57	34.89	35.24	*Pseudohastigerina micra & P. naguewichiensis*	-2.07	-1.08			This study
612,17X-2, 7-9	137.77	34.89	35.25	*Pseudohastigerina micra & P. naguewichiensis*	-2.82	-1.05			This study
612,17X-2, 28-30	137.98	34.90	35.25	*Pseudohastigerina micra & P. naguewichiensis*		-2.09			This study
612,17X-2, 47-49	138.17	34.90	35.26	*Pseudohastigerina micra & P. naguewichiensis*	-2.44	-1.01			This study
612,17X-2, 65-67	138.35	34.90	35.26	*Pseudohastigerina micra & P. naguewichiensis*	-2.17	-0.99			This study
612,17X-2, 84-86	138.54	34.91	35.26	*Pseudohastigerina micra & P. naguewichiensis*	-1.96	-0.82			This study
612,17X-2, 104-106	138.74	34.91	35.27	*Pseudohastigerina micra & P. naguewichiensis*	-1.69	-0.63			This study
612,17X-2, 140-142	139.10	34.92	35.27	*Pseudohastigerina micra & P. naguewichiensis*	-1.76	-0.94			This study
612,17X-3, 11-13	139.31	34.92	35.28	*Pseudohastigerina micra & P. naguewichiensis*	-2.37	-0.95			This study
612,17X-3, 30-32	139.50	34.92	35.28	*Pseudohastigerina micra & P. naguewichiensis*	-1.60	-0.64			This study
612,17X-3, 51-53	139.71	34.93	35.28	*Pseudohastigerina micra & P. naguewichiensis*	-2.11	-0.76			This study
612,17X-3,71-73	139.91	34.93	35.29	*Pseudohastigerina micra & P. naguewichiensis*	-1.53	-0.60			This study
612,17X-3, 90-92	140.10	34.93	35.29	*Pseudohastigerina micra & P. naguewichiensis*	-1.94	-0.83			This study
612,17X-3, 110-112	140.30	34.94	35.30	*Pseudohastigerina micra & P. naguewichiensis*	-2.19	-1.05			This study
612,16X-6, 127-129	135.47	33.07	33.24	*Turborotalia ampliapertura & T. increbescens*	-2.13	0.43			This study
612,16X-6, 143-145	135.63	33.25	33.43	*Turborotalia ampliapertura & T. increbescens*	-2.80	-0.81			This study
612,16X-7, 3-5	135.73	33.36	33.54	*Turborotalia ampliapertura & T. increbescens*	-2.10	-1.11			This study
612,16X-7, 25-27	135.95	33.61	33.80	*Turborotalia ampliapertura & T. increbescens*	-1.66	-0.75			This study
612,16X-CC, 10-12	136.08	33.86	34.09	*Turborotalia ampliapertura & T. increbescens*	-1.84	0.56			This study
612,17X-1, 0-2	136.20	34.00	34.24	*Turborotalia ampliapertura & T. increbescens*	-1.76	-0.22			This study
612,17X-1, 6.5-8.5	136.27	34.07	34.31	*Turborotalia ampliapertura & T. increbescens*	-2.75	0.11			This study
612,17X-1, 13-15	136.33	34.15	34.39	*Turborotalia ampliapertura & T. increbescens*	-1.70	-0.16			This study
612,17X-1, 20-22	136.40	34.87	35.22	*Turborotalia ampliapertura & T. increbescens*	-1.33	-0.29			This study

Sample ID	Depth (mbsf)	AGE (CK95)* (Ma)	AGE (GTS12) (Ma)	Species	$\delta^{18}O$ vs PDB unadj.	$\delta^{13}C$ vs PDB unadj.	Combined Cibs. adj. $\delta^{18}O$ ‰ VPDB	Combined Cibs. adj. $\delta^{13}C$ ‰ VPDB	Data source
612,17X-1, 39-41	136.59	34.87	35.23	*Turborotalia ampliapertura & T. increbescens*	-1.76	0.09			This study
612,17X-1, 59-61	136.79	34.87	35.23	*Turborotalia ampliapertura & T. increbescens*	-1.53	0.16			This study
612,17X-1, 78-80	136.98	34.88	35.23	*Turborotalia ampliapertura & T. increbescens*	-1.89	0.07			This study
612,17X-1, 98-100	137.18	34.88	35.24	*Turborotalia ampliapertura & T. increbescens*	-1.83	0.00			This study
612,17X-1, 117-119	137.37	34.88	35.24	*Turborotalia ampliapertura & T. increbescens*	-1.91	0.05			This study
612,17X-1, 137-139	137.57	34.89	35.24	*Turborotalia ampliapertura & T. increbescens*	-1.77	-0.04			This study
612,17X-2, 7-9	137.77	34.89	35.25	*Turborotalia ampliapertura & T. increbescens*	-1.53	0.00			This study
612,17X-2, 28-30	137.98	34.90	35.25	*Turborotalia ampliapertura & T. increbescens*	-1.93	-0.16			This study
612,17X-2, 47-49	138.17	34.90	35.26	*Turborotalia ampliapertura & T. increbescens*	-1.99	0.08			This study
612,17X-2, 65-67	138.35	34.90	35.26	*Turborotalia ampliapertura & T. increbescens*	-1.63	-0.03			This study
612,17X-2, 84-86	138.54	34.91	35.26	*Turborotalia ampliapertura & T. increbescens*	-1.62	0.39			This study
612,17X-2, 104-106	138.74	34.91	35.27	*Turborotalia ampliapertura & T. increbescens*	-1.61	0.34			This study
612,17X-2, 140-142	139.10	34.92	35.27	*Turborotalia ampliapertura & T. increbescens*	-1.44	0.11			This study
612,17X-3, 11-13	139.31	34.92	35.28	*Turborotalia ampliapertura & T. increbescens*	-1.35	-0.09			This study
612,17X-3, 30-32	139.50	34.92	35.28	*Turborotalia ampliapertura & T. increbescens*	-2.42	0.23			This study
612,17X-3, 51-53	139.71	34.93	35.28	*Turborotalia ampliapertura & T. increbescens*	-2.05	0.54			This study
612,17X-3,71-73	139.91	34.93	35.29	*Turborotalia ampliapertura & T. increbescens*	-1.66	0.62			This study
612,17X-3, 90-92	140.10	34.93	35.29	*Turborotalia ampliapertura & T. increbescens*	-1.87	0.31			This study
612,17X-3, 110-112	140.30	34.94	35.30	*Turborotalia ampliapertura & T. increbescens*	-1.85	0.23			This study
612,16X-6, 127-129	135.47	33.07	33.24	*Catapsydrax unicavus & C. dissimilis*	-1.54	-0.55			This study
612,16X-6, 143-145	135.63	33.25	33.43	*Catapsydrax unicavus & C. dissimilis*	-1.06	-1.06			This study
612,16X-7, 3-5	135.73	33.36	33.54	*Catapsydrax unicavus & C. dissimilis*	-0.43	-1.80			This study
612,16X-7, 25-27	135.95	33.61	33.80	*Catapsydrax unicavus & C. dissimilis*	-1.39	-1.17			This study
612,16X-CC, 10-12	136.08	33.86	34.09	*Catapsydrax unicavus & C. dissimilis*	-0.43	0.20			This study
612,17X-1, 0-2	136.20	34.00	34.24	*Catapsydrax unicavus & C. dissimilis*	-0.23	-0.35			This study
612,17X-1, 6.5-8.5	136.27	34.07	34.31	*Catapsydrax unicavus & C. dissimilis*	-0.31	-0.40			This study
612,17X-1, 13-15	136.33	34.15	34.39	*Catapsydrax unicavus & C. dissimilis*	-0.40	-0.33			This study
612,17X-1, 20-22	136.40	34.87	35.22	*Catapsydrax unicavus & C. dissimilis*	-0.70	-0.27			This study
612,17X-1, 39-41	136.59	34.87	35.23	*Catapsydrax unicavus & C. dissimilis*	-0.42	-0.38			This study
612,17X-1, 59-61	136.79	34.87	35.23	*Catapsydrax unicavus & C. dissimilis*	-0.52	-0.39			This study
612,17X-1, 78-80	136.98	34.88	35.23	*Catapsydrax unicavus & C. dissimilis*	-0.22	-0.29			This study
612,17X-1, 98-100	137.18	34.88	35.24	*Catapsydrax unicavus & C. dissimilis*	-0.12	-0.18			This study
612,17X-1, 117-119	137.37	34.88	35.24	*Catapsydrax unicavus & C. dissimilis*	-0.63	-0.19			This study
612,17X-1, 137-139	137.57	34.89	35.24	*Catapsydrax unicavus & C. dissimilis*	-0.18	-0.40			This study
612,17X-2, 7-9	137.77	34.89	35.25	*Catapsydrax unicavus & C. dissimilis*	-0.75	-0.40			This study
612,17X-2, 28-30	137.98	34.90	35.25	*Catapsydrax unicavus & C. dissimilis*	-0.31	-0.58			This study
612,17X-2, 47-49	138.17	34.90	35.26	*Catapsydrax unicavus & C. dissimilis*	-0.45	-0.26			This study
612,17X-2, 65-67	138.35	34.90	35.26	*Catapsydrax unicavus & C. dissimilis*	-0.60	-0.33			This study
612,17X-2, 84-86	138.54	34.91	35.26	*Catapsydrax unicavus & C. dissimilis*	-0.20	-0.05			This study
612,17X-2, 104-106	138.74	34.91	35.27	*Catapsydrax unicavus & C. dissimilis*	-0.54	0.08			This study
612,17X-2, 140-142	139.10	34.92	35.27	*Catapsydrax unicavus & C. dissimilis*	-0.48	-0.19			This study
612,17X-3, 11-13	139.31	34.92	35.28	*Catapsydrax unicavus & C. dissimilis*	-0.27	-0.04			This study

Sample ID	Depth (mbsf)	AGE (CK95)* (Ma)	AGE (GTS12) (Ma)	Species	$\delta^{18}O$ vs PDB unadj.	$\delta^{13}C$ vs PDB unadj.	Combined Cibs. adj. $\delta^{18}O$ ‰ VPDB	Combined Cibs. adj. $\delta^{13}C$ ‰ VPDB	Data source
612,17X-3, 30-32	139.50	34.92	35.28	*Catapsydrax unicavus & C. dissimilis*	-0.40	0.07			This study
612,17X-3, 51-53	139.71	34.93	35.28	*Catapsydrax unicavus & C. dissimilis*	-1.59	0.33			This study
612,17X-3,71-73	139.91	34.93	35.29	*Catapsydrax unicavus & C. dissimilis*	-0.39	0.08			This study
612,17X-3, 90-92	140.10	34.93	35.29	*Catapsydrax unicavus & C. dissimilis*	-0.57	0.04			This study
612,17X-3, 110-112	140.30	34.94	35.30	*Catapsydrax unicavus & C. dissimilis*	-0.55	-0.08			This study
612-16X-6, 116,5-119	135.37	32.95	33.12	*Cibicidoides spp.*	1.07	-0.39	1.07	-0.39	This study
612-16X-6, 122-124	135.42	33.01	33.18	*Hanzawaia spp.*	0.53	0.16	0.59	0.24	This study
612,16X-6, 127-129	135.47	33.07	33.24	*Hanzawaia ammophila*	0.71	-0.09	0.88	-0.01	Coxall et al., 2018
612-16X-6, 134-136	135.54	33.15	33.32	*Cibicidoides spp.*	0.51	0.15	0.51	0.15	This study
612-16X-6, 147-149	135.67	33.29	33.47	*Cibicidoides spp.*	0.69	-2.35	0.69	-2.35	This study
612-16X-7, 3-5	135.73	33.36	33.54	*Cibicidoides spp.*	0.78	-2.76	0.78	-2.76	This study
612-16X-7, 5-7	135.75	33.39	33.57	*Cibicidoides spp.*	0.57	-0.55	0.57	-0.55	This study
612-16X-7, 10-12	135.80	33.44	33.63	*Cibicidoides spp.*	0.61	-0.89	0.61	-0.89	This study
612-16X-7, 17-19	135.87	33.52	33.71	*Cibicidoides spp.*	0.77	-1.48	0.77	-1.48	This study
612,16X-7, 26-30	135.96	33.63	33.81	*Cibicidoides spp.*	0.66	-1.70	0.66	-1.70	Miller et al., 1991
612,16-CC	136.00	33.67	33.86	*Cibicidoides spp.*	0.57	-0.29	0.57	-0.29	Miller et al., 1991
612-16X-CC, 3-5	136.01	33.68	33.87	*Cibicidoides spp.*	0.66	-1.03	0.66	-1.03	This study
612,16X-CC, 10-12	136.08	33.86	34.09	*Hanzawaia spp.*	0.59	0.56	0.69	0.64	This study
612-16X-CC, 15-17	136.13	33.92	34.15	*Hanzawaia spp.*	0.60	0.14	0.71	0.22	This study
612-16X-CC, 18,5-20,5	136.17	33.96	34.19	*Hanzawaia spp.*	0.68	-0.05	0.85	0.03	This study
612,17X-1, 0-2	136.20	34.00	34.24	*Hanzawaia ammophila*	-0.12	0.15	-0.46	0.23	Coxall et al., 2018
612-17X-1, 3-5	136.23	34.03	34.27	*Cibicidoides spp.*	0.13	0.22	0.13	0.22	This study
612-17X-1, 3-5	136.23	34.03	34.27	*Hanzawaia spp.*	0.51	0.05	0.56	0.13	This study
612,17X-1, 6.5-8.5	136.27	34.07	34.31	*Hanzawaia ammophila*	0.33	-0.40	0.27	-0.32	Coxall et al., 2018
612-17X-1, 10-12	136.30	34.11	34.35	*Cibicidoides spp.*	0.80	-0.09	0.80	-0.09	This study
612-17X-1, 10-12	136.30	34.11	34.35	*Hanzawaia spp.*	0.52	0.19	0.58	0.27	This study
612,17X-1, 13-15	136.33	34.15	34.39	*Hanzawaia spp.*	0.23	0.03	0.11	0.11	This study
612-17X-1, 15-17	136.35	34.17	34.41	*Cibicidoides spp.*	0.65	0.03	0.65	0.03	This study
612-17X-1, 15-17	136.35	34.17	34.41	*Hanzawaia spp.*	0.51	0.15	0.57	0.23	This study
612,17X-1, 20-22	136.40	34.87	35.22	*Hanzawaia ammophila*	0.62	-0.79	0.75	-0.71	Coxall et al., 2018
612-17X-1, 29-31	136.49	34.87	35.22	*Hanzawaia spp.*	0.50	-0.17	0.54	-0.09	This study
612,17X-1, 39-41	136.59	34.87	35.23	*Hanzawaia ammophila*	0.45	-0.26	0.46	-0.18	Coxall et al., 2018
612-17X-1, 50-51	136.70	34.87	35.23	*Cibicidoides spp.*	0.22	0.00	0.22	0.00	This study
612-17X-1, 50-51	136.70	34.87	35.23	*Hanzawaia spp.*	0.39	0.00	0.37	0.08	This study
612-17X-1, 59-61	136.79	34.87	35.23	*Cibicidoides spp.*	0.64	-0.37	0.64	-0.37	This study
612-17X-1, 59-61	136.79	34.87	35.23	*Hanzawaia spp.*	0.58	0.27	0.68	0.35	This study
612-17X-1, 68-70	136.88	34.87	35.23	*Cibicidoides spp.*	0.59	-0.23	0.59	-0.23	This study
612-17X-1, 68-70	136.88	34.87	35.23	*Hanzawaia spp.*	0.43	-0.05	0.44	0.03	This study
612,17X-1, 78-80	136.98	34.88	35.23	*Hanzawaia ammophila*	0.84	-0.16	1.10	-0.08	Coxall et al., 2018
612,17X-1, 98-100	137.18	34.88	35.24	*Hanzawaia ammophila*	0.50	-0.58	0.56	-0.50	Coxall et al., 2018
612,17X-1, 117-119	137.37	34.88	35.24	*Hanzawaia ammophila*	0.85	0.15	1.12	0.23	Coxall et al., 2018
612,17X-1, 137-139	137.57	34.89	35.24	*Hanzawaia ammophila*	0.30	-0.34	0.23	-0.26	Coxall et al., 2018

Sample ID	Depth (mbsf)	AGE (CK95)* (Ma)	AGE (GTS12) (Ma)	Species	$\delta^{18}O$ vs PDB unadj.	$\delta^{13}C$ vs PDB unadj.	Combined Cibs. adj. $\delta^{18}O$ ‰ VPDB	Combined Cibs. adj. $\delta^{13}C$ ‰ VPDB	Data source
612,17-1, 140-144	137.60	34.89	35.25	*Cibicidoides spp.*	0.19	-0.07	0.19	-0.07	Miller et al., 1991
612,17-1, 140-144	137.60	34.89	35.25	*Cibicidoides spp.*	0.26	-0.33	0.26	-0.33	Miller et al., 1991
612,17X-2, 7-9	137.77	34.89	35.25	*Hanzawaia ammophila*	0.85	-0.39	1.12	-0.31	Coxall et al., 2018
612,17X-2, 28-30	137.98	34.90	35.25	*Hanzawaia ammophila*	0.18	-0.08	0.03	0.00	Coxall et al., 2018
612,17X-2, 47-49	138.17	34.90	35.26	*Hanzawaia ammophila*	-0.27	-0.18	-0.70	-0.10	Coxall et al., 2018
612-17X-2, 49-50	138.19	34.90	35.26	*Cibicidoides spp.*	0.94	-0.07	0.94	-0.07	This study
612-17X-2, 49-50	138.19	34.90	35.26	*Hanzawaia spp.*	0.62	0.10	0.75	0.18	This study
612,17X-2, 65-67	138.35	34.90	35.26	*Hanzawaia ammophila*	0.14	-0.28	-0.03	-0.20	Coxall et al., 2018
612,17X-2, 84-86	138.54	34.91	35.26	*Hanzawaia ammophila*	0.57	0.08	0.66	0.16	Coxall et al., 2018
612,17X-2, 104-106	138.74	34.91	35.27	*Hanzawaia ammophila*	0.10	0.77	-0.10	0.85	Coxall et al., 2018
612-17X-2, 126-128	138.96	34.91	35.27	*Cibicidoides spp.*	0.99	-0.21	0.99	-0.21	This study
612,17X-2, 140-142	139.10	34.92	35.27	*Hanzawaia ammophila*	0.33	0.00	0.28	0.08	Coxall et al., 2018
612,17-2,140-144	139.10	34.92	35.27	*Cibicidoides spp.*	0.29	-0.06	0.29	-0.06	Miller et al., 1991
612,17X-3, 11-13	139.31	34.92	35.28	*Hanzawaia ammophila*	0.00	-0.22	-0.26	-0.14	Coxall et al., 2018
612,17X-3, 30-32	139.50	34.92	35.28	*Hanzawaia ammophila*	0.63	0.20	0.76	0.28	Coxall et al., 2018
612,17X-3, 51-53	139.71	34.93	35.28	*Hanzawaia ammophila*	0.64	-0.15	0.77	-0.07	Coxall et al., 2018
612,17X-3,71-73	139.91	34.93	35.29	*Hanzawaia ammophila*	-0.20	0.21	-0.59	0.29	Coxall et al., 2018
612,17X-3, 90-92	140.10	34.93	35.29	*Hanzawaia ammophila*	-0.75	0.22	-1.47	0.30	Coxall et al., 2018
612-17X-3, 129-131	140.49	34.94	35.30	*Hanzawaia ammophila*	1.10	-0.56	1.52	-0.48	This study
612,17-3, 140-144	140.60	34.94	35.30	*Cibicidoides spp.*	0.42	-0.22	0.42	-0.22	Miller et al., 1991
612-17X-3, 148-150	140.68	34.95	35.30	*Cibicidoides spp.*	0.78	-0.63	0.78	-0.63	This study
612-17X-4, 19-21	140.89	34.95	35.31	*Hanzawaia ammophila*	1.04	-0.37	1.42	-0.29	This study
612-17X-4, 38-40	141.08	34.95	35.31	*Hanzawaia ammophila*	0.58	-0.29	0.67	-0.21	This study
612-17X-4, 58-60	141.28	34.96	35.31	*Cibicidoides spp.*	0.89	0.04	0.89	0.04	This study
612-17X-4, 76-78	141.46	34.96	35.32	*Hanzawaia ammophila*	0.89	0.34	1.18	0.42	This study
612,17X-5, 140-144	143.60	35.00	35.36	*Cibicidoides spp.*	0.13	0.24	0.13	0.24	Miller et al., 1991
612,17X-6,140-144	145.10	35.03	35.38	*Cibicidoides spp.*	0.20	-0.17	0.20	-0.17	Miller et al., 1991
612,18X-1,60-64	146.30	35.05	35.41	*Cibicidoides spp.*	0.25	0.36	0.25	0.36	Miller et al., 1991
612,18X-3,60-64	149.30	35.11	35.46	*Cibicidoides spp.*	0.35	0.11	0.35	0.11	Miller et al., 1991
612,18X-4,60-64	150.80	35.13	35.49	*Cibicidoides spp.*	0.47	0.40	0.47	0.40	Miller et al., 1991
612,18X-CC	154.70	35.21	35.56	*Cibicidoides spp.*	0.24	0.67	0.24	0.67	Miller et al., 1991
612,19X-1,60-64	155.80	35.23	35.58	*Cibicidoides spp.*	0.15	0.20	0.15	0.20	Miller et al., 1991
612,19X-2,60-64	157.30	35.25	35.61	*Cibicidoides spp.*	0.32	0.27	0.32	0.27	Miller et al., 1991
612,19X-3,60-64	158.80	35.28	35.64	*Cibicidoides spp.*	0.34	0.33	0.34	0.33	Miller et al., 1991
612,19X-4,60-64	160.30	35.31	35.67	*Cibicidoides spp.*	0.31	0.00	0.31	0.00	Miller et al., 1991
612,19X-6,60-64	163.30	35.42	35.78	*Cibicidoides spp.*	0.08	0.24	0.08	0.24	Miller et al., 1991
612,19X-CC	164.50	35.48	35.84	*Cibicidoides spp.*	0.01	0.56	0.01	0.56	Miller et al., 1991
612,20X-1,60-64	165.30	35.52	35.88	*Cibicidoides spp.*	0.05	0.89	0.05	0.89	Miller et al., 1991
612,20X-2,60-64	166.80	35.59	35.95	*Cibicidoides spp.*	0.14	0.96	0.14	0.96	Miller et al., 1991
612,20X-3,60-64	168.30	35.66	36.03	*Cibicidoides spp.*	0.15	0.91	0.15	0.91	Miller et al., 1991
612,20X-4,60-64	169.80	35.74	36.10	*Cibicidoides spp.*	0.08	1.03	0.08	1.03	Miller et al., 1991
612,20X-5,60-64	171.30	35.81	36.17	*Cibicidoides spp.*	0.18	1.17	0.18	1.17	Miller et al., 1991
612,21X-4,60-64	179.30	36.20	36.56	*Cibicidoides spp.*	-0.02	0.64	-0.02	0.64	Miller et al., 1991

Sample ID	Depth (mbsf)	AGE (CK95)* (Ma)	AGE (GTS12) (Ma)	Species	$\delta^{18}O$ vs PDB unadj.	$\delta^{13}C$ vs PDB unadj.	Combined Cibs. adj. $\delta^{18}O$ ‰ VPDB	Combined Cibs. adj. $\delta^{13}C$ ‰ VPDB	Data source
612,21X-5,113-114	181.33	36.30	36.66	*Cibicidoides spp.*	0.01	0.21	0.01	0.21	Pusz et al., 2009
612,21X-5,114-115	181.34	36.30	36.66	*Cibicidoides spp.*	0.20	0.16	0.20	0.16	Pusz et al., 2009
612,21X-5,116-117	181.36	36.30	36.67	*Cibicidoides spp.*	0.09	0.31	0.09	0.31	Pusz et al., 2009
612,21X-5,117-118	181.37	36.30	36.67	*Cibicidoides spp.*	0.31	0.64	0.31	0.64	Pusz et al., 2009
612,21X-5,118-119	181.38	36.30	36.67	*Cibicidoides spp.*	0.35	0.68	0.35	0.68	Pusz et al., 2009

Table IV b. Surface, mixed layer, thermocline and ocean floor paleotemperatures, calculated from foraminifera shell- oxygen stable isotopes (see Table IV. a) using different $\delta^{18}O_{SW}$ values (see Table 1). (*) indicates that latitudinal correction (Zachos et al., 1994) was applied.

Depth (mbsf)	$\delta^{18}O_{CaCO3}$ (VPDB) (‰)	Paleotemperature (°C)							Species	Equation used	Data source
		$\delta^{18}O_{SW}$ from Shackleton and Kennett, 1975 (VSMOW)	$\delta^{18}O_{SW}$ from Cramer et al., 2011	$\delta^{18}O_{SW}$ from Zachos et al., 1994	$\delta^{18}O_{SW}$ from Tindall et al., 2010	$\delta^{18}O_{SW}$ from Huber et al., 2003	$\delta^{18}O_{SW}$ from Roberts et al., 2009	Mean			
135.73	-1.37	18.11 *	18.62 *	19.04 *	18.99	19.33	19.84	18.99	*Pseudohastigerina micra*	Kim and O'Neil.,1997	This study
135.95	-3.72	29.07 *	29.59 *	30.01 *	29.96	30.30	30.82	29.96	*Pseudohastigerina micra*	Kim and O'Neil.,1997	This study
136.08	-2.76	24.55 *	25.06 *	25.48 *	25.43	25.77	26.28	25.43	*Pseudohastigerina micra*	Kim and O'Neil.,1997	This study
136.2	-1.92	20.65 *	21.17 *	21.59 *	21.54	21.87	22.39	21.53	*Pseudohastigerina micra*	Kim and O'Neil.,1997	This study
136.265	-2.15	21.74 *	22.25 *	22.67 *	22.62	22.96	23.47	22.62	*Pseudohastigerina micra*	Kim and O'Neil.,1997	This study
136.33	-2.06	21.28 *	21.79 *	22.21 *	22.16	22.50	23.01	22.16	*Pseudohastigerina micra*	Kim and O'Neil.,1997	This study
136.4	-2.96	25.50 *	26.02 *	26.44 *	26.39	26.73	27.24	26.39	*Pseudohastigerina micra*	Kim and O'Neil.,1997	This study
136.59	-2.38	22.80 *	23.31 *	23.73 *	23.68	24.02	24.53	23.68	*Pseudohastigerina micra*	Kim and O'Neil.,1997	This study
136.79	-2.09	21.45 *	21.96 *	22.38 *	22.33	22.67	23.18	22.33	*Pseudohastigerina micra*	Kim and O'Neil.,1997	This study
136.98	-2.02	21.11 *	21.62 *	22.04 *	21.99	22.33	22.84	21.99	*Pseudohastigerina micra*	Kim and O'Neil.,1997	This study
137.18	-2.20	21.95 *	22.47 *	22.89 *	22.84	23.18	23.69	22.83	*Pseudohastigerina micra*	Kim and O'Neil.,1997	This study
137.37	-2.15	21.73 *	22.25 *	22.67 *	22.62	22.95	23.47	22.61	*Pseudohastigerina micra*	Kim and O'Neil.,1997	This study
137.57	-2.07	21.37 *	21.88 *	22.30 *	22.25	22.59	23.10	22.25	*Pseudohastigerina micra*	Kim and O'Neil.,1997	This study
137.77	-2.82	24.85 *	25.37 *	25.79 *	25.74	26.08	26.59	25.74	*Pseudohastigerina micra*	Kim and O'Neil.,1997	This study
138.17	-2.44	23.06 *	23.57 *	23.99 *	23.94	24.28	24.80	23.94	*Pseudohastigerina micra*	Kim and O'Neil.,1997	This study
138.35	-2.17	21.82 *	22.34 *	22.76 *	22.71	23.04	23.56	22.70	*Pseudohastigerina micra*	Kim and O'Neil.,1997	This study
138.54	-1.96	20.84 *	21.35 *	21.77 *	21.72	22.06	22.57	21.72	*Pseudohastigerina micra*	Kim and O'Neil.,1997	This study
138.74	-1.69	19.60 *	20.11 *	20.53 *	20.48	20.81	21.33	20.47	*Pseudohastigerina micra*	Kim and O'Neil.,1997	This study
139.1	-1.76	19.88 *	20.39 *	20.81 *	20.76	21.10	21.61	20.76	*Pseudohastigerina micra*	Kim and O'Neil.,1997	This study
139.31	-2.37	22.76 *	23.27 *	23.69 *	23.64	23.98	24.50	23.64	*Pseudohastigerina micra*	Kim and O'Neil.,1997	This study
139.5	-1.60	19.17 *	19.69 *	20.10 *	20.05	20.39	20.90	20.05	*Pseudohastigerina micra*	Kim and O'Neil.,1997	This study
139.71	-2.11	21.54 *	22.05 *	22.47 *	22.42	22.76	23.27	22.42	*Pseudohastigerina micra*	Kim and O'Neil.,1997	This study
139.91	-1.53	18.81 *	19.33 *	19.75 *	19.69	20.03	20.54	19.69	*Pseudohastigerina micra*	Kim and O'Neil.,1997	This study
140.1	-1.94	20.73 *	21.24 *	21.66 *	21.61	21.95	22.46	21.61	*Pseudohastigerina micra*	Kim and O'Neil.,1997	This study
140.3	-2.19	21.93 *	22.44 *	22.86 *	22.81	23.15	23.66	22.81	*Pseudohastigerina micra*	Kim and O'Neil.,1997	This study
135.47	-2.13	21.63 *	22.14 *	22.56 *	23.05	22.85	23.36	22.60	*Turborotalia ampliapertura & increbescens*	Kim and O'Neil.,1997	This study
135.63	-2.80	24.74 *	25.25 *	25.67 *	26.16	25.96	26.47	25.71	*Turborotalia ampliapertura & increbescens*	Kim and O'Neil.,1997	This study
135.73	-2.10	21.49 *	22.00 *	22.42 *	22.90	22.71	23.22	22.46	*Turborotalia ampliapertura & increbescens*	Kim and O'Neil.,1997	This study
135.95	-1.66	19.44 *	19.95 *	20.37 *	20.86	20.66	21.17	20.41	*Turborotalia ampliapertura & increbescens*	Kim and O'Neil.,1997	This study
136.08	-1.84	20.26 *	20.78 *	21.19 *	21.68	21.48	22.00	21.23	*Turborotalia ampliapertura & increbescens*	Kim and O'Neil.,1997	This study
136.2	-1.76	19.91 *	20.42 *	20.84 *	21.33	21.13	21.64	20.88	*Turborotalia ampliapertura & increbescens*	Kim and O'Neil.,1997	This study
136.265	-2.75	24.53 *	25.05 *	25.47 *	25.96	25.76	26.27	25.50	*Turborotalia ampliapertura & increbescens*	Kim and O'Neil.,1997	This study
136.33	-1.70	19.63 *	20.15 *	20.57 *	21.05	20.85	21.37	20.60	*Turborotalia ampliapertura & increbescens*	Kim and O'Neil.,1997	This study
136.4	-1.33	17.92 *	18.43 *	18.85 *	19.34	19.14	19.65	18.89	*Turborotalia ampliapertura & increbescens*	Kim and O'Neil.,1997	This study
136.59	-1.76	19.92 *	20.43 *	20.85 *	21.33	21.14	21.65	20.89	*Turborotalia ampliapertura & increbescens*	Kim and O'Neil.,1997	This study
136.79	-1.53	18.83 *	19.34 *	19.76 *	20.25	20.05	20.56	19.80	*Turborotalia ampliapertura & increbescens*	Kim and O'Neil.,1997	This study
136.98	-1.89	20.51 *	21.02 *	21.44 *	21.93	21.73	22.24	21.48	*Turborotalia ampliapertura & increbescens*	Kim and O'Neil.,1997	This study

Depth (mbsf)	$\delta^{18}O_{CaCO3}$ (VPDB) (‰)	Paleotemperature (°C)							Species	Equation used	Data source
		$\delta^{18}O_{SW}$ from Shackleton and Kennett, 1975 (VSMOW)	$\delta^{18}O_{SW}$ from Cramer et al., 2011	$\delta^{18}O_{SW}$ from Zachos et al., 1994	$\delta^{18}O_{SW}$ from Tindall et al., 2010	$\delta^{18}O_{SW}$ from Huber et al., 2003	$\delta^{18}O_{SW}$ from Roberts et al., 2009	Mean			
137.18	-1.83	20.24 *	20.76 *	21.18 *	21.66	21.46	21.98	21.21	*Turborotalia ampliapertura & increbescens*	Kim and O'Neil.,1997	This study
137.37	-1.91	20.59 *	21.10 *	21.52 *	22.01	21.81	22.32	21.56	*Turborotalia ampliapertura & increbescens*	Kim and O'Neil.,1997	This study
137.57	-1.77	19.93 *	20.44 *	20.86 *	21.35	21.15	21.66	20.90	*Turborotalia ampliapertura & increbescens*	Kim and O'Neil.,1997	This study
137.77	-1.53	18.84 *	19.36 *	19.78 *	20.26	20.06	20.57	19.81	*Turborotalia ampliapertura & increbescens*	Kim and O'Neil.,1997	This study
137.98	-1.93	20.69 *	21.20 *	21.62 *	22.10	21.91	22.42	21.65	*Turborotalia ampliapertura & increbescens*	Kim and O'Neil.,1997	This study
138.17	-1.99	20.97 *	21.48 *	21.90 *	22.39	22.19	22.70	21.94	*Turborotalia ampliapertura & increbescens*	Kim and O'Neil.,1997	This study
138.35	-1.63	19.31 *	19.82 *	20.24 *	20.72	20.53	21.04	20.27	*Turborotalia ampliapertura & increbescens*	Kim and O'Neil.,1997	This study
138.54	-1.62	19.23 *	19.74 *	20.16 *	20.65	20.45	20.96	20.20	*Turborotalia ampliapertura & increbescens*	Kim and O'Neil.,1997	This study
138.74	-1.61	19.19 *	19.70 *	20.12 *	20.60	20.40	20.92	20.15	*Turborotalia ampliapertura & increbescens*	Kim and O'Neil.,1997	This study
139.1	-1.44	18.41 *	18.93 *	19.34 *	19.83	19.63	20.14	19.38	*Turborotalia ampliapertura & increbescens*	Kim and O'Neil.,1997	This study
139.31	-1.35	17.98 *	18.49 *	18.91 *	19.39	19.20	19.71	18.95	*Turborotalia ampliapertura & increbescens*	Kim and O'Neil.,1997	This study
139.5	-2.42	22.98 *	23.50 *	23.92 *	24.40	24.21	24.72	23.95	*Turborotalia ampliapertura & increbescens*	Kim and O'Neil.,1997	This study
139.71	-2.05	21.26 *	21.77 *	22.19 *	22.68	22.48	22.99	22.23	*Turborotalia ampliapertura & increbescens*	Kim and O'Neil.,1997	This study
139.91	-1.66	19.45 *	19.96 *	20.38 *	20.86	20.66	21.18	20.41	*Turborotalia ampliapertura & increbescens*	Kim and O'Neil.,1997	This study
140.1	-1.87	20.42 *	20.93 *	21.35 *	21.84	21.64	22.15	21.39	*Turborotalia ampliapertura & increbescens*	Kim and O'Neil.,1997	This study
140.3	-1.85	20.30 *	20.81 *	21.23 *	21.72	21.52	22.03	21.27	*Turborotalia ampliapertura & increbescens*	Kim and O'Neil.,1997	This study
135.47	-1.54	17.37	17.88	18.30				17.85	*Catapsydrax dissimilis & unicavus*	Kim and O'Neil.,1997	This study
135.63	-1.06	15.12	15.63	16.05				15.60	*Catapsydrax dissimilis & unicavus*	Kim and O'Neil.,1997	This study
135.73	-0.43	12.20	12.70	13.12				12.67	*Catapsydrax dissimilis & unicavus*	Kim and O'Neil.,1997	This study
135.95	-1.39	16.64	17.15	17.57				17.12	*Catapsydrax dissimilis & unicavus*	Kim and O'Neil.,1997	This study
136.08	-0.43	12.20	12.71	13.13				12.68	*Catapsydrax dissimilis & unicavus*	Kim and O'Neil.,1997	This study
136.2	-0.23	11.29	11.79	12.21				11.76	*Catapsydrax dissimilis & unicavus*	Kim and O'Neil.,1997	This study
136.265	-0.31	11.66	12.17	12.59				12.14	*Catapsydrax dissimilis & unicavus*	Kim and O'Neil.,1997	This study
136.33	-0.40	12.09	12.60	13.02				12.57	*Catapsydrax dissimilis & unicavus*	Kim and O'Neil.,1997	This study
136.4	-0.70	13.46	13.97	14.38				13.94	*Catapsydrax dissimilis & unicavus*	Kim and O'Neil.,1997	This study
136.59	-0.42	12.14	12.65	13.07				12.62	*Catapsydrax dissimilis & unicavus*	Kim and O'Neil.,1997	This study
136.79	-0.52	12.62	13.13	13.54				13.10	*Catapsydrax dissimilis & unicavus*	Kim and O'Neil.,1997	This study
136.98	-0.22	11.25	11.76	12.17				11.73	*Catapsydrax dissimilis & unicavus*	Kim and O'Neil.,1997	This study
137.18	-0.12	10.78	11.29	11.70				11.25	*Catapsydrax dissimilis & unicavus*	Kim and O'Neil.,1997	This study
137.37	-0.63	13.15	13.65	14.07				13.62	*Catapsydrax dissimilis & unicavus*	Kim and O'Neil.,1997	This study
137.57	-0.18	11.05	11.56	11.97				11.53	*Catapsydrax dissimilis & unicavus*	Kim and O'Neil.,1997	This study
137.77	-0.75	13.69	14.20	14.62				14.17	*Catapsydrax dissimilis & unicavus*	Kim and O'Neil.,1997	This study
137.98	-0.31	11.67	12.18	12.59				12.15	*Catapsydrax dissimilis & unicavus*	Kim and O'Neil.,1997	This study
138.17	-0.45	12.28	12.79	13.21				12.76	*Catapsydrax dissimilis & unicavus*	Kim and O'Neil.,1997	This study
138.35	-0.60	13.00	13.51	13.93				13.48	*Catapsydrax dissimilis & unicavus*	Kim and O'Neil.,1997	This study
138.54	-0.20	11.16	11.67	12.08				11.64	*Catapsydrax dissimilis & unicavus*	Kim and O'Neil.,1997	This study
138.74	-0.54	12.72	13.23	13.64				13.20	*Catapsydrax dissimilis & unicavus*	Kim and O'Neil.,1997	This study
139.1	-0.48	12.44	12.94	13.36				12.91	*Catapsydrax dissimilis & unicavus*	Kim and O'Neil.,1997	This study
139.31	-0.27	11.46	11.97	12.39				11.94	*Catapsydrax dissimilis & unicavus*	Kim and O'Neil.,1997	This study
139.5	-0.40	12.09	12.60	13.02				12.57	*Catapsydrax dissimilis & unicavus*	Kim and O'Neil.,1997	This study
139.71	-1.59	17.59	18.10	18.52				18.07	*Catapsydrax dissimilis & unicavus*	Kim and O'Neil.,1997	This study

Depth (mbsf)	$\delta^{18}O_{CaCO3}$ (VPDB) (‰)	Paleotemperature (°C)						Mean	Species	Equation used	Data source
		$\delta^{18}O_{SW}$ from Shackleton and Kennett, 1975 (VSMOW)	$\delta^{18}O_{SW}$ from Cramer et al., 2011	$\delta^{18}O_{SW}$ from Zachos et al., 1994	$\delta^{18}O_{SW}$ from Tindall et al., 2010	$\delta^{18}O_{SW}$ from Huber et al., 2003	$\delta^{18}O_{SW}$ from Roberts et al., 2009				
139.91	-0.39	12.04	12.55	12.96				12.52	*Catapsydrax dissimilis & unicavus*	Kim and O'Neil.,1997	This study
140.1	-0.57	12.88	13.39	13.80				13.36	*Catapsydrax dissimilis & unicavus*	Kim and O'Neil.,1997	This study
140.3	-0.55	12.78	13.29	13.71				13.26	*Catapsydrax dissimilis & unicavus*	Kim and O'Neil.,1997	This study
135.365	1.07	4.95	5.47	5.90				5.44	*Cibicidoides spp.*	Lynch-Stieglitz et al., 1999	This study
135.42	0.53	7.54	8.06	8.49				8.03	*Hanzawaia ammophila*	Lynch-Stieglitz et al., 1999	This study
135.47	0.71	6.68	7.20	7.63				7.17	*Hanzawaia ammophila*	Lynch-Stieglitz et al., 1999	Coxall et al., 2018
135.54	0.51	7.63	8.15	8.58				8.12	*Cibicidoides spp.*	Lynch-Stieglitz et al., 1999	This study
135.67	0.69	6.78	7.30	7.73				7.27	*Cibicidoides spp.*	Lynch-Stieglitz et al., 1999	This study
135.73	0.78	6.32	6.84	7.27				6.81	*Cibicidoides spp.*	Lynch-Stieglitz et al., 1999	This study
135.75	0.57	7.33	7.85	8.28				7.82	*Cibicidoides spp.*	Lynch-Stieglitz et al., 1999	This study
135.8	0.61	7.16	7.69	8.11				7.65	*Cibicidoides spp.*	Lynch-Stieglitz et al., 1999	This study
135.87	0.77	6.41	6.93	7.36				6.90	*Cibicidoides spp.*	Lynch-Stieglitz et al., 1999	This study
135.96	0.66	6.91	7.44	7.87				7.41	*Cibicidoides spp.*	Lynch-Stieglitz et al., 1999	Miller et al., 1991
136	0.57	7.34	7.87	8.29				7.83	*Cibicidoides spp.*	Lynch-Stieglitz et al., 1999	Miller et al., 1991
136.01	0.66	6.91	7.44	7.87				7.41	*Cibicidoides spp.*	Lynch-Stieglitz et al., 1999	This study
136.08	0.59	7.25	7.77	8.20				7.74	*Hanzawaia ammophila*	Lynch-Stieglitz et al., 1999	This study
136.13	0.60	7.20	7.73	8.15				7.69	*Hanzawaia ammophila*	Lynch-Stieglitz et al., 1999	This study
136.165	0.68	6.80	7.32	7.75				7.29	*Hanzawaia ammophila*	Lynch-Stieglitz et al., 1999	This study
136.2	-0.12	10.63	11.15	11.58				11.12	*Hanzawaia ammophila*	Lynch-Stieglitz et al., 1999	Coxall et al., 2018
136.23	0.13	9.42	9.94	10.37				9.91	*Cibicidoides spp.*	Lynch-Stieglitz et al., 1999	This study
136.23	0.51	7.65	8.17	8.60				8.14	*Hanzawaia ammophila*	Lynch-Stieglitz et al., 1999	This study
136.265	0.33	8.48	9.01	9.44				8.98	*Hanzawaia ammophila*	Lynch-Stieglitz et al., 1999	Coxall et al., 2018
136.3	0.80	6.25	6.77	7.20				6.74	*Cibicidoides spp.*	Lynch-Stieglitz et al., 1999	This study
136.3	0.52	7.59	8.11	8.54				8.08	*Hanzawaia ammophila*	Lynch-Stieglitz et al., 1999	This study
136.33	0.23	8.96	9.49	9.92				9.46	*Hanzawaia ammophila*	Lynch-Stieglitz et al., 1999	This study
136.35	0.65	6.98	7.50	7.93				7.47	*Cibicidoides spp.*	Lynch-Stieglitz et al., 1999	This study
136.35	0.51	7.61	8.14	8.57				8.11	*Hanzawaia ammophila*	Lynch-Stieglitz et al., 1999	This study
136.4	0.62	7.10	7.63	8.06				7.60	*Hanzawaia ammophila*	Lynch-Stieglitz et al., 1999	Coxall et al., 2018
136.49	0.55	7.43	7.95	8.38				7.92	*Cibicidoides spp.*	Lynch-Stieglitz et al., 1999	This study
136.49	0.50	7.69	8.21	8.64				8.18	*Hanzawaia ammophila*	Lynch-Stieglitz et al., 1999	This study
136.59	0.45	7.91	8.44	8.86				8.40	*Hanzawaia ammophila*	Lynch-Stieglitz et al., 1999	Coxall et al., 2018
136.7	0.22	9.02	9.54	9.97				9.51	*Cibicidoides spp.*	Lynch-Stieglitz et al., 1999	This study
136.7	0.39	8.20	8.72	9.15				8.69	*Hanzawaia ammophila*	Lynch-Stieglitz et al., 1999	This study
136.79	0.64	7.01	7.53	7.96				7.50	*Cibicidoides spp.*	Lynch-Stieglitz et al., 1999	This study
136.79	0.58	7.30	7.82	8.25				7.79	*Hanzawaia ammophila*	Lynch-Stieglitz et al., 1999	This study
136.88	0.59	7.23	7.75	8.18				7.72	*Cibicidoides spp.*	Lynch-Stieglitz et al., 1999	This study
136.88	0.43	7.99	8.52	8.94				8.48	*Hanzawaia ammophila*	Lynch-Stieglitz et al., 1999	This study
136.98	0.84	6.06	6.58	7.01				6.55	*Hanzawaia ammophila*	Lynch-Stieglitz et al., 1999	Coxall et al., 2018
137.18	0.50	7.67	8.20	8.63				8.17	*Hanzawaia ammophila*	Lynch-Stieglitz et al., 1999	Coxall et al., 2018
137.37	0.85	6.01	6.53	6.96				6.50	*Hanzawaia ammophila*	Lynch-Stieglitz et al., 1999	Coxall et al., 2018

Depth (mbsf)	$\delta^{18}O_{CaCO3}$ (VPDB) (‰)	Paleotemperature (°C)							Species	Equation used	Data source
		$\delta^{18}O_{SW}$ from Shackleton and Kennett, 1975 (VSMOW)	$\delta^{18}O_{SW}$ from Cramer et al., 2011	$\delta^{18}O_{SW}$ from Zachos et al., 1994	$\delta^{18}O_{SW}$ from Tindall et al., 2010	$\delta^{18}O_{SW}$ from Huber et al., 2003	$\delta^{18}O_{SW}$ from Roberts et al., 2009	Mean			
137.57	0.30	8.63	9.15	9.58				9.12	*Hanzawaia ammophila*	Lynch-Stieglitz et al., 1999	Coxall et al., 2018
137.6	0.19	9.15	9.67	10.10				9.64	*Cibicidoides spp.*	Lynch-Stieglitz et al., 1999	Miller et al., 1991
137.6	0.26	8.82	9.34	9.77				9.31	*Cibicidoides spp.*	Lynch-Stieglitz et al., 1999	Miller et al., 1991
137.77	0.85	6.01	6.53	6.96				6.50	*Hanzawaia ammophila*	Lynch-Stieglitz et al., 1999	Coxall et al., 2018
137.98	0.18	9.20	9.72	10.15				9.69	*Hanzawaia ammophila*	Lynch-Stieglitz et al., 1999	Coxall et al., 2018
138.17	-0.27	11.34	11.86	12.29				11.83	*Hanzawaia ammophila*	Lynch-Stieglitz et al., 1999	Coxall et al., 2018
138.19	0.94	5.60	6.13	6.56				6.10	*Cibicidoides spp.*	Lynch-Stieglitz et al., 1999	This study
138.19	0.62	7.09	7.61	8.04				7.58	*Hanzawaia ammophila*	Lynch-Stieglitz et al., 1999	This study
138.35	0.14	9.39	9.91	10.34				9.88	*Hanzawaia ammophila*	Lynch-Stieglitz et al., 1999	Coxall et al., 2018
138.54	0.57	7.34	7.87	8.29				7.83	*Hanzawaia ammophila*	Lynch-Stieglitz et al., 1999	Coxall et al., 2018
138.74	0.10	9.58	10.10	10.53				10.07	*Hanzawaia ammophila*	Lynch-Stieglitz et al., 1999	Coxall et al., 2018
138.96	0.99	5.32	5.85	6.28				5.82	*Cibicidoides spp.*	Lynch-Stieglitz et al., 1999	This study
139.1	0.33	8.48	9.01	9.44				8.98	*Hanzawaia ammophila*	Lynch-Stieglitz et al., 1999	Coxall et al., 2018
139.1	0.29	8.67	9.20	9.63				9.17	*Cibicidoides spp.*	Lynch-Stieglitz et al., 1999	Miller et al., 1991
139.31	0.00	10.05	10.58	11.01				10.55	*Hanzawaia ammophila*	Lynch-Stieglitz et al., 1999	Coxall et al., 2018
139.5	0.63	7.06	7.58	8.01				7.55	*Hanzawaia ammophila*	Lynch-Stieglitz et al., 1999	Coxall et al., 2018
139.71	0.64	7.01	7.53	7.96				7.50	*Hanzawaia ammophila*	Lynch-Stieglitz et al., 1999	Coxall et al., 2018
139.91	-0.20	11.01	11.53	11.96				11.50	*Hanzawaia ammophila*	Lynch-Stieglitz et al., 1999	Coxall et al., 2018
140.1	-0.75	13.62	14.15	14.58				14.12	*Hanzawaia ammophila*	Lynch-Stieglitz et al., 1999	Coxall et al., 2018
140.49	1.10	4.80	5.33	5.76				5.30	*Hanzawaia ammophila*	Lynch-Stieglitz et al., 1999	This study
140.6	0.42	8.06	8.58	9.01				8.55	*Cibicidoides spp.*	Lynch-Stieglitz et al., 1999	Miller et al., 1991
140.68	0.78	6.33	6.85	7.28				6.82	*Cibicidoides spp.*	Lynch-Stieglitz et al., 1999	This study
140.89	1.04	5.10	5.62	6.05				5.59	*Hanzawaia ammophila*	Lynch-Stieglitz et al., 1999	This study
141.08	0.58	7.30	7.83	8.25				7.79	*Hanzawaia ammophila*	Lynch-Stieglitz et al., 1999	This study
141.28	0.89	5.80	6.32	6.75				6.29	*Cibicidoides spp.*	Lynch-Stieglitz et al., 1999	This study
141.46	0.89	5.80	6.32	6.75				6.29	*Hanzawaia ammophila*	Lynch-Stieglitz et al., 1999	This study
143.6	0.13	9.44	9.96	10.39				9.93	*Cibicidoides spp.*	Lynch-Stieglitz et al., 1999	Miller et al., 1991
145.1	0.20	9.10	9.63	10.05				9.59	*Cibicidoides spp.*	Lynch-Stieglitz et al., 1999	Miller et al., 1991
146.3	0.25	8.86	9.39	9.82				9.36	*Cibicidoides spp.*	Lynch-Stieglitz et al., 1999	Miller et al., 1991
149.3	0.35	8.39	8.91	9.34				8.88	*Cibicidoides spp.*	Lynch-Stieglitz et al., 1999	Miller et al., 1991
150.8	0.47	7.82	8.34	8.77				8.31	*Cibicidoides spp.*	Lynch-Stieglitz et al., 1999	Miller et al., 1991
154.7	0.24	8.91	9.44	9.86				9.40	*Cibicidoides spp.*	Lynch-Stieglitz et al., 1999	Miller et al., 1991
155.8	0.15	9.34	9.86	10.29				9.83	*Cibicidoides spp.*	Lynch-Stieglitz et al., 1999	Miller et al., 1991
157.3	0.32	8.53	9.06	9.48				9.02	*Cibicidoides spp.*	Lynch-Stieglitz et al., 1999	Miller et al., 1991
158.8	0.34	8.44	8.96	9.39				8.93	*Cibicidoides spp.*	Lynch-Stieglitz et al., 1999	Miller et al., 1991
160.3	0.31	8.58	9.10	9.53				9.07	*Cibicidoides spp.*	Lynch-Stieglitz et al., 1999	Miller et al., 1991
163.3	0.08	9.67	10.20	10.63				10.17	*Cibicidoides spp.*	Lynch-Stieglitz et al., 1999	Miller et al., 1991
164.5	0.01	10.01	10.53	10.96				10.50	*Cibicidoides spp.*	Lynch-Stieglitz et al., 1999	Miller et al., 1991
165.3	0.05	9.82	10.34	10.77				10.31	*Cibicidoides spp.*	Lynch-Stieglitz et al., 1999	Miller et al., 1991
166.8	0.14	9.39	9.91	10.34				9.88	*Cibicidoides spp.*	Lynch-Stieglitz et al., 1999	Miller et al., 1991
168.3	0.15	9.34	9.86	10.29				9.83	*Cibicidoides spp.*	Lynch-Stieglitz et al., 1999	Miller et al., 1991

Depth (mbsf)	$\delta^{18}O_{CaCO3}$ (VPDB) (‰)	Paleotemperature (°C)							Species	Equation used	Data source
		$\delta^{18}O_{SW}$ from Shackleton and Kennett, 1975 (VSMOW)	$\delta^{18}O_{SW}$ from Cramer et al., 2011	$\delta^{18}O_{SW}$ from Zachos et al., 1994	$\delta^{18}O_{SW}$ from Tindall et al., 2010	$\delta^{18}O_{SW}$ from Huber et al., 2003	$\delta^{18}O_{SW}$ from Roberts et al., 2009	Mean			
169.8	0.08	9.67	10.20	10.63				10.17	*Cibicidoides spp.*	Lynch-Stieglitz et al., 1999	Miller et al., 1991
171.3	0.18	9.20	9.72	10.15				9.69	*Cibicidoides spp.*	Lynch-Stieglitz et al., 1999	Miller et al., 1991
179.3	-0.02	10.15	10.67	11.10				10.64	*Cibicidoides spp.*	Lynch-Stieglitz et al., 1999	Miller et al., 1991
181.33	0.01	10.01	10.53	10.96				10.50	*Cibicidoides spp.*	Lynch-Stieglitz et al., 1999	Pusz et al., 2009
181.34	0.20	9.10	9.63	10.05				9.59	*Cibicidoides spp.*	Lynch-Stieglitz et al., 1999	Pusz et al., 2009
181.36	0.09	9.63	10.15	10.58				10.12	*Cibicidoides spp.*	Lynch-Stieglitz et al., 1999	Pusz et al., 2009
181.37	0.31	8.58	9.10	9.53				9.07	*Cibicidoides spp.*	Lynch-Stieglitz et al., 1999	Pusz et al., 2009
181.38	0.35	8.39	8.91	9.34				8.88	*Cibicidoides spp.*	Lynch-Stieglitz et al., 1999	Pusz et al., 2009

Table IV c. Sediment fractions weigh: >106 µm, 106< >63 µm, >63 µm, 63< >38 µm, <63 µm and fine (FF) fractions. * = Estimated; Σ >63 µm =sum of all fractions higher than 63 µm (>106 and 106-63 µm); Σ <63 µm = sum of all fractions lower than 63 µm (63-38 µm and FF).

Depth (mbsf)	Initial weigh (g)	Weigh per fraction (g)						Weigh per fraction (%)		
		>106 µm*	106< >63 µm	**Σ >63 µm**	63< >38 µm	**Σ <63 µm**	FF *	**Coarse fraction (Σ >63 µm)**	**Σ <63 µm**	FF (Fine fraction)
135.365	8.3			1.6		6.6		19.9	80.1	
135.42	13.8			2.6		11.2		18.9	81.1	
135.47	7.3	0.6	0.6	1.2	1.6	6.1	4.5	16.8	83.2	61.5
135.54	13.2			1.9		11.3		14.6	85.4	
135.63	7.2	0.2	0.3	0.5	0.8	6.7	5.9	6.7	93.3	81.8
135.67	17.6			1.7		15.9		9.9	90.1	
135.73	7.7	0.3	0.2	0.5	0.7	7.1	6.4	7.1	92.9	83.2
135.75	14.9			1.3		13.6		9.0	91.0	
135.8	15.6			1.3		14.3		8.4	91.6	
135.87	20.4			1.9		18.5		9.5	90.5	
135.95	9.8	0.9	0.5	1.4	1.3	8.4	7.1	14.3	85.7	72.5
136.01	16.7			1.2		15.5		7.1	92.9	
136.08	11.0	0.6	0.4	1.0	0.9	10.1	9.1	8.9	91.1	82.6
136.13	12.4			1.5		10.8		12.2	87.8	
136.165	15.6			2.8		12.8		17.8	82.2	
136.2	7.7	0.6	0.5	1.1	0.5	6.6	6.1	13.7	86.3	79.7
136.23	17.0			2.3		14.7		13.6	86.4	
136.265	9.2	0.9	0.2	1.1	0.6	8.0	7.5	12.4	87.6	81.4
136.3	8.4			0.9		7.6		10.2	89.8	
136.33	8.2	0.5	0.5	1.0	0.6	7.2	6.6	12.5	87.5	80.1
136.35	10.6			1.2		9.5		11.2	88.8	
136.4	9.1	1.0	0.8	1.8	0.9	7.3	6.4	19.9	80.1	70.3
136.49	16.6			3.2		13.4		19.2	80.8	
136.59	8.8	0.5	0.9	1.4	0.9	7.3	6.4	16.3	83.7	73.3
136.7	19.2			2.5		16.7		12.8	87.2	
136.79	6.1	0.3	0.3	0.6	0.4	5.4	5.1	10.0	90.0	84.2
136.88	22.0			3.8		18.3		17.0	83.0	
136.98	8.4	0.5	0.3	0.8	1.0	7.5	6.5	10.0	90.0	77.7
137.18	9.0	0.8	0.5	1.3	0.8	7.6	6.8	15.0	85.0	75.7
137.37	8.6	1.0	0.4	1.3	0.8	7.2	6.4	15.5	84.5	74.8
137.57	9.9	0.9	0.3	1.2	0.9	8.7	7.8	12.4	87.6	78.8
137.77	8.3	0.5	0.5	1.0	0.7	7.3	6.6	11.9	88.1	80.0
137.98	9.3	1.2	0.4	1.6	0.7	7.7	7.0	16.9	83.1	75.4
138.17	9.2	1.0	0.4	1.4	0.8	7.8	7.0	15.5	84.5	75.5
138.19	0.8			0.2		0.7		18.2	81.8	
138.35	9.4	0.8	0.5	1.3	0.7	8.1	7.4	13.4	86.6	79.2
138.54	8.7	0.5	0.4	0.9	0.7	7.8	7.1	10.3	89.7	81.6
138.74	9.3	0.4	0.3	0.7	0.7	8.6	7.9	7.8	92.2	84.9
138.96	11.8	0.6	0.2	0.8	0.8	11.0	10.2	6.7	93.3	86.1
139.1	7.9	0.5	0.2	0.8	0.7	7.1	6.4	9.9	90.1	81.0

Depth (mbsf)	Initial weigh (g)	Weigh per fraction (g)						Weigh per fraction (%)		
		>106 µm*	106< >63 µm	**Σ >63 µm**	63< >38 µm	**Σ <63 µm**	FF *	**Coarse fraction (Σ >63 µm)**	**Σ <63 µm**	FF (Fine fraction)
139.31	9.8	0.3	0.3	0.6	0.6	9.2	8.6	6.2	93.8	87.9
139.5	9.3	0.6	0.4	1.0	0.8	8.3	7.4	10.7	89.3	80.3
139.69	0.2			0.1		0.2		32.7	67.3	
139.71	10.1	0.5	0.3	0.8	0.8	9.3	8.5	7.7	92.3	84.5
139.91	9.1	0.6	0.3	0.9	0.7	8.1	7.4	10.2	89.8	81.7
140.1	9.5	0.5	0.4	0.9	0.7	8.6	7.9	9.2	90.8	83.3
140.3	8.9	0.5	0.3	0.8	0.8	8.1	7.4	8.9	91.1	82.6
140.49	9.1	0.5	0.3	0.9	0.8	8.2	7.4	9.6	90.4	81.2
140.68	8.4	0.6	0.4	1.1	0.8	7.3	6.5	13.0	87.0	77.9
140.89	9.5	0.6	0.5	1.0	0.6	8.5	7.8	10.7	89.3	82.4
141.08	9.3	0.8	0.3	1.2	0.7	8.2	7.5	12.4	87.6	80.3
141.19	0.1			0.0		0.1		23.8	76.2	
141.28	8.6	0.8	0.3	1.1	0.7	7.5	6.7	12.7	87.3	78.6
141.46	8.3	0.7	0.3	1.0	0.7	7.3	6.7	12.0	88.0	80.2

Table IV d1. Planktic foraminifera assemblage: census. Warm colors correspond to high abundances and cold colors to low (this applies to all assemblage databases displayed in this appendix).

Sample ID (612-…)	16X-6, 127-129 cm	16X-6, 143-145 cm	16X-7, 3-5 cm	16X-7, 25-27 cm	16X-CC, 10-12 cm	17X-1, 0-2 cm	17X-1, 6.5-8.5 cm	17X-1, 13-15 cm	17X-1, 20-22 cm	17X-1, 39-41 cm	17X-1, 59-61 cm	17X-1, 78-80 cm	17X-1, 98-100 cm	17X-1, 117-119 cm	17X-1, 137-139 cm	17X-2, 7-9 cm	17X-2, 28-30 cm	17X-2, 47-49 cm	17X-2, 65-67 cm	17X-2, 84-86 cm	17X-2, 104-106 cm	17X-2, 126-128 cm	17X-2, 140-142 cm	17X-3, 11-13 cm	17X-3, 30-32 cm	17X-3, 51-53 cm	17X-3,71-73 cm	17X-3, 90-92 cm	17X-3, 110-112 cm	17X-3, 129-131 cm	17X-3, 148-150 cm	17X-4, 19-21 cm	17X-4, 38-40 cm	17X-4, 58-60 cm	17X-4, 76-78 cm	
Depth (mbsf)	135.47	135.63	135.73	135.95	136.08	136.2	136.265	136.33	136.4	136.59	136.79	136.98	137.18	137.37	137.57	137.77	137.98	138.17	138.35	138.54	138.74	138.96	139.1	139.31	139.5	139.71	139.91	140.1	140.3	140.49	140.68	140.89	141.08	141.28	141.46	**Average**
Cribrohantkenina inflata	0	0	0	0	0	0	0	0	0	0	0	0	0	0	0	0	0	0	0	0	0	0	0	0	0	0	0	1	1	0	0	0	0	0	0	0.1
Hantkenina alabamensis	0	0	0	0	9	0	1	0	0	1	1	1	1	0	3	2	12	5	3	0	0	0	1	1	1	0	2	9	0	0	0	1	0	2	1	1.6
Hantkenina compressa	0	0	0	0	4	0	0	0	0	1	1	0	0	2	0	2	0	0	0	0	0	0	0	1	0	0	0	2	0	0	0	0	0	0	0	0.4
Hantkenina nanggulanensis	0	0	0	0	0	0	0	0	0	0	0	0	0	0	0	0	2	0	1	0	0	0	0	0	0	1	1	0	0	0	0	0	1	2	0	0.2
Hantkenina primitiva	0	0	0	0	0	0	0	0	1	0	1	0	0	1	0	0	0	0	0	0	0	0	1	3	1	0	1	1	0	0	0	0	0	0	1	0.3
Pseudohastigerina micra	0	0	0	0	0	5	3	18	5	1	7	2	5	6	7	5	6	0	1	10	5	1	1	5	5	3	2	8	1	4	2	3	1	0	20	4.1
Pseudohastigerina naguewichiensis	0	0	0	0	0	1	0	2	1	1	1	0	0	0	0	1	3	0	1	0	0	2	1	0	0	0	0	0	0	0	0	0	0	0	0	0.4
Turborotalia cocoaensis	0	0	0	0	6	2	0	0	0	1	2	1	2	3	0	1	1	1	0	0	0	0	0	0	0	0	2	1	4	3	4	2	0	5	0	1.2
Turborotalia cunialensis	0	0	0	0	0	2	2	2	0	2	2	3	3	3	0	3	3	0	0	1	0	0	0	0	0	0	1	5	9	5	3	7	1	2	1	1.7
Turborotalia cerroazulensis	0	0	0	0	1	0	1	0	2	2	2	0	4	12	6	4	2	1	0	0	0	0	0	0	2	0	3	4	13	16	7	7	5	11	1	3
Turborotalia increbescens	40	47	48	74	51	31	52	30	43	28	42	20	35	33	23	15	44	39	42	38	39	37	37	22	47	38	57	33	23	24	31	28	26	33	46	37
Turborotalia ampliapertura	0	3	9	3	4	14	23	12	24	13	10	11	11	7	12	12	13	6	17	12	14	6	5	4	1	5	9	10	4	5	2	1	4	10	0	8.5
Catapsydrax unicavus	0	0	0	0	0	1	0	1	0	1	1	1	0	0	0	0	0	2	0	0	0	0	0	0	3	0	0	0	0	0	0	0	0	0	0	0.3
Catapsydrax dissimilis	12	12	10	10	11	17	12	6	6	8	14	14	17	12	13	13	9	16	13	7	10	21	14	8	7	9	15	12	22	16	14	10	31	17	7	13
Dentoglobigerina galavisi	33	18	28	11	32	10	24	6	13	12	10	21	19	27	13	11	11	28	16	32	27	20	19	37	21	31	20	12	24	16	35	26	25	27	34	21
Dentoglobigerina tripartita	8	12	8	4	19	16	10	7	7	17	8	15	6	26	16	32	8	15	4	11	7	5	5	2	1	12	6	2	9	3	4	3	10	5	1	9.3
Dentoglobigerina pseudovenezuelana	10	8	3	2	7	4	1	0	13	9	6	8	11	13	11	9	5	18	22	17	13	19	16	20	17	11	10	11	8	12	18	17	28	20	11	12
Dentoglobigerina venezuelana	5	4	16	29	7	4	10	2	7	1	13	9	1	0	15	8	14	11	5	17	11	18	0	7	3	9	17	7	3	5	16	17	17	13	6	9.3
Globigerina officinalis	7	3	0	3	1	2	5	14	1	3	6	4	1	2	0	2	0	0	1	2	0	0	8	4	6	4	1	4	10	4	4	4	2	4	4	3.3
Ciperoella anguliofficinalis	5	2	0	1	1	3	2	1	1	0	2	0	0	0	0	0	0	0	0	0	0	1	0	0	0	1	2	2	2	0	1	1	1	0	0	0.8
Globoturborotalita ouachitaensis	37	27	18	18	16	33	14	24	21	29	22	19	20	22	15	40	9	10	17	20	16	16	8	9	18	4	15	8	21	8	11	16	7	9	8	17
Globoturborotalita martini	8	6	5	3	3	7	2	6	3	3	11	4	4	0	1	8	3	4	5	10	6	0	3	0	2	7	2	6	1	0	5	2	0	6	0	3.9

Sample ID (612-…)	16X-6, 127-129 cm	16X-6, 143-145 cm	16X-7, 3-5 cm	16X-7, 25-27 cm	16X-CC, 10-12 cm	17X-1, 0-2 cm	17X-1, 6.5-8.5 cm	17X-1, 13-15 cm	17X-1, 20-22 cm	17X-1, 39-41 cm	17X-1, 59-61 cm	17X-1, 78-80 cm	17X-1, 98-100 cm	17X-1, 117-119 cm	17X-1, 137-139 cm	17X-2, 7-9 cm	17X-2, 28-30 cm	17X-2, 47-49 cm	17X-2, 65-67 cm	17X-2, 84-86 cm	17X-2, 104-106 cm	17X-2, 126-128 cm	17X-2, 140-142 cm	17X-3, 11-13 cm	17X-3, 30-32 cm	17X-3, 51-53 cm	17X-3,71-73 cm	17X-3, 90-92 cm	17X-3, 110-112 cm	17X-3, 129-131 cm	17X-3, 148-150 cm	17X-4, 19-21 cm	17X-4, 38-40 cm	17X-4, 58-60 cm	17X-4, 76-78 cm	
Depth (mbsf)	135.47	135.63	135.73	135.95	136.08	136.2	136.265	136.33	136.4	136.59	136.79	136.98	137.18	137.37	137.57	137.77	137.98	138.17	138.35	138.54	138.74	138.96	139.1	139.31	139.5	139.71	139.91	140.1	140.3	140.49	140.68	140.89	141.08	141.28	141.46	**Average**
Globorotaloides eovariabilis	4	4	0	0	6	3	4	4	3	3	2	7	5	2	3	4	2	6	0	1	1	0	3	3	2	6	1	5	9	1	3	2	1	0	0	2.9
Globorotaloides quadrocameratus	5	0	1	0	0	8	0	18	2	5	2	1	3	0	3	5	0	2	0	3	3	0	2	4	1	1	1	2	7	4	4	2	0	0	0	2.5
Subbotina angiporoides	8	13	6	4	7	11	15	17	8	5	18	18	15	10	15	5	7	6	12	4	14	3	11	5	8	4	6	5	6	2	2	11	14	2	3	8.6
Subbotina linaperta	13	22	11	19	6	17	21	19	18	22	22	26	16	8	32	12	14	26	17	18	25	13	31	19	26	27	9	11	11	13	12	21	13	17	21	18
Subbotina eocaena	30	43	46	49	37	23	34	25	24	15	32	33	39	16	32	23	32	38	27	28	37	39	33	30	35	30	35	27	21	24	30	30	23	23	34	31
Subbotina corpulenta	17	32	41	33	20	18	14	9	13	23	14	34	26	34	18	15	37	36	41	17	17	37	12	22	18	26	50	26	22	32	36	41	54	27	27	27
Subbotina gortanii	3	3	8	2	3	2	3	6	1	4	4	1	1	5	2	1	3	2	2	4	3	2	3	3	1	1	1	0	3	1	5	4	4	4	0	2.7
Subbotina hagni	16	9	15	12	23	21	10	3	27	20	5	6	16	8	12	8	8	6	13	13	17	13	17	3	9	3	5	22	22	17	17	39	23	21	10	14
Subbotina yeguaensis	16	8	8	7	3	22	7	11	3	12	15	26	8	15	11	5	17	9	9	18	17	12	14	9	18	21	20	16	7	11	6	8	6	15	15	12
Subbotina projecta	0	6	4	0	1	1	0	0	0	0	0	0	0	0	1	0	1	4	6	8	1	6	7	5	10	4	7	12	1	1	4	3	1	4	2	2.9
Paragloborotalia nana	4	5	0	4	3	14	12	13	13	10	2	2	1	7	4	5	3	1	1	4	4	2	6	2	6	2	2	2	4	7	5	1	0	3	1	4.4
Paragloborotalia griffinoides	11	6	9	12	7	8	15	14	16	13	2	6	6	11	3	5	7	9	7	8	23	5	12	5	6	16	3	27	20	28	19	19	6	10	4	11
Turborotalita praequinqueloba	1	3	6	0	3	5	6	12	4	7	2	3	6	2	7	4	3	0	0	5	4	4	3	2	0	2	0	0	6	1	2	1	0	6	3	3.2
Streptochilus martini	0	0	0	0	0	0	0	4	1	1	1	0	1	0	0	0	0	0	0	0	0	0	0	0	0	0	0	5	0	0	0	0	0	0	0	0.4
Chiloguembelina cubensis	0	0	0	0	0	0	1	1	1	0	3	0	0	1	0	0	0	0	0	0	0	0	0	0	0	0	0	0	0	0	0	0	0	0	0	0.2
Chiloguembelina ototara	2	0	0	0	0	1	2	4	4	8	10	3	8	3	4	4	3	1	9	3	0	14	6	10	2	7	0	4	6	8	3	1	1	7	31	4.8
Tenuitella gemma	0	0	0	0	0	0	0	4	0	6	1	0	0	4	1	6	0	0	0	0	0	0	1	5	2	5	1	1	3	4	2	0	0	0	0	1.3
Tenuitella praegemma	0	0	0	0	0	4	2	4	10	3	5	0	5	4	5	21	12	0	1	1	2	6	6	14	17	4	1	6	1	4	0	0	0	0	5	4.1
Tenuitella patefacta	0	1	0	0	0	3	1	3	5	10	0	4	5	7	7	12	7	1	7	1	0	12	14	36	10	9	0	2	7	17	6	3	8	2	3	5.8
Dipsidripella danvillensis	0	0	0	0	0	0	0	0	0	0	0	0	0	0	1	0	3	0	0	0	0	0	0	0	1	0	0	1	0	2	1	2	0	0	0	0.3
Acarinina collactea	8	4	0	0	9	0	0	0	0	0	1	2	0	0	4	1	0	2	1	4	1	0	1	2	1	2	0	0	2	4	4	6	4	1	0	1.8
Number of total counted specimens	303	301	300	300	300	313	309	302	301	300	303	305	301	306	300	304	304	305	301	317	317	314	301	302	308	305	308	312	313	302	318	339	317	308	300	

Table IV d2. Planktic foraminifera assemblage: relative abundances (%).

Sample ID (612-…)	16X-6, 127-129 cm	16X-6, 143-145 cm	16X-7, 3-5 cm	16X-7, 25-27 cm	16X-CC, 10-12 cm	17X-1, 0-2 cm	17X-1, 6.5-8.5 cm	17X-1, 13-15 cm	17X-1, 20-22 cm	17X-1, 39-41 cm	17X-1, 59-61 cm	17X-1, 78-80 cm	17X-1, 98-100 cm	17X-1, 117-119 cm	17X-1, 137-139 cm	17X-2, 7-9 cm	17X-2, 28-30 cm	17X-2, 47-49 cm	17X-2, 65-67 cm	17X-2, 84-86 cm	17X-2, 104-106 cm	17X-2, 126-128 cm	17X-2, 140-142 cm	17X-3, 11-13 cm	17X-3, 30-32 cm	17X-3, 51-53 cm	17X-3,71-73 cm	17X-3, 90-92 cm	17X-3, 110-112 cm	17X-3, 129-131 cm	17X-3, 148-150 cm	17X-4, 19-21 cm	17X-4, 38-40 cm	17X-4, 58-60 cm	17X-4, 76-78 cm	Average
Depth (mbsf)	135.47	135.63	135.73	135.95	136.08	136.2	136.265	136.33	136.4	136.59	136.79	136.98	137.18	137.37	137.57	137.77	137.98	138.17	138.35	138.54	138.74	138.96	139.1	139.31	139.5	139.71	139.91	140.1	140.3	140.49	140.68	140.89	141.08	141.28	141.46	
Cribrohantkenina inflata	0	0	0	0	0	0	0	0	0	0	0	0	0	0	0	0	0	0	0	0	0	0	0	0	0	0	0	0.3	0.3	0	0	0	0	0	0
Hantkenina alabamensis	0	0	0	0	3	0	0.3	0	0	0.3	0.3	0.3	0.3	0	1	0.7	3.9	1.6	1	0	0	0	0.3	0.3	0.3	0	0.6	2.9	0	0	0	0.3	0	0.6	0.3	0.5
Hantkenina compressa	0	0	0	0	1.3	0	0	0	0	0.3	0.3	0	0	0.7	0	0.7	0	0	0	0	0	0	0	0.3	0	0	0	0.6	0	0	0	0	0	0	0	0.1
Hantkenina nanggulanensis	0	0	0	0	0	0	0	0	0	0	0	0	0	0	0	0	0.7	0	0.3	0	0	0	0	0	0	0.3	0.3	0	0	0	0	0	0.3	0.6	0	0.1
Hantkenina primitiva	0	0	0	0	0	0	0	0	0.3	0	0.3	0	0	0.3	0	0	0	0	0	0	0	0	0.3	1	0.3	0	0.3	0.3	0	0	0	0	0	0	0.3	0.1
Pseudohastigerina micra	0	0	0	0	0	1.6	1	6	1.7	0.3	2.3	0.7	1.7	2	2.3	1.6	2	0	0.3	3.2	1.6	0.3	0.3	1.7	1.6	1	0.6	2.6	0.3	1.3	0.6	0.9	0.3	0	6.7	1.3
Pseudohastigerina naguewichiensis	0	0	0	0	0	0.3	0	0.7	0.3	0.3	0.3	0	0	0	0	0.3	1	0	0.3	0	0	0.6	0.3	0	0	0	0	0	0	0	0	0	0	0	0	0.1
Turborotalia cocoaensis	0	0	0	0	2	0.6	0	0	0	0.3	0.7	0.3	0.7	1	0	0.3	0.3	0.3	0	0	0	0	0	0	0	0	0.6	0.3	1.3	1	1.3	0.6	0	1.6	0	0.4
Turborotalia cunialensis	0	0	0	0	0	0.6	0.6	0.7	0	0.7	0.7	1	1	1	0	1	1	0	0	0.3	0	0	0	0	0	0	0.3	1.6	2.9	1.7	0.9	2.1	0.3	0.6	0.3	0.6
Turborotalia cerroazulensis	0	0	0	0	0.3	0	0.3	0	0.7	0.7	0.7	0	1.3	3.9	2	1.3	0.7	0.3	0	0	0	0	0	0	0.6	0	1	1.3	4.2	5.3	2.2	2.1	1.6	3.6	0.3	1
Turborotalia increbescens	13	16	16	25	17	9.9	17	9.9	14	9.3	14	6.6	12	11	7.7	4.9	14	13	14	12	12	12	12	7.3	15	12	19	11	7.3	7.9	9.7	8.3	8.2	11	15	12
Turborotalia ampliapertura	0	1	3	1	1.3	4.5	7.4	4	8	4.3	3.3	3.6	3.7	2.3	4	3.9	4.3	2	5.6	3.8	4.4	1.9	1.7	1.3	0.3	1.6	2.9	3.2	1.3	1.7	0.6	0.3	1.3	3.2	0	2.8
Catapsydrax unicavus	0	0	0	0	0	0.3	0	0.3	0	0.3	0.3	0.3	0	0	0	0	0	0.7	0	0	0	0	0	0	1	0	0	0	0	0	0	0	0	0	0	0.1
Catapsydrax dissimilis	4	4	3.3	3.3	3.7	5.4	3.9	2	2	2.7	4.6	4.6	5.6	3.9	4.3	4.3	3	5.2	4.3	2.2	3.2	6.7	4.7	2.6	2.3	3	4.9	3.8	7	5.3	4.4	2.9	9.8	5.5	2.3	4.1
Dentoglobigerina galavisi	11	6	9.3	3.7	11	3.2	7.8	2	4.3	4	3.3	6.9	6.3	8.8	4.3	3.6	3.6	9.2	5.3	10	8.5	6.4	6.3	12	6.8	10	6.5	3.8	7.7	5.3	11	7.7	7.9	8.8	11	7
Dentoglobigerina tripartita	2.6	4	2.7	1.3	6.3	5.1	3.2	2.3	2.3	5.7	2.6	4.9	2	8.5	5.3	11	2.6	4.9	1.3	3.5	2.2	1.6	1.7	0.7	0.3	3.9	1.9	0.6	2.9	1	1.3	0.9	3.2	1.6	0.3	3
D. pseudovenezuelana	3.3	2.7	1	0.7	2.3	1.3	0.3	0	4.3	3	2	2.6	3.7	4.2	3.7	3	1.6	5.9	7.3	5.4	4.1	6.1	5.3	6.6	5.5	3.6	3.2	3.5	2.6	4	5.7	5	8.8	6.5	3.7	3.8
Dentoglobigerina venezuelana	1.7	1.3	5.3	9.7	2.3	1.3	3.2	0.7	2.3	0.3	4.3	3	0.3	0	5	2.6	4.6	3.6	1.7	5.4	3.5	5.7	0	2.3	1	3	5.5	2.2	1	1.7	5	5	5.4	4.2	2	3
Globigerina officinalis	2.3	1	0	1	0.3	0.6	1.6	4.6	0.3	1	2	1.3	0.3	0.7	0	0.7	0	0	0.3	0.6	0	0	2.7	1.3	1.9	1.3	0.3	1.3	3.2	1.3	1.3	1.2	0.6	1.3	1.3	1.1
Ciperoella anguliofficinalis	1.7	0.7	0	0.3	0.3	1	0.6	0.3	0.3	0	0.7	0	0	0	0	0	0	0	0	0	0	0.3	0	0	0	0.3	0.6	0.6	0.6	0	0.3	0.3	0.3	0	0	0.3
Globoturborotalita ouachitaensis	12	9	6	6	5.3	11	4.5	7.9	7	9.7	7.3	6.2	6.6	7.2	5	13	3	3.3	5.6	6.3	5	5.1	2.7	3	5.8	1.3	4.9	2.6	6.7	2.6	3.5	4.7	2.2	2.9	2.7	5.6
Globoturborotalita martini	2.6	2	1.7	1	1	2.2	0.6	2	1	1	3.6	1.3	1.3	0	0.3	2.6	1	1.3	1.7	3.2	1.9	0	1	0	0.6	2.3	0.6	1.9	0.3	0	1.6	0.6	0	1.9	0	1.3
Globorotaloides eovariabilis	1.3	1.3	0	0	2	1	1.3	1.3	1	1	0.7	2.3	1.7	0.7	1	1.3	0.7	2	0	0.3	0.3	0	1	1	0.6	2	0.3	1.6	2.9	0.3	0.9	0.6	0.3	0	0	0.9
Globorotaloides quadrocameratus	1.7	0	0.3	0	0	2.6	0	6	0.7	1.7	0.7	0.3	1	0	1	1.6	0	0.7	0	0.9	0.9	0	0.7	1.3	0.3	0.3	0.3	0.6	2.2	1.3	1.3	0.6	0	0	0	0.8
Subbotina angiporoides	2.6	4.3	2	1.3	2.3	3.5	4.9	5.6	2.7	1.7	5.9	5.9	5	3.3	5	1.6	2.3	2	4	1.3	4.4	1	3.7	1.7	2.6	1.3	1.9	1.6	1.9	0.7	0.6	3.2	4.4	0.6	1	2.8
Subbotina linaperta	4.3	7.3	3.7	6.3	2	5.4	6.8	6.3	6	7.3	7.3	8.5	5.3	2.6	11	3.9	4.6	8.5	5.6	5.7	7.9	4.1	10	6.3	8.4	8.9	2.9	3.5	3.5	4.3	3.8	6.2	4.1	5.5	7	5.9
Subbotina eocaena	9.9	14	15	16	12	7.3	11	8.3	8	5	11	11	13	5.2	11	7.6	11	12	9	8.8	12	12	11	9.9	11	9.8	11	8.7	6.7	7.9	9.4	8.8	7.3	7.5	11	10
Subbotina corpulenta	5.6	11	14	11	6.7	5.8	4.5	3	4.3	7.7	4.6	11	8.6	11	6	4.9	12	12	14	5.4	5.4	12	4	7.3	5.8	8.5	16	8.3	7	11	11	12	17	8.8	9	8.7

Sample ID (612-…)	16X-6, 127-129 cm	16X-6, 143-145 cm	16X-7, 3-5 cm	16X-7, 25-27 cm	16X-CC, 10-12 cm	17X-1, 0-2 cm	17X-1, 6.5-8.5 cm	17X-1, 13-15 cm	17X-1, 20-22 cm	17X-1, 39-41 cm	17X-1, 59-61 cm	17X-1, 78-80 cm	17X-1, 98-100 cm	17X-1, 117-119 cm	17X-1, 137-139 cm	17X-2, 7-9 cm	17X-2, 28-30 cm	17X-2, 47-49 cm	17X-2, 65-67 cm	17X-2, 84-86 cm	17X-2, 104-106 cm	17X-2, 126-128 cm	17X-2, 140-142 cm	17X-3, 11-13 cm	17X-3, 30-32 cm	17X-3, 51-53 cm	17X-3,71-73 cm	17X-3, 90-92 cm	17X-3, 110-112 cm	17X-3, 129-131 cm	17X-3, 148-150 cm	17X-4, 19-21 cm	17X-4, 38-40 cm	17X-4, 58-60 cm	17X-4, 76-78 cm	Average
Depth (mbsf)	135.47	135.63	135.73	135.95	136.08	136.2	136.265	136.33	136.4	136.59	136.79	136.98	137.18	137.37	137.57	137.77	137.98	138.17	138.35	138.54	138.74	138.96	139.1	139.31	139.5	139.71	139.91	140.1	140.3	140.49	140.68	140.89	141.08	141.28	141.46	
Subbotina gortanii	1	1	2.7	0.7	1	0.6	1	2	0.3	1.3	1.3	0.3	0.3	1.6	0.7	0.3	1	0.7	0.7	1.3	0.9	0.6	1	1	0.3	0.3	0.3	0	1	0.3	1.6	1.2	1.3	1.3	0	0.9
Subbotina hagni	5.3	3	5	4	7.7	6.7	3.2	1	9	6.7	1.7	2	5.3	2.6	4	2.6	2.6	2	4.3	4.1	5.4	4.1	5.6	1	2.9	1	1.6	7.1	7	5.6	5.3	12	7.3	6.8	3.3	4.5
Subbotina yeguaensis	5.3	2.7	2.7	2.3	1	7	2.3	3.6	1	4	5	8.5	2.7	4.9	3.7	1.6	5.6	3	3	5.7	5.4	3.8	4.7	3	5.8	6.9	6.5	5.1	2.2	3.6	1.9	2.4	1.9	4.9	5	4
Subbotina projecta	0	2	1.3	0	0.3	0.3	0	0	0	0	0	0	0	0	0.3	0	0.3	1.3	2	2.5	0.3	1.9	2.3	1.7	3.2	1.3	2.3	3.8	0.3	0.3	1.3	0.9	0.3	1.3	0.7	0.9
Paragloborotalia nana	1.3	1.7	0	1.3	1	4.5	3.9	4.3	4.3	3.3	0.7	0.7	0.3	2.3	1.3	1.6	1	0.3	0.3	1.3	1.3	0.6	2	0.7	1.9	0.7	0.6	0.6	1.3	2.3	1.6	0.3	0	1	0.3	1.4
Paragloborotalia griffinoides	3.6	2	3	4	2.3	2.6	4.9	4.6	5.3	4.3	0.7	2	2	3.6	1	1.6	2.3	3	2.3	2.5	7.3	1.6	4	1.7	1.9	5.2	1	8.7	6.4	9.3	6	5.6	1.9	3.2	1.3	3.5
Turborotalita praequinqueloba	0.3	1	2	0	1	1.6	1.9	4	1.3	2.3	0.7	1	2	0.7	2.3	1.3	1	0	0	1.6	1.3	1.3	1	0.7	0	0.7	0	0	1.9	0.3	0.6	0.3	0	1.9	1	1.1
Streptochilus martini	0	0	0	0	0	0	0	1.3	0.3	0.3	0.3	0	0.3	0	0	0	0	0	0	0	0	0	0	0	0	0	0	1.6	0	0	0	0	0	0	0	0.1
Chiloguembelina cubensis	0	0	0	0	0	0	0.3	0.3	0.3	0	1	0	0	0.3	0	0	0	0	0	0	0	0	0	0	0	0	0	0	0	0	0	0	0	0	0	0	0.1
Chiloguembelina ototara	0.7	0	0	0	0	0.3	0.6	1.3	1.3	2.7	3.3	1	2.7	1	1.3	1.3	1	0.3	3	0.9	0	4.5	2	3.3	0.6	2.3	0	1.3	1.9	2.6	0.9	0.3	0.3	2.3	10	1.6
Tenuitella gemma	0	0	0	0	0	0	0	1.3	0	2	0.3	0	0	1.3	0.3	2	0	0	0	0	0	0	0.3	1.7	0.6	1.6	0.3	0.3	1	1.3	0.6	0	0	0	0	0.4
Tenuitella praegemma	0	0	0	0	0	1.3	0.6	1.3	3.3	1	1.7	0	1.7	1.3	1.7	6.9	3.9	0	0.3	0.3	0.6	1.9	2	4.6	5.5	1.3	0.3	1.9	0.3	1.3	0	0	0	0	1.7	1.3
Tenuitella patefacta	0	0.3	0	0	0	1	0.3	1	1.7	3.3	0	1.3	1.7	2.3	2.3	3.9	2.3	0.3	2.3	0.3	0	3.8	4.7	12	3.2	3	0	0.6	2.2	5.6	1.9	0.9	2.5	0.6	1	1.9
Dipsidripella danvillensis	0	0	0	0	0	0	0	0	0	0	0	0	0	0	0.3	0	1	0	0	0	0	0	0	0	0.3	0	0	0.3	0	0.7	0.3	0.6	0	0	0	0.1
Acarinina collactea	2.6	1.3	0	0	3	0	0	0	0	0	0.3	0.7	0	0	1.3	0.3	0	0.7	0.3	1.3	0.3	0	0.3	0.7	0.3	0.7	0	0	0.6	1.3	1.3	1.8	1.3	0.3	0	0.6
TOTAL	100	100	100	100	100	100	100	100	100	100	100	100	100	100	100	100	100	100	100	100	100	100	100	100	100	100	100	100	100	100	100	100	100	100	100	

Table IV d3. Planktic foraminifera assemblage: Absolute abundances (N g^{-1}).

Sample ID (612-…)	16X-6, 127-129 cm	16X-6, 143-145 cm	16X-7, 3-5 cm	16X-7, 25-27 cm	16X-CC, 10-12 cm	17X-1, 0-2 cm	17X-1, 6.5-8.5 cm	17X-1, 13-15 cm	17X-1, 20-22 cm	17X-1, 39-41 cm	17X-1, 59-61 cm	17X-1, 78-80 cm	17X-1, 98-100 cm	17X-1, 117-119 cm	17X-1, 137-139 cm	17X-2, 7-9 cm	17X-2, 28-30 cm	17X-2, 47-49 cm	17X-2, 65-67 cm	17X-2, 84-86 cm	17X-2, 104-106 cm	17X-2, 126-128 cm	17X-2, 140-142 cm	17X-3, 11-13 cm	17X-3, 30-32 cm	17X-3, 51-53 cm	17X-3,71-73 cm	17X-3, 90-92 cm	17X-3, 110-112 cm	17X-3, 129-131 cm	17X-3, 148-150 cm	17X-4, 19-21 cm	17X-4, 38-40 cm	17X-4, 58-60 cm	17X-4, 76-78 cm
Depth (mbsf)	135.47	135.63	135.73	135.95	136.08	136.2	136.27	136.33	136.4	136.59	136.79	136.98	137.18	137.37	137.57	137.77	137.98	138.17	138.35	138.54	138.74	138.96	139.1	139.31	139.5	139.71	139.91	140.1	140.3	140.49	140.68	140.89	141.08	141.28	141.46
Cribrohantkenina inflata	0	0	0	0	0	0	0	0	0	0	0	0	0	0	0	0	0	0	0	0	0	0	0	0	0	0	0	4.5	3.4	0	0	0	0	0	0
Hantkenina alabamensis	0	0	0	0	5.2	0	4	0	0	3.8	2.1	2	5.7	0	20	4.4	61	12	4.3	0	0	0	3.3	1	4.3	0	6.1	40	0	0	0	3.5	0	13	6.8
Hantkenina compressa	0	0	0	0	2.3	0	0	0	0	3.8	2.1	0	0	11	0	4.4	0	0	0	0	0	0	0	1	0	0	0	8.9	0	0	0	0	0	0	0
Hantkenina nanggulanensis	0	0	0	0	0	0	0	0	0	0	0	0	0	0	0	0	10	0	1.4	0	0	0	0	0	0	3.3	3	0	0	0	0	0	3	13	0
Hantkenina primitiva	0	0	0	0	0	0	0	0	5.7	0	2.1	0	0	5.7	0	0	0	0	0	0	0	0	3.3	3.1	4.3	0	3	4.5	0	0	0	0	0	0	6.8
Pseudohastigerina micra	0	0	0	0	0	30	12	11	28	3.8	15	4	29	34	46	11	31	0	1.4	33	8.3	2.7	3.3	5.1	21	10	6.1	36	3.4	14	3	10	3	0	136
Pseudohastigerina naguewichiensis	0	0	0	0	0	5.9	0	1.2	5.7	3.8	2.1	0	0	0	0	2.2	15	0	1.4	0	0	5.4	3.3	0	0	0	0	0	0	0	0	0	0	0	0
Turborotalia cocoaensis	0	0	0	0	3.5	12	0	0	0	3.8	4.3	2	11	17	0	2.2	5.1	2.4	0	0	0	0	0	0	0	0	6.1	4.5	14	11	6	7	0	32	0
Turborotalia cunialensis	0	0	0	0	0	12	7.9	1.2	0	7.6	4.3	5.9	17	17	0	6.5	15	0	0	3.3	0	0	0	0	0	0	3	22	31	18	4.5	24	3	13	6.8
Turborotalia cerroazulensis	0	0	0	0	0.6	0	4	0	11	7.6	4.3	0	23	69	40	8.7	10	2.4	0	0	0	0	0	0	8.6	0	9.1	18	44	57	11	24	15	69	6.8
Turborotalia increbescens	109	21	147	105	30	184	206	18	244	106	89	40	201	190	152	33	224	95	61	127	64	101	124	23	201	126	174	147	79	85	47	97	78	208	312
Turborotalia ampliapertura	0	1.4	28	4.3	2.3	83	91	7.1	136	49	21	22	63	40	79	26	66	15	25	40	23	16	17	4.1	4.3	17	27	45	14	18	3	3.5	12	63	0
Catapsydrax unicavus	0	0	0	0	0	5.9	0	0.6	0	3.8	2.1	2	0	0	0	0	0	4.9	0	0	0	0	0	0	13	0	0	0	0	0	0	0	0	0	0
Catapsydrax dissimilis	33	5.4	31	14	6.4	101	47	3.5	34	30	30	28	98	69	86	28	46	39	19	23	17	57	47	8.2	30	30	46	54	75	57	21	35	93	107	47
Dentoglobigerina galavisi	90	8.1	86	16	19	59	95	3.5	74	46	21	42	109	155	86	24	56	68	23	107	45	54	64	38	90	103	61	54	82	57	53	90	75	170	230
Dentoglobigerina tripartita	22	5.4	25	5.7	11	95	40	4.1	40	64	17	30	34	149	106	70	41	37	5.8	37	12	14	17	2	4.3	40	18	8.9	31	11	6	10	30	32	6.8
Dentoglobigerina pseudovenezuelana	27	3.6	9.2	2.8	4.1	24	4	0	74	34	13	16	63	75	73	20	25	44	32	57	21	52	54	20	73	37	30	49	27	42	27	59	84	126	75
Dentoglobigerina venezuelana	14	1.8	49	41	4.1	24	40	1.2	40	3.8	28	18	5.7	0	99	17	71	27	7.2	57	18	49	0	7.2	13	30	52	31	10	18	24	59	51	82	41
Globigerina officinalis	19	1.4	0	4.3	0.6	12	20	8.3	5.7	11	13	7.9	5.7	11	0	4.4	0	0	1.4	6.7	0	0	27	4.1	26	13	3	18	34	14	6	14	6	25	27
Ciperoella angulioffícinalis	14	0.9	0	1.4	0.6	18	7.9	0.6	5.7	0	4.3	0	0	0	0	0	0	0	0	0	0	2.7	0	0	0	3.3	6.1	8.9	6.8	0	1.5	3.5	3	0	0
Globoturborotalita ouachitaensis	101	12	55	26	9.3	196	55	14	119	110	47	38	115	126	99	87	46	24	25	67	26	44	27	9.2	77	13	46	36	72	28	17	56	21	57	54
Globoturborotalita martini	22	2.7	15	4.3	1.7	42	7.9	3.5	17	11	23	7.9	23	0	6.6	17	15	9.8	7.2	33	9.9	0	10	0	8.6	23	6.1	27	3.4	0	7.5	7	0	38	0
Globorotaloides eovariabilis	11	1.8	0	0	3.5	18	16	2.4	17	11	4.3	14	29	11	20	8.7	10	15	0	3.3	1.7	0	10	3.1	8.6	20	3	22	31	3.5	4.5	7	3	0	0
Globorotaloides quadrocameratus	14	0	3.1	0	0	48	0	11	11	19	4.3	2	17	0	20	11	0	4.9	0	10	5	0	6.7	4.1	4.3	3.3	3	8.9	24	14	6	7	0	0	0
Subbotina angiporoides	22	5.9	18	5.7	4.1	65	59	10	45	19	38	36	86	57	99	11	36	15	17	13	23	8.2	37	5.1	34	13	18	22	21	7.1	3	38	42	13	20
Subbotina linaperta	35	9.9	34	27	3.5	101	83	11	102	83	47	51	92	46	211	26	71	63	25	60	41	35	104	19	111	90	27	49	38	46	18	73	39	107	142
Subbotina eocaena	81	19	141	70	21	137	135	15	136	57	68	65	224	92	211	50	163	93	39	94	61	106	110	31	150	100	107	120	72	85	45	104	69	145	230
Subbotina corpulenta	46	14	126	47	12	107	55	5.3	74	87	30	67	149	195	119	33	188	88	59	57	28	101	40	23	77	86	152	116	75	113	54	143	162	170	183
Subbotina gortanii	8.1	1.4	25	2.8	1.7	12	12	3.5	5.7	15	8.5	2	5.7	29	13	2.2	15	4.9	2.9	13	5	5.4	10	3.1	4.3	3.3	3	0	10	3.5	7.5	14	12	25	0
Subbotina hagni	43	4.1	46	17	13	125	40	1.8	153	76	11	12	92	46	79	17	41	15	19	43	28	35	57	3.1	39	10	15	98	75	60	26	136	69	132	68
Subbotina yeguaensis	43	3.6	25	9.9	1.7	131	28	6.5	17	46	32	51	46	86	73	11	86	22	13	60	28	33	47	9.2	77	70	61	71	24	39	9	28	18	95	102
Subbotina projecta	0	2.7	12	0	0.6	5.9	0	0	0	0	0	0	0	0	6.6	0	5.1	9.8	8.6	27	1.7	16	23	5.1	43	13	21	54	3.4	3.5	6	10	3	25	14
Paragloborotalia nana	11	2.3	0	5.7	1.7	83	47	7.7	74	38	4.3	4	5.7	40	26	11	15	2.4	1.4	13	6.6	5.4	20	2	26	6.6	6.1	8.9	14	25	7.5	3.5	0	19	6.8

Sample ID (612-…)	16X-6, 127-129 cm	16X-6, 143-145 cm	16X-7, 3-5 cm	16X-7, 25-27 cm	16X-CC, 10-12 cm	17X-1, 0-2 cm	17X-1, 6.5-8.5 cm	17X-1, 13-15 cm	17X-1, 20-22 cm	17X-1, 39-41 cm	17X-1, 59-61 cm	17X-1, 78-80 cm	17X-1, 98-100 cm	17X-1, 117-119 cm	17X-1, 137-139 cm	17X-2, 7-9 cm	17X-2, 28-30 cm	17X-2, 47-49 cm	17X-2, 65-67 cm	17X-2, 84-86 cm	17X-2, 104-106 cm	17X-2, 126-128 cm	17X-2, 140-142 cm	17X-3, 11-13 cm	17X-3, 30-32 cm	17X-3, 51-53 cm	17X-3,71-73 cm	17X-3, 90-92 cm	17X-3, 110-112 cm	17X-3, 129-131 cm	17X-3, 148-150 cm	17X-4, 19-21 cm	17X-4, 38-40 cm	17X-4, 58-60 cm	17X-4, 76-78 cm
Depth (mbsf)	135.47	135.63	135.73	135.95	136.08	136.2	136.27	136.33	136.4	136.59	136.79	136.98	137.18	137.37	137.57	137.77	137.98	138.17	138.35	138.54	138.74	138.96	139.1	139.31	139.5	139.71	139.91	140.1	140.3	140.49	140.68	140.89	141.08	141.28	141.46
Paragloborotalia griffinoides	30	2.7	28	17	4.1	48	59	8.3	91	49	4.3	12	34	63	20	11	36	22	10	27	38	14	40	5.1	26	53	9.1	120	68	99	29	66	18	63	27
Turborotalita praequinqueloba	2.7	1.4	18	0	1.7	30	24	7.1	23	27	4.3	5.9	34	11	46	8.7	15	0	0	17	6.6	11	10	2	0	6.6	0	0	21	3.5	3	3.5	0	38	20
Streptochilus martini	0	0	0	0	0	0	0	2.4	5.7	3.8	2.1	0	5.7	0	0	0	0	0	0	0	0	0	0	0	0	0	0	22	0	0	0	0	0	0	0
Chiloguembelina cubensis	0	0	0	0	0	0	4	0.6	5.7	0	6.4	0	0	5.7	0	0	0	0	0	0	0	0	0	0	0	0	0	0	0	0	0	0	0	0	0
Chiloguembelina ototara	5.4	0	0	0	0	5.9	7.9	2.4	23	30	21	5.9	46	17	26	8.7	15	2.4	13	10	0	38	20	10	8.6	23	0	18	21	28	4.5	3.5	3	44	210
Tenuitella gemma	0	0	0	0	0	0	0	2.4	0	23	2.1	0	0	23	6.6	13	0	0	0	0	0	0	3.3	5.1	8.6	17	3	4.5	10	14	3	0	0	0	0
Tenuitella praegemma	0	0	0	0	0	24	7.9	2.4	57	11	11	0	29	23	33	46	61	0	1.4	3.3	3.3	16	20	14	73	13	3	27	3.4	14	0	0	0	0	34
Tenuitella patefacta	0	0.5	0	0	0	18	4	1.8	28	38	0	7.9	29	40	46	26	36	2.4	10	3.3	0	33	47	37	43	30	0	8.9	24	60	9	10	24	13	20
Dipsidripella danvillensis	0	0	0	0	0	0	0	0	0	0	0	0	0	0	6.6	0	15	0	0	0	0	0	0	0	4.3	0	0	4.5	0	7.1	1.5	7	0	0	0
Acarinina collactea	22	1.8	0	0	5.2	0	0	0	0	0	2.1	4	0	0	26	2.2	0	4.9	1.4	13	1.7	0	3.3	2	4.3	6.6	0	0	6.8	14	6	21	12	6.3	0
# specimens in fraction	189	244	442	523	120	112	350	46	484	78	488	158	243	235	306	172	224	430	255	288	304	158	248	190	382	159	133	207	149	302	126	350	553	519	265
Fractionation	32	4	16	8	16	128	32	32	32	128	8	32	64	64	64	32	64	16	16	32	16	64	32	16	32	64	64	64	64	32	32	32	16	32	64
Initial weigh (g)	7.3	7.2	7.7	9.8	11.0	7.7	9.2	8.2	9.1	8.8	6.1	8.4	9.0	8.6	9.9	8.3	9.3	9.2	9.4	8.7	9.3	11.8	7.9	9.8	9.3	10.1	9.1	9.5	8.9	9.1	8.4	9.5	9.3	8.6	8.3
Absolute abundance (#specimens*Fractionation/Initial weigh)	823	136	919	426	174	1861	1223	179	1710	1138	645	604	1728	1758	1979	663	1546	744	434	1060	524	854	1007	309	1320	1012	938	1391	1071	1067	480	1179	950	1940	2034

Table IV e1. Benthic foraminifera assemblage: census. In blue, epifaunal taxa; agglutinated taxa marked with (*).

Depth (mbsf)	135.47	135.63	135.73	135.95	136.08	136.2	136.265	136.33	136.4	136.59	136.79	136.98	137.18	137.37	137.57	137.77	137.98	138.17	138.35	138.54	138.74	138.96	139.1	139.31	139.5	139.71	139.91	140.1	140.3	140.49	140.68	140.89	141.08	141.28	141.46
Alabamina cf. *A. dissonata*	17	15	34	7	13	4	3	2	1	5	14	8	15	14	9	4	7	28	10	10	7	12	14	18	15	15	7	16	4	13	22	16	44	0	0
Ammobaculites sp.*	0	0	0	0	0	0	0	0	0	0	0	0	0	0	0	0	0	0	0	0	0	0	0	0	0	1	0	0	0	0	1	0	0	0	0
Anomalinoides alazanensis	0	0	0	0	0	0	0	0	0	0	0	0	1	0	1	0	0	2	1	0	0	2	0	0	0	0	0	2	0	0	0	0	0	0	0
Anomalinoides spissiformis	0	0	0	1	0	0	0	0	0	0	0	0	0	0	0	1	0	0	0	0	0	0	0	0	0	0	0	0	0	0	0	0	4	2	5
Anomalinoides sp.	0	0	0	0	0	0	0	0	0	0	0	0	0	0	0	0	0	0	0	0	0	0	0	0	0	0	0	0	0	0	0	1	0	0	1
Aragonia aragonensis	0	0	0	0	0	0	0	0	0	0	0	0	1	1	1	0	1	4	2	2	1	4	0	0	0	0	0	0	0	0	0	0	2	0	0
Arenobulimina sp.*	0	0	0	0	0	0	0	0	0	0	1	1	0	0	0	0	1	0	1	0	1	0	0	0	0	0	0	0	0	0	0	0	0	0	0
Bigerina sp.	0	0	0	0	0	0	0	0	0	0	0	0	0	0	0	0	1	0	0	0	1	0	0	0	2	0	0	0	0	0	0	0	0	0	0
Bolivina antiqua	0	0	0	0	0	0	0	0	0	0	9	1	3	4	0	0	0	0	1	0	0	0	0	0	1	0	0	0	0	0	1	2	0	0	9
Bolivina spp.	2	1	3	2	1	2	12	0	0	2	0	0	5	8	5	11	16	10	4	9	3	14	38	1	18	15	16	16	16	10	1	16	4	6	2
Bolivinoides crenulatus	1	0	0	0	0	25	29	33	29	39	0	1	0	0	0	0	0	0	0	0	0	1	0	0	0	0	1	0	0	31	0	0	0	0	0
Brizalina carinata	0	0	0	0	0	13	7	8	17	27	5	0	0	0	2	6	2	0	3	4	6	7	14	0	7	6	9	21	43	132	4	7	3	6	1
Brizalina tectiformis	36	11	8	15	48	14	24	21	19	12	50	60	49	63	97	62	113	220	63	62	69	108	62	40	48	85	55	58	37	34	44	52	40	32	58
Bulimina alazanensis	6	1	6	7	16	18	8	5	2	21	54	78	34	27	62	24	33	93	47	39	39	12	5	8	11	15	29	23	12	18	24	27	25	25	21
Bulimina mexicana	7	13	4	1	9	3	4	4	3	7	10	13	5	2	2	4	1	7	1	3	10	10	5	12	2	2	3	2	2	3	3	4	0	0	0
Bulimina semicostata	0	0	0	0	0	0	0	0	0	0	0	0	0	0	0	0	0	0	0	0	0	0	0	0	0	0	0	0	0	0	0	0	0	0	2
Bulimina trinidaensis	1	1	0	2	4	0	0	0	0	0	0	3	0	0	0	2	0	2	1	0	0	1	0	0	2	3	0	0	0	1	0	1	0	1	3
Bulimina tuxpamensis	0	0	0	0	2	0	0	1	0	1	3	6	6	3	27	8	8	9	10	8	12	7	5	18	4	10	3	10	6	5	8	5	0	0	1
Cancris sp.	0	0	0	0	0	0	0	0	0	0	0	1	0	0	0	0	0	0	0	0	0	0	0	0	0	0	1	1	1	0	0	0	0	0	0
Cassidulina havanensis	0	0	0	0	0	0	0	0	0	0	0	0	0	1	0	0	0	0	0	0	1	0	0	0	0	1	0	0	0	0	0	0	0	0	0
Cibicidoides sp.	0	1	0	0	0	0	0	0	0	0	0	0	0	0	0	0	0	0	0	0	0	0	0	0	0	0	0	0	0	0	0	1	1	0	0
Cibicidoides hadjibulakensis	1	5	6	5	3	1	6	4	1	1	0	5	2	5	2	10	12	2	6	0	0	2	1	1	0	0	0	0	1	0	0	0	0	0	0
Cibicidoides laurisae	0	0	0	0	0	0	0	0	0	0	0	0	0	0	0	0	0	0	0	0	0	0	0	0	0	0	0	0	0	0	0	0	2	0	0
Cibicidoides mundulus	0	0	1	1	4	2	0	0	1	0	5	4	3	5	10	6	2	8	5	6	1	1	0	5	4	8	2	4	1	0	3	4	2	2	1
Cibicidoides tuxpamensis	0	0	0	0	0	0	0	0	0	0	0	0	0	0	0	0	0	0	1	0	6	1	0	0	0	0	0	0	0	0	0	0	1	0	1
Chrysalogonium spp.	0	7	1	3	2	3	10	5	20	9	2	1	0	7	6	2	2	3	1	3	0	1	0	2	1	0	4	0	2	0	3	0	0	1	2
Clavulinoides angularis *	0	0	0	0	0	0	0	0	0	0	2	3	2	1	0	0	1	1	0	0	0	2	0	2	2	1	3	1	2	0	1	0	0	0	0
Dentalina spp.	3	7	0	5	3	2	4	3	0	1	4	2	2	1	4	4	3	5	1	3	5	4	1	0	2	5	2	4	2	0	4	1	1	2	2
Dorothia brevis *	0	0	0	0	1	0	0	0	0	0	0	1	0	0	0	0	0	0	1	0	2	0	0	0	0	1	0	0	0	0	0	0	0	0	0
Eggerella sp. *	0	0	0	0	0	1	0	0	0	0	0	0	0	0	0	0	0	0	0	0	0	0	0	0	0	0	0	0	0	0	1	0	0	0	0
Ellipsoidella sp.	0	0	0	0	0	0	0	0	0	0	0	0	0	0	0	0	0	0	0	0	0	0	0	0	0	0	0	0	0	0	2	0	0	0	0
Epistominella exigua	0	0	0	0	0	0	0	0	0	0	1	0	0	0	0	0	0	0	0	0	0	0	0	0	0	0	0	0	0	0	0	0	0	0	0
Eponides cf. *E. abatissae*	0	7	3	0	2	1	0	0	0	0	0	1	0	0	0	0	0	0	0	0	0	0	0	1	0	0	0	0	0	0	0	0	0	0	0
Fissurina spp.	0	0	2	0	0	2	0	0	0	0	0	0	1	0	0	0	1	3	3	4	1	0	0	2	1	0	1	3	2	1	2	1	1	1	3
Fursenkoina dibollensis	0	0	0	0	0	0	0	0	0	0	0	0	0	0	0	0	0	1	0	3	1	0	1	2	1	0	2	0	0	1	1	3	2	2	1
Gaudyna cf. *G. concinna* *	0	0	0	0	0	0	0	0	0	0	0	0	0	0	0	0	0	0	0	0	0	0	0	0	0	2	0	0	0	0	0	0	0	0	0
Gaudryna arenata *	1	0	1	0	0	0	0	0	0	0	0	0	0	0	0	0	0	0	0	0	0	0	0	0	2	0	0	0	0	0	0	0	0	0	0
Glandulina spp.	0	0	0	0	0	1	0	0	0	0	0	0	0	0	0	0	0	0	0	0	0	0	0	0	0	1	1	0	0	0	4	1	0	0	0
Glandulonodosaria ambigua	0	0	0	0	0	0	0	0	0	0	0	0	0	0	0	0	0	0	0	0	1	0	2	0	0	0	0	0	0	0	0	0	0	1	0
Glandulonodosaria trincherasensis	0	0	1	0	0	2	0	1	0	0	0	0	0	0	0	0	0	0	0	0	0	0	0	0	0	0	0	0	0	0	0	0	0	0	0
Glandulonodosaria sp.	0	0	0	0	0	0	0	0	0	0	0	0	0	0	0	0	0	0	0	0	0	0	0	0	0	0	0	0	0	0	1	0	0	0	0
Globocassidulina subglobosa	1	0	0	0	0	0	0	0	0	0	1	1	1	0	0	2	0	0	3	1	0	1	0	0	0	1	0	0	0	0	0	0	2	0	0

Depth (mbsf)	135.47	135.63	135.73	135.95	136.08	136.2	136.265	136.33	136.4	136.59	136.79	136.98	137.18	137.37	137.57	137.77	137.98	138.17	138.35	138.54	138.74	138.96	139.1	139.31	139.5	139.71	139.91	140.1	140.3	140.49	140.68	140.89	141.08	141.28	141.46
Globobulimina cf. *G. ovata*	0	2	0	0	1	0	0	0	1	0	1	1	1	0	0	1	0	0	0	0	1	0	0	0	1	2	0	4	2	2	0	1	0	1	0
Guttulina spp.	0	8	1	0	5	1	1	0	0	2	2	3	0	0	0	1	1	3	3	1	0	1	1	5	5	5	4	3	3	2	4	2	2	2	3
Gyroidinoides acutus	1	0	0	0	0	0	0	0	0	0	1	0	0	0	0	0	0	0	0	1	0	0	1	0	0	0	0	0	0	0	0	0	1	0	
Gyroidinoides girardanus	5	9	6	10	8	3	2	2	4	4	5	3	1	2	6	0	3	4	1	5	6	3	1	6	2	5	1	6	2	1	1	9	2	2	0
Gyroidinoides cf. *G. laevigatus*	0	0	2	0	0	0	0	0	0	0	0	0	0	0	0	4	0	0	2	2	0	0	0	2	0	2	0	0	1	0	2	0	0	0	2
Hanzawaia ammophila	0	0	0	0	0	0	0	0	0	0	1	1	0	1	2	0	0	0	2	0	0	0	0	0	0	0	0	0	0	0	1	0	0	0	0
Heterolepa grimsdalei	0	1	3	4	1	1	0	0	0	0	1	3	0	0	0	0	1	1	9	0	0	0	0	0	0	4	0	0	0	0	0	0	0	1	0
Heterolepa mexicana	5	3	0	0	0	0	0	0	0	2	2	2	0	0	1	1	0	0	0	0	0	0	1	0	0	0	0	0	0	0	0	0	1	0	0
Karrenulina coniformis *	0	0	0	0	0	0	0	0	0	0	0	0	0	0	0	0	0	0	0	0	0	0	0	0	0	0	0	0	0	0	0	0	0	0	1
Karreriella chapapotensis *	0	0	0	0	0	0	0	0	0	0	0	1	0	0	0	0	0	0	0	0	0	0	0	0	0	0	0	0	0	0	0	0	0	0	1
Karreriella bradyi *	0	0	0	2	1	1	0	0	0	0	0	1	0	0	0	0	0	0	0	1	0	0	0	0	0	0	0	0	0	0	0	0	0	0	0
Karreriella subglabra *	0	0	0	0	0	0	0	0	0	0	0	0	0	0	0	0	0	0	0	0	0	0	0	0	0	0	0	0	0	0	0	0	0	0	1
Lagena asperoides	0	0	0	0	0	0	0	0	0	0	0	0	0	0	0	0	0	0	0	0	0	0	0	0	0	0	0	0	0	0	1	0	0	0	
Lenticulina spp.	0	3	0	1	0	0	0	0	0	0	0	3	0	0	0	0	0	1	0	0	0	0	0	0	0	0	0	0	1	0	1	0	0	1	0
Lenticulina cultrata	0	0	0	0	0	0	0	0	0	0	0	0	0	0	2	0	0	0	0	0	0	3	0	0	1	3	0	0	0	1	0	0	0	0	0
Lenticulina peregrina	0	0	0	0	0	0	0	0	0	0	0	0	0	0	0	0	0	0	0	0	0	0	0	0	0	0	0	0	0	0	0	0	0	0	1
Lenticulina rotulata	1	0	2	0	0	1	0	0	1	4	4	0	2	2	4	0	0	0	5	0	3	2	1	5	2	5	3	4	0	0	0	2	0	0	0
Lenticulina turbinata	0	0	0	0	0	0	0	0	0	0	0	0	0	0	0	0	0	0	0	0	0	0	0	0	1	0	0	0	0	0	0	0	0	0	0
Lenticulina velascoensis	0	0	0	0	2	0	0	0	1	0	0	0	0	0	0	0	0	0	1	0	0	0	0	0	0	0	0	0	0	1	0	0	1	0	0
Marginulina sp.	1	0	0	0	0	1	0	0	0	0	0	0	0	0	0	0	0	0	0	2	1	0	0	0	0	0	0	0	0	0	1	0	0	0	0
Marginulinopsis sp.	0	0	0	0	0	0	0	0	0	0	0	0	0	0	0	0	0	0	0	0	0	0	0	0	0	0	0	0	0	0	0	0	0	0	1
Marssonella floridana	0	0	0	0	1	0	0	0	0	0	0	0	0	0	0	0	0	2	0	0	0	1	0	0	0	0	0	0	0	0	0	0	1	0	0
Martinottiella sp. *	0	0	0	0	0	0	0	0	0	0	0	0	0	0	0	0	0	0	0	0	0	0	0	0	0	0	1	1	0	0	0	0	0	0	0
Melonis sp.	0	2	0	0	0	0	0	0	0	0	0	0	0	0	0	0	0	0	0	0	0	0	0	0	0	0	0	0	0	0	0	0	0	0	0
Melonis affinis	7	5	5	8	9	4	1	0	1	3	9	11	8	2	8	5	4	12	3	5	6	5	5	5	11	13	17	4	7	2	10	8	13	8	13
Melonis havanensis	1	0	0	2	5	0	0	0	0	0	0	1	0	0	0	0	2	0	2	0	0	0	0	1	0	0	0	0	0	0	0	0	0	0	0
Mucronina spp.	2	19	2	1	0	5	1	2	2	8	0	0	0	0	0	0	0	0	0	1	0	1	0	0	1	1	0	0	0	0	1	0	0	0	0
Neugeborina longiscata	7	22	6	10	4	1	1	2	5	3	1	5	1	3	3	4	1	4	3	1	2	0	3	3	3	6	5	2	2	3	5	2	4	4	4
Nodosariella robusta	0	0	0	1	0	1	1	0	1	0	0	0	0	0	0	0	0	0	0	0	1	2	0	0	0	1	0	0	0	1	0	0	1	0	0
Nuttallides cf. *umbonifera*	0	0	0	0	0	0	0	0	0	0	0	0	0	0	0	0	0	0	0	0	0	0	0	0	0	0	0	0	0	0	0	0	2	2	0
Obesopleurostomella sp.	3	0	0	1	1	1	0	0	0	0	1	1	2	0	0	0	4	2	5	3	1	2	1	0	1	1	5	0	0	0	0	0	2	0	0
Oridorsalis umbonatus	13	2	4	2	20	0	1	0	1	3	6	6	1	3	10	7	6	3	2	3	0	5	1	4	3	7	2	3	3	2	7	6	5	3	1
Orthomorfina cf. *jedlitschkai*	2	1	0	0	6	39	135	97	60	0	0	1	0	0	1	0	0	0	0	0	0	0	0	0	0	0	0	0	0	0	0	0	0	0	0
Osangularia cf. *plummerae*	16	34	15	27	20	0	2	0	0	1	1	5	0	0	2	2	2	7	2	1	5	3	5	5	5	4	5	3	2	2	7	1	1	1	0
Planulina marialana	0	0	0	0	0	0	0	0	0	0	0	0	0	0	2	0	0	0	0	0	0	0	0	0	0	0	0	0	0	0	0	0	0	0	0
Planulina renzi	0	0	0	0	1	1	1	0	0	1	0	3	0	4	2	1	2	7	7	2	2	0	0	0	0	2	0	1	0	0	0	1	2	0	1
Pleurostomella parviapertura	0	1	1	0	2	0	1	0	1	0	0	1	0	0	0	0	0	0	5	0	0	0	0	0	0	0	1	3	0	0	0	0	1	0	0
Pleurostomella brevis	0	0	0	0	0	0	0	0	0	0	0	0	0	1	0	1	0	3	0	0	0	0	0	1	0	0	0	0	0	3	0	0	0	0	0
Pleurostomella obtusa	3	0	0	5	16	1	4	1	0	0	2	4	0	4	3	3	2	6	3	3	5	4	5	1	4	5	2	6	3	4	2	2	2	4	3
Pleurostomella spp.	0	0	0	0	0	0	0	0	0	0	0	0	0	0	0	0	0	0	0	0	0	0	0	0	0	0	0	0	3	1	0	2	3	0	3
Pseudoclavulina trinidaensis	2	0	0	0	0	2	0	0	0	0	1	1	1	0	0	0	0	0	0	0	0	2	0	0	0	0	0	0	0	0	0	0	0	1	0
Pullenia bulloides	12	14	9	2	9	1	1	2	0	4	3	8	8	4	6	7	7	8	7	4	5	6	0	12	7	3	4	8	4	3	13	3	7	5	1
Pullenia quinqueloba	4	4	3	4	2	2	0	0	0	1	2	0	0	1	1	1	1	1	3	2	0	0	1	0	2	3	0	2	0	0	2	0	3	0	2
Quinqueloculina sp.	0	0	1	0	0	0	1	1	0	0	0	1	0	0	0	0	0	1	0	0	1	0	0	0	3	0	0	3	0	0	0	0	0	0	0

Depth (mbsf)	135.47	135.63	135.73	135.95	136.08	136.2	136.265	136.33	136.4	136.59	136.79	136.98	137.18	137.37	137.57	137.77	137.98	138.17	138.35	138.54	138.74	138.96	139.1	139.31	139.5	139.71	139.91	140.1	140.3	140.49	140.68	140.89	141.08	141.28	141.46
Rhabdammina sp. *	0	0	0	0	0	0	0	0	0	0	0	0	0	0	0	0	0	0	0	0	0	0	0	0	0	0	0	1	0	0	1	1	0	0	0
Rosalina sp.	0	0	0	0	0	0	0	0	0	0	0	0	1	0	0	0	0	0	0	0	0	0	0	0	0	0	0	0	0	0	0	0	0	0	0
Sigmoilopsis spp.	0	2	0	0	0	0	0	0	0	0	0	0	0	0	1	0	0	1	3	0	0	0	2	1	1	0	2	0	0	0	0	3	0	1	2
Siphonodosaria annulifera	1	1	0	1	2	1	0	6	1	2	2	0	0	2	2	5	5	2	0	0	2	2	2	0	4	2	4	8	3	2	2	0	0	0	0
Siphonodosaria curvatura	5	15	0	0	0	0	1	0	0	0	0	0	3	2	3	0	2	0	0	3	0	0	1	0	1	0	0	1	0	0	0	0	0	0	0
Siphonodosaria gracillima	0	0	0	0	0	0	0	0	0	0	2	0	0	1	1	2	1	18	5	0	1	0	0	1	1	4	5	12	5	8	5	8	3	4	5
Siphonodosaria jacksonensis	15	48	31	26	21	1	7	8	1	21	9	14	4	5	9	7	9	28	12	21	22	22	8	8	21	22	22	40	21	34	18	12	2	9	17
Siphonodosaria lepidula	4	2	0	3	2	30	25	23	20	9	0	0	0	0	0	1	0	0	1	0	0	0	0	0	1	0	0	6	3	1	9	13	2	2	4
Siphonodosaria pomuligera	0	0	1	0	0	0	0	0	0	0	3	0	0	0	0	0	0	0	1	0	1	0	0	0	1	0	0	0	0	1	0	6	3	0	0
Siphonodosaria subspinosa	1	3	1	1	2	0	0	0	1	0	0	1	0	0	0	0	0	0	0	2	0	0	1	0	1	2	0	4	0	0	4	0	0	0	0
Siphotextularia sp. *	0	0	1	0	0	1	0	0	1	2	29	6	0	3	3	5	10	7	2	0	0	1	0	0	2	4	0	0	0	0	0	0	0	0	0
Spiroplectammina spectabilis *	1	0	0	0	0	0	0	0	0	0	0	0	0	0	0	1	0	0	0	0	3	2	0	0	0	0	0	0	1	1	1	6	12	3	10
Staffia tosta	0	0	1	0	0	0	0	0	0	0	0	0	0	0	0	0	0	0	0	0	0	0	0	0	0	0	0	0	0	0	0	0	0	0	0
Stilostomella rugosa	0	0	0	0	0	0	0	0	0	0	0	0	0	0	0	0	0	0	0	0	0	0	0	0	0	0	0	0	0	0	0	1	0	0	0
Strictocostella fistuca	0	0	0	0	0	0	0	0	0	0	0	0	0	0	0	0	0	0	0	0	0	0	0	0	0	0	0	0	0	1	1	0	0	0	0
Strictocostella japonica	10	14	4	3	5	11	16	23	16	19	1	1	2	3	2	4	0	4	6	6	5	10	9	2	6	14	6	18	6	22	26	31	34	21	77
Strictocostella scharbergana	10	7	3	8	7	48	152	42	76	48	4	1	5	12	0	0	0	0	0	2	4	0	0	0	0	0	0	0	0	0	0	0	0	0	0
Textularia sp. *	0	1	1	0	0	0	0	0	0	0	0	0	0	0	0	0	0	0	0	0	0	1	1	1	0	0	0	1	1	0	0	0	0	3	0
Trifarina wilcoxensis	5	8	1	1	0	39	16	14	20	21	26	34	4	11	9	6	3	4	7	11	8	7	5	22	13	7	5	7	1	2	4	6	1	12	13
Trifarina sp.	0	0	0	1	0	0	0	0	0	0	0	0	1	1	1	0	0	4	0	0	2	0	0	0	0	1	1	0	0	2	0	2	2	3	0
Uvigerina galloway	29	56	22	18	7	0	0	0	0	0	0	0	0	0	0	0	0	0	0	0	0	0	0	0	0	0	0	0	0	0	0	0	0	0	0
Uvigerina hispida	1	0	1	0	0	0	0	0	0	0	0	0	1	0	0	0	0	2	0	2	0	1	0	1	1	1	0	2	0	0	1	0	0	0	1
Uvigerina rippensis	11	4	2	5	4	2	4	5	15	10	28	22	25	21	37	14	4	4	2	1	1	0	0	7	2	2	0	2	1	3	0	5	4	5	7
Vaginulina sp.	0	0	0	0	0	0	0	0	0	0	0	0	0	0	0	0	0	0	0	0	0	0	0	0	1	1	1	1	1	0	0	0	0	0	0
Valvulineria sp.	0	0	0	1	0	0	0	0	0	0	0	0	0	0	0	0	1	0	1	0	0	0	0	0	0	0	1	0	0	0	0	0	0	0	0
Vulvulina spinosa *	0	1	1	0	0	1	0	0	0	0	0	0	0	0	0	0	0	0	1	0	0	0	0	0	0	0	0	0	0	0	0	1	0	0	0
Undetermined specimen	0	0	0	0	0	0	0	0	0	0	0	0	0	0	0	0	0	0	0	0	0	0	0	1	0	0	0	0	0	0	0	0	0	0	0
N° of counted specimens	254	361	200	197	272	294	481	315	322	293	308	335	201	230	349	229	275	537	271	242	255	276	203	205	231	304	236	317	207	354	259	277	250	180	287
Total specimens	1016	361	800	197	1088	1176	3848	2520	5152	2344	1232	1340	1608	1840	2792	1832	2200	2148	1084	484	510	1104	812	410	924	608	944	634	828	1416	518	1108	2000	1440	1148
TOTAL ABUNDANCE	553	201	416	80	394	611	1681	1222	2275	1068	814	640	715	860	1129	883	949	930	461	223	220	373	412	167	399	242	416	266	372	625	246	466	859	673	551

Table IV e2. Benthic foraminifera assemblage: relative abundances (%).

Depth (mbsf)	135.47	135.63	135.73	135.95	136.08	136.2	136.265	136.33	136.4	136.59	136.79	136.98	137.18	137.37	137.57	137.77	137.98	138.17	138.35	138.54	138.74	138.96	139.1	139.31	139.5	139.71	139.91	140.1	140.3	140.49	140.68	140.89	141.08	141.28	141.46
Alabamina cf. *A. dissonata*	7	4	17	4	5	1	1	1	0	2	5	2	7	6	3	2	3	5	4	4	3	4	7	9	6	5	3	5	2	4	8	6	18	0	0
Ammobaculites sp.	0	0	0	0	0	0	0	0	0	0	0	0	0	0	0	0	0	0	0	0	0	0	0	0	0	0	0	0	0	0	0	0	0	0	0
Anomalinoides alazanensis	0	0	0	0	0	0	0	0	0	0	0	0	0	0	0	0	0	0	0	0	0	1	0	0	0	0	0	1	0	0	0	0	0	0	0
Anomalinoides spissiformis	0	0	0	1	0	0	0	0	0	0	0	0	0	0	0	0	0	0	0	0	0	0	0	0	0	0	0	0	0	0	0	0	2	1	2
Anomalinoides sp.	0	0	0	0	0	0	0	0	0	0	0	0	0	0	0	0	0	0	0	0	0	0	0	0	0	0	0	0	0	0	0	0	0	0	0
Aragonia aragonensis	0	0	0	0	0	0	0	0	0	0	0	0	0	0	0	0	0	1	1	1	0	1	0	0	0	0	0	0	0	0	0	0	1	0	0
Arenobulimina sp.	0	0	0	0	0	0	0	0	0	0	0	0	0	0	0	0	0	0	0	0	0	0	0	0	0	0	0	0	0	0	0	0	0	0	0
Bigerina sp.	0	0	0	0	0	0	0	0	0	0	0	0	0	0	0	0	0	0	0	0	0	0	0	0	1	0	0	0	0	0	0	0	0	0	0
Bolivina antiqua	0	0	0	0	0	0	0	0	0	0	3	0	1	2	0	0	0	0	0	0	0	0	0	0	0	0	0	0	0	0	0	1	0	0	3
Bolivina spp.	1	0	2	1	0	1	2	0	0	1	0	0	2	3	1	5	6	2	1	4	1	5	19	0	8	5	7	5	8	3	0	6	2	3	1
Bolivinoides crenulatus	0	0	0	0	0	9	6	10	9	13	0	0	0	0	0	0	0	0	0	0	0	0	0	0	0	0	0	0	0	9	0	0	0	0	0
Brizalina carinata	0	0	0	0	0	4	1	3	5	9	2	0	0	0	1	3	1	0	1	2	2	3	7	0	3	2	4	7	21	37	2	3	1	3	0
Brizalina tectiformis	14	3	4	8	18	5	5	7	6	4	16	18	24	27	28	27	41	41	23	26	27	39	31	20	21	28	23	18	18	10	17	19	16	18	20
Bulimina alazanensis	2	0	3	4	6	6	2	2	1	7	18	23	17	12	18	10	12	17	17	16	15	4	2	4	5	5	12	7	6	5	9	10	10	14	7
Bulimina mexicana	3	4	2	1	3	1	1	1	1	2	3	4	2	1	1	2	0	1	0	1	4	4	2	6	1	1	1	1	1	1	1	1	0	0	0
Bulimina semicostata	0	0	0	0	0	0	0	0	0	0	0	0	0	0	0	0	0	0	0	0	0	0	0	0	0	0	0	0	0	0	0	0	0	0	1
Bulimina trinidaensis	0	0	0	1	1	0	0	0	0	0	0	1	0	0	0	1	0	0	0	0	0	0	0	0	1	1	0	0	0	0	0	0	0	1	1
Bulimina tuxpamensis	0	0	0	0	1	0	0	0	0	0	1	2	3	1	8	3	3	2	4	3	5	3	2	9	2	3	1	3	3	1	3	2	0	0	0
Cancris sp.	0	0	0	0	0	0	0	0	0	0	0	0	0	0	0	0	0	0	0	0	0	0	0	0	0	0	0	0	0	0	0	0	0	0	0
Cassidulina havanensis	0	0	0	0	0	0	0	0	0	0	0	0	0	0	0	0	0	0	0	0	0	0	0	0	0	0	0	0	0	0	0	0	0	0	0
Cibicidoides sp.	0	0	0	0	0	0	0	0	0	0	0	0	0	0	0	0	0	0	0	0	0	0	0	0	0	0	0	0	0	0	0	0	0	0	0
Cibicidoides hadjibulakensis	0	1	3	3	1	0	1	1	0	0	0	1	1	2	1	4	4	0	2	0	0	1	0	0	0	0	0	0	0	0	0	0	0	0	0
Cibicidoides laurisae	0	0	0	0	0	0	0	0	0	0	0	0	0	0	0	0	0	0	0	0	0	0	0	0	0	0	0	0	0	0	0	0	1	0	0
Cibicidoides mundulus	0	0	1	1	1	1	0	0	0	0	2	1	1	2	3	3	1	1	2	2	0	0	0	2	2	3	1	1	0	0	1	1	1	1	0
Cibicidoides tuxpamensis	0	0	0	0	0	0	0	0	0	0	0	0	0	0	0	0	0	0	0	0	2	0	0	0	0	0	0	0	0	0	0	0	0	0	0
Chrysalogonium spp.	0	2	1	2	1	1	2	2	6	3	1	0	0	3	2	1	1	1	0	1	0	0	0	1	0	0	2	0	1	0	1	0	0	1	1
Clavulinoides angularis	0	0	0	0	0	0	0	0	0	0	1	1	1	0	0	0	0	0	0	0	0	1	0	1	1	0	1	0	1	0	0	0	0	0	0
Dentalina spp.	1	2	0	3	1	1	1	1	0	0	1	1	1	0	1	2	1	1	0	1	2	1	0	0	1	2	1	1	1	0	2	0	0	1	1
Dorothia brevis	0	0	0	0	0	0	0	0	0	0	0	0	0	0	0	0	0	0	0	0	1	0	0	0	0	0	0	0	0	0	0	0	0	0	0
Eggerella sp.	0	0	0	0	0	0	0	0	0	0	0	0	0	0	0	0	0	0	0	0	0	0	0	0	0	0	0	0	0	0	0	0	0	0	0
Ellipsoidella sp.	0	0	0	0	0	0	0	0	0	0	0	0	0	0	0	0	0	0	0	0	0	0	0	0	0	0	0	0	0	0	1	0	0	0	0
Epistominella exigua	0	0	0	0	0	0	0	0	0	0	0	0	0	0	0	0	0	0	0	0	0	0	0	0	0	0	0	0	0	0	0	0	0	0	0
Eponides cf. *E. abatissae*	0	2	2	0	1	0	0	0	0	0	0	0	0	0	0	0	0	0	0	0	0	0	0	0	0	0	0	0	0	0	0	0	0	0	0
Fissurina spp.	0	0	1	0	0	1	0	0	0	0	0	0	0	0	0	0	0	1	1	2	0	0	0	1	0	0	0	1	1	0	1	0	0	1	1
Fursenkoina dibollensis	0	0	0	0	0	0	0	0	0	0	0	0	0	0	0	0	0	0	0	1	0	0	0	1	0	0	1	0	0	0	0	1	1	1	0
Gaudyna cf. *G. concinna*	0	0	0	0	0	0	0	0	0	0	0	0	0	0	0	0	0	0	0	0	0	0	0	0	0	1	0	0	0	0	0	0	0	0	0
Gaudryna arenata	0	0	1	0	0	0	0	0	0	0	0	0	0	0	0	0	0	0	0	0	0	0	0	0	1	0	0	0	0	0	0	0	0	0	0
Glandulina spp.	0	0	0	0	0	0	0	0	0	0	0	0	0	0	0	0	0	0	0	0	0	0	0	0	0	0	0	0	0	0	2	0	0	0	0
Glandulonodosaria ambigua	0	0	0	0	0	0	0	0	0	0	0	0	0	0	0	0	0	0	0	0	0	0	1	0	0	0	0	0	0	0	0	0	0	1	0
Glandulonodosaria trincherasensis	0	0	1	0	0	1	0	0	0	0	0	0	0	0	0	0	0	0	0	0	0	0	0	0	0	0	0	0	0	0	0	0	0	0	0
Glandulonodosaria sp.	0	0	0	0	0	0	0	0	0	0	0	0	0	0	0	0	0	0	0	0	0	0	0	0	0	0	0	0	0	0	0	0	0	0	0

Depth (mbsf)	135.47	135.63	135.73	135.95	136.08	136.2	136.265	136.33	136.4	136.59	136.79	136.98	137.18	137.37	137.57	137.77	137.98	138.17	138.35	138.54	138.74	138.96	139.1	139.31	139.5	139.71	139.91	140.1	140.3	140.49	140.68	140.89	141.08	141.28	141.46
Globocassidulina subglobosa	0	0	0	0	0	0	0	0	0	0	0	0	0	0	0	1	0	0	1	0	0	0	0	0	0	0	0	0	0	0	0	0	1	0	0
Globobulimina cf. *G. ovata*	0	1	0	0	0	0	0	0	0	0	0	0	0	0	0	0	0	0	0	0	0	0	0	0	0	1	0	1	1	1	0	0	0	1	0
Guttulina spp.	0	2	1	0	2	0	0	0	0	1	1	1	0	0	0	0	0	1	1	0	0	0	0	2	2	2	2	1	1	1	2	1	1	1	1
Gyroidinoides acutus	0	0	0	0	0	0	0	0	0	0	0	0	0	0	0	0	0	0	0	0	0	0	0	0	0	0	0	0	0	0	0	0	0	1	0
Gyroidinoides girardanus	2	2	3	5	3	1	0	1	1	1	2	1	0	1	2	0	1	1	0	2	2	1	0	3	1	2	0	2	1	0	0	3	1	1	0
Gyroidinoides cf. *G. laevigatus*	0	0	1	0	0	0	0	0	0	0	0	0	0	0	0	2	0	0	1	1	0	0	0	1	0	1	0	0	0	0	1	0	0	0	1
Hanzawaia ammophila	0	0	0	0	0	0	0	0	0	0	0	0	0	0	1	0	0	0	1	0	0	0	0	0	0	0	0	0	0	0	0	0	0	0	0
Heterolepa grimsdalei	0	0	2	2	0	0	0	0	0	0	0	1	0	0	0	0	0	0	3	0	0	0	0	0	0	1	0	0	0	0	0	0	0	1	0
Heterolepa mexicana	2	1	0	0	0	0	0	0	0	1	1	1	0	0	0	0	0	0	0	0	0	0	0	0	0	0	0	0	0	0	0	0	0	0	0
Karrenulina coniformis	0	0	0	0	0	0	0	0	0	0	0	0	0	0	0	0	0	0	0	0	0	0	0	0	0	0	0	0	0	0	0	0	0	0	0
Karreriella chapapotensis	0	0	0	0	0	0	0	0	0	0	0	0	0	0	0	0	0	0	0	0	0	0	0	0	0	0	0	0	0	0	0	0	0	0	0
Karreriella bradyi	0	0	0	1	0	0	0	0	0	0	0	0	0	0	0	0	0	0	0	0	0	0	0	0	0	0	0	0	0	0	0	0	0	0	0
Karreriella subglabra	0	0	0	0	0	0	0	0	0	0	0	0	0	0	0	0	0	0	0	0	0	0	0	0	0	0	0	0	0	0	0	0	0	0	0
Lagena asperoides	0	0	0	0	0	0	0	0	0	0	0	0	0	0	0	0	0	0	0	0	0	0	0	0	0	0	0	0	0	0	0	0	0	0	0
Lenticulina spp.	0	1	0	1	0	0	0	0	0	0	0	1	0	0	0	0	0	0	0	0	0	0	0	0	0	0	0	0	0	0	0	0	0	1	0
Lenticulina cultrata	0	0	0	0	0	0	0	0	0	0	0	0	0	0	1	0	0	0	0	0	0	1	0	0	0	1	0	0	0	0	0	0	0	0	0
Lenticulina peregrina	0	0	0	0	0	0	0	0	0	0	0	0	0	0	0	0	0	0	0	0	0	0	0	0	0	0	0	0	0	0	0	0	0	0	0
Lenticulina rotulata	0	0	1	0	0	0	0	0	0	1	1	0	1	1	1	0	0	0	2	0	1	1	0	2	1	2	1	1	0	0	0	1	0	0	0
Lenticulina turbinata	0	0	0	0	0	0	0	0	0	0	0	0	0	0	0	0	0	0	0	0	0	0	0	0	0	0	0	0	0	0	0	0	0	0	0
Lenticulina velascoensis	0	0	0	0	1	0	0	0	0	0	0	0	0	0	0	0	0	0	0	0	0	0	0	0	0	0	0	0	0	0	0	0	0	0	0
Marginulina sp.	0	0	0	0	0	0	0	0	0	0	0	0	0	0	0	0	0	0	0	1	0	0	0	0	0	0	0	0	0	0	0	0	0	0	0
Marginulinopsis sp.	0	0	0	0	0	0	0	0	0	0	0	0	0	0	0	0	0	0	0	0	0	0	0	0	0	0	0	0	0	0	0	0	0	0	0
Marssonella floridana	0	0	0	0	0	0	0	0	0	0	0	0	0	0	0	0	0	0	0	0	0	0	0	0	0	0	0	0	0	0	0	0	0	0	0
Martinottiella sp.	0	0	0	0	0	0	0	0	0	0	0	0	0	0	0	0	0	0	0	0	0	0	0	0	0	0	0	0	0	0	0	0	0	0	0
Melonis sp.	0	1	0	0	0	0	0	0	0	0	0	0	0	0	0	0	0	0	0	0	0	0	0	0	0	0	0	0	0	0	0	0	0	0	0
Melonis affinis	3	1	3	4	3	1	0	0	0	1	3	3	4	1	2	2	1	2	1	2	2	2	2	2	5	4	7	1	3	1	4	3	5	4	5
Melonis havanensis	0	0	0	1	2	0	0	0	0	0	0	0	0	0	0	0	1	0	1	0	0	0	0	0	0	0	0	0	0	0	0	0	0	0	0
Mucronina spp.	1	5	1	1	0	2	0	1	1	3	0	0	0	0	0	0	0	0	0	0	0	0	0	0	0	0	0	0	0	0	0	0	0	0	0
Neugeborina longiscata	3	6	3	5	1	0	0	1	2	1	0	1	0	1	1	2	0	1	1	0	1	0	1	1	1	2	2	1	1	1	2	1	2	2	1
Nodosariella robusta	0	0	0	1	0	0	0	0	0	0	0	0	0	0	0	0	0	0	0	0	0	1	0	0	0	0	0	0	0	0	0	0	0	0	0
Nuttallides cf. *umbonifera*	0	0	0	0	0	0	0	0	0	0	0	0	0	0	0	0	0	0	0	0	0	0	0	0	0	0	0	0	0	0	0	0	1	1	0
Obesopleurostomella sp.	1	0	0	1	0	0	0	0	0	0	0	0	1	0	0	0	1	0	2	1	0	1	0	0	0	0	2	0	0	0	0	0	1	0	0
Oridorsalis umbonatus	5	1	2	1	7	0	0	0	0	1	2	2	0	1	3	3	2	1	1	1	0	2	0	2	1	2	1	1	1	1	3	2	2	2	0
Orthomorfina cf. *jedlitschkai*	1	0	0	0	2	13	28	31	19	0	0	0	0	0	0	0	0	0	0	0	0	0	0	0	0	0	0	0	0	0	0	0	0	0	0
Osangularia cf. *plummerae*	6	9	8	14	7	0	0	0	0	0	0	1	0	0	1	1	1	1	1	0	2	1	2	2	2	1	2	1	1	1	3	0	0	1	0
Planulina marialana	0	0	0	0	0	0	0	0	0	0	0	0	0	0	1	0	0	0	0	0	0	0	0	0	0	0	0	0	0	0	0	0	0	0	0
Planulina renzi	0	0	0	0	0	0	0	0	0	0	0	1	0	2	1	0	1	1	3	1	1	0	0	0	0	1	0	0	0	0	0	0	1	0	0
Pleurostomella parviapertura	0	0	1	0	1	0	0	0	0	0	0	0	0	0	0	0	0	0	2	0	0	0	0	0	0	0	0	1	0	0	0	0	0	0	0
Pleurostomella brevis	0	0	0	0	0	0	0	0	0	0	0	0	0	0	0	0	0	1	0	0	0	0	0	0	0	0	0	0	0	1	0	0	0	0	0
Pleurostomella obtusa	1	0	0	3	6	0	1	0	0	0	1	1	0	2	1	1	1	1	1	1	2	1	2	0	2	2	1	2	1	1	1	1	1	2	1
Pleurostomella spp.	0	0	0	0	0	0	0	0	0	0	0	0	0	0	0	0	0	0	0	0	0	0	0	0	0	0	0	0	1	0	0	1	1	0	1
Pseudoclavulina trinidaensis	1	0	0	0	0	1	0	0	0	0	0	0	0	0	0	0	0	0	0	0	0	1	0	0	0	0	0	0	0	0	0	0	0	1	0
Pullenia bulloides	5	4	5	1	3	0	0	1	0	1	1	2	4	2	2	3	3	1	3	2	2	2	0	6	3	1	2	3	2	1	5	1	3	3	0
Pullenia quinqueloba	2	1	2	2	1	1	0	0	0	0	1	0	0	0	0	0	0	0	1	1	0	0	0	0	1	1	0	1	0	0	1	0	1	0	1

Depth (mbsf)	135.47	135.63	135.73	135.95	136.08	136.2	136.265	136.33	136.4	136.59	136.79	136.98	137.18	137.37	137.57	137.77	137.98	138.17	138.35	138.54	138.74	138.96	139.1	139.31	139.5	139.71	139.91	140.1	140.3	140.49	140.68	140.89	141.08	141.28	141.46
Quinqueloculina sp.	0	0	1	0	0	0	0	0	0	0	0	0	0	0	0	0	0	0	0	0	0	0	0	0	1	0	0	1	0	0	0	0	0	0	0
Rhabdammina sp.	0	0	0	0	0	0	0	0	0	0	0	0	0	0	0	0	0	0	0	0	0	0	0	0	0	0	0	0	0	0	0	0	0	0	0
Rosalina sp.	0	0	0	0	0	0	0	0	0	0	0	0	0	0	0	0	0	0	0	0	0	0	0	0	0	0	0	0	0	0	0	0	0	0	0
Sigmoilopsis spp.	0	1	0	0	0	0	0	0	0	0	0	0	0	0	0	0	0	0	1	0	0	0	1	0	0	0	1	0	0	0	0	1	0	1	1
Siphonodosaria annulifera	0	0	0	1	1	0	0	2	0	1	1	0	0	1	1	2	2	0	0	0	1	1	1	0	2	1	2	3	1	1	1	0	0	0	0
Siphonodosaria curvatura	2	4	0	0	0	0	0	0	0	0	0	0	1	1	1	0	1	0	0	1	0	0	0	0	0	0	0	0	0	0	0	0	0	0	0
Siphonodosaria gracillima	0	0	0	0	0	0	0	0	0	0	1	0	0	0	0	1	0	3	2	0	0	0	0	0	0	1	2	4	2	2	2	3	1	2	2
Siphonodosaria jacksonensis	6	13	16	13	8	0	1	3	0	7	3	4	2	2	3	3	3	5	4	9	9	8	4	4	9	7	9	13	10	10	7	4	1	5	6
Siphonodosaria lepidula	2	1	0	2	1	10	5	7	6	3	0	0	0	0	0	0	0	0	0	0	0	0	0	0	0	0	0	2	1	0	3	5	1	1	1
Siphonodosaria pomuligera	0	0	1	0	0	0	0	0	0	0	1	0	0	0	0	0	0	0	0	0	0	0	0	0	0	0	0	0	0	0	0	2	1	0	0
Siphonodosaria subspinosa	0	1	1	1	1	0	0	0	0	0	0	0	0	0	0	0	0	0	0	1	0	0	0	0	0	1	0	1	0	0	2	0	0	0	0
Siphotextularia sp.	0	0	1	0	0	0	0	0	0	1	9	2	0	1	1	2	4	1	1	0	0	0	0	0	1	1	0	0	0	0	0	0	0	0	0
Spiroplectammina spectabilis	0	0	0	0	0	0	0	0	0	0	0	0	0	0	0	0	0	0	0	0	1	1	0	0	0	0	0	0	0	0	0	2	5	2	3
Staffia tosta	0	0	1	0	0	0	0	0	0	0	0	0	0	0	0	0	0	0	0	0	0	0	0	0	0	0	0	0	0	0	0	0	0	0	0
Stilostomella rugosa	0	0	0	0	0	0	0	0	0	0	0	0	0	0	0	0	0	0	0	0	0	0	0	0	0	0	0	0	0	0	0	0	0	0	0
Strictocostella fistuca	0	0	0	0	0	0	0	0	0	0	0	0	0	0	0	0	0	0	0	0	0	0	0	0	0	0	0	0	0	0	0	0	0	0	0
Strictocostella japonica	4	4	2	2	2	4	3	7	5	6	0	0	1	1	1	2	0	1	2	2	2	4	4	1	3	5	3	6	3	6	10	11	14	12	27
Strictocostella scharbergana	4	2	2	4	3	16	32	13	24	16	1	0	2	5	0	0	0	0	0	1	2	0	0	0	0	0	0	0	0	0	0	0	0	0	0
Textularia sp.	0	0	1	0	0	0	0	0	0	0	0	0	0	0	0	0	0	0	0	0	0	0	0	0	0	0	0	0	0	0	0	0	0	2	0
Trifarina wilcoxensis	2	2	1	1	0	13	3	4	6	7	8	10	2	5	3	3	1	1	3	5	3	3	2	11	6	2	2	2	0	1	2	2	0	7	5
Trifarina sp.	0	0	0	1	0	0	0	0	0	0	0	0	0	0	0	0	0	1	0	0	1	0	0	0	0	0	0	0	0	1	0	1	1	2	0
Uvigerina galloway	11	16	11	9	3	0	0	0	0	0	0	0	0	0	0	0	0	0	0	0	0	0	0	0	0	0	0	0	0	0	0	0	0	0	0
Uvigerina hispida	0	0	1	0	0	0	0	0	0	0	0	0	0	0	0	0	0	0	0	1	0	0	0	0	0	0	0	1	0	0	0	0	0	0	0
Uvigerina rippensis	4	1	1	3	1	1	1	2	5	3	9	7	12	9	11	6	1	1	1	0	0	0	0	3	1	1	0	1	0	1	0	2	2	3	2
Vaginulina sp.	0	0	0	0	0	0	0	0	0	0	0	0	0	0	0	0	0	0	0	0	0	0	0	0	0	0	0	0	0	0	0	0	0	0	0
Valvulineria sp.	0	0	0	1	0	0	0	0	0	0	0	0	0	0	0	0	0	0	0	0	0	0	0	0	0	0	0	0	0	0	0	0	0	0	0
Vulvulina spinosa	0	0	1	0	0	0	0	0	0	0	0	0	0	0	0	0	0	0	0	0	0	0	0	0	0	0	0	0	0	0	0	0	0	0	0
Undetermined specimen	0	0	0	0	0	0	0	0	0	0	0	0	0	0	0	0	0	0	0	0	0	0	0	0	0	0	0	0	0	0	0	0	0	0	0
TOTAL	100	100	100	100	100	100	100	100	100	100	100	100	100	100	100	100	100	100	100	100	100	100	100	100	100	100	100	100	100	100	100	100	100	100	100

Table IV e3. Benthic foraminifera assemblage: absolute abundances (N g^{-1}).

Depth (mbsf)	135.47	135.63	135.73	135.95	136.08	136.2	136.265	136.33	136.4	136.59	136.79	136.98	137.18	137.37	137.57	137.77	137.98	138.17	138.35	138.54	138.74	138.96	139.1	139.31	139.5	139.71	139.91	140.1	140.3	140.49	140.68	140.89	141.08	141.28	141.46
Alabamina cf. *A. dissonata*	37	8	71	3	19	8	10	8	7	18	37	15	53	52	29	15	24	48	17	9	6	16	28	15	26	12	12	13	7	23	21	27	151	0	0
Ammobaculites sp.	0	0	0	0	0	0	0	0	0	0	0	0	0	0	0	0	0	0	0	0	0	0	0	0	0	1	0	0	0	0	1	0	0	0	0
Anomalinoides alazanensis	0	0	0	0	0	0	0	0	0	0	0	0	4	0	3	0	0	3	2	0	0	3	0	0	0	0	0	2	0	0	0	0	0	0	0
Anomalinoides spissiformis	0	0	0	0	0	0	0	0	0	0	0	0	0	0	0	4	0	0	0	0	0	0	0	0	0	0	0	0	0	0	0	0	14	7	10
Anomalinoides sp.	0	0	0	0	0	0	0	0	0	0	0	0	0	0	0	0	0	0	0	0	0	0	0	0	0	0	0	0	0	0	0	2	0	0	2
Aragonia aragonensis	0	0	0	0	0	0	0	0	0	0	0	0	4	4	3	0	3	7	3	2	1	5	0	0	0	0	0	0	0	0	0	0	7	0	0
Arenobulimina sp.	0	0	0	0	0	0	0	0	0	0	3	2	0	0	0	0	3	0	2	0	1	0	0	0	0	0	0	0	0	0	0	0	0	0	0
Bigerina sp.	0	0	0	0	0	0	0	0	0	0	0	0	0	0	0	0	3	0	0	0	1	0	0	0	3	0	0	0	0	0	0	0	0	0	0
Bolivina antiqua	0	0	0	0	0	0	0	0	0	0	24	2	11	15	0	0	0	0	2	0	0	0	0	0	2	0	0	0	0	0	1	3	0	0	17
Bolivina spp.	4	1	6	1	1	4	42	0	0	7	0	0	18	30	16	42	55	17	7	8	3	19	77	1	31	12	28	13	29	18	1	27	14	22	4
Bolivinoides crenulatus	2	0	0	0	0	52	101	128	205	142	0	2	0	0	0	0	0	0	0	0	0	1	0	0	0	0	2	0	0	55	0	0	0	0	0
Brizalina carinata	0	0	0	0	0	27	24	31	120	98	13	0	0	0	6	23	7	0	5	4	5	9	28	0	12	5	16	18	77	233	4	12	10	22	2
Brizalina tectiformis	78	6	17	6	70	29	84	81	134	44	132	115	174	236	314	239	390	381	107	57	59	146	126	33	83	68	97	49	66	60	42	88	137	120	111
Bulimina alazanensis	13	1	12	3	23	37	28	19	14	77	143	149	121	101	201	93	114	161	80	36	34	16	10	7	19	12	51	19	22	32	23	45	86	93	40
Bulimina mexicana	15	7	8	0	13	6	14	16	21	26	26	25	18	7	6	15	3	12	2	3	9	14	10	10	3	2	5	2	4	5	3	7	0	0	0
Bulimina semicostata	0	0	0	0	0	0	0	0	0	0	0	0	0	0	0	0	0	0	0	0	0	0	0	0	0	0	0	0	0	0	0	0	0	0	4
Bulimina trinidaensis	2	1	0	1	6	0	0	0	0	0	0	6	0	0	0	8	0	3	2	0	0	1	0	0	3	2	0	0	0	2	0	2	0	4	6
Bulimina tuxpamensis	0	0	0	0	3	0	0	4	0	4	8	11	21	11	87	31	28	16	17	7	10	9	10	15	7	8	5	8	11	9	8	8	0	0	2
Cancris sp.	0	0	0	0	0	0	0	0	0	0	0	2	0	0	0	0	0	0	0	0	0	0	0	0	0	0	2	1	2	0	0	0	0	0	0
Cassidulina havanensis	0	0	0	0	0	0	0	0	0	0	0	0	4	0	0	0	0	0	0	0	1	0	0	0	0	1	0	0	0	0	0	0	0	0	0
Cibicidoides sp.	0	1	0	0	0	0	0	0	0	0	0	0	0	0	0	0	0	0	0	0	0	0	0	0	0	0	0	0	0	0	0	2	3	0	0
Cibicidoides hadjibulakensis	2	3	12	2	4	2	21	16	7	4	0	10	7	19	6	39	41	3	10	0	0	3	2	1	0	0	0	0	2	0	0	0	0	0	0
Cibicidoides laurisae	0	0	0	0	0	0	0	0	0	0	0	0	0	0	0	0	0	0	0	0	0	0	0	0	0	0	0	0	0	0	0	0	7	0	0
Cibicidoides mundulus	0	0	2	0	6	4	0	0	7	0	13	8	11	19	32	23	7	14	9	6	1	1	0	4	7	6	4	3	2	0	3	7	7	7	2
Cibicidoides tuxpamensis	0	0	0	0	0	0	0	0	0	0	0	0	0	0	0	0	0	0	2	0	5	1	0	0	0	0	0	0	0	0	0	0	3	0	2
Chrysalogonium spp.	0	4	2	1	3	6	35	19	141	33	5	2	0	26	19	8	7	5	2	3	0	1	0	2	2	0	7	0	4	0	3	0	0	4	4
Clavulinoides angularis	0	0	0	0	0	0	0	0	0	0	5	6	7	4	0	0	3	2	0	0	0	3	0	2	3	1	5	1	4	0	1	0	0	0	0
Dentalina spp.	7	4	0	2	4	4	14	12	0	4	11	4	7	4	13	15	10	9	2	3	4	5	2	0	3	4	4	3	4	0	4	2	3	7	4
Dorothia brevis	0	0	0	0	1	0	0	0	0	0	0	2	0	0	0	0	0	0	2	0	2	0	0	0	0	1	0	0	0	0	0	0	0	0	0
Eggerella sp.	0	0	0	0	0	2	0	0	0	0	0	0	0	0	0	0	0	0	0	0	0	0	0	0	0	0	0	0	0	0	1	0	0	0	0
Ellipsoidella sp.	0	0	0	0	0	0	0	0	0	0	0	0	0	0	0	0	0	0	0	0	0	0	0	0	0	0	0	0	0	0	2	0	0	0	0
Epistominella exigua	0	0	0	0	0	0	0	0	0	0	3	0	0	0	0	0	0	0	0	0	0	0	0	0	0	0	0	0	0	0	0	0	0	0	0
Eponides cf. *E. abatissae*	0	4	6	0	3	2	0	0	0	0	0	2	0	0	0	0	0	0	0	0	0	0	0	1	0	0	0	0	0	0	0	0	0	0	0
Fissurina spp.	0	0	4	0	0	4	0	0	0	0	0	0	4	0	0	0	3	5	5	4	1	0	0	2	2	0	2	3	4	2	2	2	3	4	6
Fursenkoina dibollensis	0	0	0	0	0	0	0	0	0	0	0	0	0	0	0	0	0	2	0	3	1	0	2	2	2	0	4	0	0	2	1	5	7	7	2
Gaudyna cf. *G. concinna*	0	0	0	0	0	0	0	0	0	0	0	0	0	0	0	0	0	0	0	0	0	0	0	0	0	2	0	0	0	0	0	0	0	0	0
Gaudryna arenata	2	0	2	0	0	0	0	0	0	0	0	0	0	0	0	0	0	0	0	0	0	0	0	0	3	0	0	0	0	0	0	0	0	0	0
Glandulina spp.	0	0	0	0	0	2	0	0	0	0	0	0	0	0	0	0	0	0	0	0	0	0	0	0	0	1	2	0	0	0	4	2	0	0	0
Glandulonodosaria ambigua	0	0	0	0	0	0	0	0	0	0	0	0	0	0	0	0	0	0	0	0	1	0	4	0	0	0	0	0	0	0	0	0	0	4	0

Depth (mbsf)	135.47	135.63	135.73	135.95	136.08	136.2	136.265	136.33	136.4	136.59	136.79	136.98	137.18	137.37	137.57	137.77	137.98	138.17	138.35	138.54	138.74	138.96	139.1	139.31	139.5	139.71	139.91	140.1	140.3	140.49	140.68	140.89	141.08	141.28	141.46
Glandulonodosaria trincherasensis	0	0	2	0	0	4	0	4	0	0	0	0	0	0	0	0	0	0	0	0	0	0	0	0	0	0	0	0	0	0	0	0	0	0	0
Glandulonodosaria sp.	0	0	0	0	0	0	0	0	0	0	0	0	0	0	0	0	0	0	0	0	0	0	0	0	0	0	0	0	0	0	1	0	0	0	0
Globocassidulina subglobosa	2	0	0	0	0	0	0	0	0	0	3	2	4	0	0	8	0	0	5	1	0	1	0	0	0	1	0	0	0	0	0	0	7	0	0
Globobulimina cf. *G. ovata*	0	1	0	0	1	0	0	0	7	0	3	2	4	0	0	4	0	0	0	0	1	0	0	0	2	2	0	3	4	4	0	2	0	4	0
Guttulina spp.	0	4	2	0	7	2	3	0	0	7	5	6	0	0	0	4	3	5	5	1	0	1	2	4	9	4	7	3	5	4	4	3	7	7	6
Gyroidinoides acutus	2	0	0	0	0	0	0	0	0	0	3	0	0	0	0	0	0	0	0	1	0	0	2	0	0	0	0	0	0	0	0	0	0	4	0
Gyroidinoides girardanus	11	5	12	4	12	6	7	8	28	15	13	6	4	7	19	0	10	7	2	5	5	4	2	5	3	4	2	5	4	2	1	15	7	7	0
Gyroidinoides cf. *G. laevigatus*	0	0	4	0	0	0	0	0	0	0	0	0	0	0	0	15	0	0	3	2	0	0	0	2	0	2	0	0	2	0	2	0	0	0	4
Hanzawaia ammophila	0	0	0	0	0	0	0	0	0	0	3	2	0	4	6	0	0	0	3	0	0	0	0	0	0	0	0	0	0	0	1	0	0	0	0
Heterolepa grimsdalei	0	1	6	2	1	2	0	0	0	0	3	6	0	0	0	0	3	2	15	0	0	0	0	0	0	3	0	0	0	0	0	0	0	4	0
Heterolepa mexicana	11	2	0	0	0	0	0	0	0	7	5	4	0	0	3	4	0	0	0	0	0	0	2	0	0	0	0	0	0	0	0	0	3	0	0
Karrenulina coniformis	0	0	0	0	0	0	0	0	0	0	0	0	0	0	0	0	0	0	0	0	0	0	0	0	0	0	0	0	0	0	0	0	0	0	2
Karreriella chapapotensis	0	0	0	0	0	0	0	0	0	0	0	2	0	0	0	0	0	0	0	0	0	0	0	0	0	0	0	0	0	0	0	0	0	0	2
Karreriella bradyi	0	0	0	1	1	2	0	0	0	0	0	2	0	0	0	0	0	0	0	1	0	0	0	0	0	0	0	0	0	0	0	0	0	0	0
Karreriella subglabra	0	0	0	0	0	0	0	0	0	0	0	0	0	0	0	0	0	0	0	0	0	0	0	0	0	0	0	0	0	0	0	0	0	0	2
Lagena asperoides	0	0	0	0	0	0	0	0	0	0	0	0	0	0	0	0	0	0	0	0	0	0	0	0	0	0	0	0	0	0	0	2	0	0	0
Lenticulina spp.	0	2	0	0	0	0	0	0	0	0	0	6	0	0	0	0	0	2	0	0	0	0	0	0	0	0	0	0	2	0	1	0	0	4	0
Lenticulina cultrata	0	0	0	0	0	0	0	0	0	0	0	0	0	0	6	0	0	0	0	0	0	4	0	0	2	2	0	0	0	2	0	0	0	0	0
Lenticulina peregrina	0	0	0	0	0	0	0	0	0	0	0	0	0	0	0	0	0	0	0	0	0	0	0	0	0	0	0	0	0	0	0	0	0	0	2
Lenticulina rotulata	2	0	4	0	0	2	0	0	7	15	11	0	7	7	13	0	0	0	9	0	3	3	2	4	3	4	5	3	0	0	0	3	0	0	0
Lenticulina turbinata	0	0	0	0	0	0	0	0	0	0	0	0	0	0	0	0	0	0	0	0	0	0	0	0	2	0	0	0	0	0	0	0	0	0	0
Lenticulina velascoensis	0	0	0	0	3	0	0	0	7	0	0	0	0	0	0	0	0	0	2	0	0	0	0	0	0	0	0	0	0	2	0	0	3	0	0
Marginulina sp.	2	0	0	0	0	2	0	0	0	0	0	0	0	0	0	0	0	0	0	2	1	0	0	0	0	0	0	0	0	0	1	0	0	0	0
Marginulinopsis sp.	0	0	0	0	0	0	0	0	0	0	0	0	0	0	0	0	0	0	0	0	0	0	0	0	0	0	0	0	0	0	0	0	0	0	2
Marssonella floridana	0	0	0	0	1	0	0	0	0	0	0	0	0	0	0	0	0	3	0	0	0	1	0	0	0	0	0	0	0	0	0	0	3	0	0
Martinottiella sp.	0	0	0	0	0	0	0	0	0	0	0	0	0	0	0	0	0	0	0	0	0	0	0	0	0	0	2	1	0	0	0	0	0	0	0
Melonis sp.	0	1	0	0	0	0	0	0	0	0	0	0	0	0	0	0	0	0	0	0	0	0	0	0	0	0	0	0	0	0	0	0	0	0	0
Melonis affinis	15	3	10	3	13	8	3	0	7	11	24	21	28	7	26	19	14	21	5	5	5	7	10	4	19	10	30	3	13	4	10	13	45	30	25
Melonis havanensis	2	0	0	1	7	0	0	0	0	0	0	2	0	0	0	0	7	0	3	0	0	0	0	1	0	0	0	0	0	0	0	0	0	0	0
Mucronina spp.	4	11	4	0	0	10	3	8	14	29	0	0	0	0	0	0	0	0	0	1	0	1	0	0	2	1	0	0	0	0	1	0	0	0	0
Neugeborina longiscata	15	12	12	4	6	2	3	8	35	11	3	10	4	11	10	15	3	7	5	1	2	0	6	2	5	5	9	2	4	5	5	3	14	15	8
Nodosariella robusta	0	0	0	0	0	2	3	0	7	0	0	0	0	0	0	0	0	0	0	0	1	3	0	0	0	1	0	0	0	2	0	0	3	0	0
Nuttallides cf. *umbonifera*	0	0	0	0	0	0	0	0	0	0	0	0	0	0	0	0	0	0	0	0	0	0	0	0	0	0	0	0	0	0	0	0	7	7	0
Obesopleurostomella sp.	7	0	0	0	1	2	0	0	0	0	3	2	7	0	0	0	14	3	9	3	1	3	2	0	2	1	9	0	0	0	0	0	7	0	0
Oridorsalis umbonatus	28	1	8	1	29	0	3	0	7	11	16	11	4	11	32	27	21	5	3	3	0	7	2	3	5	6	4	3	5	4	7	10	17	11	2
Orthomorfina cf. *jedlitschkai*	4	1	0	0	9	81	472	376	424	0	0	2	0	0	3	0	0	0	0	0	0	0	0	0	0	0	0	0	0	0	0	0	0	0	0
Osangularia cf. *plummerae*	35	19	31	11	29	0	7	0	0	4	3	10	0	0	6	8	7	12	3	1	4	4	10	4	9	3	9	3	4	4	7	2	3	4	0
Planulina marialana	0	0	0	0	0	0	0	0	0	0	0	0	0	0	6	0	0	0	0	0	0	0	0	0	0	0	0	0	0	0	0	0	0	0	0
Planulina renzi	0	0	0	0	1	2	3	0	0	4	0	6	0	15	6	4	7	12	12	2	2	0	0	0	0	2	0	1	0	0	0	2	7	0	2
Pleurostomella parviapertura	0	1	2	0	3	0	3	0	7	0	0	2	0	0	0	0	0	0	9	0	0	0	0	0	0	0	2	3	0	0	0	0	3	0	0
Pleurostomella brevis	0	0	0	0	0	0	0	0	0	0	0	0	0	4	0	4	0	5	0	0	0	0	0	1	0	0	0	0	0	5	0	0	0	0	0
Pleurostomella obtusa	7	0	0	2	23	2	14	4	0	0	5	8	0	15	10	12	7	10	5	3	4	5	10	1	7	4	4	5	5	7	2	3	7	15	6

Depth (mbsf)	135.47	135.63	135.73	135.95	136.08	136.2	136.265	136.33	136.4	136.59	136.79	136.98	137.18	137.37	137.57	137.77	137.98	138.17	138.35	138.54	138.74	138.96	139.1	139.31	139.5	139.71	139.91	140.1	140.3	140.49	140.68	140.89	141.08	141.28	141.46
Pleurostomella spp.	0	0	0	0	0	0	0	0	0	0	0	0	0	0	0	0	0	0	0	0	0	0	0	0	0	0	0	0	5	2	0	3	10	0	6
Pseudoclavulina trinidaensis	4	0	0	0	0	4	0	0	0	0	3	2	4	0	0	0	0	0	0	0	0	3	0	0	0	0	0	0	0	0	0	0	0	4	0
Pullenia bulloides	26	8	19	1	13	2	3	8	0	15	8	15	28	15	19	27	24	14	12	4	4	8	0	10	12	2	7	7	7	5	12	5	24	19	2
Pullenia quinqueloba	9	2	6	2	3	4	0	0	0	4	5	0	0	4	3	4	3	2	5	2	0	0	2	0	3	2	0	2	0	0	2	0	10	0	4
Quinqueloculina sp.	0	0	2	0	0	0	3	4	0	0	0	2	0	0	0	0	0	2	0	0	1	0	0	0	5	0	0	3	0	0	0	0	0	0	0
Rhabdammina sp.	0	0	0	0	0	0	0	0	0	0	0	0	0	0	0	0	0	0	0	0	0	0	0	0	0	0	0	1	0	0	1	2	0	0	0
Rosalina sp.	0	0	0	0	0	0	0	0	0	0	0	0	4	0	0	0	0	0	0	0	0	0	0	0	0	0	0	0	0	0	0	0	0	0	0
Sigmoilopsis spp.	0	1	0	0	0	0	0	0	0	0	0	0	0	0	3	0	0	2	5	0	0	0	4	1	2	0	4	0	0	0	0	5	0	4	4
Siphonodosaria annulifera	2	1	0	0	3	2	0	23	7	7	5	0	0	7	6	19	17	3	0	0	2	3	4	0	7	2	7	7	5	4	2	0	0	0	0
Siphonodosaria curvatura	11	8	0	0	0	0	3	0	0	0	0	0	11	7	10	0	7	0	0	3	0	0	2	0	2	0	0	1	0	0	0	0	0	0	0
Siphonodosaria gracillima	0	0	0	0	0	0	0	0	0	0	5	0	0	4	3	8	3	31	9	0	1	0	0	1	2	3	9	10	9	14	5	13	10	15	10
Siphonodosaria jacksonensis	33	27	64	11	30	2	24	31	7	77	24	27	14	19	29	27	31	48	20	19	19	30	16	7	36	18	39	34	38	60	17	20	7	34	33
Siphonodosaria lepidula	9	1	0	1	3	62	87	89	141	33	0	0	0	0	0	4	0	0	2	0	0	0	0	0	2	0	0	5	5	2	9	22	7	7	8
Siphonodosaria pomuligera	0	0	2	0	0	0	0	0	0	0	8	0	0	0	0	0	0	0	2	0	1	0	0	0	2	0	0	0	0	2	0	10	10	0	0
Siphonodosaria subspinosa	2	2	2	0	3	0	0	0	7	0	0	2	0	0	0	0	0	0	0	2	0	0	2	0	2	2	0	3	0	0	4	0	0	0	0
Siphotextularia sp.	0	0	2	0	0	2	0	0	7	7	77	11	0	11	10	19	35	12	3	0	0	1	0	0	3	3	0	0	0	0	0	0	0	0	0
Spiroplectammina spectabilis	2	0	0	0	0	0	0	0	0	0	0	0	0	0	0	4	0	0	0	0	3	3	0	0	0	0	0	0	2	2	1	10	41	11	19
Staffia tosta	0	0	2	0	0	0	0	0	0	0	0	0	0	0	0	0	0	0	0	0	0	0	0	0	0	0	0	0	0	0	0	0	0	0	0
Stilostomella rugosa	0	0	0	0	0	0	0	0	0	0	0	0	0	0	0	0	0	0	0	0	0	0	0	0	0	0	0	0	0	0	2	0	0	0	0
Strictocostella fistuca	0	0	0	0	0	0	0	0	0	0	0	0	0	0	0	0	0	0	0	0	0	0	0	0	0	0	0	0	2	1	0	0	0	0	0
Strictocostella japonica	22	8	8	1	7	23	56	89	113	69	3	2	7	11	6	15	0	7	10	6	4	14	18	2	10	11	11	15	11	39	25	52	117	79	148
Strictocostella scharbergana	22	4	6	3	10	100	531	163	537	175	11	2	18	45	0	0	0	0	0	2	3	0	0	0	0	0	0	0	0	0	0	0	0	0	0
Textularia sp.	0	1	2	0	0	0	0	0	0	0	0	0	0	0	0	0	0	0	0	0	0	1	2	1	0	0	0	1	2	0	0	0	0	11	0
Trifarina wilcoxensis	11	4	2	0	0	81	56	54	141	77	69	65	14	41	29	23	10	7	12	10	7	9	10	18	22	6	9	6	2	4	4	10	3	45	25
Trifarina sp.	0	0	0	0	0	0	0	0	0	0	0	0	4	4	3	0	0	7	0	0	2	0	0	0	0	1	2	0	0	4	0	3	7	11	0
Uvigerina galloway	63	31	46	7	10	0	0	0	0	0	0	0	0	0	0	0	0	0	0	0	0	0	0	0	0	0	0	0	0	0	0	0	0	0	0
Uvigerina hispida	2	0	2	0	0	0	0	0	0	0	0	0	4	0	0	0	0	3	0	2	0	1	0	1	2	1	0	2	0	0	1	0	0	0	2
Uvigerina rippensis	24	2	4	2	6	4	14	19	106	36	74	42	89	79	120	54	14	7	3	1	1	0	0	6	3	2	0	2	2	5	0	8	14	19	13
Vaginulina sp.	0	0	0	0	0	0	0	0	0	0	0	0	0	0	0	0	0	0	0	0	0	0	0	0	2	1	2	1	2	0	0	0	0	0	0
Valvulineria sp.	0	0	0	0	0	0	0	0	0	0	0	0	0	0	0	0	3	0	2	0	0	0	0	0	0	0	2	0	0	0	0	0	0	0	0
Vulvulina spinosa	0	1	2	0	0	2	0	0	0	0	0	0	0	0	0	0	0	0	2	0	0	0	0	0	0	0	0	0	0	0	2	0	0	0	0
Undetermined specimen	0	0	0	0	0	0	0	0	0	0	0	0	0	0	0	0	0	0	0	0	0	0	0	1	0	0	0	0	0	0	0	0	0	0	0
N° of counted specimens	254	361	200	197	272	294	481	315	322	293	308	335	201	230	349	229	275	537	271	242	255	276	203	205	231	304	236	317	207	354	259	277	250	180	287
Total specimens	1016	361	800	197	1088	1176	3848	2520	5152	2344	1232	1340	1608	1840	2792	1832	2200	2148	1084	484	510	1104	812	410	924	608	944	634	828	1416	518	1108	2000	1440	1148
TOTAL ABUNDANCE	553	201	416	80	394	611	1681	1222	2275	1068	814	640	715	860	1129	883	949	930	461	223	220	373	412	167	399	242	416	266	372	625	246	466	859	673	551

Table IV f1. Calcareous nannofossil assemblage: census. FOV=Fields of view.

Depth (mbsf)	135.47	135.63	135.73	135.95	136.08	136.2	136.27	136.33	136.4	136.59	136.79	136.98	137.18	137.37	137.57	137.77	137.98	138.17	138.35	138.54	138.74	138.96	139.1	139.31	139.5	139.71	139.91	140.1	140.3	140.49	140.68	140.89	141.08	141.28	141.46
# FOV	60	38	33	71	35	36	38	42	42	45	29	39	27	35	34	33	31	32	35	29	35	40	45	28	34	36	36	34	31	46	60	42	39	36	31
Blackites spp.	5	6	4	1	5	6	9	4	2	1	4	3	2	1	5	7	5	5	3	4	5	6	5	5	6	4	3	8	7	3	3	9	5	5	3
Bramlettei serraculoides	0	0	0	0	0	0	0	0	1	0	0	0	0	0	0	0	2	2	0	2	0	0	0	0	0	0	0	1	0	0	0	0	0	0	1
Chiasmolithus spp.	0	0	0	0	0	0	0	0	0	0	0	0	0	0	0	0	0	0	1	0	0	0	1	0	1	0	0	0	0	0	0	0	0	1	0
Chiasmolithus oamaruensis	0	0	0	0	0	0	0	1	1	1	0	0	1	0	1	0	0	1	0	0	1	0	0	0	0	0	0	0	0	1	0	1	0	0	0
Chaismolithus modestus	0	0	0	0	0	0	0	0	0	0	0	0	0	2	0	0	0	0	0	0	0	0	0	0	0	0	0	0	0	0	0	0	0	0	0
Chiasmolithus altus	0	0	0	0	1	1	0	0	0	0	0	0	0	0	0	0	0	0	0	0	0	0	0	0	0	0	0	0	0	0	0	0	0	0	0
Calcidiscus patecus	0	0	0	0	0	0	0	0	0	0	0	0	0	0	0	0	0	0	0	0	0	0	0	0	0	0	1	1	0	0	0	0	0	0	0
Clausicoccus obrutus	3	1	2	1	3	1	3	4	1	1	6	4	3	1	3	5	6	3	2	1	6	0	3	2	3	4	0	3	2	4	2	1	2	1	1
Clausicoccus fenestraus	1	0	0	0	0	0	0	0	0	2	0	0	0	0	1	1	0	2	1	0	1	1	0	0	0	0	0	0	0	0	0	0	0	0	2
Clausicoccus subdistichus	4	1	0	0	2	3	1	3	2	0	2	4	3	0	2	3	2	0	4	1	4	0	2	1	2	2	1	0	0	3	0	1	3	1	6
Coccolithus cachaoi (7-11µ)	0	1	0	0	0	0	1	0	0	0	0	1	0	1	0	0	0	1	0	0	0	0	0	0	0	0	0	0	0	0	0	0	0	0	0
Coccolithus eopelagicus	2	1	0	0	0	0	1	0	0	0	0	0	0	0	0	0	0	0	0	0	0	0	0	0	0	0	0	0	0	0	0	0	0	0	1
Coccolithus pelagicus (3-7µ)	11	8	10	12	15	11	9	6	9	12	10	8	6	6	11	10	10	12	12	8	10	4	6	5	10	7	11	6	10	14	10	12	6	10	13
Coccolithus pelagicus (7-11µ)	18	13	9	13	12	10	15	11	14	12	9	17	6	12	14	6	11	7	10	8	17	24	1	6	12	10	13	11	10	19	20	17	17	8	8
Coccolithus pelagicus (11-16µ)	0	0	0	0	0	4	2	1	0	2	1	2	1	1	2	1	1	3	0	0	1	1	0	1	0	0	1	0	1	0	1	0	0	0	2
Coccolithus formosus (7-11µ)	4	1	1	2	4	4	5	4	3	1	3	2	3	5	3	4	3	1	1	1	2	5	6	2	3	3	2	5	2	5	8	4	5	4	1
Coccolithus formosus (11-16µ)	1	1	1	0	0	0	0	1	1	0	0	1	0	2	0	0	0	0	0	0	0	1	0	0	0	1	1	0	0	1	1	2	0	1	1
Corpnocyclus bramlettei	0	0	2	0	2	3	2	3	2	1	2	1	2	2	4	1	0	1	0	3	3	2	1	4	4	3	2	2	5	4	3	2	3	0	4
Corpnocyclus netiscens	0	0	0	0	0	0	0	0	0	0	0	0	0	0	0	1	0	1	0	0	0	0	0	0	0	0	0	0	0	0	0	0	0	0	0
Cyclicargolithus sp. (3-5µ)	12	18	13	18	16	8	13	10	7	10	7	7	7	6	5	14	8	10	14	3	8	10	8	8	9	7	10	21	2	4	6	11	7	13	10
Cyclicargolithus sp. (5-7µ)	11	12	8	12	9	14	17	10	14	13	10	8	6	3	13	10	5	13	17	11	9	7	15	13	10	15	11	9	9	11	19	11	15	14	9
Cyclicargolithus sp. (7-9µ)	2	0	0	1	0	0	0	0	0	0	0	0	2	1	0	0	0	0	2	0	0	0	0	0	0	0	0	1	0	0	0	0	0	0	0
Cyclicargolithus floridanus (3-5µ)	6	4	3	7	1	1	2	1	3	4	1	3	3	3	2	2	2	5	6	3	5	5	3	3	3	3	1	5	5	4	3	1	4	0	4
Cyclicargolithus floridanus (5-7µ)	3	0	0	2	3	0	4	0	1	3	2	2	0	0	3	5	3	5	1	1	1	2	2	0	1	0	1	6	2	6	3	0	4	2	2
Cyclicargolithus floridanus (7-9µ)	0	0	0	0	0	0	0	0	0	0	0	0	0	0	0	0	0	0	0	0	1	0	0	0	0	0	0	0	0	0	0	0	0	0	0
Dictyococcites bisectus	9	3	5	10	5	4	8	7	7	7	4	1	4	2	4	7	7	1	6	3	5	4	0	1	3	1	2	3	2	4	3	5	2	5	4
Dictyococcited callidus	2	1	4	6	3	1	3	6	8	3	11	9	4	8	9	2	10	2	6	5	3	7	5	3	8	7	7	10	6	7	4	3	9	7	5
Dictyococcites daviesii	25	21	24	30	19	23	35	17	28	38	8	15	7	22	20	20	15	7	14	16	21	25	19	16	18	19	15	23	19	30	21	29	16	22	21
Dictyococcites stavensis	1	4	5	4	5	2	3	2	3	3	2	2	1	3	3	3	4	2	1	0	2	2	3	2	5	1	1	1	2	8	5	3	4	5	2
Dictyococcites stavensis (>14µ)	2	0	1	0	0	1	0	0	0	0	0	1	2	0	0	1	1	0	0	1	1	1	1	1	0	1	2	1	0	0	0	0	1	0	0
Discoaster spp.	6	1	1	1	0	1	1	0	1	2	1	2	2	2	0	1	2	1	0	1	2	0	1	0	1	1	1	0	0	0	2	1	3	0	1
Discoaster barbadiensis	0	0	0	0	0	0	0	0	2	0	0	1	0	0	0	1	0	0	1	0	2	2	1	0	0	0	0	0	0	1	0	0	0	0	0
Discoaster deflandrei	0	0	0	0	0	0	0	3	0	1	0	0	0	0	1	0	0	0	0	0	0	0	0	0	0	0	0	0	0	0	0	0	0	0	0
Discoaster saipanensis	0	0	0	0	0	0	0	0	2	0	0	0	1	0	2	1	1	1	1	1	0	1	0	0	0	1	0	0	0	1	0	0	0	1	0
Discoaster nodifer	0	1	0	1	1	4	0	1	1	1	2	1	0	0	0	0	2	0	1	0	0	0	0	0	0	0	0	0	0	1	1	0	0	2	0
Discoaster tanii	0	1	0	0	0	0	0	0	0	0	0	0	0	0	0	0	0	0	0	0	0	0	0	0	0	0	0	0	0	0	0	0	0	0	0
Hayella situliformis	1	0	0	0	2	0	0	0	0	1	0	0	0	0	0	0	0	0	0	0	0	0	0	0	0	0	0	0	0	0	0	0	0	0	0
Helicosphaera bramlettei	1	0	0	0	2	1	2	3	1	1	2	0	0	0	3	1	1	2	1	1	2	2	2	2	3	0	5	2	2	1	2	2	2	1	0
Helicosphaera compacta	1	1	2	1	2	2	4	2	0	2	1	2	2	2	0	0	0	2	1	2	2	2	2	2	2	2	3	2	2	1	1	0	2	1	2
Helicosphaera euphratis	0	0	1	0	0	0	0	0	0	0	0	0	2	0	0	0	0	0	1	2	0	0	1	1	0	0	1	0	1	0	1	0	0	1	0

Depth (mbsf)	135.47	135.63	135.73	135.95	136.08	136.2	136.27	136.33	136.4	136.59	136.79	136.98	137.18	137.37	137.57	137.77	137.98	138.17	138.35	138.54	138.74	138.96	139.1	139.31	139.5	139.71	139.91	140.1	140.3	140.49	140.68	140.89	141.08	141.28	141.46
Helicosphaera seminulum	0	0	0	0	0	0	0	0	0	0	1	0	0	0	0	0	0	0	0	0	0	0	0	0	0	0	0	0	0	0	0	0	0	0	0
Isthmolithus recurvus	8	12	7	3	7	10	10	8	10	13	10	3	8	8	10	13	12	5	5	10	8	11	8	14	6	5	5	5	6	7	10	7	4	6	3
Lanthernithus minutus	0	0	0	0	0	0	2	0	0	0	0	0	1	0	0	0	3	0	1	0	0	0	0	0	1	0	0	0	0	0	1	0	0	0	0
Pedinolcyclus	0	0	1	0	0	0	0	0	0	1	0	1	0	0	0	0	1	1	1	0	0	0	0	0	1	0	1	0	0	0	0	0	0	0	0
Pontosphaera multipora	4	2	0	0	0	3	3	4	3	1	4	2	1	2	1	2	3	2	1	3	3	5	0	2	2	2	5	1	5	3	0	1	5	3	3
Pontosphaera pygmea	1	1	2	2	1	5	7	4	3	3	9	2	10	5	4	8	4	9	6	7	8	5	2	6	6	3	2	3	5	4	5	6	2	2	7
Pontosphaera puclheroides	2	0	1	0	1	2	0	1	1	1	0	1	0	4	0	4	1	2	1	3	2	2	3	4	2	0	2	2	1	2	0	0	0	1	1
Reticulofenestra circus	0	0	0	0	0	0	0	0	1	0	0	1	0	1	1	1	3	1	0	1	1	0	1	0	0	0	0	1	0	0	1	0	0	3	1
Reticulofenestra dictyoda (3-5µ)	46	34	38	55	41	27	41	27	41	12	13	22	21	28	22	25	25	16	25	15	20	22	23	24	32	24	16	21	28	21	13	21	21	19	17
Reticulofenestra dictyoda (5-7µ)	21	11	8	14	13	9	6	2	8	10	12	9	26	11	14	8	8	8	13	10	18	14	18	23	16	18	20	19	20	19	19	23	19	9	13
Reticulofenestra dictyoda (7-9µ)	2	0	0	1	0	0	0	0	0	1	0	1	1	1	0	1	0	0	0	0	0	1	0	0	0	0	0	0	0	0	0	0	0	0	0
Reticulofenestra flecwinzii (5-7µ)	4	7	6	7	4	3	3	1	2	1	0	0	1	1	2	1	1	0	0	0	0	1	0	0	0	0	0	0	1	3	0	2	0	3	4
Reticulofenestra flecwinzii (7-10µ)	5	2	2	0	2	0	2	1	1	3	0	1	1	2	0	2	0	1	1	0	1	1	1	0	0	1	0	3	1	0	0	0	1	0	2
Reticulofenestra flecwinzii (9-11µ)	1	0	0	0	0	0	0	0	0	0	1	1	1	0	0	0	0	1	0	0	2	0	0	0	0	1	2	0	0	0	0	0	0	0	0
Reticulofenestra hillae	2	4	3	5	4	1	2	0	0	0	1	0	1	1	1	1	2	2	4	2	1	1	4	3	1	3	6	2	3	3	4	3	3	3	3
Reticulofenestra lockeri (3-5µ)	2	4	6	6	3	2	1	8	4	6	9	2	5	6	5	5	7	7	5	3	6	5	2	5	3	5	6	3	1	1	3	4	7	3	1
Reticulofenestra lockeri (5-7µ)	7	5	13	9	9	7	12	9	4	3	2	4	4	4	1	2	5	1	4	1	4	3	3	1	4	6	3	3	3	9	1	3	2	3	2
Reticulofenestra lockeri (7-9µ)	0	0	0	0	0	0	0	0	0	0	0	0	0	0	1	0	1	0	0	0	0	0	0	0	0	0	0	0	0	0	0	0	0	0	0
Reticulofenestra rupeliensis	2	0	0	2	1	2	2	2	1	2	0	2	0	0	0	0	0	0	1	0	1	0	0	0	0	0	0	0	0	0	1	0	0	0	0
R. samodurovii (10-12µ)	1	1	1	1	1	4	2	3	4	5	1	0	0	1	3	0	2	0	1	0	1	4	1	0	0	1	0	1	0	0	0	1	0	1	0
R. samodurovii (12-14µ)	0	2	1	0	0	4	5	3	1	2	2	1	2	4	1	2	3	0	0	0	0	0	0	1	3	0	1	2	1	1	2	0	0	2	2
Reticulofenestra scrippsae (3-5µ)	0	1	1	2	3	1	1	0	0	0	0	0	0	0	0	0	0	0	0	0	0	0	0	0	0	0	0	0	0	4	0	0	0	0	0
Reticulofenestra scrippsae (5-7µ)	5	5	4	10	4	1	2	5	2	1	0	1	1	3	1	2	1	0	2	0	0	1	4	1	1	0	1	1	0	0	1	2	0	3	2
Reticulofenestra umbilicus	3	0	2	5	2	2	5	3	2	4	2	4	2	3	6	4	0	5	3	7	6	7	9	7	4	3	4	3	4	1	6	3	5	5	6
Reticulofenestra waedae (3-5µ)	0	0	0	0	0	0	0	0	0	0	0	1	1	0	0	2	2	0	0	0	2	1	0	1	0	0	0	0	0	0	0	0	0	0	1
Reticulofenestra waedae (5-7µ)	0	0	0	0	0	0	0	0	0	0	0	3	1	0	0	0	0	0	0	0	0	0	2	4	4	5	0	2	1	0	0	0	2	0	0
Reticulofenestra waedae (7-9µ)	0	0	0	0	0	0	0	0	0	0	0	0	0	0	0	0	0	0	0	0	0	0	3	0	0	0	0	0	0	0	0	0	0	0	0
Sphenolithus moriformis	2	2	3	0	3	1	2	1	1	1	0	3	0	1	3	3	1	2	1	1	2	0	2	1	2	2	1	1	0	1	1	1	1	2	0
Sphenolithus predistentus	4	6	6	5	3	5	2	2	2	3	2	5	6	4	3	4	0	6	2	3	5	1	4	4	4	2	2	0	1	1	5	2	1	1	2
Sphenolithus tribulosus	2	1	0	1	1	0	0	0	0	0	0	1	0	1	2	0	4	0	0	4	0	7	2	5	6	2	6	6	5	5	5	3	4	8	3
Zigrhrablithus bijugathus	1	0	0	2	0	3	3	2	1	2	3	1	4	0	2	2	1	0	4	2	2	1	2	0	2	1	1	2	0	1	1	3	2	2	0
Small placoliths	0	1	1	0	0	0	0	0	1	0	1	2	0	0	0	0	1	0	2	4	7	1	1	0	2	4	1	0	0	3	2	2	3	3	2
Small reticulofenestrids	65	119	112	84	116	117	142	134	105	124	159	163	162	141	152	144	135	147	155	161	148	126	123	149	114	133	145	126	139	116	112	120	115	128	147
Campylosphaera	0	0	0	0	0	0	0	0	0	0	0	0	0	0	0	0	0	0	0	0	0	0	0	0	0	0	1	1	1	2	2	0	1	1	1
Reticulofenestra reticulata	0	0	0	0	0	0	0	0	0	0	0	0	1	0	2	0	0	0	2	0	0	0	0	0	0	0	0	0	0	0	0	0	0	0	0
Neococcolithus minutus	0	0	0	0	0	0	0	1	0	0	0	0	0	0	0	0	1	0	0	0	0	0	0	0	0	0	0	0	0	0	0	0	0	0	0
Cruciplacolithus	0	0	0	0	1	0	0	0	0	0	0	0	0	1	0	0	0	0	0	0	0	0	0	0	0	0	0	0	0	0	0	0	0	0	0
Calcidiscus protoanulus	0	0	0	0	0	0	0	0	0	1	0	0	0	0	0	0	0	0	0	0	0	0	0	0	0	0	0	0	0	0	0	0	0	0	0
Transversopontis	2	0	0	0	0	0	0	0	0	0	0	0	0	0	0	0	0	0	0	0	0	0	0	0	0	0	0	0	0	0	0	0	0	0	0
Triquetrorhabdulus	1	0	0	0	0	0	0	0	0	0	0	0	0	0	0	0	0	0	0	0	0	0	0	0	0	0	0	0	0	0	0	0	0	0	0
TOTAL	324	320	314	336	332	314	395	321	312	322	320	334	330	318	346	343	328	306	345	315	362	334	306	333	320	313	326	329	315	340	314	322	308	316	326

Table IV f2. Calcareous nannofossil assemblage: relative abundances (%).

Depth (mbsf)	135.47	135.63	135.73	135.95	136.08	136.20	136.27	136.33	136.40	136.59	136.79	136.98	137.18	137.37	137.57	137.77	137.98	138.17	138.35	138.54	138.74	138.96	139.10	139.31	139.50	139.71	139.91	140.10	140.30	140.49	140.68	140.89	141.08	141.28	141.46
Blackites spp.	1.5	1.9	1.3	0.3	1.5	1.9	2.3	1.2	0.6	0.3	1.3	0.9	0.6	0.3	1.4	2.0	1.5	1.6	0.9	1.3	1.4	1.8	1.6	1.5	1.9	1.3	0.9	2.4	2.2	0.9	1.0	2.8	1.6	1.6	0.9
Bramlettei serraculoides	0	0	0	0	0	0	0	0	0.3	0	0	0	0	0	0	0	0.6	0.7	0	0.6	0	0	0	0	0	0	0	0.3	0	0	0	0	0	0	0.3
Chiasmolithus spp.	0	0	0	0	0	0	0	0	0	0	0	0	0	0	0	0	0	0	0.3	0	0	0	0.3	0	0.3	0	0	0	0	0	0	0	0	0.3	0
Chiasmolithus oamaruensis	0	0	0	0	0	0	0	0.3	0.3	0.3	0	0	0.3	0	0.3	0	0	0.3	0	0	0.3	0	0	0	0	0	0	0	0	0.3	0	0.3	0	0	0
Chaismolithus modestus	0	0	0	0	0	0	0	0	0	0	0	0	0	0.6	0	0	0	0	0	0	0	0	0	0	0	0	0	0	0	0	0	0	0	0	0
Chiasmolithus altus	0	0	0	0	0.3	0.3	0	0	0	0	0	0	0	0	0	0	0	0	0	0	0	0	0	0	0	0	0	0	0	0	0	0	0	0	0
Calcidiscus patecus	0	0	0	0	0	0	0	0	0	0	0	0	0	0	0	0	0	0	0	0	0	0	0	0	0	0	0.3	0.3	0	0	0	0	0	0	0
Clausicoccus obrutus	0.9	0.3	0.6	0.3	0.9	0.3	0.8	1.2	0.3	0.3	1.9	1.2	0.9	0.3	0.9	1.5	1.8	1.0	0.6	0.3	1.7	0	1.0	0.6	0.9	1.3	0	0.9	0.6	1.2	0.6	0.3	0.6	0.3	0.3
Clausicoccus fenestraus	0.3	0	0	0	0	0	0	0	0	0.6	0	0	0	0	0.3	0.3	0	0.7	0.3	0	0.3	0.3	0	0	0	0	0	0	0	0	0	0	0	0	0.6
Clausicoccus subdistichus	1.2	0.3	0	0	0.6	1.0	0.3	0.9	0.6	0	0.6	1.2	0.9	0	0.6	0.9	0.6	0	1.2	0.3	1.1	0	0.7	0.3	0.6	0.6	0.3	0	0	0.9	0	0.3	1.0	0.3	1.8
Coccolithus cachaoi (7-11µ)	0	0.3	0	0	0	0	0.3	0	0	0	0	0.3	0	0.3	0	0	0	0.3	0	0	0	0	0	0	0	0	0	0	0	0	0	0	0	0	0
Coccolithus eopelagicus	0.6	0.3	0	0	0	0	0.3	0	0	0	0	0	0	0	0	0	0	0	0	0	0	0	0	0	0	0	0	0	0	0	0	0	0	0	0.3
Coccolithus pelagicus (3-7µ)	3.4	2.5	3.2	3.6	4.5	3.5	2.3	1.9	2.9	3.7	3.1	2.4	1.8	1.9	3.2	2.9	3.0	3.9	3.5	2.5	2.8	1.2	2.0	1.5	3.1	2.2	3.4	1.8	3.2	4.1	3.2	3.7	1.9	3.2	4.0
Coccolithus pelagicus (7-11µ)	5.6	4.1	2.9	3.9	3.6	3.2	3.8	3.4	4.5	3.7	2.8	5.1	1.8	3.8	4.0	1.7	3.4	2.3	2.9	2.5	4.7	7.2	0.3	1.8	3.8	3.2	4.0	3.3	3.2	5.6	6.4	5.3	5.5	2.5	2.5
Coccolithus pelagicus (11-16µ)	0	0	0	0	0	1.3	0.5	0.3	0	0.6	0.3	0.6	0.3	0.3	0.6	0.3	0.3	1.0	0	0	0.3	0.3	0	0.3	0	0	0.3	0	0.3	0	0.3	0	0	0	0.6
Coccolithus formosus (7-11µ)	1.2	0.3	0.3	0.6	1.2	1.3	1.3	1.2	1.0	0.3	0.9	0.6	0.9	1.6	0.9	1.2	0.9	0.3	0.3	0.3	0.6	1.5	2.0	0.6	0.9	1.0	0.6	1.5	0.6	1.5	2.5	1.2	1.6	1.3	0.3
Coccolithus formosus (11-16µ)	0.3	0.3	0.3	0	0	0	0	0.3	0.3	0	0	0.3	0	0.6	0	0	0	0	0	0	0	0.3	0	0	0	0.3	0.3	0	0	0.3	0.3	0.6	0	0.3	0.3
Corpnocyclus bramlettei	0	0	0.6	0	0.6	1.0	0.5	0.9	0.6	0.3	0.6	0.3	0.6	0.6	1.2	0.3	0	0.3	0	1.0	0.8	0.6	0.3	1.2	1.3	1.0	0.6	0.6	1.6	1.2	1.0	0.6	1.0	0	1.2
Corpnocyclus netiscens	0	0	0	0	0	0	0	0	0	0	0	0	0	0	0	0.3	0	0.3	0	0	0	0	0	0	0	0	0	0	0	0	0	0	0	0	0
Cyclicargolithus sp. (3-5µ)	3.7	5.6	4.1	5.4	4.8	2.5	3.3	3.1	2.2	3.1	2.2	2.1	2.1	1.9	1.4	4.1	2.4	3.3	4.1	1.0	2.2	3.0	2.6	2.4	2.8	2.2	3.1	6.4	0.6	1.2	1.9	3.4	2.3	4.1	3.1
Cyclicargolithus sp. (5-7µ)	3.4	3.8	2.5	3.6	2.7	4.5	4.3	3.1	4.5	4.0	3.1	2.4	1.8	0.9	3.8	2.9	1.5	4.2	4.9	3.5	2.5	2.1	4.9	3.9	3.1	4.8	3.4	2.7	2.9	3.2	6.1	3.4	4.9	4.4	2.8
Cyclicargolithus sp. (7-9µ)	0.6	0	0	0.3	0	0	0	0	0	0	0	0	0.6	0.3	0	0	0	0	0.6	0	0	0	0	0	0	0	0	0.3	0	0	0	0	0	0	0
Cyclicargolithus floridanus (3-5µ)	1.9	1.3	1.0	2.1	0.3	0.3	0.5	0.3	1.0	1.2	0.3	0.9	0.9	0.9	0.6	0.6	0.6	1.6	1.7	1.0	1.4	1.5	1.0	0.9	0.9	1.0	0.3	1.5	1.6	1.2	1.0	0.3	1.3	0	1.2
Cyclicargolithus floridanus (5-7µ)	0.9	0	0	0.6	0.9	0	1.0	0	0.3	0.9	0.6	0.6	0	0	0.9	1.5	0.9	1.6	0.3	0.3	0.3	0.6	0.7	0	0.3	0	0.3	1.8	0.6	1.8	1.0	0	1.3	0.6	0.6
Cyclicargolithus floridanus (7-9µ)	0	0	0	0	0	0	0	0	0	0	0	0	0	0	0	0	0	0	0	0	0.3	0	0	0	0	0	0	0	0	0	0	0	0	0	0
Dictyococcites bisectus	2.8	0.9	1.6	3.0	1.5	1.3	2.0	2.2	2.2	2.2	1.3	0.3	1.2	0.6	1.2	2.0	2.1	0.3	1.7	1.0	1.4	1.2	0	0.3	0.9	0.3	0.6	0.9	0.6	1.2	1.0	1.6	0.6	1.6	1.2
Dictyococcited callidus	0.6	0.3	1.3	1.8	0.9	0.3	0.8	1.9	2.6	0.9	3.4	2.7	1.2	2.5	2.6	0.6	3.0	0.7	1.7	1.6	0.8	2.1	1.6	0.9	2.5	2.2	2.1	3.0	1.9	2.1	1.3	0.9	2.9	2.2	1.5
Dictyococcites daviesii	7.7	6.6	7.6	8.9	5.7	7.3	8.9	5.3	9.0	11.8	2.5	4.5	2.1	6.9	5.8	5.8	4.6	2.3	4.1	5.1	5.8	7.5	6.2	4.8	5.6	6.1	4.6	7.0	6.0	8.8	6.7	9.0	5.2	7.0	6.4
Dictyococcites stavensis	0.3	1.3	1.6	1.2	1.5	0.6	0.8	0.6	1.0	0.9	0.6	0.6	0.3	0.9	0.9	0.9	1.2	0.7	0.3	0	0.6	0.6	1.0	0.6	1.6	0.3	0.3	0.3	0.6	2.4	1.6	0.9	1.3	1.6	0.6
Dictyococcites stavensis (>14µ)	0.6	0	0.3	0	0	0.3	0	0	0	0	0	0.3	0.6	0	0	0.3	0.3	0	0	0.3	0.3	0.3	0.3	0.3	0	0.3	0.6	0.3	0	0	0	0	0.3	0	0
Discoaster spp.	1.9	0.3	0.3	0.3	0	0.3	0.3	0	0.3	0.6	0.3	0.6	0.6	0.6	0	0.3	0.6	0.3	0	0.3	0.6	0	0.3	0	0.3	0.3	0.3	0	0	0	0.6	0.3	1.0	0	0.3
Discoaster barbadiensis	0	0	0	0	0	0	0	0	0.6	0	0	0.3	0	0	0	0.3	0	0	0.3	0	0.6	0.6	0.3	0	0	0	0	0	0	0.3	0	0	0	0	0
Discoaster deflandrei	0	0	0	0	0	0	0	0.9	0	0.3	0	0	0	0	0.3	0	0	0	0	0	0	0	0	0	0	0	0	0	0	0	0	0	0	0	0	0
Discoaster saipanensis	0	0	0	0	0	0	0	0	0.6	0	0	0	0.3	0	0.6	0.3	0.3	0.3	0.3	0.3	0	0.3	0	0	0	0	0.3	0	0	0	0.3	0	0	0.3	0
Discoaster nodifer	0	0.3	0	0.3	0.3	1.3	0	0.3	0.3	0.3	0.6	0.3	0	0	0	0	0.6	0	0.3	0	0	0	0	0	0	0	0	0	0	0.3	0.3	0	0	0.6	0
Discoaster tanii	0	0.3	0	0	0	0	0	0	0	0	0	0	0	0	0	0	0	0	0	0	0	0	0	0	0	0	0	0	0	0	0	0	0	0	0
Hayella situliformis	0.3	0	0	0	0.6	0	0	0	0	0.3	0	0	0	0	0	0	0	0	0	0	0	0	0	0	0	0	0	0	0	0	0	0	0	0	0	0
Helicosphaera bramlettei	0.3	0	0	0	0.6	0.3	0.5	0.9	0.3	0.3	0.6	0	0	0	0.9	0.3	0.3	0.7	0.3	0.3	0.6	0.6	0.7	0.6	0.9	0	1.5	0.6	0.6	0.3	0.6	0.6	0.6	0.3	0
Helicosphaera compacta	0.3	0.3	0.6	0.3	0.6	0.6	1.0	0.6	0	0.6	0.3	0.6	0.6	0.6	0	0	0	0.7	0.3	0.6	0.6	0.6	0.7	0.6	0.6	0.6	0.9	0.6	0.6	0.3	0.3	0	0.6	0.3	0.6
Helicosphaera euphratis	0	0	0.3	0	0	0	0	0	0	0	0	0	0.6	0	0	0	0	0	0.3	0.6	0	0	0.3	0.3	0	0	0.3	0	0.3	0	0.3	0	0	0.3	0
Helicosphaera seminulum	0	0	0	0	0	0	0	0	0	0	0.3	0	0	0	0	0	0	0	0	0	0	0	0	0	0	0	0	0	0	0	0	0	0	0	0

Depth (mbsf)	135.47	135.63	135.73	135.95	136.08	136.20	136.27	136.33	136.40	136.59	136.79	136.98	137.18	137.37	137.57	137.77	137.98	138.17	138.35	138.54	138.74	138.96	139.10	139.31	139.50	139.71	139.91	140.10	140.30	140.49	140.68	140.89	141.08	141.28	141.46
Isthmolithus recurvus	2.5	3.8	2.2	0.9	2.1	3.2	2.5	2.5	3.2	4.0	3.1	0.9	2.4	2.5	2.9	3.8	3.7	1.6	1.4	3.2	2.2	3.3	2.6	4.2	1.9	1.6	1.5	1.5	1.9	2.1	3.2	2.2	1.3	1.9	0.9
Lanthernithus minutus	0	0	0	0	0	0	0.5	0	0	0	0	0	0.3	0	0	0	0.9	0	0.3	0	0	0	0	0	0.3	0	0	0	0	0	0.3	0	0	0	0
Pedinolcyclus	0	0	0.3	0	0	0	0	0	0	0.3	0	0.3	0	0	0	0	0.3	0.3	0.3	0	0	0	0	0	0.3	0	0.3	0	0	0	0	0	0	0	0
Pontosphaera multipora	1.2	0.6	0	0	0	1.0	0.8	1.2	1.0	0.3	1.3	0.6	0.3	0.6	0.3	0.6	0.9	0.7	0.3	1.0	0.8	1.5	0	0.6	0.6	0.6	1.5	0.3	1.6	0.9	0	0.3	1.6	0.9	0.9
Pontosphaera pygmea	0.3	0.3	0.6	0.6	0.3	1.6	1.8	1.2	1.0	0.9	2.8	0.6	3.0	1.6	1.2	2.3	1.2	2.9	1.7	2.2	2.2	1.5	0.7	1.8	1.9	1.0	0.6	0.9	1.6	1.2	1.6	1.9	0.6	0.6	2.1
Pontosphaera puclheroides	0.6	0	0.3	0	0.3	0.6	0	0.3	0.3	0.3	0	0.3	0	1.3	0	1.2	0.3	0.7	0.3	1.0	0.6	0.6	1.0	1.2	0.6	0	0.6	0.6	0.3	0.6	0	0	0	0.3	0.3
Reticulofenestra circus	0	0	0	0	0	0	0	0	0.3	0	0	0.3	0	0.3	0.3	0.3	0.9	0.3	0	0.3	0.3	0	0.3	0	0	0	0	0.3	0	0	0.3	0	0	0.9	0.3
Reticulofenestra dictyoda (3-5µ)	14.2	10.6	12.1	16.4	12.3	8.6	10.4	8.4	13.1	3.7	4.1	6.6	6.4	8.8	6.4	7.3	7.6	5.2	7.2	4.8	5.5	6.6	7.5	7.2	1 0	7.7	4.9	6.4	8.9	6.2	4.1	6.5	6.8	6.0	5.2
Reticulofenestra dictyoda (5-7µ)	6.5	3.4	2.5	4.2	3.9	2.9	1.5	0.6	2.6	3.1	3.8	2.7	7.9	3.5	4.0	2.3	2.4	2.6	3.8	3.2	5.0	4.2	5.9	6.9	5.0	5.8	6.1	5.8	6.3	5.6	6.1	7.1	6.2	2.8	4.0
Reticulofenestra dictyoda (7-9µ)	0.6	0	0	0.3	0	0	0	0	0	0.3	0	0.3	0.3	0.3	0	0.3	0	0	0	0	0	0.3	0	0	0	0	0	0	0	0	0	0	0	0	0
Reticulofenestra flecwinzii (5-7µ)	1.2	2.2	1.9	2.1	1.2	1.0	0.8	0.3	0.6	0.3	0	0	0.3	0.3	0.6	0.3	0.3	0	0	0	0	0.3	0	0	0	0	0	0	0.3	0.9	0	0.6	0	0.9	1.2
Reticulofenestra flecwinzii (7-10µ)	1.5	0.6	0.6	0	0.6	0	0.5	0.3	0.3	0.9	0	0.3	0.3	0.6	0	0.6	0	0.3	0.3	0	0.3	0.3	0.3	0	0	0.3	0	0.9	0.3	0	0	0	0.3	0	0.6
Reticulofenestra flecwinzii (9-11µ)	0.3	0	0	0	0	0	0	0	0	0	0.3	0.3	0.3	0	0	0	0	0.3	0	0	0.6	0	0	0	0	0.3	0.6	0	0	0	0	0	0	0	0
Reticulofenestra hillae	0.6	1.3	1.0	1.5	1.2	0.3	0.5	0	0	0	0.3	0	0.3	0.3	0.3	0.3	0.6	0.7	1.2	0.6	0.3	0.3	1.3	0.9	0.3	1.0	1.8	0.6	1.0	0.9	1.3	0.9	1.0	0.9	0.9
Reticulofenestra lockeri (3-5µ)	0.6	1.3	1.9	1.8	0.9	0.6	0.3	2.5	1.3	1.9	2.8	0.6	1.5	1.9	1.4	1.5	2.1	2.3	1.4	1.0	1.7	1.5	0.7	1.5	0.9	1.6	1.8	0.9	0.3	0.3	1.0	1.2	2.3	0.9	0.3
Reticulofenestra lockeri (5-7µ)	2.2	1.6	4.1	2.7	2.7	2.2	3.0	2.8	1.3	0.9	0.6	1.2	1.2	1.3	0.3	0.6	1.5	0.3	1.2	0.3	1.1	0.9	1.0	0.3	1.3	1.9	0.9	0.9	1.0	2.6	0.3	0.9	0.6	0.9	0.6
Reticulofenestra lockeri (7-9µ)	0	0	0	0	0	0	0	0	0	0	0	0	0	0	0.3	0	0.3	0	0	0	0	0	0	0	0	0	0	0	0	0	0	0	0	0	0
Reticulofenestra rupeliensis	0.6	0	0	0.6	0.3	0.6	0.5	0.6	0.3	0.6	0	0.6	0	0	0	0	0	0	0.3	0	0.3	0	0	0	0	0	0	0	0	0	0.3	0	0	0	0
Reticulofenestra samodurovii (10-12µ)	0.3	0.3	0.3	0.3	0.3	1.3	0.5	0.9	1.3	1.6	0.3	0	0	0.3	0.9	0	0.6	0	0.3	0	0.3	1.2	0.3	0	0	0.3	0	0.3	0	0	0	0.3	0	0.3	0
Reticulofenestra samodurovii (12-14µ)	0	0.6	0.3	0	0	1.3	1.3	0.9	0.3	0.6	0.6	0.3	0.6	1.3	0.3	0.6	0.9	0	0	0	0	0	0	0.3	0.9	0	0.3	0.6	0.3	0.3	0.6	0	0	0.6	0.6
Reticulofenestra scrippsae (3-5µ)	0	0.3	0.3	0.6	0.9	0.3	0.3	0	0	0	0	0	0	0	0	0	0	0	0	0	0	0	0	0	0	0	0	0	0	1.2	0	0	0	0	0
Reticulofenestra scrippsae (5-7µ)	1.5	1.6	1.3	3.0	1.2	0.3	0.5	1.6	0.6	0.3	0	0.3	0.3	0.9	0.3	0.6	0.3	0	0.6	0	0	0.3	1.3	0.3	0.3	0	0.3	0.3	0	0	0.3	0.6	0	0.9	0.6
Reticulofenestra umbilicus	0.9	0	0.6	1.5	0.6	0.6	1.3	0.9	0.6	1.2	0.6	1.2	0.6	0.9	1.7	1.2	0	1.6	0.9	2.2	1.7	2.1	2.9	2.1	1.3	1.0	1.2	0.9	1.3	0.3	1.9	0.9	1.6	1.6	1.8
Reticulofenestra waedae (3-5 m)	0	0	0	0	0	0	0	0	0	0	0	0.3	0.3	0	0	0.6	0.6	0	0	0	0.6	0.3	0	0.3	0	0	0	0	0	0	0	0	0	0	0.3
Reticulofenestra waedae (5-7)	0	0	0	0	0	0	0	0	0	0	0	0.9	0.3	0	0	0	0	0	0	0	0	0	0.7	1.2	1.3	1.6	0	0.6	0.3	0	0	0	0.6	0	0
Reticulofenestra waedae (7-9)	0	0	0	0	0	0	0	0	0	0	0	0	0	0	0	0	0	0	0	0	0	0	1.0	0	0	0	0	0	0	0	0	0	0	0	0
Sphenolithus moriformis	0.6	0.6	1.0	0	0.9	0.3	0.5	0.3	0.3	0.3	0	0.9	0	0.3	0.9	0.9	0.3	0.7	0.3	0.3	0.6	0	0.7	0.3	0.6	0.6	0.3	0.3	0	0.3	0.3	0.3	0.3	0.6	0
Sphenolithus predistentus	1.2	1.9	1.9	1.5	0.9	1.6	0.5	0.6	0.6	0.9	0.6	1.5	1.8	1.3	0.9	1.2	0	2.0	0.6	1.0	1.4	0.3	1.3	1.2	1.3	0.6	0.6	0	0.3	0.3	1.6	0.6	0.3	0.3	0.6
Sphenolithus tribulosus	0.6	0.3	0	0.3	0.3	0	0	0	0	0	0	0.3	0	0.3	0.6	0	1.2	0	0	1.3	0	2.1	0.7	1.5	1.9	0.6	1.8	1.8	1.6	1.5	1.6	0.9	1.3	2.5	0.9
Zigrhrablithus bijugathus	0.3	0	0	0.6	0	1.0	0.8	0.6	0.3	0.6	0.9	0.3	1.2	0	0.6	0.6	0.3	0	1.2	0.6	0.6	0.3	0.7	0	0.6	0.3	0.3	0.6	0	0.3	0.3	0.9	0.6	0.6	0
Small placoliths	0	0.3	0.3	0	0	0	0	0	0.3	0	0.3	0.6	0	0	0	0	0.3	0	0.6	1.3	1.9	0.3	0.3	0	0.6	1.3	0.3	0	0	0.9	0.6	0.6	1.0	0.9	0.6
Small reticulofenestrids	20.1	37.2	35.7	25.0	34.9	37.3	35.9	41.7	33.7	38.5	49.7	48.8	49.1	44.3	43.9	42.0	41.2	48.0	44.9	51.1	40.9	37.7	40.2	44.7	35.6	42.5	44.5	38.3	44.1	34.1	35.7	37.3	37.3	40.5	45.1
Campylosphaera	0	0	0	0	0	0	0	0	0	0	0	0	0	0	0	0	0	0	0	0	0	0	0	0	0	0	0.3	0.3	0.3	0.6	0.6	0	0.3	0.3	0.3
Neococcolithus minutus	0	0	0	0	0	0	0	0.3	0	0	0	0	0	0	0	0	0.3	0	0	0	0	0	0	0	0	0	0	0	0	0	0	0	0	0	0	0
Cruciplacolithus	0	0	0	0	0.3	0	0	0	0	0	0	0	0	0.3	0	0	0	0	0	0	0	0	0	0	0	0	0	0	0	0	0	0	0	0	0	0
Calcidiscus protoanulus	0	0	0	0	0	0	0	0	0	0.3	0	0	0	0	0	0	0	0	0	0	0	0	0	0	0	0	0	0	0	0	0	0	0	0	0	0
Transversopontis	0.6	0	0	0	0	0	0	0	0	0	0	0	0	0	0	0	0	0	0	0	0	0	0	0	0	0	0	0	0	0	0	0	0	0	0	0
Triquetrorhabdulus	0.3	0	0	0	0	0	0	0	0	0	0	0	0	0	0	0	0	0	0	0	0	0	0	0	0	0	0	0	0	0	0	0	0	0	0	0

Table IV f3. Calcareous nannofossil assemblage: Absolute abundances (N g^{-1}).

Depth (mbsf)	135.47	135.63	135.73	135.95	136.08	136.20	136.27	136.33	136.40	136.59	136.79	136.98	137.18	137.37	137.57	137.77	137.98	138.17	138.35	138.54	138.74	138.96	139.10	139.31	139.50	139.71	139.91	140.10	140.30	140.49	140.68	140.89	141.08	141.28	141.46
Blackites spp.	5E+07	1E+08	8E+07	9E+06	9E+07	1E+08	2E+08	6E+07	3E+07	1E+07	8E+07	5E+07	5E+07	2E+07	1E+08	1E+08	1E+08	1E+08	6E+07	9E+07	9E+07	9E+07	7E+07	1E+08	1E+08	8E+07	6E+07	2E+08	1E+08	4E+07	3E+07	1E+08	8E+07	9E+07	6E+07
Bramlettei serraculoides	0	0	0	0	0	0	0	0	2E+07	0	0	0	0	0	0	0	4E+07	4E+07	0	5E+07	0	0	0	0	0	0	0	2E+07	0	0	0	0	0	0	2E+07
Chiasmolithus spp.	0	0	0	0	0	0	0	0	0	0	0	0	0	0	0	0	0	0	2E+07	0	0	0	1E+07	0	2E+07	0	0	0	0	0	0	0	2E+07	0
Chiasmolithus oamaruensis	0	0	0	0	0	0	0	2E+07	2E+07	1E+07	0	0	2E+07	0	2E+07	0	0	2E+07	0	0	2E+07	0	0	0	0	0	0	0	0	1E+07	0	1E+07	0	0	0
Chaismolithus modestus	0	0	0	0	0	0	0	0	0	0	0	0	0	4E+07	0	0	0	0	0	0	0	0	0	0	0	0	0	0	0	0	0	0	0	0	0
Chiasmolithus altus	0	0	0	0	2E+07	2E+07	0	0	0	0	0	0	0	0	0	0	0	0	0	0	0	0	0	0	0	0	0	0	0	0	0	0	0	0	0
Calcidiscus patecus	0	0	0	0	0	0	0	0	0	0	0	0	0	0	0	0	0	0	0	0	0	0	0	0	0	0	2E+07	2E+07	0	0	0	0	0	0	0
Clausicoccus obrutus	3E+07	2E+07	4E+07	9E+06	5E+07	2E+07	5E+07	6E+07	2E+07	1E+07	1E+08	7E+07	7E+07	2E+07	6E+07	1E+08	1E+08	6E+07	4E+07	2E+07	1E+08	0	4E+07	5E+07	5E+07	8E+07	0	6E+07	4E+07	6E+07	2E+07	1E+07	3E+07	2E+07	2E+07
Clausicoccus fenestraus	1E+07	0	0	0	0	0	0	0	0	3E+07	0	0	0	0	2E+07	2E+07	0	4E+07	2E+07	0	2E+07	2E+07	0	0	0	0	0	0	0	0	0	0	0	0	4E+07
Clausicoccus subdistichus	4E+07	2E+07	0	0	4E+07	6E+07	2E+07	5E+07	3E+07	0	4E+07	7E+07	7E+07	0	4E+07	6E+07	4E+07	0	8E+07	2E+07	7E+07	0	3E+07	2E+07	4E+07	4E+07	2E+07	0	0	4E+07	0	1E+07	5E+07	2E+07	1E+08
Coccolithus cachaoi (7-11)	0	2E+07	0	0	0	0	2E+07	0	0	0	0	2E+07	0	2E+07	0	0	0	2E+07	0	0	0	0	0	0	0	0	0	0	0	0	0	0	0	0	0
Coccolithus eopelagicus	2E+07	2E+07	0	0	0	0	2E+07	0	0	0	0	0	0	0	0	0	0	0	0	0	0	0	0	0	0	0	0	0	0	0	0	0	0	0	2E+07
Coccolithus pelagicus (3-7)	1E+08	1E+08	2E+08	1E+08	3E+08	2E+08	2E+08	9E+07	1E+08	2E+08	2E+08	1E+08	1E+08	1E+08	2E+08	2E+08	2E+08	2E+08	2E+08	2E+08	2E+08	6E+07	8E+07	1E+08	2E+08	1E+08	2E+08	1E+08	2E+08	2E+08	1E+08	2E+08	1E+08	2E+08	3E+08
Coccolithus pelagicus (7-11)	2E+08	2E+08	2E+08	1E+08	2E+08	2E+08	3E+08	2E+08	2E+08	2E+08	2E+08	3E+08	1E+08	2E+08	3E+08	1E+08	2E+08	1E+08	2E+08	2E+08	3E+08	4E+08	1E+07	1E+08	2E+08	2E+08	2E+08	2E+08	2E+08	3E+08	2E+08	3E+08	3E+08	1E+08	2E+08
Coccolithus pelagicus (11-16)	0	0	0	0	0	8E+07	3E+07	2E+07	0	3E+07	2E+07	3E+07	2E+07	2E+07	4E+07	2E+07	2E+07	6E+07	0	0	2E+07	2E+07	0	2E+07	0	0	2E+07	0	2E+07	0	1E+07	0	0	0	4E+07
Coccolithus formosus (7-11)	4E+07	2E+07	2E+07	2E+07	7E+07	8E+07	9E+07	6E+07	5E+07	1E+07	6E+07	3E+07	7E+07	9E+07	6E+07	8E+07	6E+07	2E+07	2E+07	2E+07	4E+07	8E+07	8E+07	5E+07	5E+07	6E+07	4E+07	1E+08	4E+07	7E+07	9E+07	6E+07	8E+07	7E+07	2E+07
Coccolithus formosus (11-16)	1E+07	2E+07	2E+07	0	0	0	0	2E+07	2E+07	0	0	2E+07	0	4E+07	0	0	0	0	0	0	0	2E+07	0	0	0	2E+07	2E+07	0	0	1E+07	1E+07	3E+07	0	2E+07	2E+07
Corpnocyclus bramlettei	0	0	4E+07	0	4E+07	6E+07	3E+07	5E+07	3E+07	1E+07	4E+07	2E+07	5E+07	4E+07	8E+07	2E+07	0	2E+07	0	7E+07	5E+07	3E+07	1E+07	9E+07	7E+07	6E+07	4E+07	4E+07	1E+08	6E+07	3E+07	3E+07	5E+07	0	8E+07
Corpnocyclus netiscens	0	0	0	0	0	0	0	0	0	0	0	0	0	0	0	2E+07	0	2E+07	0	0	0	0	0	0	0	0	0	0	0	0	0	0	0	0	0
Cyclicargolithus sp. *(3-5)*	1E+08	3E+08	3E+08	2E+08	3E+08	2E+08	2E+08	2E+08	1E+08	1E+08	1E+08	1E+08	2E+08	1E+08	1E+08	3E+08	2E+08	2E+08	3E+08	7E+07	1E+08	2E+08	1E+08	2E+08	2E+08	1E+08	2E+08	4E+08	4E+07	6E+07	7E+07	2E+08	1E+08	2E+08	2E+08
Cyclicargolithus sp. *(5-7)*	1E+08	2E+08	2E+08	1E+08	2E+08	3E+08	3E+08	2E+08	2E+08	2E+08	2E+08	1E+08	1E+08	5E+07	3E+08	2E+08	1E+08	3E+08	3E+08	3E+08	2E+08	1E+08	2E+08	3E+08	2E+08	3E+08	2E+08	2E+08	2E+08	2E+08	2E+08	2E+08	3E+08	2E+08	2E+08
Cyclicargolithus sp. *(7-9)*	2E+07	0	0	9E+06	0	0	0	0	0	0	0	0	5E+07	2E+07	0	0	0	0	4E+07	0	0	0	0	0	0	0	0	2E+07	0	0	0	0	0	0	0
Cyclicargolithus floridanus (3-5)	6E+07	7E+07	6E+07	6E+07	2E+07	2E+07	3E+07	2E+07	5E+07	6E+07	2E+07	5E+07	7E+07	5E+07	4E+07	4E+07	4E+07	1E+08	1E+08	7E+07	9E+07	8E+07	4E+07	7E+07	5E+07	6E+07	2E+07	1E+08	1E+08	6E+07	3E+07	1E+07	7E+07	0	8E+07
Cyclicargolithus floridanus (5-7)	3E+07	0	0	2E+07	5E+07	0	7E+07	0	2E+07	4E+07	4E+07	3E+07	0	0	6E+07	1E+08	6E+07	1E+08	2E+07	2E+07	2E+07	3E+07	3E+07	0	2E+07	0	2E+07	1E+08	4E+07	9E+07	3E+07	0	7E+07	4E+07	4E+07
Cyclicargolithus floridanus (7-9)	0	0	0	0	0	0	0	0	0	0	0	0	0	0	0	0	0	0	0	0	2E+07	0	0	0	0	0	0	0	0	0	0	0	0	0	0
Dictyococcites bisectus	9E+07	5E+07	1E+08	9E+07	9E+07	8E+07	1E+08	1E+08	1E+08	1E+08	8E+07	2E+07	1E+08	4E+07	8E+07	1E+08	1E+08	2E+07	1E+08	7E+07	9E+07	6E+07	0	2E+07	5E+07	2E+07	4E+07	6E+07	4E+07	6E+07	3E+07	7E+07	3E+07	9E+07	8E+07
Dictyococcited callidus	2E+07	2E+07	8E+07	5E+07	5E+07	2E+07	5E+07	9E+07	1E+08	4E+07	2E+08	2E+08	1E+08	1E+08	2E+08	4E+07	2E+08	4E+07	1E+08	1E+08	5E+07	1E+08	7E+07	7E+07	1E+08	1E+08	1E+08	2E+08	1E+08	1E+08	4E+07	4E+07	2E+08	1E+08	1E+08
Dictyococcites daviesii	3E+08	4E+08	5E+08	3E+08	3E+08	4E+08	6E+08	3E+08	4E+08	5E+08	2E+08	3E+08	2E+08	4E+08	4E+08	4E+08	3E+08	1E+08	3E+08	4E+08	4E+08	4E+08	3E+08	4E+08	3E+08	4E+08	3E+08	4E+08	4E+08	4E+08	2E+08	4E+08	3E+08	4E+08	4E+08
Dictyococcites stavensis	1E+07	7E+07	1E+08	4E+07	9E+07	4E+07	5E+07	3E+07	5E+07	4E+07	4E+07	3E+07	2E+07	5E+07	6E+07	6E+07	8E+07	4E+07	2E+07	0	4E+07	3E+07	4E+07	5E+07	9E+07	2E+07	2E+07	2E+07	4E+07	1E+08	6E+07	4E+07	7E+07	9E+07	4E+07
Dictyococcites stavensis (>14)	2E+07	0	2E+07	0	0	2E+07	0	0	0	0	0	2E+07	5E+07	0	0	2E+07	2E+07	0	0	2E+07	2E+07	2E+07	1E+07	2E+07	0	2E+07	4E+07	2E+07	0	0	0	0	2E+07	0	0
Discoaster spp.	6E+07	2E+07	2E+07	9E+06	0	2E+07	2E+07	0	2E+07	3E+07	2E+07	3E+07	5E+07	4E+07	0	2E+07	4E+07	2E+07	0	2E+07	4E+07	0	1E+07	0	2E+07	2E+07	2E+07	0	0	0	2E+07	1E+07	5E+07	0	2E+07
Discoaster barbadiensis	0	0	0	0	0	0	0	0	3E+07	0	0	2E+07	0	0	0	2E+07	0	0	2E+07	0	4E+07	3E+07	1E+07	0	0	0	0	0	0	1E+07	0	0	0	0	0
Discoaster deflandrei	0	0	0	0	0	0	0	5E+07	0	1E+07	0	0	0	0	2E+07	0	0	0	0	0	0	0	0	0	0	0	0	0	0	0	0	0	0	0	0
Discoaster saipanensis	0	0	0	0	0	0	0	0	3E+07	0	0	0	2E+07	0	4E+07	2E+07	2E+07	2E+07	2E+07	2E+07	0	2E+07	0	0	0	2E+07	0	0	0	1E+07	0	0	0	2E+07	0
Discoaster nodifer	0	2E+07	0	9E+06	2E+07	8E+07	0	2E+07	2E+07	1E+07	4E+07	2E+07	0	0	0	0	4E+07	0	2E+07	0	0	0	0	0	0	0	0	0	0	1E+07	1E+07	0	0	4E+07	0
Discoaster tanii	0	2E+07	0	0	0	0	0	0	0	0	0	0	0	0	0	0	0	0	0	0	0	0	0	0	0	0	0	0	0	0	0	0	0	0	0
Hayella situliformis	1E+07	0	0	0	4E+07	0	0	0	0	1E+07	0	0	0	0	0	0	0	0	0	0	0	0	0	0	0	0	0	0	0	0	0	0	0	0	0
Helicosphaera bramlettei	1E+07	0	0	0	4E+07	2E+07	3E+07	5E+07	2E+07	1E+07	4E+07	0	0	0	6E+07	2E+07	2E+07	4E+07	2E+07	2E+07	4E+07	3E+07	3E+07	5E+07	5E+07	0	9E+07	4E+07	4E+07	1E+07	2E+07	3E+07	3E+07	2E+07	0

Depth (mbsf)	135.47	135.63	135.73	135.95	136.08	136.20	136.27	136.33	136.40	136.59	136.79	136.98	137.18	137.37	137.57	137.77	137.98	138.17	138.35	138.54	138.74	138.96	139.10	139.31	139.50	139.71	139.91	140.10	140.30	140.49	140.68	140.89	141.08	141.28	141.46
Helicosphaera compacta	1E+07	2E+07	4E+07	9E+06	4E+07	4E+07	7E+07	3E+07	0	3E+07	2E+07	3E+07	5E+07	4E+07	0	0	0	4E+07	2E+07	5E+07	4E+07	3E+07	3E+07	5E+07	4E+07	4E+07	6E+07	4E+07	4E+07	1E+07	1E+07	0	3E+07	2E+07	4E+07
Helicosphaera euphratis	0	0	2E+07	0	0	0	0	0	0	0	0	0	5E+07	0	0	0	0	0	2E+07	5E+07	0	0	1E+07	2E+07	0	0	2E+07	0	2E+07	0	1E+07	0	0	2E+07	0
Helicosphaera seminulum	0	0	0	0	0	0	0	0	0	0	2E+07	0	0	0	0	0	0	0	0	0	0	0	0	0	0	0	0	0	0	0	0	0	0	0	0
Isthmolithus recurvus	8E+07	2E+08	1E+08	3E+07	1E+08	2E+08	2E+08	1E+08	2E+08	2E+08	2E+08	5E+07	2E+08	1E+08	2E+08	3E+08	2E+08	1E+08	9E+07	2E+08	1E+08	2E+08	1E+08	3E+08	1E+08	9E+07	9E+07	1E+08	1E+08	1E+08	1E+08	1E+08	7E+07	1E+08	6E+07
Lanthernithus minutus	0	0	0	0	0	0	3E+07	0	0	0	0	0	2E+07	0	0	0	6E+07	0	2E+07	0	0	0	0	0	2E+07	0	0	0	0	0	1E+07	0	0	0	0
Pedinolcyclus	0	0	2E+07	0	0	0	0	0	0	1E+07	0	2E+07	0	0	0	0	2E+07	2E+07	2E+07	0	0	0	0	0	2E+07	0	2E+07	0	0	0	0	0	0	0	0
Pontosphaera multipora	4E+07	4E+07	0	0	0	6E+07	5E+07	6E+07	5E+07	1E+07	8E+07	3E+07	2E+07	4E+07	2E+07	4E+07	6E+07	4E+07	2E+07	7E+07	5E+07	8E+07	0	5E+07	4E+07	4E+07	9E+07	2E+07	1E+08	4E+07	0	1E+07	8E+07	5E+07	6E+07
Pontosphaera pygmea	1E+07	2E+07	4E+07	2E+07	2E+07	9E+07	1E+08	6E+07	5E+07	4E+07	2E+08	3E+07	2E+08	9E+07	8E+07	2E+08	8E+07	2E+08	1E+08	2E+08	1E+08	8E+07	3E+07	1E+08	1E+08	6E+07	4E+07	6E+07	1E+08	6E+07	6E+07	9E+07	3E+07	4E+07	1E+08
Pontosphaera puclheroides	2E+07	0	2E+07	0	2E+07	4E+07	0	2E+07	2E+07	1E+07	0	2E+07	0	7E+07	0	8E+07	2E+07	4E+07	2E+07	7E+07	4E+07	3E+07	4E+07	9E+07	4E+07	0	4E+07	4E+07	2E+07	3E+07	0	0	0	2E+07	2E+07
Reticulofenestra circus	0	0	0	0	0	0	0	0	2E+07	0	0	2E+07	0	2E+07	2E+07	2E+07	6E+07	2E+07	0	2E+07	2E+07	0	1E+07	0	0	0	0	2E+07	0	0	1E+07	0	0	5E+07	2E+07
Reticulofenestra dictyoda (3-5)	5E+08	6E+08	8E+08	5E+08	7E+08	5E+08	7E+08	4E+08	6E+08	2E+08	3E+08	4E+08	5E+08	5E+08	4E+08	5E+08	5E+08	3E+08	5E+08	3E+08	4E+08	3E+08	3E+08	6E+08	6E+08	5E+08	3E+08	4E+08	5E+08	3E+08	1E+08	3E+08	4E+08	3E+08	3E+08
Reticulofenestra dictyoda (5-7)	2E+08	2E+08	2E+08	1E+08	2E+08	2E+08	1E+08	3E+07	1E+08	1E+08	3E+08	2E+08	6E+08	2E+08	3E+08	2E+08	2E+08	2E+08	2E+08	2E+08	2E+08	2E+08	2E+08	5E+08	3E+08	3E+08	4E+08	4E+08	4E+08	3E+08	2E+08	3E+08	3E+08	2E+08	3E+08
Reticulofenestra dictyoda (7-9)	2E+07	0	0	9E+06	0	0	0	0	0	1E+07	0	2E+07	2E+07	2E+07	0	2E+07	0	0	0	0	0	2E+07	0	0	0	0	0	0	0	0	0	0	0	0	0
Reticulofenestra flecwinzii (5-7)	4E+07	1E+08	1E+08	6E+07	7E+07	6E+07	5E+07	2E+07	3E+07	1E+07	0	0	2E+07	2E+07	4E+07	2E+07	2E+07	0	0	0	0	2E+07	0	0	0	0	0	0	2E+07	4E+07	0	3E+07	0	5E+07	8E+07
Reticulofenestra flecwinzii (7-10)	5E+07	4E+07	4E+07	0	4E+07	0	3E+07	2E+07	2E+07	4E+07	0	2E+07	2E+07	4E+07	0	4E+07	0	2E+07	2E+07	0	2E+07	2E+07	1E+07	0	0	2E+07	0	6E+07	2E+07	0	0	0	2E+07	0	4E+07
Reticulofenestra flecwinzii (9-11)	1E+07	0	0	0	0	0	0	0	0	0	2E+07	2E+07	2E+07	0	0	0	0	2E+07	0	0	4E+07	0	0	0	0	2E+07	4E+07	0	0	0	0	0	0	0	0
Reticulofenestra hillae	2E+07	7E+07	6E+07	4E+07	7E+07	2E+07	3E+07	0	0	0	2E+07	0	2E+07	2E+07	2E+07	2E+07	4E+07	4E+07	8E+07	5E+07	2E+07	2E+07	5E+07	7E+07	2E+07	6E+07	1E+08	4E+07	6E+07	4E+07	4E+07	4E+07	5E+07	5E+07	6E+07
Reticulofenestra lockeri (3-5)	2E+07	7E+07	1E+08	5E+07	5E+07	4E+07	2E+07	1E+08	6E+07	9E+07	2E+08	3E+07	1E+08	1E+08	1E+08	1E+08	1E+08	1E+08	9E+07	7E+07	1E+08	8E+07	3E+07	1E+08	5E+07	9E+07	1E+08	6E+07	2E+07	1E+07	3E+07	6E+07	1E+08	5E+07	2E+07
Reticulofenestra lockeri (5-7)	7E+07	9E+07	3E+08	8E+07	2E+08	1E+08	2E+08	1E+08	6E+07	4E+07	4E+07	7E+07	1E+08	7E+07	2E+07	4E+07	1E+08	2E+07	8E+07	2E+07	7E+07	5E+07	4E+07	2E+07	7E+07	1E+08	6E+07	6E+07	6E+07	1E+08	1E+07	4E+07	3E+07	5E+07	4E+07
Reticulofenestra lockeri (7-9)	0	0	0	0	0	0	0	0	0	0	0	0	0	0	2E+07	0	2E+07	0	0	0	0	0	0	0	0	0	0	0	0	0	0	0	0	0	0
Reticulofenestra rupeliensis	2E+07	0	0	2E+07	2E+07	4E+07	3E+07	3E+07	2E+07	3E+07	0	3E+07	0	0	0	0	0	0	2E+07	0	2E+07	0	0	0	0	0	0	0	0	0	1E+07	0	0	0	0
Reticulofenestra samodurovii (10-12)	1E+07	2E+07	2E+07	9E+06	2E+07	8E+07	3E+07	5E+07	6E+07	7E+07	2E+07	0	0	2E+07	6E+07	0	4E+07	0	2E+07	0	2E+07	6E+07	1E+07	0	0	2E+07	0	2E+07	0	0	0	1E+07	0	2E+07	0
Reticulofenestra samodurovii (12-14)	0	4E+07	2E+07	0	0	8E+07	9E+07	5E+07	2E+07	3E+07	4E+07	2E+07	5E+07	7E+07	2E+07	4E+07	6E+07	0	0	0	0	0	0	2E+07	5E+07	0	2E+07	4E+07	2E+07	1E+07	2E+07	0	0	4E+07	4E+07
Reticulofenestra scrippsae (3-5)	0	2E+07	2E+07	2E+07	5E+07	2E+07	2E+07	0	0	0	0	0	0	0	0	0	0	0	0	0	0	0	0	0	0	0	0	0	0	6E+07	0	0	0	0	0
Reticulofenestra scrippsae (5-7)	5E+07	9E+07	8E+07	9E+07	7E+07	2E+07	3E+07	8E+07	3E+07	1E+07	0	2E+07	2E+07	5E+07	2E+07	4E+07	2E+07	0	4E+07	0	0	2E+07	5E+07	2E+07	2E+07	0	2E+07	2E+07	0	0	1E+07	3E+07	0	5E+07	4E+07
Reticulofenestra umbilicus	3E+07	0	4E+07	4E+07	4E+07	4E+07	9E+07	5E+07	3E+07	6E+07	4E+07	7E+07	5E+07	5E+07	1E+08	8E+07	0	1E+08	6E+07	2E+08	1E+08	1E+08	1E+08	2E+08	7E+07	6E+07	8E+07	6E+07	8E+07	1E+07	7E+07	4E+07	8E+07	9E+07	1E+08
Reticulofenestra waedae (3-5)	0	0	0	0	0	0	0	0	0	0	0	2E+07	2E+07	0	0	4E+07	4E+07	0	0	0	4E+07	2E+07	0	2E+07	0	0	0	0	0	0	0	0	0	0	2E+07
Reticulofenestra waedae (5-7)	0	0	0	0	0	0	0	0	0	0	0	5E+07	2E+07	0	0	0	0	0	0	0	0	0	3E+07	9E+07	7E+07	9E+07	0	4E+07	2E+07	0	0	0	3E+07	0	0
Reticulofenestra waedae (7-9)	0	0	0	0	0	0	0	0	0	0	0	0	0	0	0	0	0	0	0	0	0	0	4E+07	0	0	0	0	0	0	0	0	0	0	0	0
Sphenolithus moriformis	2E+07	4E+07	6E+07	0	5E+07	2E+07	3E+07	2E+07	2E+07	1E+07	0	5E+07	0	2E+07	6E+07	6E+07	2E+07	4E+07	2E+07	2E+07	4E+07	0	3E+07	2E+07	4E+07	4E+07	2E+07	2E+07	0	1E+07	1E+07	1E+07	2E+07	4E+07	0
Sphenolithus predistentus	4E+07	1E+08	1E+08	4E+07	5E+07	9E+07	3E+07	3E+07	3E+07	4E+07	4E+07	9E+07	1E+08	7E+07	6E+07	8E+07	0	1E+08	4E+07	7E+07	9E+07	2E+07	5E+07	9E+07	7E+07	4E+07	4E+07	0	2E+07	1E+07	6E+07	3E+07	2E+07	2E+07	4E+07
Sphenolithus tribulosus	2E+07	2E+07	0	9E+06	2E+07	0	0	0	0	0	0	2E+07	0	2E+07	4E+07	0	8E+07	0	0	9E+07	0	1E+08	3E+07	1E+08	1E+08	4E+07	1E+08	1E+08	1E+08	7E+07	6E+07	4E+07	7E+07	1E+08	6E+07
Zigrhrablithus bijugathus	1E+07	0	0	2E+07	0	6E+07	5E+07	3E+07	2E+07	3E+07	6E+07	2E+07	1E+08	0	4E+07	4E+07	2E+07	0	8E+07	5E+07	4E+07	2E+07	3E+07	0	4E+07	2E+07	2E+07	4E+07	0	1E+07	1E+07	4E+07	3E+07	4E+07	0
Small placoliths	0	2E+07	2E+07	0	0	0	0	0	2E+07	0	2E+07	3E+07	0	0	0	0	2E+07	0	4E+07	9E+07	1E+08	2E+07	1E+07	0	4E+07	8E+07	2E+07	0	0	4E+07	2E+07	3E+07	5E+07	5E+07	4E+07
Small *reticulofenestrids*	7E+08	2E+09	2E+09	8E+08	2E+09	2E+09	2E+09	2E+09	2E+09	2E+09	3E+09	3E+09	4E+09	2E+09	3E+09	3E+09	3E+09	3E+09	3E+09	4E+09	3E+09	2E+09	2E+09	3E+09	2E+09	3E+09	3E+09	2E+09	3E+09	2E+09	1E+09	2E+09	2E+09	2E+09	3E+09
Campylosphaera	0	0	0	0	0	0	0	0	0	0	0	0	0	0	0	0	0	0	0	0	0	0	0	0	0	2E+07	2E+07	2E+07	3E+07	2E+07	0	2E+07	2E+07	2E+07
Reticolofenestra reticulata	0	0	0	0	0	0	0	0	0	0	0	0	2E+07	0	4E+07	0	0	0	4E+07	0	0	0	0	0	0	0	0	0	0	0	0	0	0	0	0
Neococcolithus minutus	0	0	0	0	0	0	0	2E+07	0	0	0	0	0	0	0	0	2E+07	0	0	0	0	0	0	0	0	0	0	0	0	0	0	0	0	0	0
Cruciplacolithus	0	0	0	0	2E+07	0	0	0	0	0	0	0	0	2E+07	0	0	0	0	0	0	0	0	0	0	0	0	0	0	0	0	0	0	0	0	0

Depth (mbsf)	135.47	135.63	135.73	135.95	136.08	136.20	136.27	136.33	136.40	136.59	136.79	136.98	137.18	137.37	137.57	137.77	137.98	138.17	138.35	138.54	138.74	138.96	139.10	139.31	139.50	139.71	139.91	140.10	140.30	140.49	140.68	140.89	141.08	141.28	141.46
Calcidiscus protoanulus	0	0	0	0	0	0	0	0	0	1E+07	0	0	0	0	0	0	0	0	0	0	0	0	0	0	0	0	0	0	0	0	0	0	0	0	0
Transversopontis	2E+07	0	0	0	0	0	0	0	0	0	0	0	0	0	0	0	0	0	0	0	0	0	0	0	0	0	0	0	0	0	0	0	0	0	0	0
Triquetrorhabdulus	1E+07	0	0	0	0	0	0	0	0	0	0	0	0	0	0	0	0	0	0	0	0	0	0	0	0	0	0	0	0	0	0	0	0	0	0	0
tot	3E+09	6E+09	6E+09	3E+09	6E+09	6E+09	7E+09	5E+09	5E+09	5E+09	7E+09	6E+09	8E+09	6E+09	7E+09	7E+09	6E+09	6E+09	7E+09	7E+09	7E+09	5E+09	4E+09	8E+09	6E+09	6E+09	6E+09	6E+09	6E+09	5E+09	3E+09	5E+09	5E+09	6E+09	6E+09

Table IV g. Siliceous plankton: census and absolute abundances. Diatoms, other siliceous plankton (Si Pl) and the sum of these (total siliceous plankton = Si Pl tot).

Depth (mbsf)	Census		Absolute abundance		
	Diatoms (census)	Siliceous plankton (census)	Diatoms /g	Si Pl /g	Si Pl tot/g
135.47	175	67	4.8E+08	1.8E+08	6.6E+08
135.63	261	44	9.1E+08	1.5E+08	1.1E+09
135.73	271	35	9.0E+08	1.2E+08	1.0E+09
135.95	256	46	9.5E+08	1.7E+08	1.1E+09
136.08	271	32	1.8E+09	2.1E+08	2.0E+09
136.20	252	49	1.9E+09	3.6E+08	2.2E+09
136.27	262	48	4.3E+09	7.9E+08	5.1E+09
136.33	301	36	2.7E+09	3.2E+08	3.0E+09
136.40	272	29	1.8E+09	1.9E+08	2.0E+09
136.59	264	33	1.7E+09	2.1E+08	1.9E+09
136.79	278	24	2.1E+09	1.8E+08	2.2E+09
136.98	268	32	1.1E+09	1.3E+08	1.2E+09
137.18	281	26	1.6E+09	1.5E+08	1.8E+09
137.37	278	29	1.6E+09	1.7E+08	1.8E+09
137.57	264	39	1.1E+09	1.6E+08	1.2E+09
137.77	282	28	1.3E+09	1.2E+08	1.4E+09
137.98	275	28	1.5E+09	1.6E+08	1.7E+09
138.17	269	31	1.2E+09	1.4E+08	1.3E+09
138.35	273	30	1.2E+09	1.3E+08	1.3E+09
138.54	280	25	1.4E+09	1.2E+08	1.5E+09
138.74	262	38	1.0E+09	1.5E+08	1.2E+09
138.96	224	81	1.0E+09	3.6E+08	1.4E+09
139.10	229	72	9.7E+08	3.0E+08	1.3E+09
139.31	221	82	1.2E+09	4.6E+08	1.7E+09
139.50	244	60	1.6E+09	4.0E+08	2.0E+09
139.71	232	73	1.5E+09	4.6E+08	1.9E+09
139.91	224	79	1.2E+09	4.2E+08	1.6E+09
140.10	231	70	1.2E+09	3.7E+08	1.6E+09
140.30	234	67	9.3E+08	2.7E+08	1.2E+09
140.49	230	72	9.5E+08	3.0E+08	1.2E+09
140.68	220	80	7.4E+08	2.7E+08	1.0E+09
140.89	232	81	8.3E+08	2.9E+08	1.1E+09
141.08	222	78	8.4E+08	2.9E+08	1.1E+09
141.28	225	75	7.8E+08	2.6E+08	1.0E+09
141.46	228	75	7.7E+08	2.5E+08	1.0E+09

Table IV h. Planktic foraminifera eco-groups, built with the abundance of the species showing affinity to each environment (see Table 3). Deep-water dwellers = Σ Thermocline and Sub-thermocline dwellers; Chiloguembelinidae = *Chiloguembelina* and *Tenuitella*.

Depth	Surface mixed dwellers (%)	Thermocline dwellers (%)	Sub-thermocline dwellers (%)	Deep-water dwellers (%)	Chiloguembelinidae (%)
135.47	34.65	35.97	28.38	64.36	0.66
135.63	30.56	39.53	28.57	68.11	0.33
135.73	26.67	37.33	34.00	71.33	0
135.95	34.00	29.67	36.33	66.00	0
136.08	35.00	41.00	25.00	66.00	0
136.2	31.95	36.10	28.43	64.54	2.56
136.265	33.98	34.63	27.51	62.14	1.94
136.33	36.09	24.50	28.81	53.31	6.62
136.4	33.89	37.54	20.60	58.14	6.98
136.59	28.33	39.67	20.67	60.33	9.33
136.79	36.63	29.04	28.05	57.10	6.60
136.98	21.97	42.95	32.13	75.08	2.30
137.18	28.57	37.21	26.58	63.79	6.31
137.37	29.74	44.77	19.93	64.71	6.21
137.57	23.67	40.33	28.00	68.33	5.67
137.77	31.58	32.24	21.05	53.29	14.14
137.98	32.24	30.92	28.95	59.87	7.24
138.17	22.30	44.92	32.46	77.38	0.66
138.35	29.57	41.86	22.92	64.78	5.65
138.54	30.60	36.59	29.65	66.25	1.58
138.74	25.55	39.12	33.44	72.56	0.63
138.96	20.06	35.67	32.80	68.47	10.19
139.1	21.93	39.20	29.24	68.44	8.97
139.31	16.89	37.42	24.50	61.92	21.52
139.5	27.27	34.74	28.25	62.99	10.06
139.71	21.31	38.03	31.80	69.84	8.20
139.91	31.82	36.04	32.47	68.51	0.65
140.1	30.13	29.81	34.94	64.74	5.77
140.3	29.07	35.14	29.71	64.86	5.43
140.49	24.17	34.77	30.79	65.56	10.93
140.68	23.27	41.82	32.08	73.90	3.46
140.89	23.01	47.49	28.61	76.11	1.18
141.08	16.40	52.68	28.08	80.76	2.84
141.28	27.60	41.23	27.92	69.16	2.92
141.46	27.33	36.33	22.67	59.00	13.00
Max.	36.63	52.68	36.33	80.76	21.52
Min.	16.40	24.50	19.93	53.29	0
Avg.	27.94	37.61	28.44	66.05	5.44

Table IV. i. Benthic foraminifera eco-groups. *= Deep infaunal conical and flattened biserial (high food supply) (%); E=Epifaunal; I=Infaunal.

Depth (mbsf)	AGE (CK95)	Deep infaunal* (%)	Elongate or Extinction Gp (%)	Agglutinated taxa (%)	E/I ratio	Epifaunal taxa (%)	Epifaunal phytodetritus (>106µm)	Epifaunal phytodetritus (63-106µm)
135.47	33.07	22.83	22.83	1.57	0.26	15.75	6.69	36.40
135.63	33.25	9.70	33.52	0.55	0.24	19.11	4.16	38.02
135.73	33.36	11.00	24.00	2.00	0.53	32.50	17.00	42.74
135.95	33.61	14.72	30.96	1.02	0.32	23.35	3.55	51.21
136.08	33.86	29.41	25.37	1.10	0.32	16.91	4.78	6.27
136.20	34.00	38.78	46.26	2.04	0.04	3.74	1.36	0.60
136.27	34.07	20.79	73.39	0.00	0.03	2.70	0.62	1.86
136.33	34.15	27.30	65.71	0.00	0.02	2.22	0.63	1.40
136.40	34.87	27.95	62.73	0.31	0.02	1.55	0.31	1.36
136.59	34.87	44.37	37.88	0.68	0.06	4.78	1.71	0.72
136.79	34.87	50.97	8.44	10.71	0.13	9.42	4.87	1.04
136.98	34.88	58.51	8.66	4.18	0.14	10.75	2.39	6.88
137.18	34.88	53.23	7.46	1.49	0.14	11.44	7.46	11.07
137.37	34.88	51.74	17.39	1.74	0.17	13.48	6.09	10.84
137.57	34.89	58.74	8.60	0.86	0.15	10.32	2.58	5.93
137.77	34.89	53.71	12.66	2.62	0.16	10.48	1.75	7.36
137.98	34.90	64.00	8.00	4.73	0.14	9.82	2.55	7.66
138.17	34.90	64.99	12.66	1.86	0.12	10.24	5.21	4.19
138.35	34.90	50.55	13.65	1.85	0.23	18.08	3.69	1.55
138.54	34.91	56.20	16.94	0.41	0.10	7.85	4.13	19.18
138.74	34.91	58.43	17.25	2.75	0.11	9.80	2.75	15.46
138.96	34.91	60.51	14.86	3.26	0.12	8.70	4.35	22.75
139.10	34.92	66.01	15.27	0.49	0.13	10.84	6.90	17.91
139.31	34.92	49.27	8.78	1.46	0.23	17.07	8.78	18.06
139.50	34.92	45.89	19.05	3.46	0.17	13.42	6.49	34.15
139.71	34.93	47.37	18.42	2.96	0.19	13.49	4.93	20.67
139.91	34.93	51.69	20.76	1.69	0.09	7.63	2.97	32.57
140.10	34.93	43.22	31.55	1.26	0.12	10.09	5.05	23.83
140.30	34.94	56.52	23.19	1.93	0.06	4.35	1.93	29.66
140.49	34.94	67.23	22.88	0.28	0.06	4.80	3.67	16.19
140.68	34.95	34.36	30.12	1.93	0.19	13.51	8.49	16.36
140.89	34.95	44.04	27.80	2.89	0.13	9.39	5.78	25.29
141.08	34.95	30.00	22.00	5.20	0.33	22.80	17.60	25.00
141.28	34.96	47.22	25.56	3.89	0.06	3.89	0.00	9.01
141.46	34.96	38.33	40.07	4.53	0.02	1.39	0.00	4.33
Max.		67.23	73.39	10.71	0.53	32.50	17.60	51.21
Min.		9.70	7.46	0.00	0.02	1.39	0.00	0.60
Avg.		44.27	24.99	2.22	0.15	11.02	4.61	16.21

Table IV j1. Factor analysis results extended: Factor loadings for a) Benthic foraminifera; b) Planktic foraminifera; and c) Calcareous nannofossils. Loadings of samples significant for each factor highlighted in grey (>0.6), light grey (second highest >0.6 loading) and blue (highest loading but not >0.6). Expl.Var= Explained variance; Prp. Totl= Total explained variance.

Depth (mbsf)	a) Benthic foraminifera			b) Planktic foraminifera			c) Calcareous nannofossils		
	$F1_{BF}$	$F2_{BF}$	$F3_{BF}$	$F1_{PF}$	$F2_{PF}$	$F3_{PF}$	$F1_{CN}$	$F2_{CN}$	$F3_{CN}$
135.47	0.27	0.12	0.87	0.75	0.25	0.32	0.37	0.74	0.45
135.63	-0.13	0.19	0.89	0.75	0.26	0.51	0.28	0.82	0.36
135.73	0.16	-0.04	0.89	0.87	0.22	0.32	0.33	0.77	0.42
135.95	0.14	0.09	0.88	0.84	0.26	0.27	0.35	0.81	0.28
136.08	0.44	-0.06	0.77	0.79	0.21	0.42	0.41	0.78	0.36
136.2	0.22	0.91	0.04	0.53	0.07	0.76	0.24	0.54	0.72
136.26	0.05	0.91	0.18	0.64	0.10	0.58	0.41	0.63	0.59
136.33	0.04	0.90	0.16	0.07	-0.19	0.73	0.28	0.55	0.68
136.4	-0.03	0.92	0.03	0.40	0.38	0.52	0.43	0.64	0.58
136.59	0.22	0.82	-0.08	0.31	0.45	0.65	0.29	0.61	0.62
136.79	0.82	0.04	-0.03	0.63	0.11	0.35	0.48	0.30	0.74
136.98	0.75	-0.05	0.14	0.73	0.28	0.41	0.57	0.33	0.56
137.18	0.84	-0.02	0.11	0.47	0.54	0.54	0.41	0.38	0.75
137.37	0.77	0.17	0.10	0.34	0.57	0.54	0.45	0.61	0.49
137.57	0.82	-0.11	-0.03	0.53	0.40	0.45	0.57	0.49	0.56
137.77	0.84	0.05	-0.02	0.18	0.28	0.56	0.42	0.47	0.68
137.98	0.86	-0.15	0.06	0.54	0.48	0.35	0.48	0.51	0.44
138.17	0.90	-0.01	0.29	0.80	0.39	0.28	0.53	0.29	0.62
138.35	0.89	0.07	0.09	0.63	0.59	0.23	0.53	0.51	0.53
138.54	0.89	0.20	0.10	0.85	0.20	0.23	0.80	0.22	0.39
138.74	0.83	0.20	0.19	0.81	0.21	0.39	0.56	0.30	0.67
138.96	0.85	0.15	0.12	0.52	0.73	0.08	0.71	0.47	0.29
139.1	0.68	0.33	0.13	0.28	0.72	0.37	0.66	0.34	0.29
139.31	0.66	-0.16	0.20	0.13	0.90	0.03	0.78	0.24	0.39
139.5	0.87	0.18	0.16	0.33	0.73	0.28	0.79	0.31	0.42
139.71	0.86	0.19	0.18	0.59	0.56	0.11	0.74	0.35	0.40
139.91	0.81	0.31	0.16	0.82	0.35	0.28	0.74	0.50	0.26
140.1	0.82	0.32	0.14	0.64	0.46	0.16	0.73	0.49	0.27
140.3	0.74	0.31	-0.01	0.49	0.46	0.35	0.80	0.35	0.34
140.49	0.44	0.64	-0.10	0.36	0.81	0.11	0.62	0.61	0.29
140.68	0.69	0.32	0.42	0.77	0.50	0.00	0.70	0.48	0.31
140.89	0.84	0.34	0.20	0.79	0.46	0.08	0.61	0.62	0.35
141.08	0.70	0.24	0.35	0.70	0.56	0.04	0.82	0.34	0.33
141.28	0.69	0.48	0.10	0.81	0.41	0.00	0.62	0.68	0.17
141.46	0.66	0.50	0.15	0.39	0.68	0.01	0.62	0.47	0.40
Expl.Var	15.93	5.88	4.52	13.24	7.73	5.20	11.53	9.76	8.18
Prp.Totl	46%	17%	13%	38%	22%	15%	33%	28%	23%

Table IV j2. Factor analysis results extended: Factor scores for a) Benthic foraminifera; b) Planktic foraminifera; and c) Calcareous nannofossils. In green, highest scores corresponding to significant species for each factor.

a) Benthic foraminifera species	Factor Scores		
	F1	F2	F3
Alabamina cf. A. dissonata	0.67	-0.59	1.19
Agglutinata	0.35	-0.61	-0.46
Bolivina spp.	0.76	-0.13	-1.01
Bolivinoides crenulatus	-1.60	1.60	-1.37
Brizalina carinata	-0.10	1.45	-1.91
Brizalina tectiformis	2.88	0.41	0.76
Bulimina alazanensis	2.00	-0.02	-0.29
Bulimina mexicana	-0.32	-0.37	0.08
Bulimina tuxpamensis	0.59	-1.02	-1.42
Cibicidoides hadjibulakensis	-0.83	-0.73	-0.18
Cibicidoides mundulus	-0.05	-0.93	-0.96
Chrysalogonium spp.	-0.95	0.25	-0.59
Dentalina spp.	-0.53	-0.44	-0.33
Glandulonodosariidae	-0.99	1.65	0.98
Gyroidinoides girardanus	-0.56	-0.40	0.44
Lenticulina spp.	-0.46	-0.57	-0.70
Melonis affinis	0.37	-0.47	0.28
Oridorsalis umbonatus	-0.15	-0.84	0.14
Osangularia cf. plummerae	-0.76	-0.85	1.73
Pleurostomellidae	0.17	-0.45	-0.12
Pullenia bulloides	0.09	-0.76	0.50
Siphonodosaria spp.	1.08	1.40	1.68
Strictocostella spp.	-0.18	2.73	0.91
Trifarina wilcoxensis	0.31	0.85	-0.83
Uvigerina galloway	-1.77	-0.85	1.81
Uvigerina rippensis	0.00	-0.30	-0.34

b) Planktic foraminifera species	Factor Scores		
	F1	F2	F3
Turborotalia increbescens	1.29	0.98	1.38
Turborotalia ampliapertura	-0.15	-0.90	0.95
Pseudohastigerina spp.	-1.02	-0.41	-0.19
Catapsydrax spp.	0.46	0.33	-0.06
Subbotina angiporoides	-0.02	-0.81	0.72
Subbotina linaperta	0.34	0.69	0.82
Subbotina eocaena	1.14	0.97	1.02
Subbotina corpulenta	1.16	1.23	-0.05
Subbotina hagni	0.62	0.21	-0.16
Subbotina yeguaensis	0.41	0.16	-0.10
Dentoglobigerina galavisi	1.06	1.02	-0.45
Dentoglobigerina tripartita	-0.02	-0.98	1.08
Dentogl. pseudovenezuelana	0.24	1.32	-1.59
Dentoglobigerina venezuelana	1.79	-1.14	-2.36
Globoturborotalita ouachitaensis	0.17	-0.20	2.00
Chiloguembelinoides	-1.16	0.71	-1.12
Paragloborotalia nana	-0.95	-0.86	0.57
Globigerina officinalis	-0.58	-0.75	-1.09
Globoturborotalita martini	0.51	-2.03	-0.93
Globorotaloides spp.	-0.75	-0.84	0.59
Paragloborotalia griffinoides	0.25	0.09	-0.28
Turborotalita praequinqueloba	-0.65	-1.30	-0.12
Tenuitella praegemma	-2.04	0.65	0.02
Tenuitella patefacta	-2.08	1.86	-0.62

c) Calcareous nannofossil species	Factor Scores		
	F1	F2	F3
Blackites spp.	0.43	-0.31	-0.09
Clausicoccus subdistichus	-0.27	-1.10	1.42
Coccolithus pelagicus (3-7µ)	0.39	0.64	0.58
C. pelagicus (7-11µ)	0.77	0.87	0.36
C. pelagicus (11-16µ)	-1.29	-1.17	0.47
Coccolithus formosus	0.04	0.25	-0.67
Coronocyclus spp	0.17	-1.38	0.07
Cyclicargolithus sp.	1.23	1.27	0.89
Cyclicargolithus floridanus	0.48	-0.17	-0.13
Dictyococcites bisectus	-1.23	0.89	0.30
Dictyococcited callidus	1.01	-0.45	-0.26
Dictyococcites daviesii	1.16	1.75	0.31
Dictyococcites stavensis	-0.19	0.41	-0.68
Discoaster spp.	-1.46	-0.11	0.35
Helicosphaera spp.	0.46	-0.90	-0.04
Isthmolithus recurvus	0.10	0.10	1.04
Pontosphaera spp.	0.89	-1.20	1.60
Reticulofenestra dictyoda	1.97	1.65	1.30
Reticulofenestra flecwinzii	-1.68	1.41	-0.48
Reticulofenestra hillae	0.24	0.34	-1.91
Reticulofenestra lockeri	-0.27	0.79	0.96
Reticulofenestra samodurovii	-1.53	0.26	0.40
Reticulofenestra scrippsae	-1.69	1.78	-1.39
Reticulofenestra umbilicus	0.84	-1.00	-0.16
Reticulofenestra waedae	0.17	-1.82	-0.48
Sphenolithus moriformis	-0.83	-0.27	-0.54
Sphenolithus predistentus	-0.85	-0.44	0.79
Sphenolithus tribulosus	1.61	-0.22	-3.06
Zigrhrablithus bijugathus	-0.83	-0.89	0.23
Small placoliths	0.16	-0.98	-1.18

Table IV k. Initial observation of the sediment with qualitative/semiquantitative data. Blue line corresponds to the EOB. Ech= echinoderm spines; R= radiolarians; Ft= fish teeth; Os= ostracods; Spic= Sponge spicules; PF= Planktic foraminifera; BF= Benthic foraminifera; Glt= Glauconite grains/spheres; Gp= Gypsum crystals; Qtz= quartz grains; Py= pyritized tests; Mca= Mica; M2= unknown mineral 2; M3= unknown mineral 3; VA= Very abundant; A or 4= Abundant; C or 3= Common; F or 2= Few; R or 1= Rare; VR= Very rare; ( ) or 0= Absent; x= Present; >= Increased (from bottom to top); <= Decreased (from bottom to top); L= low preservation; G= good; QG= quite good; VG= very good; Rc= Recrystallized.

Depth (mbsf)	Biogenic remains							Inorganic remains								Preser-vation	Disso-lution	Fragmen-tation	Remarks
	Ech	R (~%)	Ft	Os	Spic	Pf (~%)	Bf	Glt	Gp	Qtz	Py	Glass	Mca	M2	M3				
135.47	F	A (60)	F	x	x	F (15)	F	4		A	C			C	F	L		x	Some Qz > 500 µm
135.63	x	A (60)	C		x	F (15)	A	4		F			R		A	L	x		
135.73	x	C (40)	R	x	x	C (30)	F (<)	3		C	C	x	R	C	F	L		A	
135.95	x	x	x	x	x			2	A			A			A	L		>	
136.08	F	C (35)	R	x	C			4		C	C				F	QG		x	
136.20	F	C (35)	x	x	R	C (30)		2		R	F				F	G			
136.27	F	C (30)	x		C			2		F	R					G			BF= further increase of the uniserial-elongate taxa
136.33	x	x	x		x											G			
136.40	R	C (45)	F		F			1		R					R	G			
136.59	x	x	x	x	x											G			BF= marked increase of the uniserial-elongate taxa
136.79	F	C (30)	x	A	F			1		F	F				R	G			
136.98	x	x	x	x	x											QG		x	
137.18	x	C (40)	R	F	A			2					R		F	QG		x	
137.37	x	x	x	x	x											QG		x	
137.57	x	C (30)	F		A			1			F				F	QG		x	
137.77	x	x			x											G			
137.98	F	C (20)	F	A	A			2							R	QG		x	
138.17	F	C (20)	F	A	A			2							R	G			Not well cleaned
138.35	x	C (20)	F	x	x			0								QG			F fish vertebrae; Not well cleaned
138.54	x	x		R	x			0								L		A	A and extremely big *P. micra* compared to younger samples
138.74	F	C (20)	R	F	A			0								G			
138.96	x	x	F		x			0								G			*Pseudohastigerina* small size (>150 or smaller)
139.10	x	x		R	x			0								QG/ Rc?			F chiloguembelinids
139.31	x	x			x			0								VG			
139.50	x	x	x	A	x			0								QG		x	
139.71	x	x			x			0								G			
139.91	x	x		x	x			0								G			
140.10	x	x	x	x	x			0								G			R chiloguembelinids
140.30	x	x			x			0								QG		x	A *T. cerroazulensis* group (peak)
140.49	x	x			x			0								G			A T. cerroazulensis group; VR chiloguembelinids
140.68	x	x	x	x	x			0								G			Not very clean sample; VR chiloguembelinids
140.89	x	x		x	x			0								G	x		VR chiloguembelinids
141.08		x			x			0								G			R chiloguembelinids
141.28		x	x		x			0								G/Rc			A chiloguembelinids
141.46	x	x		x	x			0								G		F	VA chiloguembelinids

Table IV.I. Studied samples, performed analysis type and sampling intervals. A= assemblage analysis, B= biostratigraphy; W= weighing; PF= planktic foraminifera; BF= benthic foraminifera; δ= stable isotope analysis.

Sample	Depth (msb)	AGE (CK95)* (Ma)	AGE (GPTS12) (Ma)	Analysis type				Sampling intervals (cm)
				A & B	W	PF δ	BF δ	
612,16X-6, 116,5-119	135.37	32.95	33.12		x		x	6
612,16X-6, 122-124	135.42	33.01	33.18		x		x	6
612,16X-6, 127-129	135.47	33.07	33.24	x	x	x		6
612,16X-6, 134-136	135.54	33.15	33.32		x		x	6
612,16X-6, 143-145	135.63	33.25	33.43	x	x	x		6
612,16X-6, 147-149	135.67	33.29	33.47		x		x	6
612,16X-7, 3-5	135.73	33.36	33.54	x	x	x	x	6
612,16X-7, 5-7	135.75	33.39	33.57		x		x	6
612,16X-7, 10-12	135.80	33.44	33.63		x		x	6
612,16X-7, 17-19	135.87	33.52	33.71		x		x	6
612,16X-7, 25-27	135.95	33.61	33.80	x	x	x		6
612,16X-CC, 3-5	136.01	33.68	33.87		x		x	6
612,16X-CC, 10-12	136.08	33.86	34.09	x	x	x	x	6
612,16X-CC, 15-17	136.13	33.92	34.15		x		x	3
612,16X-CC, 18,5-20,5	136.17	33.96	34.19		x		x	3
612,17X-1, 0-2	136.20	34.00	34.24	x	x	x		3
612,17X-1, 3-5	136.23	34.03	34.27		x		x	3
612,17X-1, 6.5-8.5	136.27	34.07	34.31	x	x	x		3
612,17X-1, 10-12	136.30	34.11	34.35		x		x	3
612,17X-1, 13-15	136.33	34.15	34.39	x	x	x	x	3
612,17X-1, 15-17	136.35	34.17	34.41		x		x	3
612,17X-1, 20-22	136.40	34.87	35.22	x	x	x		10
612,17X-1, 29-31	136.49	34.87	35.22		x		x	10
612,17X-1, 39-41	136.59	34.87	35.23	x	x	x		10
612,17X-1, 50-51	136.70	34.87	35.23		x		x	10
612,17X-1, 59-61	136.79	34.87	35.23	x	x	x	x	10
612,17X-1, 68-70	136.88	34.87	35.23		x		x	10
612,17X-1, 78-80	136.98	34.88	35.23	x	x	x		20
612,17X-1, 98-100	137.18	34.88	35.24	x	x	x		20
612,17X-1, 117-119	137.37	34.88	35.24	x	x	x		20
612,17X-1, 137-139	137.57	34.89	35.24	x	x	x		20
612,17X-2, 7-9	137.77	34.89	35.25	x	x	x		20
612,17X-2, 28-30	137.98	34.90	35.25	x	x	x		20
612,17X-2, 47-49	138.17	34.90	35.26	x	x	x		20
612,17X-2, 49-50	138.19	34.90	35.26		x		x	20
612,17X-2, 65-67	138.35	34.90	35.26	x	x	x		20
612,17X-2, 84-86	138.54	34.91	35.26	x	x	x		20
612,17X-2, 104-106	138.74	34.91	35.27	x	x	x		20
612,17X-2, 126-128	138.96	34.91	35.27	x	x		x	20
612,17X-2, 140-142	139.10	34.92	35.27	x	x	x		20
612,17X-3, 11-13	139.31	34.92	35.28	x	x	x		20

Sample	Depth (msb)	AGE (CK95)* (Ma)	AGE (GPTS12) (Ma)	Analysis type				Sampling intervals (cm)
				A & B	W	PF δ	BF δ	
612,17X-3, 30-32	139.50	34.92	35.28	x	x	x		20
612,17 X-3,49-50	139.69	34.93	35.28		x			20
612,17X-3, 51-53	139.71	34.93	35.28	x	x	x		20
612,17X-3,71-73	139.91	34.93	35.29	x	x	x		20
612,17X-3, 90-92	140.10	34.93	35.29	x	x	x		20
612,17X-3, 110-112	140.30	34.94	35.30	x	x	x		20
612,17X-3, 129-131	140.49	34.94	35.30	x	x		x	20
612,17X-3, 148-150	140.68	34.95	35.30	x	x		x	20
612,17X-4, 19-21	140.89	34.95	35.31	x	x		x	20
612,17X-4, 38-40	141.08	34.95	35.31	x	x		x	20
612,17 X-4,49-50	141.19	34.95	35.31		x			20
612,17X-4, 58-60	141.28	34.96	35.31	x	x		x	20
612,17X-4, 76-78	141.46	34.96	35.32	x	x		x	20

Table IV.m. Previously studied samples in Site 612 for biostratigraphy (Diatoms (Abbott, 1987); calcareous nannofossils (Bukry, 1987); planktic foraminifera (Miller and Hart, 1987) and radiolaria (Palmer, 1987)), benthic foraminifera assemblage analysis (Miller and Katz, 1987) and stable C and O isotopes in benthic foraminifera (Coxall et al., 2018; Miller et al., 1991; Pusz et al., 2009).

Site	Depth (msb)	AGE (CK95)* (Ma)	AGE (GTS12) (Ma)	Analysis type	Microfossil group	Data source
612-17X-1, 50-51	136.70	34.87	35.23	Biostratigraphy	Diatoms	Abbott, 1987
612,16-CC	136.00	33.67	33.86	Biostratigraphy	Calcareous nannofossils	Bukry, 1987
612,17X-3, 110-112	140.30	34.94	35.30	Biostratigraphy	Calcareous nannofossils	Bukry, 1987
612,16-CC	136.00	33.67	33.86	Biostratigraphy	Planktic foraminifera	Miller and Hart, 1987
612, 17-4, 60-64	141.31	34.96	35.31	Biostratigraphy	Planktic foraminifera	Miller and Hart, 1987
612,16-CC	136.00	33.67	33.86	Biostratigraphy	Radiolaria	Palmer, 1987
612,17X-1, 110-112	137.20	34.88	35.24	Biostratigraphy	Radiolaria	Palmer, 1987
612,17X-3, 110-112	140.30	34.94	35.30	Biostratigraphy	Radiolaria	Palmer, 1987
612,16X-7, 26-30	135.95	33.61	33.80	Assemblage analysis	Benthic foraminifera	Miller and Katz, 1987
612,16-CC	136.00	33.67	33.86	Assemblage analysis	Benthic foraminifera	Miller and Katz, 1987
612,17-1, 140-144	137.60	34.89	35.25	Assemblage analysis	Benthic foraminifera	Miller and Katz, 1987
612,17-2,140-144	139.10	34.92	35.27	Assemblage analysis	Benthic foraminifera	Miller and Katz, 1987
612,17-3, 140-144	140.60	34.94	35.30	Assemblage analysis	Benthic foraminifera	Miller and Katz, 1987
612,17-4, 60-64	141.28	34.96	35.31	Assemblage analysis	Benthic foraminifera	Miller and Katz, 1987
612,16X-6, 127-129	135.47	33.07	33.24	Stable C and O isotopes	Benthic foraminifera	Coxall et al., 2018
612,17X-1, 0-2	136.20	34.00	34.24	Stable C and O isotopes	Benthic foraminifera	Coxall et al., 2018
612,17X-1, 6.5-8.5	136.27	34.07	34.31	Stable C and O isotopes	Benthic foraminifera	Coxall et al., 2018
612,17X-1, 20-22	136.40	34.87	35.22	Stable C and O isotopes	Benthic foraminifera	Coxall et al., 2018
612,17X-1, 39-41	136.59	34.87	35.23	Stable C and O isotopes	Benthic foraminifera	Coxall et al., 2018
612,17X-1, 78-80	136.98	34.88	35.23	Stable C and O isotopes	Benthic foraminifera	Coxall et al., 2018
612,17X-1, 98-100	137.18	34.88	35.24	Stable C and O isotopes	Benthic foraminifera	Coxall et al., 2018
612,17X-1, 117-119	137.37	34.88	35.24	Stable C and O isotopes	Benthic foraminifera	Coxall et al., 2018
612,17X-1, 137-139	137.57	34.89	35.24	Stable C and O isotopes	Benthic foraminifera	Coxall et al., 2018
612,17X-2, 7-9	137.77	34.89	35.25	Stable C and O isotopes	Benthic foraminifera	Coxall et al., 2018
612,17X-2, 28-30	137.98	34.90	35.25	Stable C and O isotopes	Benthic foraminifera	Coxall et al., 2018

Site	Depth (msb)	AGE (CK95)* (Ma)	AGE (GTS12) (Ma)	Analysis type	Microfossil group	Data source
612,17X-2, 47-49	138.17	34.90	35.26	Stable C and O isotopes	Benthic foraminifera	Coxall et al., 2018
612,17X-2, 65-67	138.35	34.90	35.26	Stable C and O isotopes	Benthic foraminifera	Coxall et al., 2018
612,17X-2, 84-86	138.54	34.91	35.26	Stable C and O isotopes	Benthic foraminifera	Coxall et al., 2018
612,17X-2, 104-106	138.74	34.91	35.27	Stable C and O isotopes	Benthic foraminifera	Coxall et al., 2018
612,17X-2, 140-142	139.10	34.92	35.27	Stable C and O isotopes	Benthic foraminifera	Coxall et al., 2018
612,17X-3, 11-13	139.31	34.92	35.28	Stable C and O isotopes	Benthic foraminifera	Coxall et al., 2018
612,17X-3, 30-32	139.50	34.92	35.28	Stable C and O isotopes	Benthic foraminifera	Coxall et al., 2018
612,17X-3, 51-53	139.71	34.93	35.28	Stable C and O isotopes	Benthic foraminifera	Coxall et al., 2018
612,17X-3,71-73	139.91	34.93	35.29	Stable C and O isotopes	Benthic foraminifera	Coxall et al., 2018
612,17X-3, 90-92	140.10	34.93	35.29	Stable C and O isotopes	Benthic foraminifera	Coxall et al., 2018
612,16X-7, 26-30	135.96	33.63	33.81	Stable C and O isotopes	Benthic foraminifera	Miller et al., 1991
612,16-CC	136.00	33.67	33.86	Stable C and O isotopes	Benthic foraminifera	Miller et al., 1991
612,17-1, 140-144	137.60	34.89	35.25	Stable C and O isotopes	Benthic foraminifera	Miller et al., 1991
612,17-1, 140-144	137.60	34.89	35.25	Stable C and O isotopes	Benthic foraminifera	Miller et al., 1991
612,17-2,140-144	139.10	34.92	35.27	Stable C and O isotopes	Benthic foraminifera	Miller et al., 1991
612,17-3, 140-144	140.60	34.94	35.30	Stable C and O isotopes	Benthic foraminifera	Miller et al., 1991
612,17X-5, 140-144	143.60	35.00	35.36	Stable C and O isotopes	Benthic foraminifera	Miller et al., 1991
612,17X-6,140-144	145.10	35.03	35.38	Stable C and O isotopes	Benthic foraminifera	Miller et al., 1991
612,18X-1,60-64	146.30	35.05	35.41	Stable C and O isotopes	Benthic foraminifera	Miller et al., 1991
612,18X-3,60-64	149.30	35.11	35.46	Stable C and O isotopes	Benthic foraminifera	Miller et al., 1991
612,18X-4,60-64	150.80	35.13	35.49	Stable C and O isotopes	Benthic foraminifera	Miller et al., 1991
612,18X-CC	154.70	35.21	35.56	Stable C and O isotopes	Benthic foraminifera	Miller et al., 1991
612,19X-1,60-64	155.80	35.23	35.58	Stable C and O isotopes	Benthic foraminifera	Miller et al., 1991
612,19X-2,60-64	157.30	35.25	35.61	Stable C and O isotopes	Benthic foraminifera	Miller et al., 1991
612,19X-3,60-64	158.80	35.28	35.64	Stable C and O isotopes	Benthic foraminifera	Miller et al., 1991
612,19X-4,60-64	160.30	35.31	35.67	Stable C and O isotopes	Benthic foraminifera	Miller et al., 1991
612,19X-6,60-64	163.30	35.42	35.78	Stable C and O isotopes	Benthic foraminifera	Miller et al., 1991
612,19X-CC	164.50	35.48	35.84	Stable C and O isotopes	Benthic foraminifera	Miller et al., 1991

Site	Depth (msb)	AGE (CK95)* (Ma)	AGE (GTS12) (Ma)	Analysis type	Microfossil group	Data source
612,20X-1,60-64	165.30	35.52	35.88	Stable C and O isotopes	Benthic foraminifera	Miller et al., 1991
612,20X-2,60-64	166.80	35.59	35.95	Stable C and O isotopes	Benthic foraminifera	Miller et al., 1991
612,20X-3,60-64	168.30	35.66	36.03	Stable C and O isotopes	Benthic foraminifera	Miller et al., 1991
612,20X-4,60-64	169.80	35.74	36.10	Stable C and O isotopes	Benthic foraminifera	Miller et al., 1991
612,20X-5,60-64	171.30	35.81	36.17	Stable C and O isotopes	Benthic foraminifera	Miller et al., 1991
612,21X-4,60-64	179.30	36.20	36.56	Stable C and O isotopes	Benthic foraminifera	Miller et al., 1991
612,21X-5,113-114	181.33	36.30	36.66	Stable C and O isotopes	Benthic foraminifera	Pusz et al., 2009
612,21X-5,114-115	181.34	36.30	36.66	Stable C and O isotopes	Benthic foraminifera	Pusz et al., 2009
612,21X-5,116-117	181.36	36.30	36.67	Stable C and O isotopes	Benthic foraminifera	Pusz et al., 2009
612,21X-5,117-118	181.37	36.30	36.67	Stable C and O isotopes	Benthic foraminifera	Pusz et al., 2009
612,21X-5,118-119	181.38	36.30	36.67	Stable C and O isotopes	Benthic foraminifera	Pusz et al., 2009

Table IV.n. Detailed biostratigraphy. * = reworked: R= rare; x= present, but not counted within the 300 specimens.

Sample	Depth (mbsf)	Epoch	PF Biozone	CP Zones	**Planktic foraminifera:**	*Turborotalia cocoaensis*	*Turborotalia cunialensis*	*Turborotalia cerroazulensis*	*Hantkenina alabamensis*	*Hantkenina compressa*	*Hantkenina nanggulanensis*	*Hantkenina primitiva*	*Cribrohantkenina lazarii*	*Pseudohastigerina micra*	*Pseudohastigerina naguewichiensis*	**Calcareous nannofossils:**	*Discoaster barbadiensis*	*Discoaster saipanensis*	*Clausicoccus obrutus*
95-612,16X-6, 127-129	135.47	Oligocene	O1	CNE 21										x					R
95-612,16X-6, 143-145	135.63	Oligocene	O1	CNE 21															R
95-612,16X-7, 3-5	135.73	Oligocene	O1	CNE 21															R
95-612,16X-7, 25-27	135.95	Oligocene	O1	CNE 21					x*										R
95-612,16X-CC, 10-12	136.08	Eocene	E15/E16	CNE 21		6		1	9	4		x		x					R
95-612,17X-1, 0-2	136.20	Eocene	E15/E16	CNE 21		2	2		x					5	1				
95-612,17X-1, 6.5-8.5	136.27	Eocene	E15/E16	CNE 21		x	2	1	1					3					
95-612,17X-1, 13-15	136.33	Eocene	E15/E16	CNE 21			2							18	2				
612,17X-1, 20-22	136.40	Eocene	E15/E16	CNE19 / CNE20		x		2				1		5	1		2	1	
95-612,17X-1, 39-41	136.59	Eocene	E15/E16	CNE19 / CNE20		1	2	2	1	1				1	1		0	1	
95-612,17X-1, 59-61	136.79	Eocene	E15/E16	CNE19 / CNE20		2	2	2	1	1		1		7	1		3	0	
95-612,17X-1, 78-80	136.98	Eocene	E15/E16	CNE19 / CNE20		1	3		1					2					
95-612,17X-1, 98-100	137.18	Eocene	E15/E16	CNE19 / CNE20		2	3	4	1			x		5	x				
95-612,17X-1, 117-119	137.37	Eocene	E15/E16	CNE19 / CNE20		3	3	12		2		1		6					
95-612,17X-1, 137-139	137.57	Eocene	E15/E16	CNE19 / CNE20		x	x	6	3					7	x				
95-612,17X-2, 7-9	137.77	Eocene	E15/E16	CNE19 / CNE20		1	3	4	2	2				5	1				
95-612,17X-2, 28-30	137.98	Eocene	E15/E16	CNE19 / CNE20		1	3	2	12	x	2	x		6	3				
95-612,17X-2, 47-49	138.17	Eocene	E15/E16	CNE19 / CNE20		1		1	5										
95-612,17X-2, 65-67	138.35	Eocene	E15/E16	CNE19 / CNE20					3		1	x		1	1				
95-612,17X-2, 84-86	138.54	Eocene	E15/E16	CNE19 / CNE20			1							10					
95-612,17X-2, 104-106	138.74	Eocene	E15/E16	CNE19 / CNE20										5					
95-612,17X-2,126-128	138.96	Eocene	E15/E16	CNE19 / CNE20					x					1	2				
95-612,17X-2, 140-142	139.10	Eocene	E15/E16	CNE19 / CNE20					1			1		1	1				
95-612,17X-3, 11-13	139.31	Eocene	E15/E16	CNE19 / CNE20					1	1		3		5					
95-612,17X-3, 30-32	139.50	Eocene	E15/E16	CNE19 / CNE20				2	1			1		5					
95-612,17X-3, 51-53	139.71	Eocene	E15/E16	CNE19 / CNE20							1			3					
95-612,17X-3,71-73	139.91	Eocene	E15/E16	CNE19 / CNE20		2	1	3	2		1	1		2					
95-612,17X-3, 90-92	140.10	Eocene	E15/E16	CNE19 / CNE20		1	5	4	9	2		1	1	8					
95-612,17X-3, 110-112	140.30	Eocene	E15/E16	CNE19 / CNE20		4	9	13	x				1	1					
95-612,17X-3, 129-131	140.49	Eocene	E15/E16	CNE19 / CNE20		3	5	16						4					
95-612,17X-3, 148-150	140.68	Eocene	E15/E16	CNE19 / CNE20		4	3	7						2					
95-612,17X-4, 19-21	140.89	Eocene	E15/E16	CNE19 / CNE20		2	7	7	1					3					
95-612,17X-4, 38-40	141.08	Eocene	E15/E16	CNE19 / CNE20			1	5			1			1					
95-612,17X-4, 58-60	141.28	Eocene	E15/E16	CNE19 / CNE20		5	2	11	2		2								
95-612,17X-4, 76-78	141.46	Eocene	E15/E16	CNE19 / CNE20			1	1	1			1		20					

Appendix V. Supplementary information

Details on planktic and benthic foraminifera sample preparation

Samples (a split of 10 cc) were oven-dried (<40°C), desiccated, weighed, disaggregated in buffered water and then washed over a 38 μm mesh sized sieve. The obtained washed residues were dried, dry sieved to obtain 63 and 106 μm size fractions, weighed and separated into two equal parts using a precision micro-splitter; for the >106 μm fraction, one half of residue was used for the picking of foraminiferal specimens for isotopical analysis in Stockholm University, the other half was split again into two parts. One quarter was used for the study of planktic foraminiferal assemblages at Uppsala University (A. Legarda-Lisarri), the other quarter for the analyses of benthic foraminifera at Pavia University (N. Mancin). The >63 μm fraction was split only once, one half was used for the picking of specimens for isotopical analysis and the other half for the analyses of benthic foraminifera.

Samples for planktic foraminifera analysis were dry sieved again to obtain the >150 μm fraction (CLIMAP, 1976), weighed and examined with a reflected-light microscope. In representative splits of each fraction, we counted at least 300 specimens and identified into species level. For biostratigraphic purposes only, >63 μm fraction was revised to determine the presence of biostratigraphical markers, such as Turborotalia cerroazulensis group and species of the Family Hantkeninidae. As the primary species abundance data omits some smaller species such as *Pseudohastigerina* lineage, a total of 300 planktic foraminiferal specimens in three categories (*Pseudohastigerina micra*, *Pseudohastigerina naguewichiensis* and others) was identified for each sediment fraction (i.e. 250< > 150 μm, 150< > 125 μm and 125< >106 μm) in order to detect its distinctive reduction in size (Wade & Pearson, 2008). Census and detailed biostratigraphic data are reported in Appendix IV. Tables d and n respectively.

Quantitative analysis of benthic foraminifera was based on the study of both >106 µm and 63-106 µm fractions in order to avoid the underestimation of small-size ecological indexes, as some phytodetritus species (e.g. Gooday & Jorissen, 2011; Murray, 2006) and the elongate uniserial taxa belonging to the Elongate group (e.g. Hayward, Kawagata, & Sabaa, 2012 and references therein). In representative splits of each fraction, 300 specimens per sample were counted, except in samples containing less specimens. In these samples the whole fraction was analyzed and all the benthic specimens were counted. In order to avoid an overestimation of the counting, for the commonly fragmented elongate-uniserial taxa, three small fragments of the same species were considered as one specimen. Census data is reported in Appendix IV. Table e.

Relative abundance of planktic and benthic foraminifera was calculated as a percentage (%) of the total foraminiferal census counts together with their absolute abundance (N g^{-1}), calculated as the number of foraminiferal specimens per gram of dry bulk sediments (Appendix IV. Tables d and f).

Details on calcareous nannofossil sample preparation

Samples (35) were prepared with the drop technique which avoids selective settling effects, assures slides with even particle distribution, allows calculation of coccolith absolute abundances per gram of dry sediment (N g^{-1}) and provides good reproducibility, for both absolute and relative abundances (Bordiga, Bartol, & Henderiks, 2015). Calcareous nannofossils were examined under polarized light (LM) at 1000X magnification. At least 300 specimens were counted in each slide and identified at species or genus level. Additional observations were performed to detect the occurrence of rare species, especially biostratigraphical markers. Taxonomy follows Young et al. (2014 and references therein). To calculate absolute abundances the number of fields of view (FOV) observed was also noted, ranging from a minimum of 27 FOVs

(0.32 mm^2) to a maximum of 71 FOVs (0.84 mm^2). Census data, together with relative (%) and absolute abundances (N g^{-1}), is reported in Appendix IV. Table f.

Appendix VI. Publications

Coxall, Helen K., Huck, C. E., Huber, M., Lear, C. H., Legarda-Lisarri, A., O'Regan, M., et al. (2018). Export of nutrient rich Northern Component Water preceded early Oligocene Antarctic glaciation. *Nature Geoscience*, *11*(3), 190–196. https://doi.org/10.1038/s41561-018-0069-9

Bordiga, M., Henderiks, J., Tori, F., Monechi, S., Fenero, R., Legarda-Lisarri, A., & Thomas, E. (2015). Microfossil evidence for trophic changes during the Eocene-Oligocene transition in the South Atlantic (ODP Site 1263, Walvis Ridge). *Climate of the Past*, *11*(9), 1249–1270. https://doi.org/10.5194/cp-11-1249-2015

Legarda-Lisarri, A., Molina, E., Arenillas, I. Esparza-Alvarez, M.A. (2014). Cambios paleoambientales basados en foraminíferos planctónicos del Tetis durante el tránsito Eoceno-Oligoceno. En: New Insights on Ancient Life (G. Arreguín-Rodríguez, J. Colmenar, E. Díaz-Berenguer, J. Galán, A. Legarda-Lisarri, J. Parrilla-Bel, E. Puértolas-Pascual & R. Silva-Casal, Eds.), 49-52. Boltaña, Huesca.


Photo: Mustis Persson

Alba Legarda Lisarri is a specialist in Eocene-Oligocene planktic foraminifera with a focus on paleoecology, paleoceanography and paleoclimate. She studied Geology (Licenciatura en Geología; 2005-2010) in Basque Country University (EHU) and as exchange student in the UK (Cardiff University) and Mexico City (UNAM). She completed her masters in Marine Ecology in the Mexican Pacific coast (UMAR) and in Introduction to research in Geology in Spain (Zaragoza University) (2010-2012). In 2013 she started the doctoral studies in Zaragoza and continued in Stockholm University, under the supervision of Eustoquio Molina, Helen Coxall and Ignacio Arenillas.

Supervised by:

Eustoquio Molina
Departamento de Ciencias de la Tierra (Paleontología), Facultad de Ciencias, Instituto Universitario de Investigación de Ciencias Ambientales de Aragón (IUCA)
Universidad de Zaragoza, Spain

Helen K. Coxall
Department of Geological Sciences
Stockholm University and Bolin Centre for Climate Research, Sweden

Ignacio Arenillas
Departamento de Ciencias de la Tierra (Paleontología), Facultad de Ciencias, Instituto Universitario de Investigación de Ciencias Ambientales de Aragón (IUCA)
Universidad de Zaragoza, Spain

Stockholm University
Universidad Zaragoza
1542
Facultad de Ciencias Universidad Zaragoza
iuca
Instituto Universitario de Investigación en Ciencias Ambientales de Aragón
Universidad Zaragoza